AGH UNIVERSITY OF SCIENCE AND TECHNOLOGY

FIELD OF SCIENCE"ENGINEERING AND TECHNOLOGY"

SCIENTIFIC DISCIPLINE AUTOMATION, AND ELECTRONICS AND ELECTRICAL ENGINEERING

DOCTORAL THESIS

THE OPTIMIZATION OF CONTROL IN INDUSTRIAL FACILITIES CONSIDERING MINIMIZATION OF ENERGY CONSUMPTION

Author: mgr inż. Paweł Król

First supervisor: prof. dr hab. inż. Tadeusz Uhl
Assisting supervisor: dr hab. inż. Alberto Gallina

Completed in:
AGH UNIVERSITY OF SCIENCE AND TECHNOLOGY
THE FACULTY OF MECHANICAL ENGINEERING AND ROBOTICS
DEPARTMENT OF ROBOTICS AND MECHATRONICS

Kraków, 2022

AKADEMIA GÓRNICZO-HUTNICZA IM. STANISŁAWA STASZICA W KRAKOWIE

DZIEDZINA NAUK INŻYNIERYJNO-TECHNICZNYCH

DYSCYPLINA AUTOMATYKA, ELEKTRONIKA I ELEKTROTECHNIKA

ROZPRAWA DOKTORSKA

OPTYMALIZACJA STEROWANIA OBIEKTAMI PRZEMYSŁOWYMI Z UWZGLĘDNIENIEM KRYTERIUM MINIMALIZACJI ZUŻYCIA ENERGII

Autor: mgr inż. Paweł Król

Promotor rozprawy: prof. dr hab. inż. Tadeusz Uhl
Promotor pomocniczy: dr hab. inż. Alberto Gallina

Praca wykonana:
AKADEMIA GÓRNICZO-HUTNICZA
WYDZIAŁ INŻYNIERII MECHANICZNEJ i ROBOTYKI
KATEDRA ROBOTYKI I MECHATRONIKI

Kraków, 2022

Składam serdeczne podziękowania dla
prof. dra hab. Tadeusza Uhla za inspirację do podjęcia tematu oraz
dra hab. Alberto Galliny za wsparcie w analizach

I would like to express my sincere thanks to
prof. dr hab. Tadeusz Uhl for inspiration to take up the topic and
dr hab. Alberto Gallina for his support in the analysis

The doctoral thesis is a part of the InnoEnergy PhD School supported by EIT InnoEnergy. This research is under the GEKON program (contract number GEKON2/O2/266926/3/2015) and dean's grants support. Conducted in AGH UST Center of Energy.

Praca doktorska jest częścią Szkoły Doktorskiej InnoEnergy wspieranej przez EIT InnoEnergy. Badania realizowane są w ramach projektu GEKON (umowa GEKON2/O2/266926/3/2015) oraz przy wsparciu grantów dziekańskich. Zrealizowano w Centrum Energetyki AGH.

Abstract

Currently, the energy industry is at the time of a groundbreaking transformation which results in the dispersion of energy sources. The need for transformation is caused by the climate change observed in recent years, which entails the need to reduce CO_2 emissions. The effect is an increase in electricity prices, prompting industry to minimize energy consumption. The author's interests focus especially on the issues of energy installations in industrial applications.

The author has put forward the thesis that "*Comprehensive modeling of the industrial facilities like wastewater treatment plants can be used in optimization of control leading to minimization of electric energy consumption."* The author assumes that complex energy optimization algorithms can be implemented numerically in the installation of an industrial facility such as the above-mentioned sewage treatment plant (WWTP). Such a model is based on data from the existing Płaszów WWTP in Krakow.

Modelling of wastewater treatment plants has been chosen as the main topic. Aeration has been analyzed, as it is the most energy-consuming part of the process. The available modifications to the control of the installation have been discussed. The target implementation compared the performance of the reactor model and blowers with the available measurement data. A Matlab/Simulink model has been prepared to enable energy optimization of the treatment plant facility. Thanks to this numerical image, it is possible to freely test various energy optimization algorithms without the need to interfere with the operation of the existing installation.

The operation of virtual WWTP is validated. A proprietary uncertainty testing procedure in a complex strategy for controlling reactors and blowers has been prepared. Actions are performed to validate the parameters implemented in the model. Morris analysis has revealed the parameters of the most essential introduction process. The author has taken the state estimation to check the cleaning efficiency and identify the parameters with the Extended Kalman Filter.

The main purpose of the work is to use the optimization algorithms in the control of wastewater treatment plants with the use of numerical models of WWTP. The author has decided on the practice of changing the switching time and downtime of the blowers' in order to select the optimal operation of the station of six blowers in the installation. Subsequently, the energy optimization of the blowers has been thereby carried out in terms of reducing electricity consumption.

One can acknowledge the dissertation's contribution to the current scientific resources. The work covers the implementation of a complex biological simulation of sewage reactors in Płaszów Sewage Treatment Plant in Kraków. Thanks to their use, it was possible to achieve the aim of the dissertation - to prove the possibility of using energy optimization algorithms in industrial installations of sewage treatment plants. To the best of author's knowledge, this analysis is the first such approach for the Kraków sewage treatment plant.

Streszczenie

Obecnie branża energetyczna jest w momencie przełomowej transformacji. Obserwowane w ostatnich latach zmiany klimatu, pociągają za sobą potrzebę redukcji emisji CO_2, co skutkuje wzrostem cen energii elektrycznej. To z kolei skłania przemysł do minimalizacji zużycia energii. Zainteresowania autora koncentrują się na kwestiach działania instalacji energetycznych w zastosowaniach przemysłowych.

Autor stawia następującą tezę: „*Kompleksowe modelowanie obiektów przemysłowych takich jak oczyszczalnie ścieków może być wykorzystane w optymalizacji sterowania prowadzącej do minimalizacji zużycia energii*". Autor zakłada, że złożone algorytmy optymalizacji energetycznej mogą być zaimplementowane numerycznie w instalacji takiego obiektu przemysłowego, jakim jest wspomniana powyżej oczyszczalnia ścieków. Praca bazuje na danych pochodzących z Zakładu Oczyszczania Ścieków Płaszów w Krakowie.

Głównym tematem pracy jest modelowanie oczyszczalni ścieków. Przeanalizowano proces napowietrzania ścieków, ponieważ jest to najbardziej energochłonna część procesu. Omówiono dostępne modyfikacje sterowania instalacją. W realizacji docelowej porównano wydajność modelu reaktora i dmuchaw z dostępnymi danymi pomiarowymi. Przygotowano model Matlab/Simulink, aby umożliwić optymalizację energetyczną oczyszczalni ścieków. Dzięki temu liczbowemu obrazowi możliwe jest swobodne testowanie różnych algorytmów optymalizacji energetycznej bez konieczności ingerencji w pracę istniejącej instalacji.

Sprawdzono działanie wirtualnej oczyszczalni ścieków. Przygotowano autorską procedurę testowania niepewności w złożonej strategii sterowania reaktorami i dmuchawami. Wykonano działania, które badają parametry zaimplementowane w modelu. Analiza Morrisa ujawniła parametry najistotniejsze w procesie oczyszczania ścieków. Autor zaimplementował estymację stanu w celu sprawdzenia wydajności oczyszczalni ścieków i identyfikacji parametrów za pomocą Rozszerzonego Filtru Kalmana (EKF).

Głównym celem pracy jest wykorzystanie algorytmów optymalizacji w sterowaniu oczyszczalniami ścieków z wykorzystaniem modeli numerycznych oczyszczalni ścieków. Autor zdecydował się na praktykę polegającą na zmianie czasu przełączenia oraz przestoju dmuchaw w celu doboru optymalnej pracy stacji sześciu dmuchaw w instalacji. W dalszej kolejności w ten sposób przeprowadzono optymalizację energetyczną dmuchaw pod kątem redukcji zużycia elektryczności.

Można znaleźć wkład rozprawy do aktualnych zasobów naukowych. Praca obejmuje wykonanie kompleksowej symulacji biologicznej reaktorów ściekowych w Oczyszczalni Ścieków Płaszów w Krakowie. Dzięki ich wykorzystaniu udało się zrealizować cel rozprawy - udowodnić możliwość stosowania algorytmów optymalizacji energetycznej w przemysłowych instalacjach oczyszczalni ścieków. Według obecnej najlepszej wiedzy taka analiza jest pierwszym takim podejściem dla krakowskiej oczyszczalni ścieków.

Table of Contents

1 Aim and scope of the thesis

1.1 Motivation and the aim of the dissertation

MOTIVATION: We observe the continuous progress in various fields. For example, technological development leads to the modernization of production techniques, improvement of process management and efficiency of operation. Nowadays, a conscious environmental policy is particularly taken into account, which forces the industries to reduce CO_2 emissions. Next decades are likely to witness a considerable emphasis on the reduction of electricity consumption. This impacts the industry that also needs to reduce the impact on the environment to preserve the nature for the future. It is not only economically justified, but it also reduces long-term costs of operation. This direction of development has inspired the author to choose this subject of research.

OBJECTIVE: In the author's forgoing research, it has been examined that wastewater treatment plants (WWTPs) are considerable energy consumers. Therefore, research of this industry is taken into consideration. Indeed, the main motivation of dissertation is to investigate the process of industrial wastewater treatment in terms of the reduction of electricity consumption. To carry out the study, a simulation environment that implements optimization control strategy in order to reduce energy consumption has been conducted.

THE AIM OF WORK: The author explored tools for simulation of the wastewater treatment process and later exploited one in a numerical implementation. Such virtualization simplifies virtual prototyping of the operation of sewage treatment plants. The main aim of the work is to investigate the operation of industrial wastewater treatment considering electricity and optimization of its consumption. It is carried out by simulations utilizing optimization algorithms and implementation of efficient control strategies.

BACKGROUND: Doctoral dissertation is supported by the dean's grants, the place of work is the AGH Center of Energy. The research conducted as part of this doctoral dissertation was carried out with financial support under the GEKON-EPOS program (contract number GEKON2/02/266926/3/2015)[1].

1.2 The context of research within the GEKON project

GEKON project included the implementation of Integrated System for Energy Efficiency Integrated System EEIS (ZSEE Zintegrowany System Efektywności Energetycznej) as a superior system to the control system of the Płaszów Sewage Treatment Plant existing for several years. The system has been built so that IT and communication solutions are compatible with the standards adopted and used in the Płaszów Sewage Treatment Plant [1][2].The research is carried out as part of this project. The aim of the work is to carry out the model of the internal processes of the sewage treatment plant in terms of energy optimization[3].

[1] More information can be found on websites
http://krim.agh.edu.pl/projekty/epos/
https://www.astor.com.pl/klienci-astor/wdrozenia/10368-mpwik-krakow-zintegrowany-system-efektywnosci-energetycznej-w-oczyszczalni-plaszow.html

1.3 Scope of the dissertation

The selected area concerns environmental engineering, in particular technical aspects of the operation of sewage treatment plants. The industry is dictated by the need to analyze the energy consumption of the aeration process, which is the most energy-intensive purification process. The simulation framework presented in the thesis is based on algorithms describing the operation of wastewater treatment plants. The goal of work is to present the implementation aspects of algorithms used in the topic of reduction of industrial energy consumption using control optimization criteria.

The work focuses on the analysis of optimization algorithms of the wastewater treatment process. A simulation model of biological reactors of the treatment plant has been prepared and measurements of the control system installed in the existing treatment plant have been used. The case study includes a treatment plant in Płaszów Sewage Treatment Plant in Kraków. The available modifications of the control of the municipal sewage treatment plant object are discussed. The purpose of the work is to develop optimal algorithms for controlling blowers taking into account the criterion of minimizing energy consumption.

The above considerations discuss different approaches to energy optimization of industrial facilities. The dissertation focuses on algorithms and energy optimization, which aims to losslessly minimize the energy costs of the industrial process. In particular, the focus was on researching the energy aspects of facilities such as sewage treatment plants.

The main assumption of the work is to prepare Matlab/Simulink model which unambiguously determines the air blow based on the demand for oxygen in the wastewater. A detailed numerical model of wastewater treatment plants that includes blowers is described. The simulation prepared in this way integrates the BSM1 model with the blower design.

Subsequently, such a simulation constructed a numerical environment, which allows testing the energy efficiency of the oxygenation process without interfering in the existing treatment plant. Such simulation allows to model and validate the operation of wastewater treatment plants based on a numerical model – the modification in blower's control algorithm allows to validate electricity consumption during the aeration process.

1.4 Thesis and original contribution of the work

The author follows the thesis that

> *Comprehensive modeling of the industrial facilities like wastewater treatment plants can be used in optimization of control leading to minimization of electric energy consumption.*

Numerous activities have been described in order to implement the task.

First, the BSM1 model has been thoroughly tested and its structure has been rebuilt so that the parameters currently correspond to those in the Płaszów sewage treatment plant. The BSM1 model has been integrated with blowers, thus creating a full system. This complex simulation of the sewage biological reactors in Płaszów WWTP is the first novelty presented in the study.

Further, the author uses this model for simulation to reduce power consumption. In order to achieve this goal optimization algorithm running on BSM1 model of the WWTP is proposed. Despite the high uncertainty, the observations have a cognitive value. The author assumes that this approach meets the criteria of novelty.

More specifically, the following issues are considered new:

- Complete numerical model of Płaszów WWTP based on BSM1 in Matlab/Simulink;
- Uncertainty treatment and identification procedure in complex blowers' control strategy;
- Optimization of WWTP's control by modification of blowers' delays.

1.5 Structure of the dissertation

The work is divided into chapters in the order presented below.

The second chapter introduces the reader to important economic and environmental background – the reduction of electricity consumption in industrial units. The introduction of the work includes an in-depth analysis of the current state of theoretical knowledge in the field of highly-efficient energy sources and effective methods of controlling receivers.

In the third chapter, the author presents the idea of a municipal wastewater treatment plant simulation using BSM1 model based on ASM mathematical equations. The detailed description of the model is presented.

In chapter four, the author shows the model of Płaszów WWTP as the object of research. The paragraph describes in detail the design assumptions and practical aspects considered in simulation based on the real object.

Later in the fifth paragraph, the author discusses the practical implementation of BSM1 model and aeration system in such municipal WWTP. The model has been used and the optimization is presented in the next paragraph.

Chapters six and seven present the model validation based on two independent ideas. The former presents a numeric model of reactor characterized by model sensitivity. The latter discusses the Kalman filter for model validation.

In paragraph eight, the simulations calculating the electricity demand, taking into consideration different parameters wastewater influent are presented. The discussed results are collected in tables.

In paragraph nine, the author introduces us to the optimization of electric energy consumption utilizing numerical implementation of WWTP. They lead to assumptions that such model can be used in optimization of control leading to minimization of electric energy consumption.

In paragraph ten, discussion of results paying special attention to minimization of electricity consumption is presented.

2 Electric energy consumption in large industrial facilities

2.1 Energy aspects of industrial facilities

According to the [4], the industry is responsible for 33% of global energy consumption and 38% of CO_2 emissions in the atmosphere. Such proportion of industrial consumption in the relation to the whole economy is presented in Fig. 1. According to the American Energy Information Administration (EIA), the industry can be divided into three groups: energy-intensive production, non-energy-intensive production, and services (agriculture, construction) [5]. The energy balance depends, to a large extent, on the specifics of the country being studied.

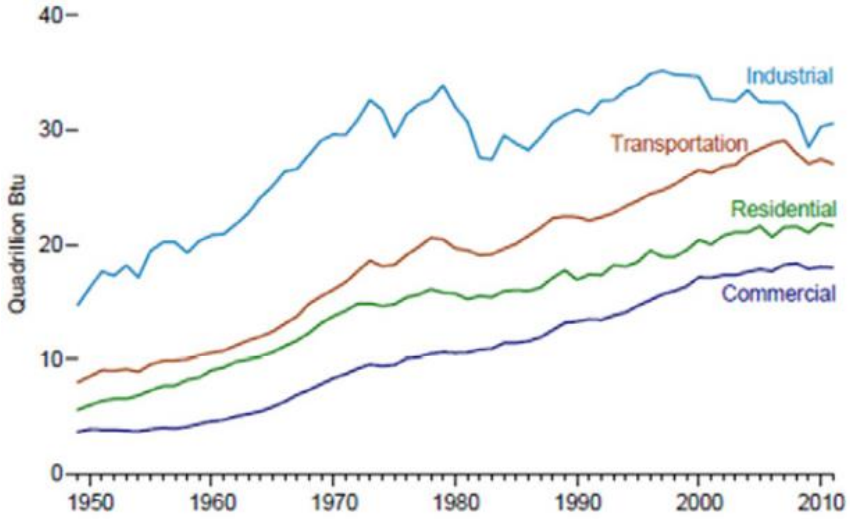

Fig. 1. The use of energy by end customers [4]

Each process improvement in the industrial process can generate observable savings which contribute to measurable economic benefits in the long term. An example of an energy-intensive industry is the metallurgical industry. For instance, the Chinese steel industry accounts for 15.2% of total national electric energy consumption, 14% of wastewater production and 6% of solid waste [6]. The share of only four energy-intensive branches of industry in Poland (chemical, non-ferrous metals, ferrous and paper) amounts to approximately 70% of the electricity consumed in the industry [7]. Nevertheless, there are industrial recipients in other manufacturing sectors. Ramirez and Patel analyzes non-energy intensive industries concerning its energy intensity, value-added, the value of production and energy cost [8]. The analysis points out the strong relationship between manufacturing output and energy consumption in the non-energy intensive sectors which certainly does not include metallurgy. Indisputably, slight improvement in the energy-consuming process generates significant savings.

How can energy neutrality be implemented in practice in the case of large industrial facilities? In principle, two options to local electricity generation in industry can be distinguished: on-site local generation using internal resources– photovoltaic, waste biogas combustion, waste heat recovery; and energy saving through the on-site improvement of ongoing industrial process.

2.2 Wastewater treatment as energy-consuming processes

What does this energetic aspect look like in the non-intensive industry like municipal services? In a report prepared by organization ESMAP around 4 percent of global electricity production is used for a municipal water supply and wastewater treatment (WWT). The high potential for electricity reduction is in the wastewater treatment industry [9].

The issue of electric energy consumption in large industrial facilities such as sewage treatment plants can be considered through on-site generation and the implementation of optimization algorithms. Optimization algorithms are used to improve the operation of wastewater treatment plants. In [10], authors analyze the economic aspects of modernization of wastewater treatment plants to optimize electric energy consumption. Authors analyze the modernization of diffusers to more effective ones. In [11], energy consumption in selected sewage treatment plants in Japan has been presented. In [12], authors describe the energy consumption of the Slovak sewage treatment plant. In [13], authors propose enhancement of Polish WWTP through biogas implementation.

The object of the Płaszów Sewage Treatment Plant in Kraków is a modern facility that meets most of the latest environmental and energy standards. More information about the Płaszów Sewage Treatment Plant in Kraków is presented in [14]. The municipal sewage treatment plant is an example of an installation serving a large area of the Kraków agglomeration. Therefore, due to the significant size of the utility its importance is noticeable – the facility is a significant consumer of electricity. The dissertation discusses control techniques to reduce electricity consumption taking Płaszów WWTP as a reference. They allow modernization of the process in a way that avoids costly investments so that society can benefit from cleaning costs. This issue will be discussed in the following paragraphs of this dissertation. In the following chapters of the work, two approaches to minimize the cost of electricity consumption are presented. At first, on-site generation is a way of increasing self-sufficiency. Later, optimization algorithms are discussed and the implementation possibilities are presented. The reduction of electric energy consumption is the effect of such optimization.

2.3 On-site generation as a method of reducing energy consumption

2.3.1 On-site local generation using internal resources

With the increase of consumer awareness, manufacturers are paying more and more attention to the sources of electricity that power production processes. The generation of electricity using on-site local resources can be considered as an energy-efficient solution. This is because the plant does not have to purchase electricity from external suppliers. Such a solution increases the efficiency of the industrial process and reduces operating costs. However, the costs of implementation of a certain solution in a company are significant.

Part of this attention focuses on the use of green electricity. Thanks to this attitude, the companies reduce the environmental impact of the production processes, which then reaches customers' expectations. This attitude is positively perceived by customers to

increase the entrepreneur's profits. These processes are analyzed on the example of global corporations[15].

The largest share is from non-renewable energy sources, with the indication of renewable energy growing in industrial plants (Fig. 2). For example, according to [16], the company Facebook declares to cover 25% of electricity consumption by renewable energy. The biggest retailer in the US, Wal-Mart, invested in a wind farm in Red Bluff distribution center to supply 15 to 20% of the facility's electricity needs at substantial cost savings over the next 15 years. In report [17], authors suggest the distribution of electricity sources in industrial plants.

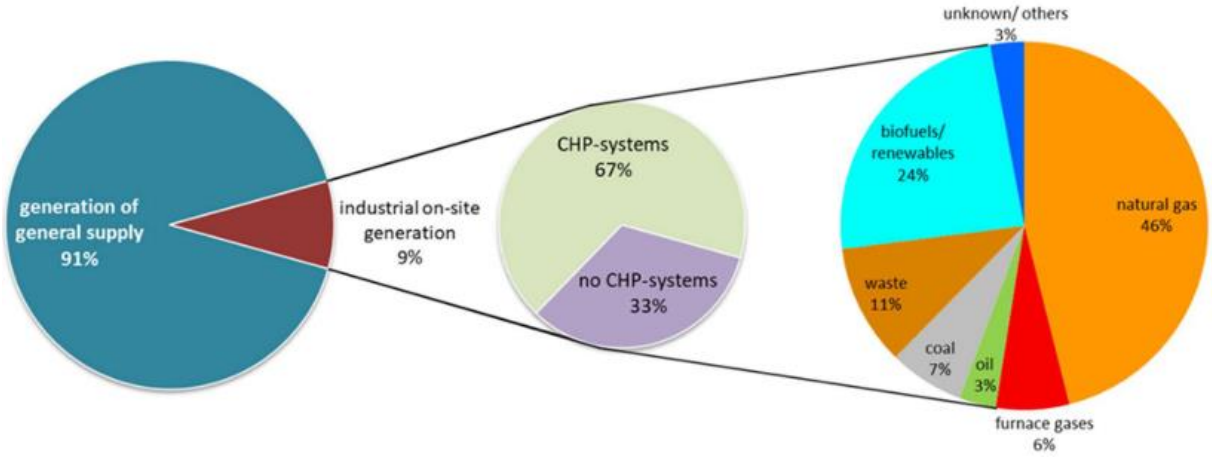

Fig. 2. Industrial on-site generation of total electricity production share (left),
CHP- systems of on-site generated electricity share (middle),
main energy sources of on-site generate electricity for 2017 (right) [17]

2.3.2 Biogas combustion

In research, the author discusses the sewage treatment plant installations. In their case, biogas from the decomposition of wastewater is the most valuable resource. The schematic of the process is presented below (Fig.3)[18].

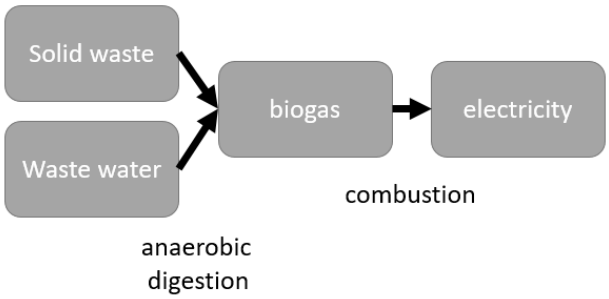

Fig. 3. Schematic of waste utilization be electricity production [18]

Anaerobic digestion is a primary method of utilization of products such as plant remains, agricultural products or organic waste. These are natural processes by which microorganisms break down biodegradable material in the absence of oxygen – the amount of organic matter is reduced by the extraction of gases. The process intensifies at elevated temperatures, thus external heat source is advantageous. The product of anaerobic

digestion is biogas which consists of methane (65%) and other non-flammable ingredients (carbon dioxide and water).Proper storage conditions allow one to produce biogas that releases heat (while being burned) which is utilized to generate energy [19].

The biogas potential of solid waste depends on the type of feedstock. During anaerobic digestion around 0.42m^3 of biogas is obtained by processing 1kg of biodegradable solid [20]. When the content of biodegradable ingredients in waste is 50%, the yield of biogas is reduced to 0.21m^3 per kg. Each 1m^3 of sewage contains around 0.5kg of sludge [21]. The digestion of 1 kg of sewage sludge produces approximately 0.7m^3 of biogas [22]. Biogas extracted during anaerobic digestion of both solid waste and sewage sludge can be used as a partial or complete fuel for combustion engines and as such is considered as a potential source of a renewable energy [23].

The potential of anaerobic digestion to produce biogas is presented by Houdková[24] – authors present biogas production in a laboratory and next, comment on the potential of biogas utilization and biogas production for vehicles. Matuszewska et al. [25] evaluate the biological methane potential of various feedstock for the production of biogas to supply engines in agricultural tractors. Otherwise, biogas can feed generators producing electricity in stationary local power plants. Some researchers focus on such waste management – Željko et al. [26]propose energy recovery from waste by the creation of waste management centers in regions of Croatia.

Waste digestate is utilized, incinerated or landfilled [22]. Pyrolysis of digestate is one of the utilization methods. Opatokun et al. [27] assess the energy potential of food waste energy harvesting system. The authors conclude that transitional energy base products (biogas and bio-oil) are generated through the energy harvesting system of food waste, while energy-rich solid fuels can be produced through pyrolysis at 500°C. In [28], the author proposes approaches based on anaerobic digestion and pyrolysis of sewage management.

In [29], authors analyze the potential of biogas utilization to reduce the electricity consumption in Dubrovnik city located in Croatia. In the paper, authors give examples of many low-temperature processes from which energy can be recovered in the city of Dubrovnik.

The use of fuel cells fed with biogas obtained in a sewage treatment plant is a new direction of research. Particularly interesting is the SOFC Solid Oxide Fuel Cell technology elaborated in the DEMOSOFC project [30]. Especially cogeneration (combined heat and power) in industrial applications is exploited.

Sometimes waste heat can be used to generate additional electricity [31]. The temperature scale even covers the range below 200°C. Such low-temperature recovery is possible thanks to the use of organic working fluids that change state in different conditions. In [32], issues concerning the usage of Organic Rankine Turbines (ORC)and steam process for small power generation are presented.

2.4 Selection of algorithms used in optimization of control

2.4.1 Tasks scheduling to reduce electricity consumption

Control algorithm of industrial utilities can be usually improved to a certain extent. Proper tasks scheduling could be one of the ways having a positive effect on performance of the controlled system. When using the task scheduling technique, a task should be selected, in such order that the total time of their implementation is the most advantageous. It is necessary to respect the availability of energy resources and temporary rigor of the feasibility of tasks [33].

We can distinguish two methods of making decisions about starting tasks: greedy scheduling algorithms and lazy scheduling algorithms. In the greedy approach, each task is carried out at the time of its submission as long as it has the highest priority. In the lazy task scheduling, the algorithm makes decisions during the application operation (on-line), the dispositions are supported by historical readings. Lazy algorithms enable deferment of the receiver's inclusion to match the consumption of resources to its planned availability. They are used in applications such as sensors with limited availability of resources (energy harvesting). Fig. 4 presents operation of tasks scheduling algorithms in both versions.

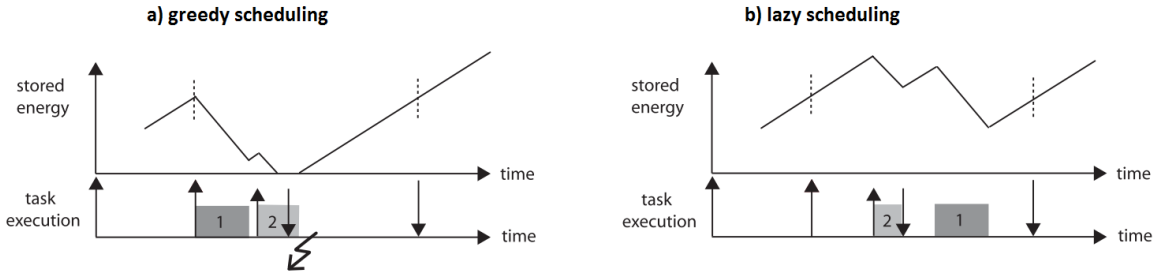

Fig. 4. Operation of algorithms using (a) greedy (b) lazy tasks scheduling[34]

The implementations of tasks scheduling in the energy industry have been published. Authors developed algorithms that predict the potential electricity availability and schedules the tasks according to prediction. The considered topic allows to improve the process of charging batteries installed in electric vehicles. In [35], authors consider two heuristic algorithms: the Earliest Start Time (EST) algorithm and the Earliest Finish Time (EFT) algorithm. EST tries to advance the start charging time to get customers in service as early as possible while EFT focuses on the possible finish charging time to get customers served as soon as possible. In [36],authors present the lazy algorithm for energy harvesting sensor nodes. T. Khatib presents the review of optimization systems used in inverters used in photovoltaic systems (PV) [37]. The publication presents that the sun is a highly unreliable power source. Thus, the sophisticated power management systems might be used. Zhang et. al. [38] propose Optimal Scheduling of Smart Homes Energy Consumption with Microgrid. Electricity consuming tasks are scheduled on the basis of different electricity tariffs, electricity task time window and forecasted renewable energy output.

The author is faced with the question of whether there is a possibility of similar scheduling of energy-intensive processes in applications, in particular, like sewage treatment plants.

2.4.2 Mathematical programming in electricity sector

Mathematical programming is a tool in which management operations are described by mathematical equations that can be used for a variety of purposes. In particular, it focuses on finding an extreme value of a certain objective function in which limits have been imposed on variables that affect the narrowing of the number of possible solutions described by the objective function $z = f(x_j) = min/max$ with constraints: $f(x_j) \leq 0;\ j = 1, \dots, m$. The task optimization problem, formulated in this way, can be solved by many methods using the available optimization environments (i.e. GAMS, AIMMS) and are used in the optimization of complex energy models [39].

The application of mathematical programming in industry has been examined. Works [40]and [41] present mathematical programming in the optimization of industrial processes. Paper [42] discusses the use of mathematical programming in the design of the wastewater treatment process itself. In [40], the use of linear programming for optimizing the planning and production process has been discussed. A discrete-time scheduling model for continuous power-intensive process networks with various power contracts has been examined in [41].

Mathematical programming is a commonly used technique in the optimization of control to reduce electric energy consumption. This type of optimization has been implemented in the electric energy industry, as described in the literature below. Mathematical programming is a basis for operation of electricity markets in electricity distribution. In [43], authors discuss tools deploying this programming technique to optimize electricity distribution at the country level. In publication *Business Models for Distributed Energy Resources: A Review and Empirical Analysis An MIT Energy Initiative Working Paper* [44], the most popular applications of dispersed electricity sources have been debated. The document considers legal incentives to apply flexible solutions. In [45], authors scrutinize the basic applications of market coupling algorithms as tools for optimization in electricity trade at the international level. In particular, the author draws attention to the publication *EUPHEMIA Public Description* [46] that shows the use of the EUPHEMIA algorithm as a tool enabling further integration of distribution on the international market. The purpose of the paper is to discuss basic algorithms applied in practice, their theoretical assumptions and the scope of recent as well as future applications. The authors provide considerations about these algorithms in the context of optimization of electricity distribution in Poland.

The task of mathematical programming is within the scope of this thesis. The author will look for the possibility of implementing this approach in the developed model of a sewage treatment plant.

2.4.3 Optimal control in electric energy distribution

Optimal control is the process of determining control and state trajectories for a dynamic system over a period of time to minimize cost criterion. The problem is derived from mathematical optimization. Each problem of optimal control requires a mathematical formulation of the process quality indicator that is to be optimal. Optimization in real systems always takes place with constraints imposed on the process variables which cannot assume any values [47].

The concept of optimal control is described as continuous-time cost functional presented below [48] and [47]:

$$J = E\left(x(t_0), t_0, x\left(t_f\right), t_f\right) + \int_{t_0}^{t_f} F(x(t), u(t), t)\, dt \tag{1}$$

$$\dot{x}(t) = f[x(t), u(t), t] \tag{2}$$

$$h[x(t), u(t), t] \leq 0 \tag{3}$$

Where:

J is a performance index is a measure of the quality of system behavior,
E and F are referred to as the Mayer term and the Lagrangian respectively,
$x(t)$ is the state, $u(t)$ is the control,
h indicates the path constraints,
t_0 is the initial time, t_f is the terminal time.

This type of optimization has been implemented in the electric energy industry, as described in the literature below.

David M. Rosewater[49] investigates the optimal control in practical application. Analysis with respect to the models is used in optimal control of battery energy storage. The author demonstrates the significance of model selection in optimal control. In this case, the task presents the optimal control equation, the form of which is a simplification of the above.

Luis I. Minchala-Avila et al. discuss some control techniques for optimal control in energy management and microgrids control [50]. The paper presents an overview of optimal control techniques used in energy management and microgrid control. Authors show optimal energy management systems (EMS) that can be used in management and control of microgrids. The paper debates numerous methodologies of optimal control. Authors discuss variable optimization methods for microgrid control: predictive optimization, mixed-integer linear programming (MILP) and non-classic optimization techniques.

The task of mathematical programming is within the scope of interest. Later in the dissertation, there is a reference described in this optimization method. In particular, the optimization of the wastewater treatment in terms of selected process parameters in time domain interests the author.

2.4.4 Brute force approach in optimization of electric energy consumption

Brute force approach in optimization (exhaustive search) is a non-complex way of searching for an optimal solution. This is an approach to calculate all possible solutions and decide afterwards which one is the best. The method is feasible for case of model with a small dimensionality. Such a solution does not allow to search for a global minimum [51].

Grid search optimization, for example, is one way to search for values using brute force approach. The task is to a grid of parameter values at equal distances. The input parameters thus form a grid of equally spaced points. An exemplary implementation of a grid of this type is shown below (Fig. 5).

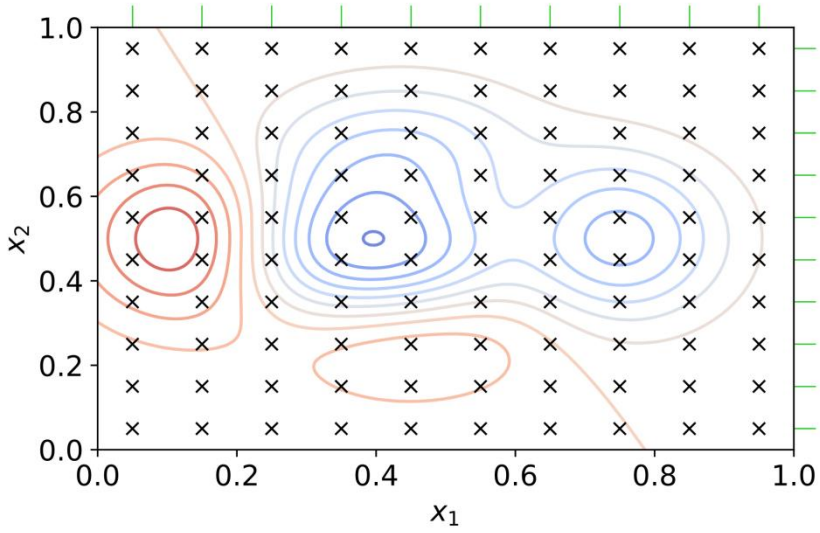

Fig. 5. Example of grid search across different values of two parameters [52]

This type of optimization has been implemented in the electric energy industry, as described in the literature below.

Anna Glazunova, Elena Aksaeva in [53] present the implementation of brute-force in the flexibility of the electric power system (EPS). Authors come up with some deterministic methods developed to study the EPS flexibility. Later, authors usebrute-force optimization to determine the most effective combinations of possible loads in electric power system.

In publication [54], Parlier Guillaume et al. propose solution of solving distribution feeder reconfiguration (DFR) problem. First, authors present the numeric implementation of DFR problem with constraints. The high number of solutions is reduced based on a graph theory pre-processing. Later, brute-force approach is used to select the most effective solution.

2.4.5 Blockchain to reduce the consumption of electricity

Blockchain has received much attention in the last decade. This paragraph presents application research of the technology of distributed database registers based on a blockchain. The algorithm is applicable among other things as a block-based transaction register.

A distributed transaction register is a base in which transactions are collected in blocks, which then, as a result of encryption algorithms, are associated with blocks containing a register of previous transactions (Fig.6) [55].

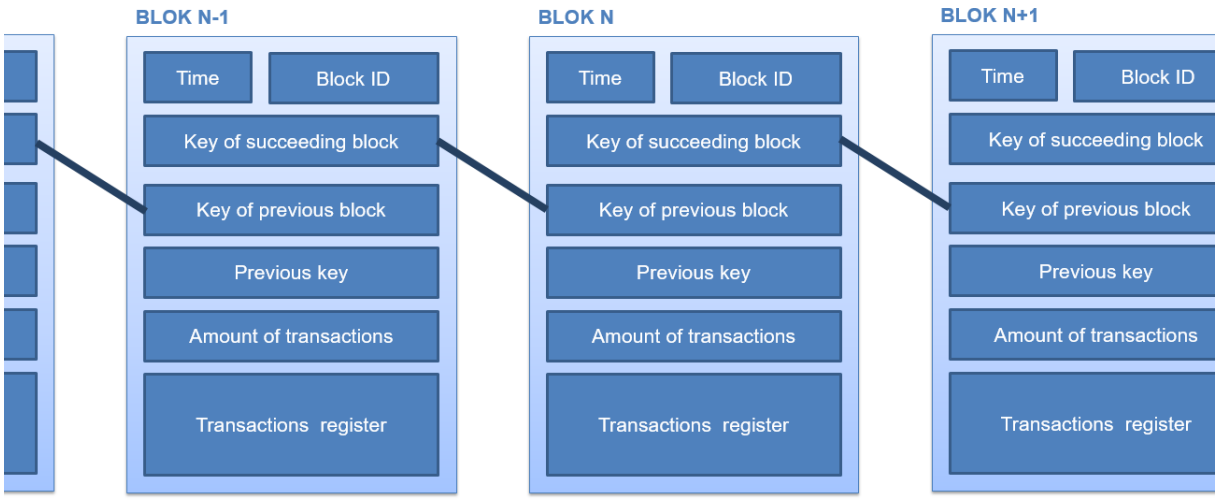

Fig. 6. Block structure of a typical blockchain [55]

Each privileged node can independently download its copy of the database in nodes - servers. The use of a distributed database gives the possibility of independent registration of certain information. To decide which node has the correct data, consensus methods guaranteeing full data security have been developed.

Two independent worlds - central and distributed databases are shown in the graphic below (Fig. 7). What are the benefits of spreading this data between different clients? The use of distributed registers allows you to secure your information on different servers without indicating the central one. Such a built-in register contains the whole history of transactions that have taken place so far. Thanks to this the base is safe to manipulate.

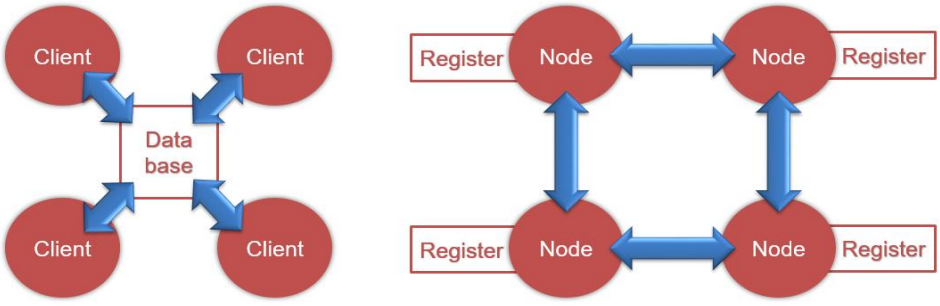

Fig. 7. Comparison of a standard device network with blockchain application

As part of the developed topic, attention is paid to the possibility of using algorithms of distributed databases on the blockchain in the optimization of industrial processes, in particular energy optimization. For this purpose, it is decided to use the open project implementing the blockchain database – Hyperledger supported by Linux Foundation. This database is dedicated for use in distributed corporate networks - closed, non-public distributed registers that cover the area of one or several companies. Transaction registration in Hyperledger is possible thanks to the use of blockchains. The algorithm introduced in this database consists of two types of nodes - client and privileged. The privileged node can enter transactions into a distributed register. The customer, on the other hand, has the option of synchronizing the account with one of the privileged nodes.

Available studies report the use of distributed databases based on the Hyperledger project in the energy sector. In [56], Zhang considers using a distributed IOE (internet of energy) system for electricity trading using the implementation of the Hyperledger environment. Ultimately, the operated power grid also supports batteries which task is to stabilize the system. Lombardi [57] discusses the distributed database application for intelligent IoT networks. An infrastructure architecture based on smart contracts has been presented which offers functionality for managing energy trading policy, conducting energy auctions on the network. The authors add that the solution is beneficial in particular in the settlement of prosumer installations.

In the paper [58], the following applications of databases dispersed in the power industry are distinguished and discussed:

- certificates of origin of electricity,
- distributed registers in energy distribution management,
- smart-contracts in prosumer accounting.

Blockchain acts as a distributed database. The distribution of the register with the data for the settlement of this information is crucial in the case of bottom-up installations, such as energy clusters. The use of blockchain in the energy sector allows to improve the exchange of data between producers. Such action lets you save on electricity by reducing its consumption.

2.5 Approach used in further considerations

The previous chapters outline two optimization approaches in order to optimize electricity management: on-site generation utilizing internal reaches and reduction by energy management.

Firstly, it is possible to produce electricity on the premises of the plant. However, on-site energy production will not fully replace the consumption of an off-site power plant. Therefore, the author focuses on the possibilities of reducing electricity consumption in the municipal sewage treatment plant.

The author has made a review of algorithms used in optimization of electric energy consumption in engineering applications. More specifically, the following methods have been described:

1. Tasks scheduling,
2. Mathematical programming,
3. Optimal control,
4. Grid search optimization (based on brute force exhaustive search),
5. Application of blockchain.

Undoubtedly, the implementation of the above-mentioned control optimization algorithms could lead to minimization of electric energy consumption[59]. The control algorithms are tested on the model of an industrial facility. The author analyzes an industrial object that consumes significant amounts of electrical energy. Due to the significant energy cost of the biological process in the treatment of wastewater, the author considers this part as a place for potential energy savings. The author proves that there are possibilities to optimize the electricity consumption in such installation and discusses possible solutions in this matter.

Author proposes novel task scheduling algorithm to reduce electricity consumption. More precisely, the lazy control policy that tries to run the blowers no later than necessary. The task is to control the activation of the blowers in such a way as to optimize the operating point of the device. Thanks to this solution, electricity consumption is reduced.

Second, the author makes an attempt to implement an optimal control task based on mathematical programming. The presented optimization covers boundary conditions were selected on the basis of the author's knowledge, literature sources and previous simulations. The work includes a series of simulations for the determined influent parameters and internal work settings of the sewage treatment plant. Due to the complexity of the topic solution is a form of grid search optimization, in other words, the brute force approach. The obtained results were compared in terms of electric energy consumption. Results are treated as a suboptimal solutions due to this method of determining the minimum.

The author did not include blockchain algorithms in his doctoral dissertation. In the author's opinion, these algorithms have great potential for implementation in the power industry. However, not in industrial wastewater treatment plants.

3 Numerical representation of wastewater treatment process

3.1 Wastewater treatment process – general description

Wastewater Treatment Plant (WWTP) –a set of technological facilities as well as associated operations for removing contaminants contained in wastewater. The wastewater treatment plant also includes the treatment and disposal of sewage sludge (or other solid contaminants) arising during wastewater treatment. Fig. 8 presents two stages of classic wastewater treatment process – a mechanical and biological one.

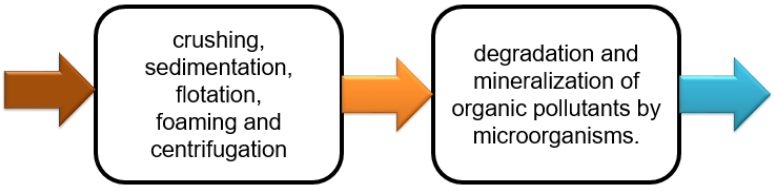

Fig. 8. Division into two basic processes during wastewater treatment

Mechanical wastewater treatment - physical and mechanical processes that result in decanted sewage and sludge. Mechanical treatment involves removing mechanical impurities from sewage, i.e. solids and suspended solids, crushing, sedimentation, flotation, foaming, and centrifugation. These processes take place employing separating grids, screens, grease separators, sand traps, settling tanks and filters.

Biological treatment of wastewater – processes with the use of aerobic and anaerobic microorganisms, as a result of which purified wastewater is generated, separated from the sludge and sludge containing biomass including pollutants. Such processes use aerobic and anaerobic microorganisms, as a result of which purified sewage is generated and sludge containing biomass including pollutants. Biological treatment processes may be used without or combined with mechanical treatment and with an increased degree of purification. The scheme of biological treatment is marked below. Recently, two types of bioreactors in WWTPs are installed [60], [61]:conventional activated sludge process bioreactors (AST) and membrane bioreactors (MBR) (Fig. 9).

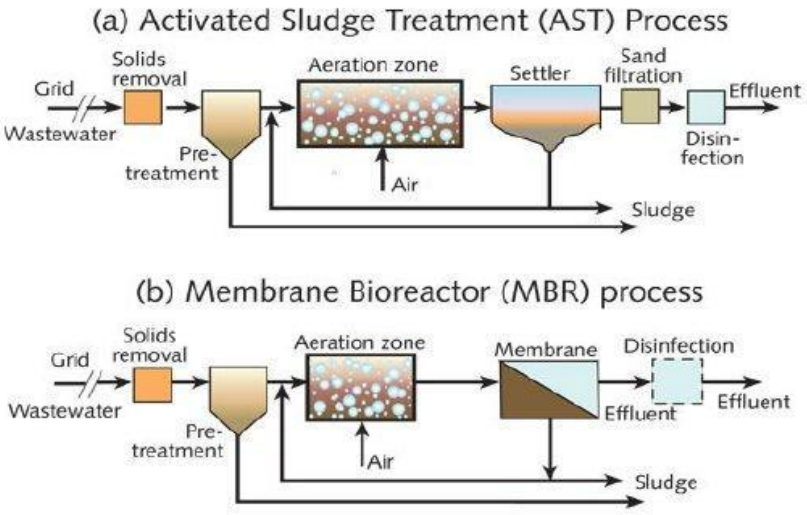

Fig. 9. Comparison of Activated Sludge Treatment system with Membrane Bioreactor (MBR) [60], [61]

Both types of sewage treatment plants are cited in the publications presented in the state of the art. In the implementation part, the author focuses on the treatment plant with activated sludge process bioreactors (Fig. 10).

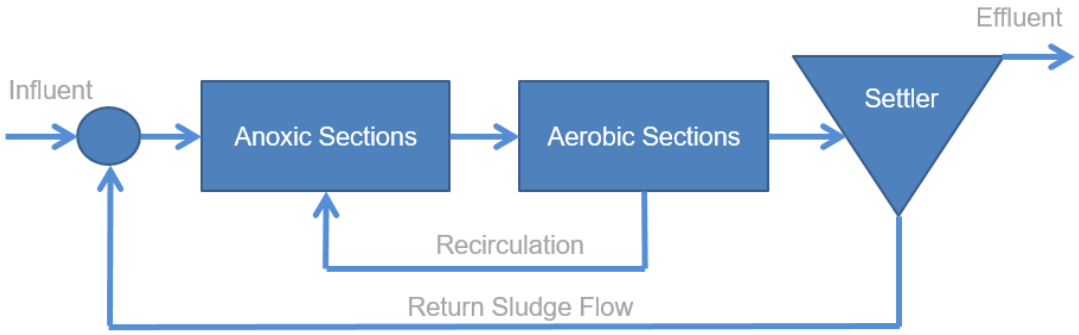

Fig. 10. Schematic of internal and external recirculation [62], [63]

3.2 Key parameters to assess wastewater quality

It is worth mentioning commonly used units describing sewage quality. They will be used in the further paragraphs of the dissertation. The key parameters describing the wastewater used in laboratories and the operation of the treatment plant are:

- Biochemical Oxygen Demand (BOD),
- Chemical Oxygen Demand (COD),
- Total Suspended Solids (TSS),
- Concentration of ammonia,
- Concentration of phosphorous,
- PH level.

Biochemical Oxygen Demand (BOD) is a parameter corresponding consumption of oxygen for oxidation in the aerobic conditions of organic compounds contained in wastewater (or in water) with the participation of microorganisms. The total mineralization of organic compounds contained in water and sewage requires a long time – about 20 days. However, the most intense biodegradation processes take place within the first five days. Therefore, BOD_5 has been adopted as an indicator of the load of water and sewage by organic substances. As the temperature has a great influence on the speed of chemical reactions, the indicator determination at 20°C without light has been accepted. Usually, a five-day BOD equals about 70% of the total BOD.

Chemical Oxygen Demand (COD) is a parameter used similarly to BOD to assess the state of water or sewage, interpreted as the amount of oxygen needed to oxidize organic and inorganic compounds contained. Oxidation is carried out using strong oxidizing compounds such as potassium dichromate ($K_2Cr_2O_7$), potassium periodate (KJO_3) or potassium permanganate ($KMnO_4$).

BOD is part of the COD, i.e. the COD value is always greater than the BOD value. Their proportion is an important indicator of the biodegradability of sewage. For example, hypothetically, if all substances would decompose naturally, i.e. $BOD/COD=1$, we are dealing with perfectly biodegradable sewage. To examine the COD and BOD values, long-term and costly analysis of sewage samples (including much more indicators than BOD and COD) is carried out [64], [65].

Total Suspended Solids (TSS) is the dry-weight of suspended particles which are not dissolved. TSS corresponds to mass concentration assessed by filtration using dedicated filters.

Ammonia and phosphorous are biogenic particles that are needed for the development of living organisms. Their presence in nature increases the fertility of rivers and lakes, causing eutrophication. It results in the massive growth of algae which, dying, cause secondary water pollution. Therefore, these elements are also studied in the purification process.

Total Kjeldahl Nitrogen (TKN) gives the results of the total organic nitrogen plus ammonia. TKN is usually requested to gain knowledge as to the total nitrogen content of the sample. Total Nitrogen is the parameter that additionally takes into consideration nitrate and nitrite. Kjeldahl analysis is the tool for the determination of ammonium and amine nitrogen.

Total Nitrogen is the sum of nitrate-nitrogen and nitrite-nitrogen, ammonia-nitrogen and organically bonded nitrogen. Generally speaking, total Nitrogen concentration(N_{TOT}) is the sum of nitrogen compoundslike: Total Kjeldahl Nitrogen (TKN); nitrate-nitrogen andnitrite-nitrogen.

In the dissertation, the author uses unit mg/l as a measure of the wastewater quality of these parameters. The literature also refers to the possibility of using the same g/m^3 units to express pollutants content in wastewater [66].

In the book [63], authors present an example characteristics of parameter values in urban wastewater for selected cities in the country. The summarized values are presented in Tab. 1.

Tab. 1. Example characteristics of parameter values in urban wastewater [63]

Parameter	Unit	ŁÓDŹ	STRYKÓW	GŁÓWNO	NAMYSŁOW
PH	-	7.4 – 7.9	7.2 – 7.5	7.2 – 7.4	7.2
BOD5	(mg/l)	140	300	290	600
COD	(mg/l)	140	300	290	600
COD/BOD	-	2.7	1.8	1.5	2.0
TSS	(mg/l)	150	250	330	500
AMMONIA	(mg N/l)	32.2	65.7	55.2	30
PHOSPHOROUS	(mg P/l)	8.3	30.2	20.1	10

3.3 BSM1 model based on ASM1

3.3.1 ASM1 as a numeric tool for modeling water treatment

The Activated Sludge Models (ASM) are sued in biological processes occurring in treatment by the formulation of mathematical equations. The basic model, named ASM1, was published in 1987 and was later extended with new functionalities [67], [68]. The primary sewage characteristics such as the content of inorganic and organic matter and alkalinity are simulated. The effluent is characterized by state variables which represent concentrations of components in the wastewater, and dynamics observed during water cleaning is described by state equations. In particular, ASM1 includes 13 state variables[69], [70].

One group of variables are biodegradable components of the Chemical Oxygen Demand (*COD*). These are: Readily biodegradable substrate S_S; Slowly biodegradable substrate X_S; Active heterotrophic biomass $X_{B,H}$; Active autotrophic biomass $X_{B,A}$. Non-biodegradable material characterized by variables unaffected by biological action in the system: S_I and X_I; Variable X_P models inert particulate matter arising from biomass decay. These components are summarized in Tab.2.

Tab. 2. Wastewater characterization for carbonaceous components [67]

COD	Biodegradable COD	Soluble - S_S
		Particulate - X_S
	Non-Biodegradable COD	Soluble - S_I
		Particulate - X_I and X_P
	Active mass COD	Heterotrophs - $X_{B,H}$
		Autotrophs - $X_{B,A}$

Remaining state variables are the concentration of dissolved oxygen S_O, the alkalinity level S_{ALK}, and 4 components of the Total Kjeldahl Nitrogen (*TKN*). The latter are: Nitrate and nitrite nitrogen S_{NO}; Biodegradable organic nitrogen X_{ND}; Soluble biodegradable organic nitrogen S_{ND}; Volumetric concentration of free and saline ammonia in dilution S_{NH}. The whole set of *TKN* components is shown in Tab. 3.

Tab. 3. Wastewater characterization for nitrogenous components [67]

<table>
<tr><td rowspan="5">TKN</td><td colspan="3">Free & Saline ammonia - S_{NH}</td></tr>
<tr><td rowspan="3">Organically bound N</td><td rowspan="2">Soluble Organic N</td><td>Nonbiodeg. NS_{NI}</td></tr>
<tr><td rowspan="2">Biodeg. NS_{ND} and X_{ND}</td></tr>
<tr><td rowspan="2">Particulate organic N</td></tr>
<tr><td>Nonbiodeg NX_{NI} and X_{NP}</td></tr>
<tr><td colspan="3">Active mass N - X_{NB}</td></tr>
<tr><td colspan="4">Nitrate and Nitrite N - S_{NO}</td></tr>
</table>

The treatment process itself is described by 8 processes reflecting natural transformations observed during sewage treatment. Tab. 4 presents all processes included in ASM1 model. State characteristics and processes are reciprocally correlated.

Tab. 4. Processes in ASM numeric models[67]

No	Process
1	Aerobic growth of heterotrophs
2	Anoxic growth of heterotrophs
3	Aerobic growth of autotrophs
4	Decay of heterotrophs
5	Decay of autotrophs
6	Ammonification of soluble organic nitrogen
7	Hydrolysis of entrapped organics
8	Hydrolysis of entrapped organic nitrogen

The processes are related to the model coefficients through a set of 5 stoichiometric and 14 kinetic parameters [68]. Stoichiometric parameters describe the relationship between the components, while kinetic – rate-concentration dependence in the process. The relations are gathered in Petersen matrix for wastewater treatment (Tab. 5).

Tab. 5. Petersen matrix for wastewater treatment (original, obtained from [68])

Component → i / j ↓ Process	1 S_I	2 S_S	3 X_I	4 X_S	5 $X_{B,H}$	6 $X_{B,A}$	7 X_P	8 S_O	9 S_{NO}	10 S_{NH}	11 S_{ND}	12 X_{ND}	13 S_{ALK}	Process Rate, ρ_j $[ML^{-3}T^{-1}]$
1 Aerobic growth of heterotrophs		$-\frac{1}{Y_H}$			1			$-\frac{1-Y_H}{Y_H}$		$-i_{XB}$			$-\frac{i_{XB}}{14}$	$\hat{\mu}_H\left(\frac{S_S}{K_S+S_S}\right)\left(\frac{S_O}{K_{O,H}+S_O}\right)X_{B,H}$
2 Anoxic growth of heterotrophs		$-\frac{1}{Y_H}$			1				$-\frac{1-Y_H}{2.86\,Y_H}$	$-i_{XB}$			$\frac{1-Y_H}{14\cdot 2.86\,Y_H}-\frac{i_{XB}}{14}$	$\hat{\mu}_H\left(\frac{S_S}{K_S+S_S}\right)\left(\frac{K_{O,H}}{K_{O,H}+S_O}\right)\times\left(\frac{S_{NO}}{K_{NO}+S_{NO}}\right)\eta_g X_{B,H}$
3 Aerobic growth of autotrophs						1		$-\frac{4.57-Y_A}{Y_A}$	$\frac{1}{Y_A}$	$-i_{XB}-\frac{1}{Y_A}$			$\frac{i_{XB}}{14}-\frac{1}{7Y_A}$	$\hat{\mu}_A\left(\frac{S_{NH}}{K_{NH}+S_{NH}}\right)\left(\frac{S_O}{K_{O,A}+S_O}\right)X_{B,A}$
4 'Decay' of heterotrophs				$1-f_P$	−1		f_P					$i_{XB}-f_P i_{XP}$		$b_H X_{B,H}$
5 'Decay' of autotrophs				$1-f_P$		−1	f_P					$i_{XB}-f_P i_{XP}$		$b_A X_{B,A}$
6 Ammonification of soluble organic nitrogen										1	−1		$\frac{1}{14}$	$k_a S_{ND} X_{B,H}$
7 'Hydrolysis' of entrapped organics		1		−1										$k_h\frac{X_S/X_{B,H}}{K_X+(X_S/X_{B,H})}\left[\left(\frac{S_O}{K_{O,H}+S_O}\right)+\eta_h\left(\frac{K_{O,H}}{K_{O,H}+S_O}\right)\left(\frac{S_{NO}}{K_{NO}+S_{NO}}\right)\right]X_{B,H}$
8 'Hydrolysis' of entrapped organic nitrogen											1	−1		$\rho_7(X_{ND}/X_S)$
Observed Conversion Rates $[ML^{-3}T^{-1}]$	$r_i=\sum_j \nu_{ij}\rho_j$													
Stoichiometric Parameters: Heterotrophic yield: Y_H Autotrophic yield: Y_A Fraction of biomass yielding particulate products: f_P Mass N/Mass COD in biomass: i_{XB} Mass N/Mass COD in products from biomass: i_{XP}	Soluble inert organic matter $[M(COD)L^{-3}]$	Readily biodegradable substrate $[M(COD)L^{-3}]$	Particulate inert organic matter $[M(COD)L^{-3}]$	Slowly biodegradable substrate $[M(COD)L^{-3}]$	Active heterotrophic biomass $[M(COD)L^{-3}]$	Active autotrophic biomass $[M(COD)L^{-3}]$	Particulate products arising from biomass decay $[M(COD)L^{-3}]$	Oxygen (negative COD) $[M(-COD)L^{-3}]$	Nitrate and nitrite nitrogen $[M(N)L^{-3}]$	$NH_4^+ + NH_3$ nitrogen $[M(N)L^{-3}]$	Soluble biodegradable organic nitrogen $[M(N)L^{-3}]$	Particulate biodegradable organic nitrogen $[M(N)L^{-3}]$	Alkalinity – Molar units	Kinetic Parameters: Heterotrophic growth and decay: $\hat{\mu}_H$, K_S, $K_{O,H}$, K_{NO}, b_H Autotrophic growth and decay: $\hat{\mu}_A$, K_{NH}, $K_{O,A}$, b_A Correction factor for anoxic growth of heterotrophs: η_g Ammonification: k_a Hydrolysis: k_h, K_X Correction factor for anoxic hydrolysis: η_h

All bio-processes considered in ASM1 model are presented in the general overview presented below (Fig. 11).

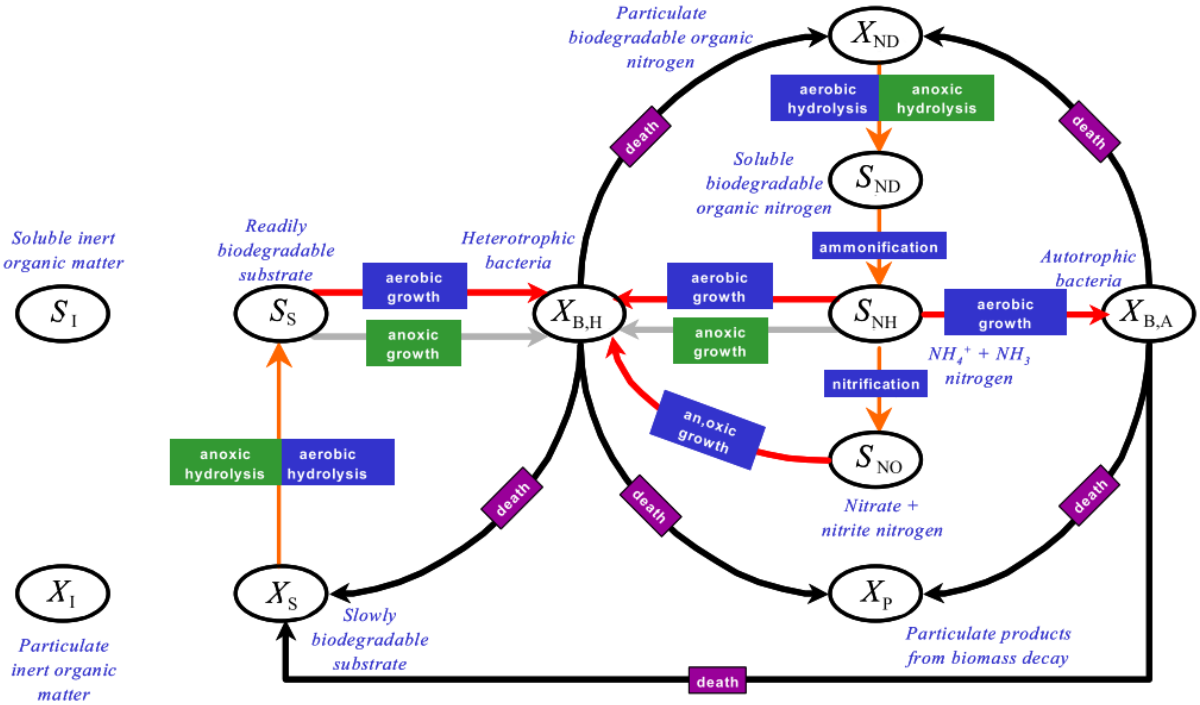

Fig. 11. General overview of ASM1 [71]

The documentation of BSM1 model [57] limits effluent quality, as presented below (Tab. 6).

Tab. 6. Wastewater characterization for nitrogenous components [67]

	Variable	Value
Total nitrogen	N_{TOT}	< 18 g N m^{-3}
Chemical oxygen demand	COD_{TOT}	< 100 g COD m^{-3}
Effluent ammonia	S_{NH}	< 4 g N m^{-3}
Total suspended solids	TSS	< 30 g SS m^{-3}
Biochemical oxygen demand	BOD_5	< 10 g BOD m^{-3}

Documentation of BSM1 model [67] proposes the following methods of calculating the following parameters. These formulas are used in research under the patronage of the institutions of the European Union [72]and in applications such as MASSFLOW [73].

$$COD_{TOTAL} = X_I + S_I + S_S + X_S + X_{BH} + X_{BA} + X_P \quad (4)$$

$$TKN = S_{NH} + S_{ND} + X_{ND} + i_{XB}(X_{BH} + X_{BA}) + i_{XP}(X_{NI} + X_{NP}) \quad (5)$$

$$N_{TOT} = S_{NO} + TKN \quad (6)$$

Assessed values of parameters are according to library: i_{XB} = 0.08; i_{XP} = 0.06; f_P = 0.08.

ASM1 model presented above has been developed to more extended versions. Activated Sludge Model no. 2 (ASM2) include nitrogen removal and biological phosphorus removal. In ASM2d denitrifying PAOs are added. In 1998 ASM3 was published – included internal storage compounds that have an important role in the metabolism of the organisms [68]. Anaerobic Digestion Model ADM1 is designed to model the dynamic of anaerobic digestion [74].

3.3.2 Development of the BSM models based on ASM

The ASM1 as a numeric simulation tool is commonly implemented in the Benchmark Simulation Model (BSM). BSM is a numerical framework that describes the entire wastewater treatment process of a WWTP. BSM1 is the first version of BSM model. Further modifications are BSM1_LT, ADM1, and BSM2 [75], [76] and [77].

The first version of numerated BSM1 has been developed by a research team at the University of Lund which has been released as a Matlab/Simulink implementation[78]. That simulation comprises activated sludge reactor divided into aerobic and anoxic sections. Secondary settlers follow the reactor. An independent version of such a model has been developed.BSM1_LT model is used in long term simulations [79].

BSM2 is a second developed simulation of BSM1 layout. It includes BSM1 for the biological treatment of the wastewater and covers a wider range of wastewater treatment – the sludge treatment. In such a model a primary clarifier, a thickener, an anaerobic digester, a thickener of secondary sludge and a dewatering unit have been added. The view of the entire cleaning process with the BSM1 model range selected is shown in the graphic below (Fig. 12).

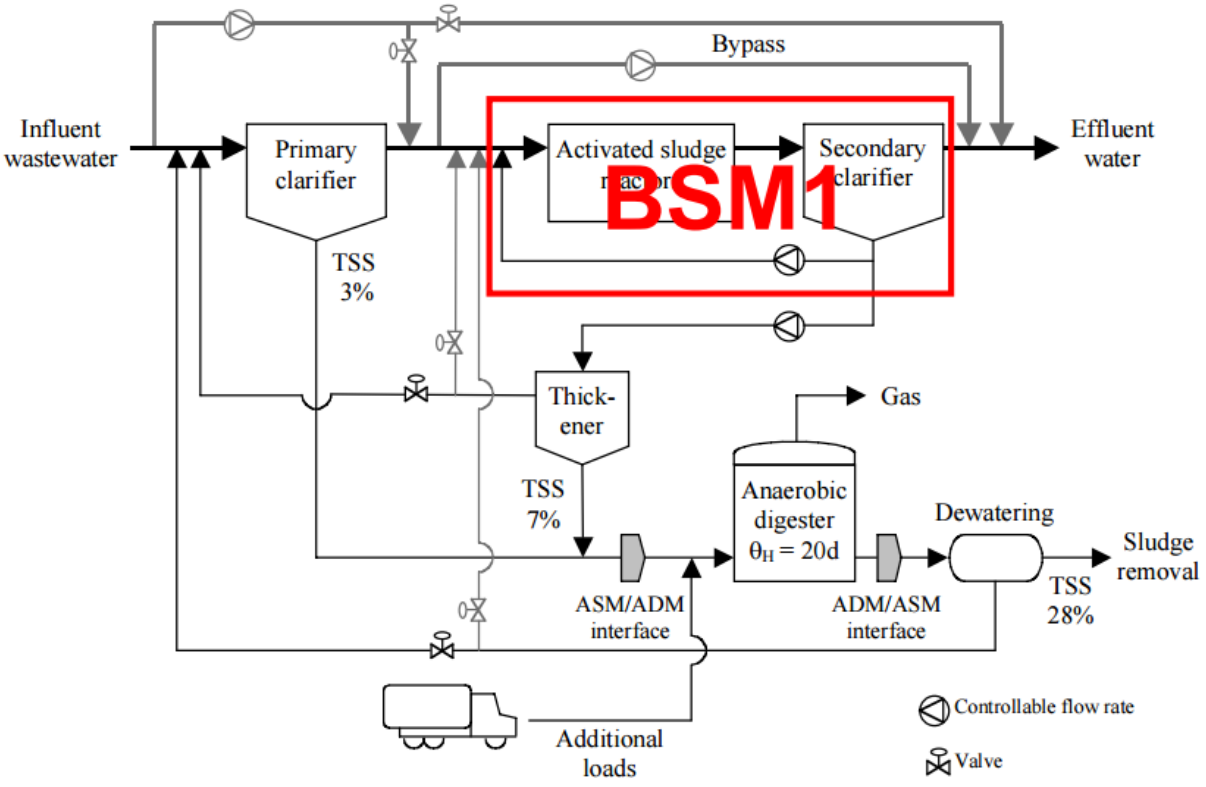

Fig. 12. Range of BSM2 model [80]

3.3.3 Demonstration of BSM1 model

The documentation [71] presents the BSM1 model including the simple reference layout (Fig. 13). The benchmark plant is composed of a sludge reactor consisting five compartments activated with two anoxic tanks followed by three aerobic tanks. In first two (anoxic ones) biological denitrification reactions take place where bacteria change nitrate into nitrogen. In the aerated sections (aerobic) nitrification takes place. It is the reaction in which the bacteria oxidize ammonium to nitrate. The activated sludge reactor is followed by a clarifier (secondary settler) in that water and activated sludge is separated. Water that is the result of treatment is directed outside of the plant. As it contains much less waste than influent to WWTP the environmental impact is reduced to a minimum. To maintain the process activated sludge is recirculated inside the reactor (internal recycle) and from settler to reactor(external recycle), and mixed with influent. The excess waste sludge is removed.

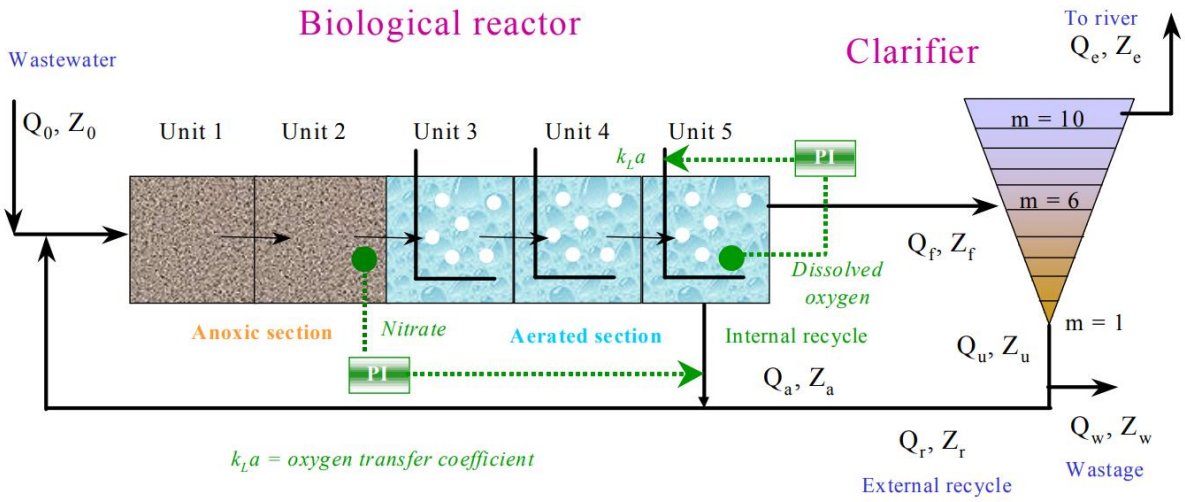

Fig. 13. General overview of the BSM1 water treatment reactor [71]

The demonstration layout model is equipped with oxygen and ammonia sensors that are used in aeration control through a dedicated algorithm. These sensors work on the principle of feedback with the use of PI regulators (as indicated in the diagram). The dynamic behavior of sensors and actuators is considered through additional measurement noise.

A basic control strategy is proposed to test the benchmark: it aims to control the dissolved oxygen level in the final compartment of the reactor by manipulation of the oxygen transfer coefficient and to control the nitrate level in the last anoxic tank by the manipulation of the internal recycle flow rate. It is crucial to mention that the KLa (oxygen transfer coefficient) is calculated on the basis of the process and used to simulate the aeration process. This aspect will be discussed in consecutive paragraphs.

BSM1 is imaged in a numeric block diagram implemented in the Matlab/Simulink environment (Fig. 14). The files can be downloaded from the website[2]. The base schematic of BSM1 model is available in MATLAB Simulink, thus the author uses this application in this dissertation. Model designs the activated sludge WWTP that operates for an average influent dry-weather flow rate of 18.446 m^3/day and an average biodegradable COD in the influent of 300 g/m^3.

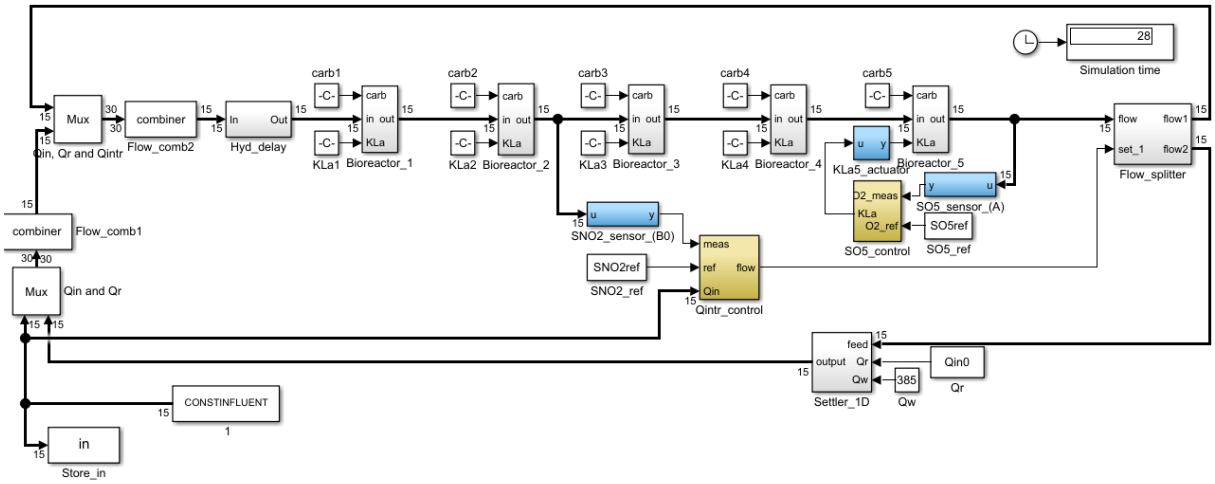

Fig. 14. The model of reference reactor in BSM1 model

A list of state variables used in BSM1, with their definition, appropriate notation and initial values of influent are presented in Tab.7.

Tab. 7. List of ASM1 variables[71]

No	Parameter	Abbreviation	Constant influent value set in BSM1
1	Soluble inert organic matter	S_I	30
2	Soluble inert organic matter	S_S	69.5
3	Particulate inert organic matter	X_I	51.2
4	Slowly biodegradable substrate	X_S	202.32
5	Active heterotrophic biomass	X_{BH}	28.17
6	Active autotrophic biomass	X_{BA}	0
7	Particulate products arising from biomass decay	X_P	0
8	Oxygen	S_O	0
9	Nitrate and nitrite nitrogen	S_{NO}	0
10	NH_4^++NH_3 nitrogen	S_{NH}	31.56
11	Soluble biodegradable organic nitrogen	S_{ND}	6.95
12	Particulate biodegradable organic nitrogen	X_{ND}	10.59
13	Alkalinity	S_{ALK}	7
14	Total Suspended Solids	T_{SS}	211.2675
15	Flow rate	Q	18 446

[2]Downloaded from http://www.iea.lth.se after contact with Ulf Jeppson (ulf.jeppsson@iea.lth.se)

In publication[81], Ulf Jeppson, who is the co-author of BSM algorithms, describes modifications in basic concepts implemented in BSM1, BSM1_LT, andBSM2.

Along with the original model of the sewage treatment plant, exemplary seven-day runs describing the parameters of flowing sewage have been provided [3].

We can mention among them the following flowing sewage routes:

- CONSTANTINFLUENT –corresponds to a non-physical situation where the parameters of the wastewater do not change (assumption of fixed values are as in Tab. 7) (Fig. 15),
- DRYINFLUENT –daily fluctuations resulting from the time of day (Fig. 16),
- STORMINFLUENT – daily fluctuations resulting from the time of day with a single-stream inflow caused by a storm (Fig. 17),
- WETINFLUENT –daily fluctuations resulting from the time of day with a two day period corresponding to the rainy weather (Fig. 18).

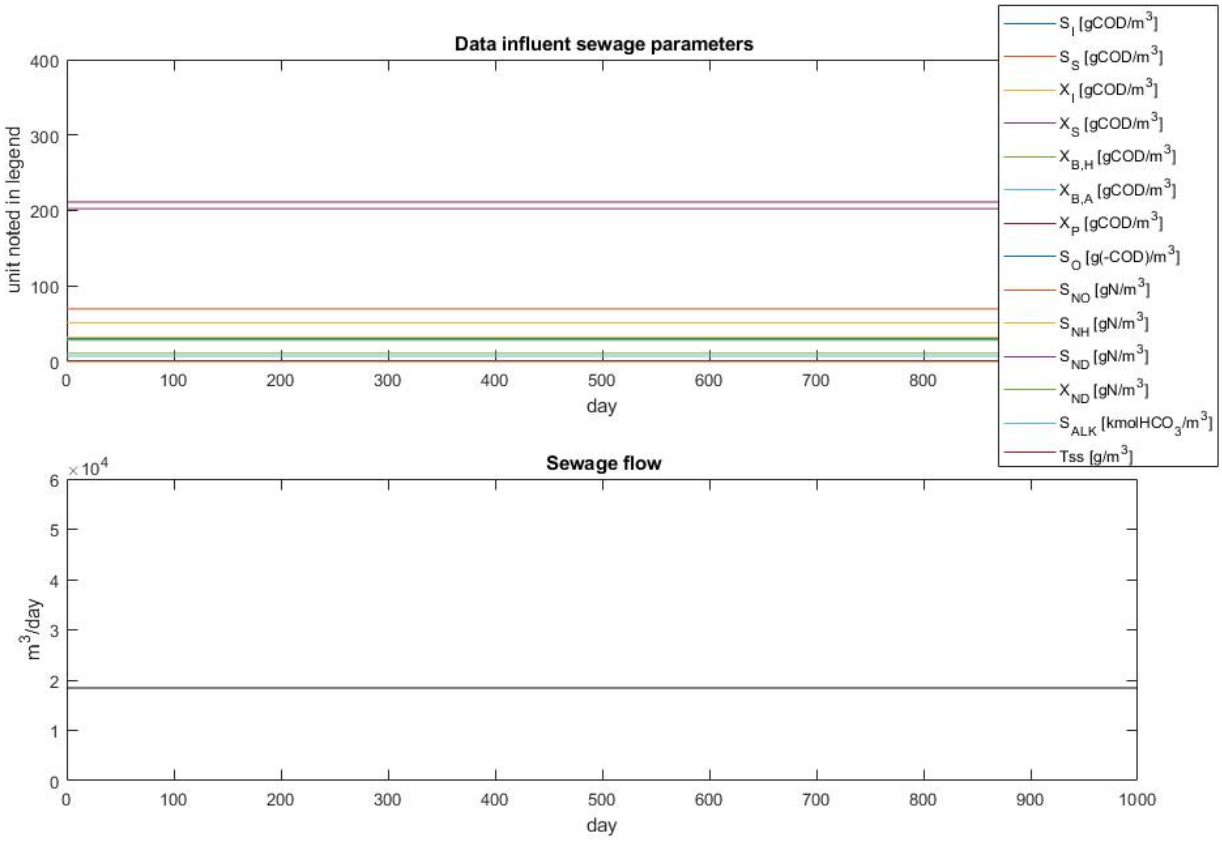

Fig. 15. Graph showing the values of wastewater parameters in the BSM1 model

[3] Downloaded from http://iwa-mia.org/benchmarking/#BSM1

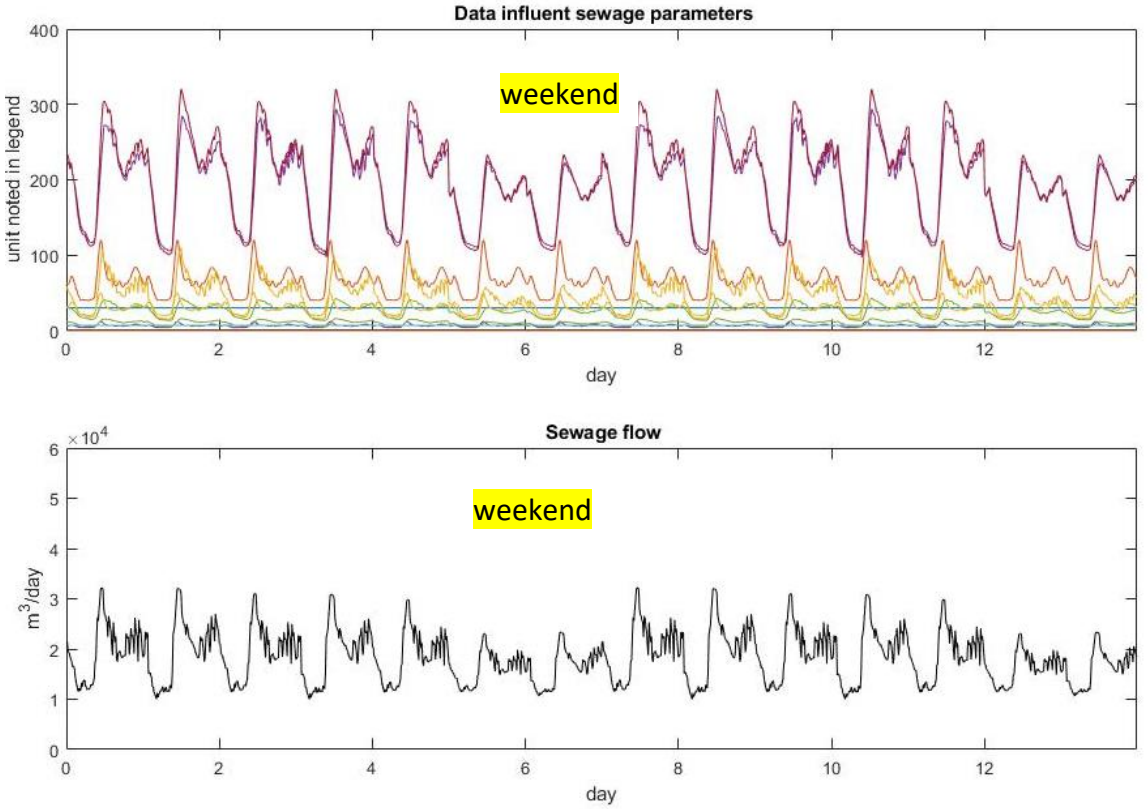

Fig. 16. Graph showing the values of wastewater parameters affected by the dry weather in the BSM1 model

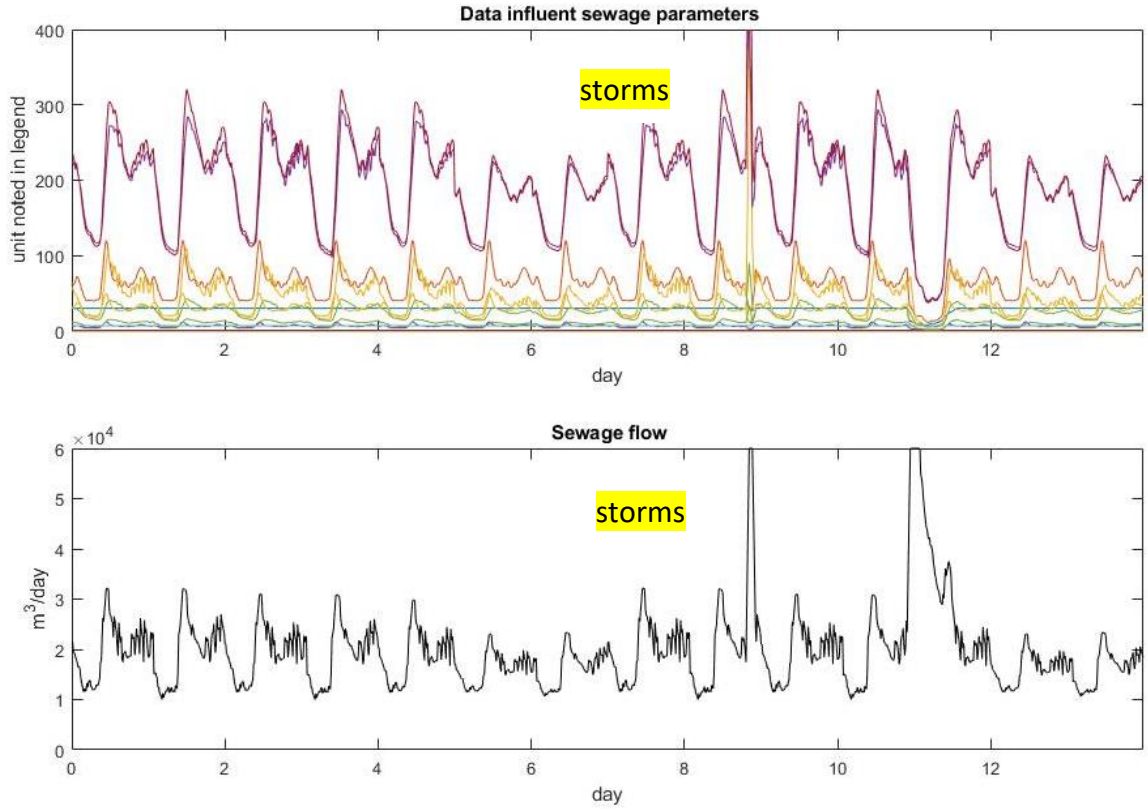

Fig. 17. Graph showing the values of wastewater parameters affected by the stormy weather in the BSM1 model

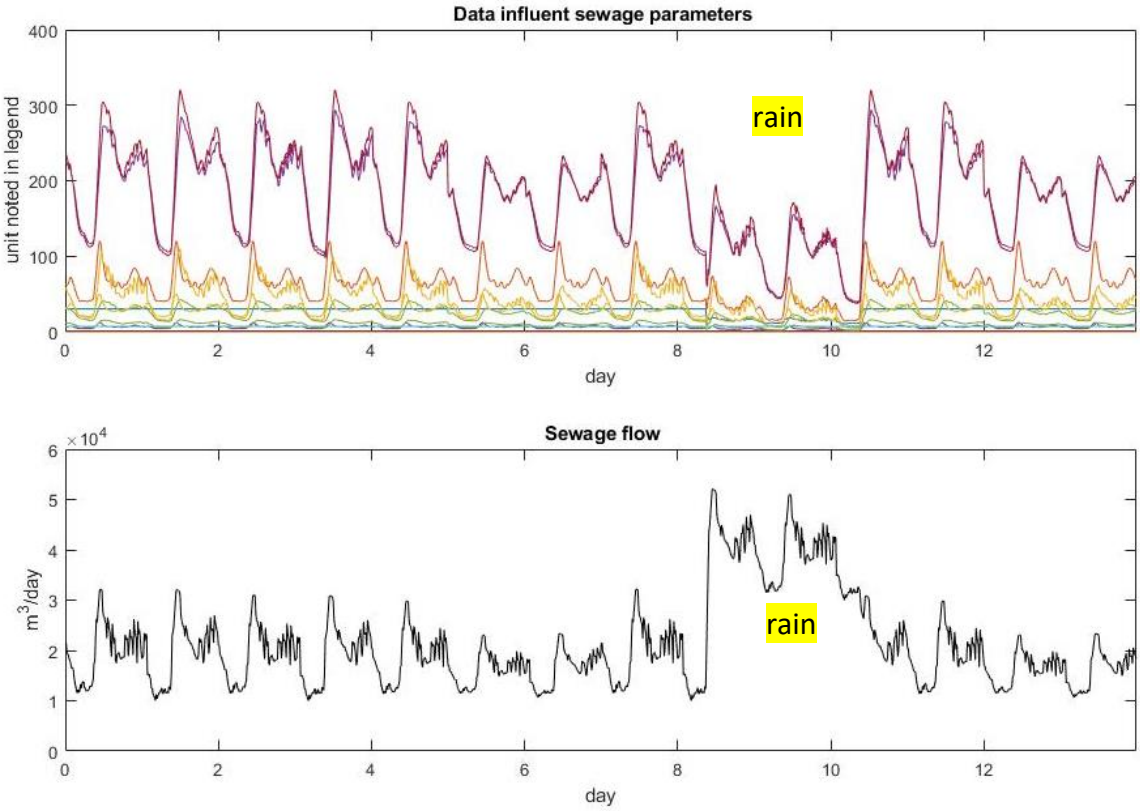

Fig. 18. Graph showing the values of wastewater parameters affected by the dry weather in the BSM1 model

3.3.4 Blowers control to maintain the treatment process

The issue of oxygenation directly arises from the operation of the reactor. Aeration control sustains treatment processes to achieve expected effluent quality regardless of the influent parameters (Fig. 19). It is worth emphasizing that aeration systems usually generate up to 60% of the costs of the total electric energy consumption during wastewater treatment [10]. Due to the significant consumption, reactors' aeration is a crucial part of WWTPs' operating control.

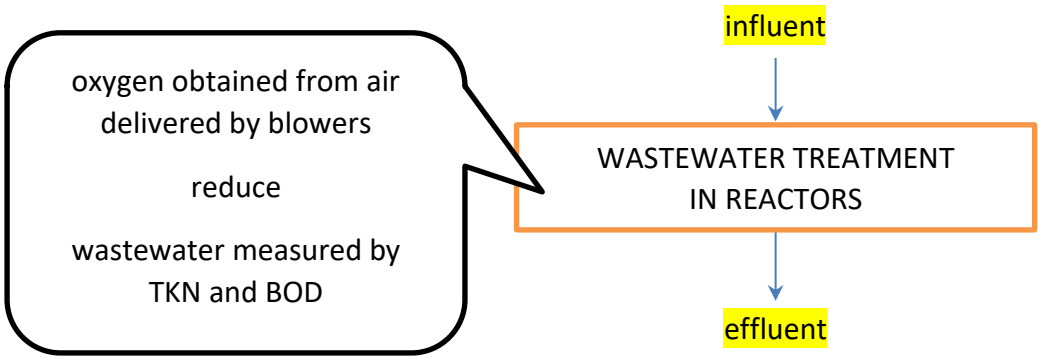

Fig. 19. Step by step schematic of the simulation presented in the dissertation

In previous paragraphs, the BSM1 numeric model of reactors is presented. It implements ASM equations in its operation. The main process objective is to reduce wastewater measured by TKN and BOD oxygen with the use of air delivered by blowers. The plant control system is critical to achieving the most efficient sequencing of the aeration blowers. The literature [82]proposes a variety of blower control techniques:

- running the smallest number of machines (blower that does not rotate and consumes no energy),
- running the largest number of machines in your most efficient range,
- avoiding idling and deflating,
- determining the sequence of operations with regard to service life and maintenance intervals.

The following types of blowers are presented [82]:

- rotary lobe blower,
- centrifugal or turbo blower,
- rotary screw compressor.

3.3.5 Oxygenation transfer implemented originally in BSM1

Numeric solutions implemented in the original BSM1 model base on the concept of KLa parameter as the transfer coefficient [78]. A simple reference layout contains the algorithm that is implemented in BSM1. The equation takes into consideration a reactor containing 5 aerated sections.

The activated sludge process consists of aerated zones. The dissolved oxygen (DO) mass balance [71]:

$$\frac{dy(t)}{dt} = \frac{Q(t)}{V}(y_{in}(t) - q(t)) + KLa\big(u(t)\big)(c^{sat} - c) - R(t) \tag{7}$$

Where:

$y(t)$ – dissolved oxygen in the zone

KLa – volumetric mass transfer coefficient

c^{sat} – dissolved oxygen saturation coefficient

c – dissolved oxygen concentration

In each section of the reactor, the oxygen concentration (C) depends on the value of the previous time step and fresh inflow by the following formula [57]:

$$\frac{dC}{dt} = (K_L a) \cdot (c^{sat} - c) \tag{8}$$

Maximal value of KLa is 240. In controlled sections, the KLa parameter ranges from 0 to this value. According to the document, to calculate the air costs aeration system must take into consideration plant peculiarities (a type of diffusers, bubble size, depth, etc.).

Aeration energy is presented in the equation below. AE is proportional to time integral of the particular volume of section and the value of the KLa coefficient designated for the section. Unfortunately, it applies only to the Degremont DP230 porous disc diffusers at an immersion depth of 4m.

$$AE = \frac{S_0^{sat}}{T \cdot 1.8 \cdot 1000} \int_{7days}^{14days} \sum_{i=1}^{5} V_i \cdot K_L a_i(t) dt \tag{9}$$

As it is presented above, BSM1 is used for simulation biological treatment. Described aeration system is limited to diffusors described in the documentation. The question how aeration in WWTPs in general operates remains unanswered.

3.4 Airflow modeling in reactors

3.4.1 Theoretical introduction to problem of oxygen transfer into wastewater

This paragraph presents the typical parameters used to describe the oxidation aspect of wastewater. The values can be extracted during the simulation to parameterize the aeration process and then, be used during the energy optimization of the model[83], [84], [85], [86].

The parameters are presented in two versions – both in undefined and standard conditions. Since 1982 standard conditions define temperature 20°C (68°F) and pressure 100 kPa (1 bar) [87], [88].Standard conditions for temperature and pressure are standard sets of conditions for experimental measurements to be established to allow comparisons to be made between different sets of data.

Oxygen Mass Transfer Coefficient (KLa), used in wastewater treatment, presents to rate with oxygen that is transferred to the activated sludge by the aerating system. KLa is a non-linear function of the airflow rate. In BSM1, the KLa allows the description of mass transfer between gas and liquid in two-phase systems and informs about the degree of mass transfer at the interface between the solid and gaseous phase for a unit of volume and allows to assess how efficiently this process is carried out.

Oxygen Transfer Rate (OTR), Standard Oxygen Transfer Rate ($SOTR$). OTR is the oxygen transfer rate in clean water in non-standard conditions. The OTR is the actual mass of oxygen transferred per time unit and is the key process variable for design WWTPs. Standard oxygen transfer rate $SOTR$ (kg/d) presents OTR in standard conditions – clean water.

Oxygen Transfer Efficiency (OTE), Standard Oxygen Transfer Efficiency ($SOTE$). Oxygen transfer efficiency presents how much of the injected oxygen becomes dissolved in water. The parameter has expressed a percentage of the oxygen mass flow pushed through blowers. The value strongly depends on the depth and type of diffusers. The default value of Standard Oxygen Transfer Efficiency 0.3 (as a fraction) represents typical estimate of the efficiency for fine bubble diffusers.

Aeration Efficiency (AE), Standard Aeration Efficiency (SAE). As noted earlier, aeration is an electricity consuming process, thus usually 60% or more of the total energy cost is spent on blowers. The most important efficiency parameter is Aeration Efficiency (AE) – the mass of oxygen transferred per unit of power input. The value is equal to the oxygen transfer rate (OTR) divided by the power input (P). SAE (kgO2/kWh) is an oxygen transfer per power input utilized in the blower.

The foundation of airflow in wastewater is the Whitman two-film theory. To imply the two-film theory to WWTP, it is assumed that the main mass transfer resistance is in the liquid film in the bubbles. The phenomenon is described in the following equation that is based on the Whitman two-film theory. The theory assumes that the concentration gradients in the gas and particle phases are confined in the "films" adjacent to the interface. The mass-transfer coefficients depends on the gas- and particle-side film thicknesses (δ_g and δ_p) (Fig. 20). The overall gas-side mass-transfer coefficient K_L is characteristic of the process environment [89].

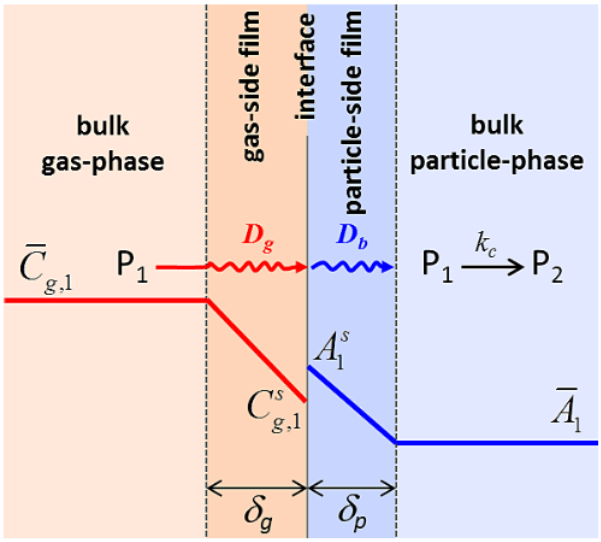

Fig. 20. The graphic representation of two-layer theory [89]

The process of oxygen permeation on the phase borders is described by Whitman's two-film theory [73].

$$\frac{dW}{dt} = K_L \cdot A_t(c^{sat} - c) \tag{10}$$

Where:

W – the weight of solute (g),

$\frac{dW}{dt}$ – rate of oxygen absorption (g/day),

K_L – overall mass transfer coefficient (1/m^3/day),

c^{sat} – dissolved oxygen saturation coefficient,

c – dissolved oxygen concentration,

Ac_t – the total interfacial area,

This parameter K_L takes possible loss into consideration due to clogging, aging and deterioration. And a characterizes liquor transfer characteristics in the phase border[90]. Since it is difficult to measure the K_L and a value separately, they are combined into one parameter. The two coefficients make the KLa strongly dependent on the process conditions.

The *KLa* parameter needs the laboratory tests of oxygen migration through the air-liquid surface. In publication [88], the author proposes a laboratory setup to define the values of this parameter. The publication develops an alternative model which includes more parameters than the standard ASCE method [91]. Fändriks [88] comes up with some alternative methods for evaluation of oxygen transfer performance in clean water. In this publication, five more complex equations are juxtaposed.

3.4.2 Numerical representation of aeration in WWTPs – state of the art

As mentioned in paragraph 3.4, the aeration system includes diffusers that blow the air into the sewage content. The numeric model of oxygen, transfer from the air in the bubbles to sewage is expected. The basic issue in the simulation of WWTP is the connection between bioreactors and blowers (Fig. 21). That issue is touched in several publications.

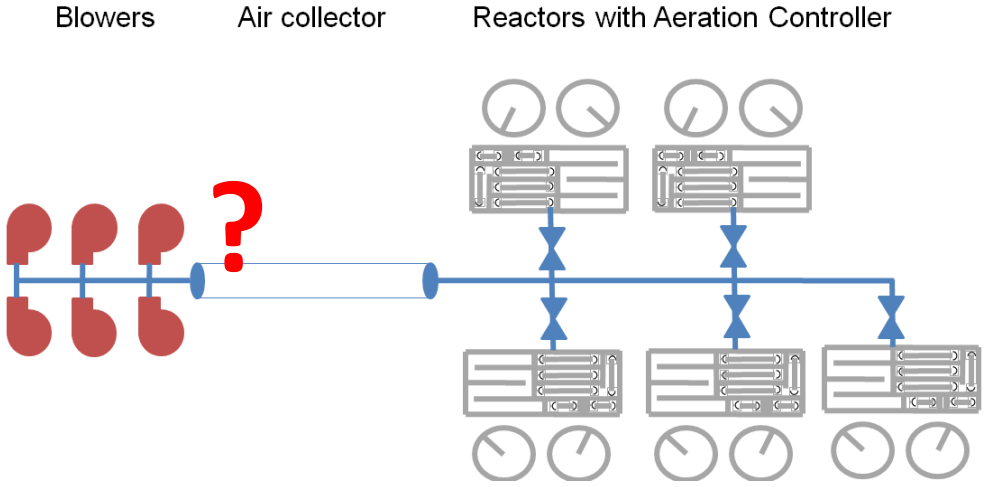

Fig. 21. Schematic of blowing system in Płaszów WWTP

Collector is a pipe connecting blowers with reactors. Authors in [77]–[80] propose the idea to model the collector as an electronic circuit (Fig. 22). Blowers are treated as a flow source, where the relationship between electric energy consumption and flow is determined from the characteristics of the devices. The collector is replaced by a condenser charged by the air stream generated by the blowers and discharged by the reactors. When the collector pipe is treated as a capacitance with negligible flow resistance, simple linear equation is established [77].

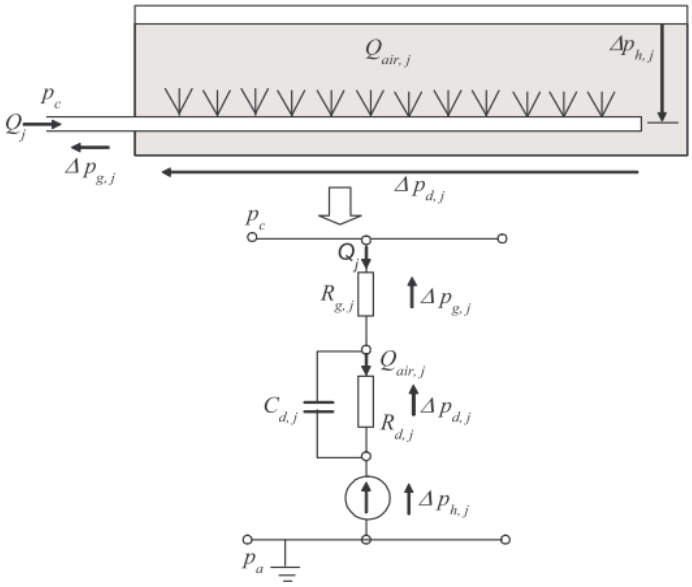

Fig. 22. The electrical analogy to collector pipeline [92]

The model can be expressed with the following equation:

$$\frac{dp_c}{dt} = \frac{1}{C_c}(Q_b - Q_c) \tag{11}$$

$$C_c = \frac{V_c}{p_c} \tag{12}$$

Where:

- C_c – collector fluid-flow capacitance,
- Q_c – collector flow,
- V_c – collector volume,
- p_c – collector pressure.

Such an idea is discussed to simulate the dynamics of collectors in the presented model. In [93], authors propose a centralized nonlinear model predictive controller of dissolved oxygen tracking and aeration system control. The research is based on WWTP in Nowy Dwór Gdański. In [94], authors analyze that schematic in WWTP located in Swarzewo, Poland. In [95], the author implements such an idea in Mątowskie Pastwiska WWTP located in Northern Poland.

Different authors around the world have also raised this issue. Casey [96] presents the diffused aerated systems and analyses the equations that can be used in the modeling of oxygen diffusion. The document [97] presents the theory of diffusion used in the construction of diffusers that are produced by OTT. In publication [98], the direct relation KLa-airflow is presented, as shown in the following figure below(Fig. 23).

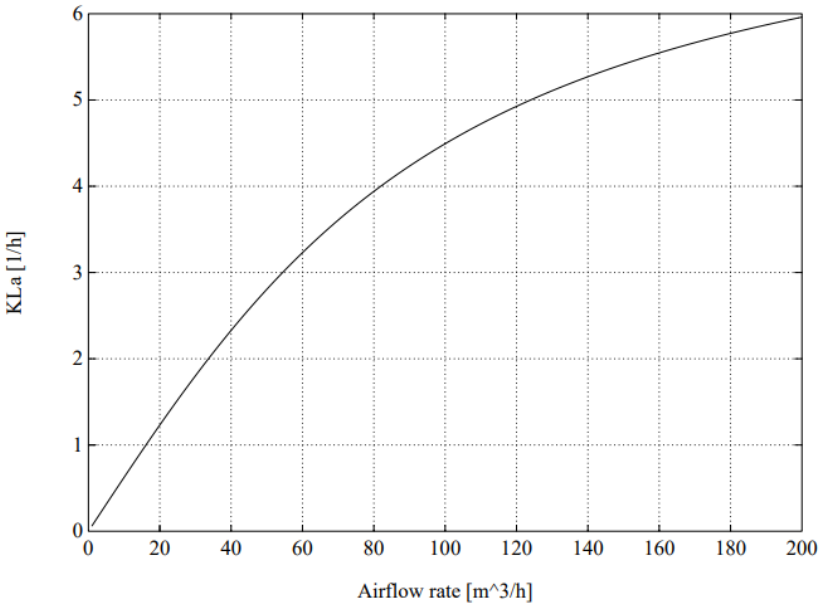

Fig. 23. The plot describing KLa-airflow relation [98]

In the thesis [61], the author models an aeration system that includes air distribution. The equation is presented below (Fig. 24). In [99], Arnell presents case studies of three full-scale WWTPs.The authors propose this equation relaying the relation between KLa and airflow.

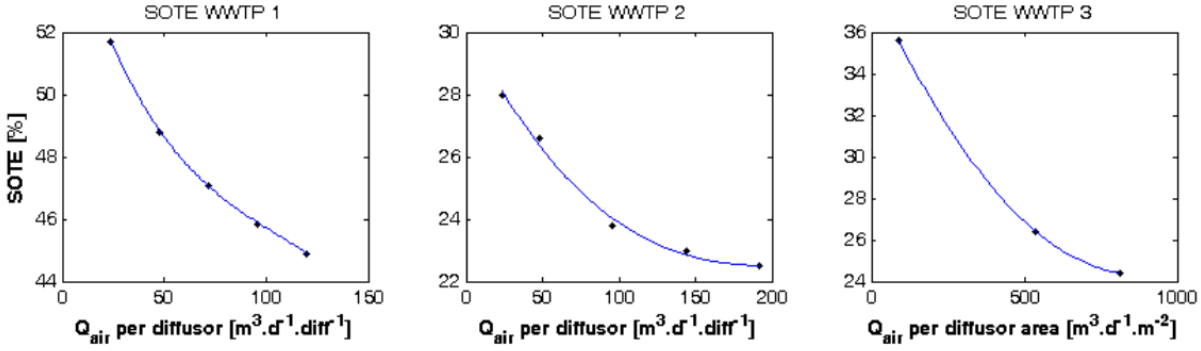

Fig. 24. The SOTE plots at actual submersion depths and diffusor densities presented in three references WWTPs [99]

Authors in [85] review the control of continuous aeration systems in municipal wastewater treatment plants. The review is supplemented with a summary of comparisons between control strategies evaluated in full-scale, pilot-scale and simulations. The figure presented below was published (Fig. 25).

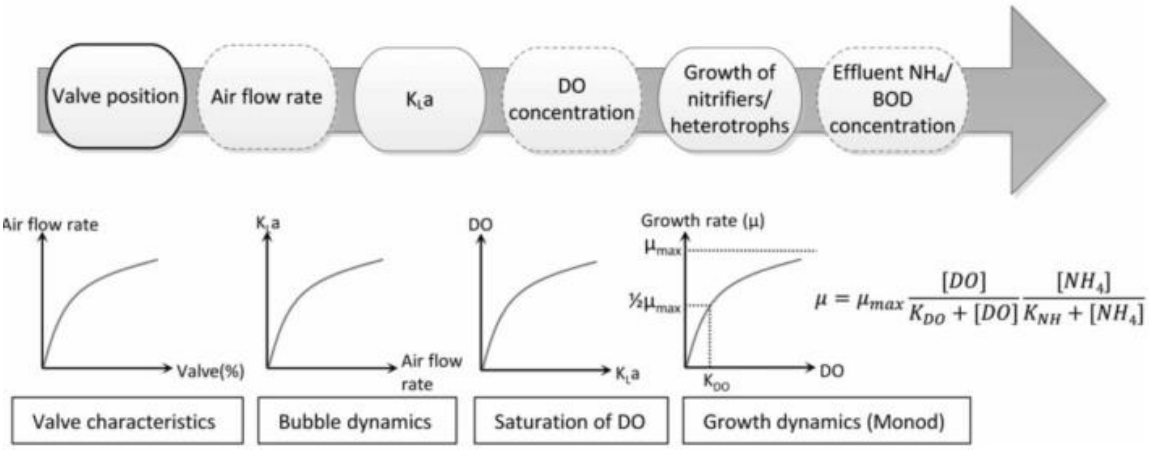

Fig. 25. Stages presenting how oxygenation affects wastewater treatment in reactors[99]

In [100], the aeration cost has been calculated based on the Oxygen Uptake Rate (OUR) model. Mathematic models are applied to simulate the transient OUR and show the impact of varying load on OTE and aeration cost.

Finally, Zhu [101] evaluates the control strategy of ASM1 model for reduction of electricity consumption.

3.4.3 Determination of airflow used in the dissertation

In Sec. 3.5.1 of dissertation, the authors presented parameters $SOTE$ and $SOTR$ describing the aeration process in wastewater in standard conditions. In engineering, the OTR factor is used to describe the flow of oxygen between the phases [83]. Oxygen Transfer Rate at field conditions is expressed with the following equation.

$$OTR_{TOTAL} = KLa \cdot (c^{sat} - c) \cdot V \tag{13}$$

Where:

OTR – oxygen transfer rate (mmol $l^{-1}h^{-1}$),

$K_L a$ – volumetric mass transfer coefficient ($1/m^3$),

V – volume of wastewater in the reactors' section,

c^{sat} – saturation value of the water or wastewater.

In [86], he presents the estimation of airflow demand based in water using desorption and absorption methods. Standard conditions (20°C and 1 atm) in clean water airflow is calculated utilizing presented equations. The author proposes the equation:

$$SOTE = \frac{SOTR}{W_{O2}} = \frac{SOTR}{0.2765\ Q_S} \tag{14}$$

Where:

$W_{O2}\ (kg/s)$ - the mass flow of oxygen in air stream,

Qs - refers to air flow rate at standard condition.

And after modification, the following relation is achieved:

$$Q_S = \frac{SOTR}{0.2765 \cdot SOTE} \tag{15}$$

According to the documentation of GPS-X [102] and [86], additional correction factors can be used to take into account the special correction factor that takes into consideration empirical research.

$$AIRFLOW = \frac{OTR}{OTE \cdot CF_1} \tag{16}$$

Where:

CF_1 – conversion factor to account for the density, molecular weight and O2 mole fraction of the standard air (U.S. Standard = 277.6533841; European Standard = 300.495893),

OTE – standard oxygen transfer efficiency.

4 The case study of the Płaszów WWTP

4.1 The general description of Płaszów Sewage Treatment Plant

Validation of the numerical model has been carried out with the use of the existing Płaszów Sewage Treatment Plant in Kraków (Fig. 26).

Fig. 26. Płaszów Sewage Treatment Plant in Kraków – reactor and settlers in the first plan

The municipal WWTP in Płaszów is a modern facility that treats sewage from Kraków agglomeration located in the south of Poland (780,000 PE - population equivalent). The facility is located on the area of about 50 hectares. The object is a complex waste treatment system that consists of mechanical and biological cleaning. The object is equipped with a comprehensive control system with appropriate control, measurement and steering equipment. The sewage treatment plant has a capacity of 328,000 m^3/day and average flow is 160,000 m^3/day.

The system responsible for complex wastewater treatment including mechanical and biological processes as well as the utilization and combustion of sludge allows reducing the impact of the treatment plant on the environment [103], [104]. Each of the above systems consists of numerous dispersed receivers, as described below [103], [105].

Mechanical treatment catches large wastewater fractions mechanically and through sedimentation. In Płaszów WWTP, this step includes rare grids, dense grates, latches, 1st, and 2nd-degree pumping stations, sand traps, pre-settling tanks and sand separator.

The biological part of the treatment plant consists of 5 biological reactors supported by 10 secondary clarifiers, a sewage recirculation and a blower station. The system additionally uses PIX station, methanol station, deactivation stations and control automatics[106].

The sedimentary part is responsible for sewage sludge management. Such installation consists of primary sludge thickeners, excess sludge operation tank, sludge thickening, and

dewatering system, sludge pre-pumping station, WKF sludge digestion chamber, sludge intermediate tank, pumping stations and sludge tank, chemical phosphorus removal station from the supernatant, sludge pumping stations after coagulation, biogas tanks, flares, desulphurization of biogas, overlaying water pumping stations, sewage pumping stations, pumping sludge and flotate pumping stations.

The installation of thermal sludge utilization (STUO) in a fluidized bed consists of: storage and transport systems with sludge drying, thermal utilization node, heat recovery system, waste gas treatment system, process, and gas monitoring system waste, control system, solidification node. Such solidified wastes do not harm the natural environment.

According to the report [14]and [1], wastewater treatment plant consumes a significant amount of electricity. The graphic below presents general decomposition of electricity consumption in a sewage treatment plant(Fig. 27).

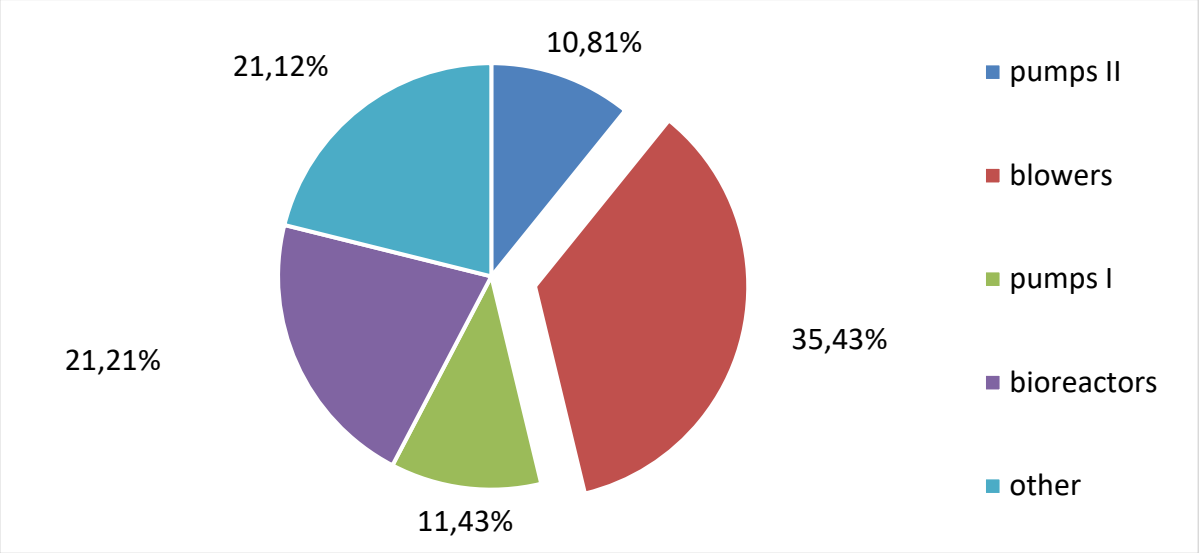

Fig. 27. Electricity consumption in Płaszów WWTP [14] and [1]

As presented in figure, few crucial devices have the biggest impact on the total consumption of electricity. Those receivers are the independent stations that are controlled by independent control procedures. Those appliances are pumps and blowers that maintain the continuity of waste-water treatment. Based on the energetic study, the following groups of receivers have been distinguished:

- pumping station I → 7pumps x 132 kW, 924kW in total),
- pumping station II → 3 pumps x 160 kW (480kW in total),
- blower station → 6 blowers x 400kW (2400kW in total).

4.2 Biological treatment in Płaszów WWTP in details

As mentioned earlier, biological treatment is the basic stage of wastewater treatment. Płaszów WWTP consists of 5 biological reactors (Fig. 28).

Fig. 28. Aerial photography ofthe Płaszów WWTP with reactor[4]

In reactors, sewage continually recirculates in 10 sections both in aerobic and anaerobic environments. Each reactor cooperates with two secondary clarifiers in which activated sludge is collected for further utilization. The flow of wastewater in reactors is fully automated. The pumps enforce an appropriate circulation - both internal and external recirculation. The reactor's layout presented below outlines the bioreactor with particular sections; additionally, the direction of effluent flow has been marked (Fig. 29).

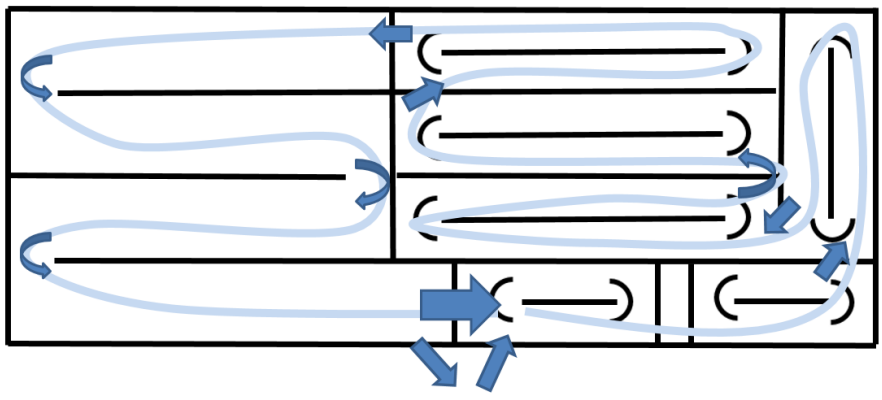

Fig. 29. Layout of the reactor in Płaszów WWTP – internal recirculation

[4] https://wodociagi.Kraków.pl/o-firmie/infrastruktura/zaklad-oczyszczania-sciekow-Płaszów.html

The wastewater flows through several internal sections sequentially as it flows through the reactor (Fig. 29 and Fig. 30). The pre-denitrification KPD chamber is to reduce the nitrates contained in the recirculation. The Redox probe indicatesthe degree of nitrate removal. KDF chamber is responsible for biological dephosphatation in aerobic conditions. Absolute oxygen conditions (presence of dissolved oxygen) and relative aerobic conditions (presence of nitrates) is used for signaling the Redox probe. The sludge concentration probe serves to determine the concentration of activated sludge in the chambers. After exceeding the preset sludge concentration, it switches off one recirculation pump. Denitrification chambers KDN1, KDN2, KDN3 are to reduce the total nitrogen by reducing nitrates. Exceptionally, denitrification chamber KDN3 has two functions. In the summer, it performs the analogous function of the KDN1 and KDN2 chambers, i.e. the removal of nitrates. In winters, KDN3 can act as an aeration chamber. In KDN3 nitrate-nitrogen (N - NO3), a sensor is installed. The nitrification chambers KN1, KN2, KN3 and KN4 are designed to reduce organic carbon, phosphate uptake and oxidation of nitrogen compounds to nitrates. Oxygen probes coupled with a control damper system with electric drives are used to control the appropriate amount of supplied oxygen. Deoxidation chamber KO is to remove dissolved oxygen contained in wastewater fed in the internal circulation stream to the KDN1 denitrification chamber.In the KO chamber, wastewater is divided into two independent streams. Volumes of sections implemented in Simulink model are listed in Tab. 8.

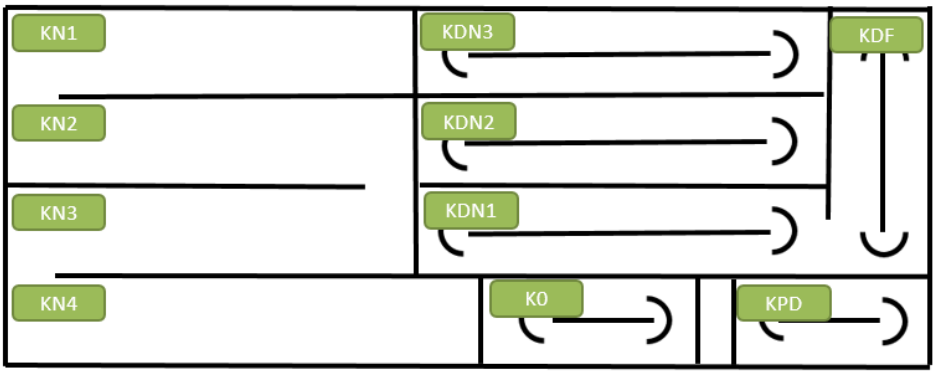

Fig. 30. Layout of the reactor in Płaszów WWTP – sections naming

Tab.8. Sections in Płaszów Sewage Treatment Plant.

	Section	Type	Aeration	Volume [m³]
1	Predenitrification KDP	Anoxic		1000
2	Dephosphatation KDF	Anaerobic		1700
3	Denitrification KDN1	Anoxic		2600
4	Denitrification KDN2	Anoxic		2600
5	Denitrification KDN3	Anoxic / Aerobic	x (sometimes)	2600
6	Nitrification KN1	Aerobic	X	2850
7	Nitrification KN2	Aerobic	X	2850
8	Nitrification KN3	Aerobic	X	2850
9	Nitrification KN4	Aerobic	X	3450
10	Deaeration KO	Deaeration		1000

In the KO chamber of the reactor, the wastewater is divided into two independent streams. Part of deoxidized material is returned inside the reactor, this process is called internal recirculation. The sediment debris is gathered in double secondary settling tanks that are integrated with each reactor. The process is called external recirculation. The second part is turned into two independent sedimentation tanks (secondary settler) in which a part of active biomass is recirculated and the other is removed. Secondary settler has a height of 4.7m with diameter 44 m.

Sewage parameters are measured during treatment by a SCADA control and monitoring system. Information about the ammonia and oxygen amount in the reactor has large importance on the treatment process control.

The ammonia sensor measures the concentration of ammonium nitrogen using a gas-sensitive electrode (GSE). The ammonium nitrogen present in the sample is converted into the ammonia gas form. Only NH_3 gas passes through the gas-permeable electrode membrane and is detected. This method guarantees a wide measurement range and is less susceptible to interference [107].

Oxygen sensors are used for continuous measurement of oxygen dissolved in wastewater. Generally, there are two types of oxygen sensors. In the amperometric probe, there are reactions on the anode and cathode, and the reference electrode provides the right electrochemical potential. Optic sensor excites dissolved oxygen molecules according to the content of dissolved oxygen in the wastewater.

The wastewater is aerated with compressed air using diaphragm diffusers. Due to the uneven distribution of oxygen demand, the number of diffusers varies in individual sections[97]. The diffusers installed in the reactors are Magnum 2000 tubular - diaphragm type [108].

The operator of Płaszów WWTP published the parameters of the sewage effluent in the treatment process in the treatment plant[106][109]. In the analyzed research, the author relies on the legal acts in force which regulate the permissible values of wastewater pollution indicators (91/271/EWG [110]). Such values are aggregated in Tab. 9.

Tab. 9. Expected values of effluent parameters in mg/l
(according to 91/271/EWG [111] and in Płaszów WWTP [106])

Parameter	Expected values of effluent parameters in mg/l (according to 91/271/EWG [111]and in Płaszów WWTP [106])
BOD5	15
COD	125
Total suspended solids	35
total nitrogen	10
total phosphorus	1,0

4.3 Aeration system with reactors in Płaszów WWTP

The photo below shows a blower station with an aeration system (Fig. 31).

Fig. 31. Picture of reactors inPłaszów WWTP with air pipes in the first plan[5]

Air is distributed to aeration tanks by diffusors that are controlled by throttling valves[112]. This demand airflow reduces the pressure p_c in collectors, the value of which the blower must "catch up". Such pressure change is measured in blowers station. Blowers are operated by a PID controller. In blowers PID controller maintains the collector pressure (p_c) at constant preset value. Nonetheless, some hysteresis is allowed. The schematic of the aeration controlsystem is presented below. The key step in the treatment is the oxygenation of the wastewater according to the diagram below (Fig. 32).

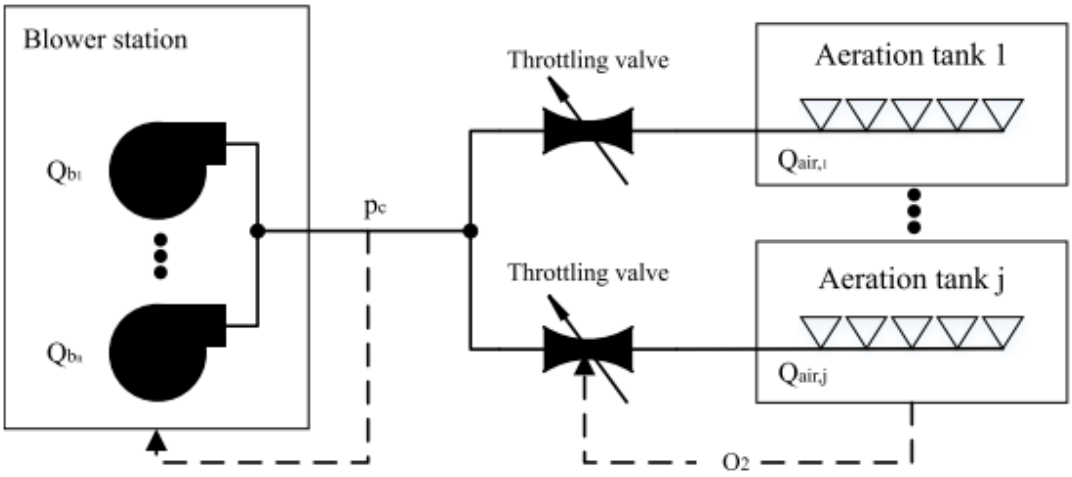

Fig. 32. Control of aeration system

[5]https://wodociagi.Kraków.pl/o-firmie/infrastruktura/zaklad-oczyszczania-sciekow-Płaszów.html

In general, the blowers installed in each treatment plant are responsible for maintaining the proper air pressure flowing through the diffusers. In Płaszów WWTP, there are six blower sets installed in the blower station building. It is estimated that electricity consumption by blowers accounts for 15% of electric energy consumption in the whole treatment plant (6 blowers of 400kW each have been installed)[1].

In details, the operation of the aeration system is to control the airflow by change of the pressure in the collector. The operation of the blowers is completely automated. The automation is supervised by a central controller cooperating with local controllers. The control process is two-step, as described below:

1. First blowers are blowing air (Q) to a common collector. The target is to maintain constant pressure in the discharge manifold – it should be maintained at 0.845 bar above the atmospheric pressure. The task of the control algorithm is to maintain such constant pressure. Their operation is based on a PID controller that tries to maintain constant pressure (p_c). To maintain pressure at a constant value, the controller operates blower blades inclination in 0-100% (the speed of the blower motor is constant). Supervision over automation is performed by characteristics that correlate efficiency, power and flow.
2. The air compressed by blowers is delivered to reactors by throttling valves that control airflow. Each section in each reactor is controlled separately. The air blown into the reactor depends on the wastewater quality parameter. The flow sensor system that controls the operation of the dampers is responsible for controlling the flow of supplied air. The position of the damper depends on the oxygen demand of the individual reactor chambers. Compressed air is supplied to the aerated section in biological reactors through aeration diffusers controlled by oxygen probes installed in four KN chambers and the KDN3 chamber.

The schematic of such process is presented below (Fig. 33).

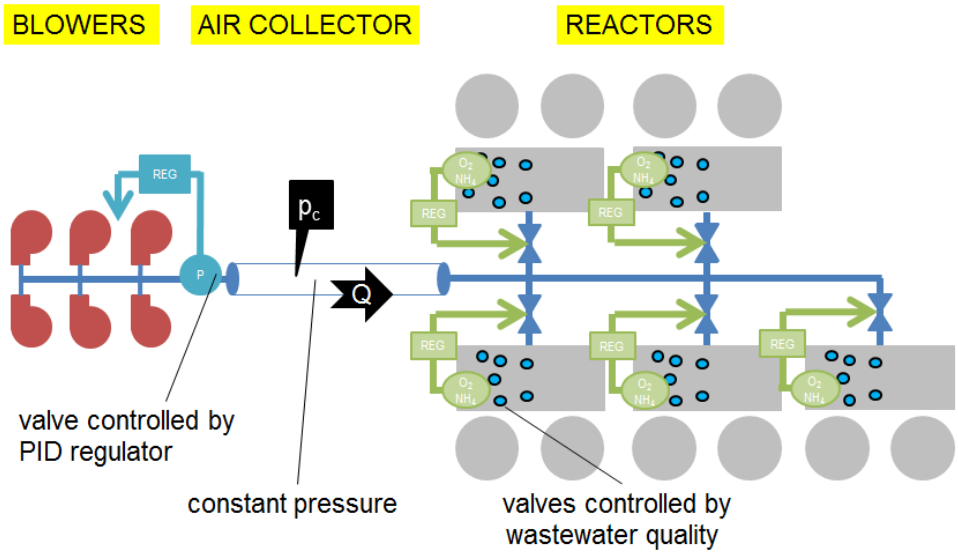

Fig. 33. Structure of the Płaszów WWTP aeration control [97]

To control blower a complex control algorithm is implemented. The number of running blowers is adjusted depending on the oxygen demand. The operation of the blowers is adjusted by switching on/off and the regulation of blades' angle.

The performance of each blower is a function of several operating conditions monitored on-line. Its settings are selected so as to minimize electric energy consumption while maintaining the assumed pressure within the defined limits. More precisely, the controller adapts to possible changes in blower performance due to changing weather conditions or degradation problems.

It should be noted that the exact implementation of the blower control system algorithm on the plant is unknown to the author. Therefore, approximate characteristics have been determined based on SCADA measurements in accordance with the assumption presented in Sec. 5.2.

4.4 Example SCADA measurements

During the implementation of the GEKON project, measurement data has been obtained from the operation of the sewage treatment plant[6].

Measurements of oxygen and NH_4^++NH_3 nitrogen (ammonia) in the discussed period are presented below (Fig. 34).

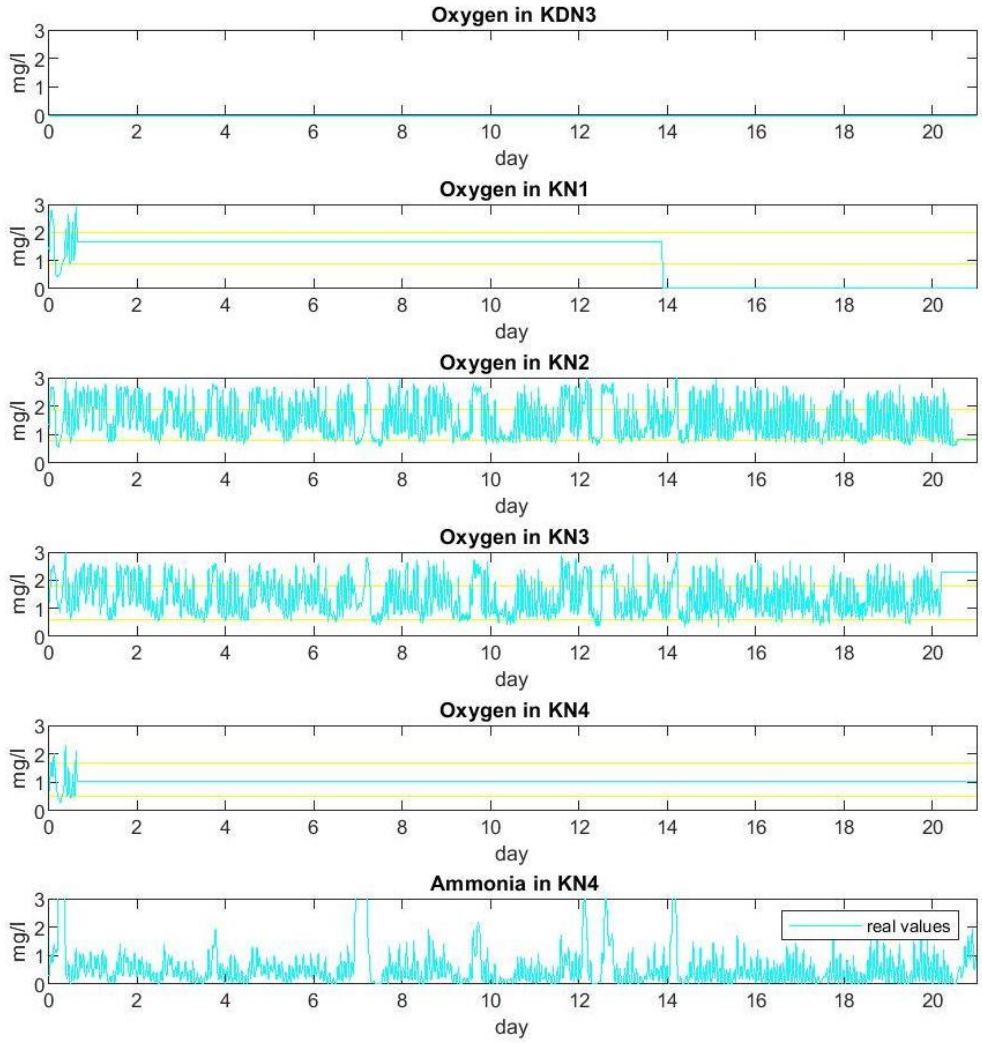

Fig. 34. Measurements of oxygen and NH_4^++NH_3 nitrogen

[6] Data obtained for two first quarters of 2017

Wastewater flow is measured at the outlet of the treatment plant. The measured quantity sewage effluent is presented below (Fig. 35). Such industrial facilities have negligible possibilities of storing sewage during treatment process. Therefore, a simplification is adopted - it is assumed that the measured quantity of the effluent is equal to the influent at the moment. This practice allows the available measurements to be taken as a quantitative characterization of the waste water influent.

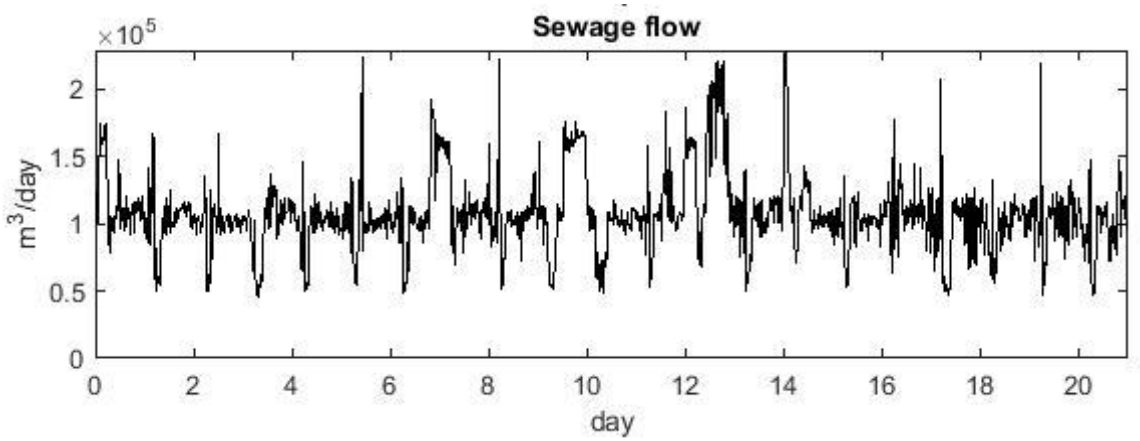

Fig. 35. Sewage influent

The airflow and power consumption values are pictured below, summing up the values for all sections. It is worth noting that increasing the flow results in an increased consumption of electricity (Fig. 36).

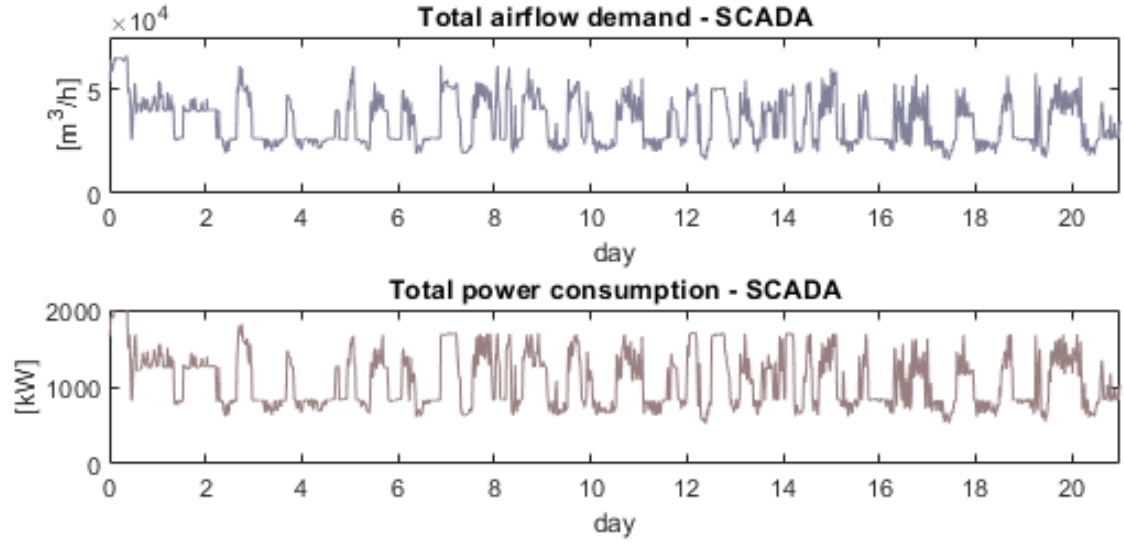

Fig. 36. Total airflow demand and total power consumption

Registered airflow in particular blowers is presented below (Fig. 37).

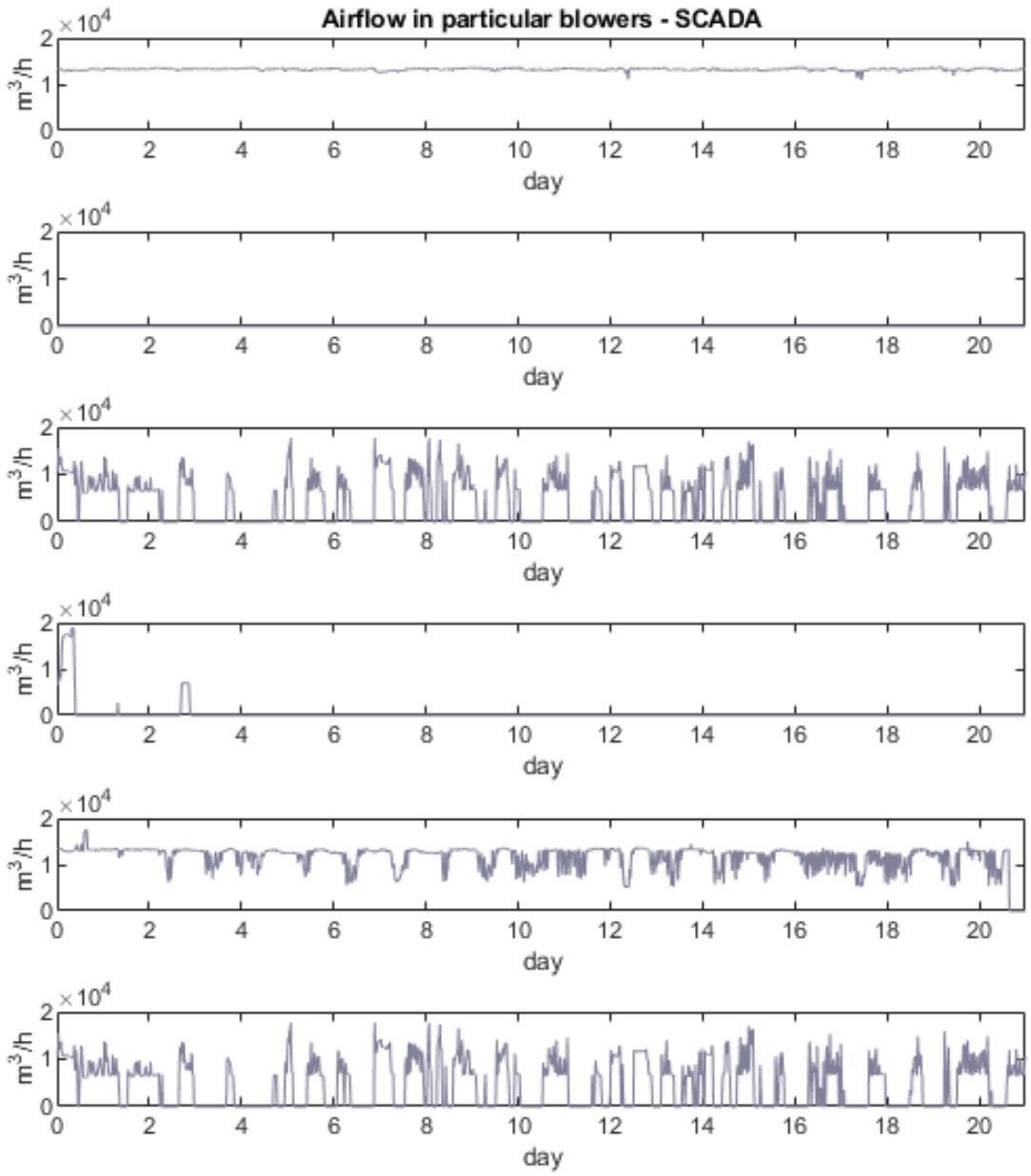

Fig. 37. Airflow registered in particular blowers

Power consumption in particular blowers is presented below (Fig. 38).

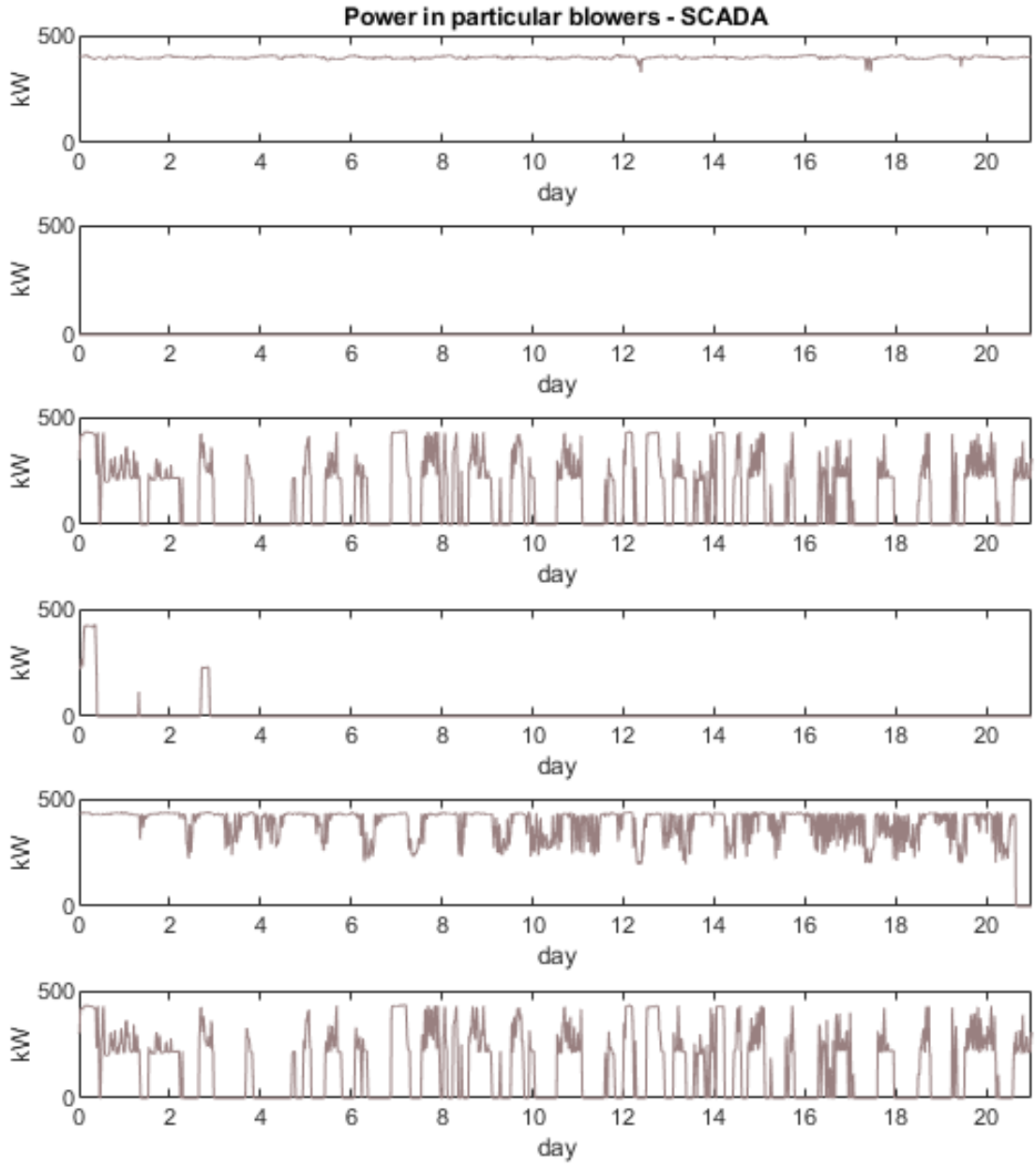

Fig. 38. Power consumption in particular blowers

It is worth adding that the signals of the airflow in blowers and the corresponding demand for power are used to determine the characteristics of the device.

The available SCADA measurements have been used to investigate the characteristics of the blowers. The following figures (Fig. 39) show the measured values of the blower power consumption. Therefore, they will be considered independently. These calculations will be used in the next chapter to determine the characteristics of individual blowers (Sec. 5).

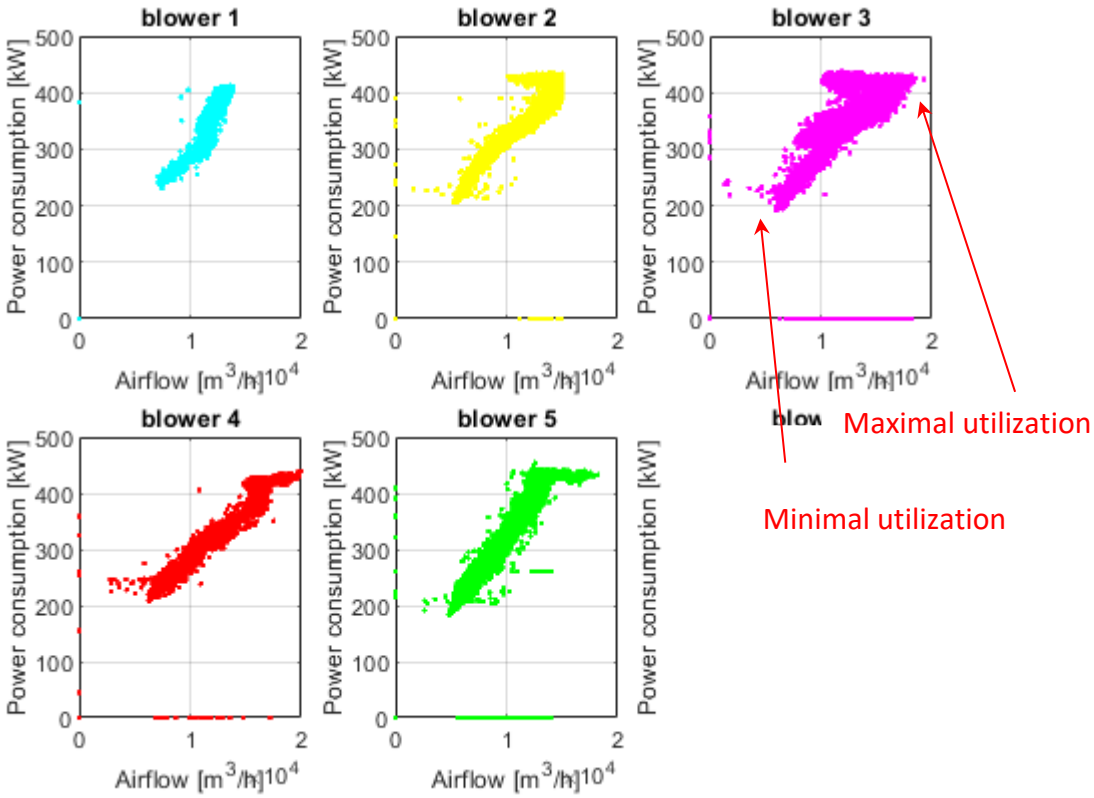

Fig. 39. Measured blower power consumption for different airflow measures and blade angle values

For next figure (Fig. 40) blowers' characteristic curves are expressed as power consumption per airflow.

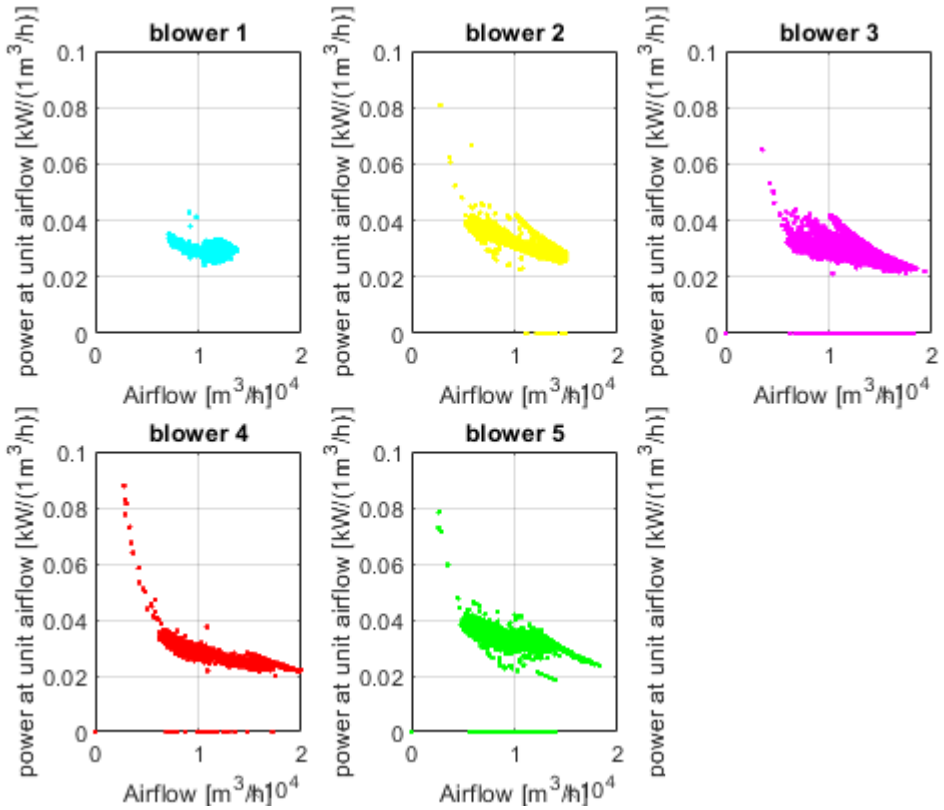

Fig. 40. Blower characteristic curves expressed as power consumption per airflow unit

5 Numeric model of Płaszów WWTP

5.1 BSM1 model of reactors in Płaszów WWTP

5.1.1 General layout of the BSM1 model of Płaszów WWTP

The BSM1 environment presented in the previous paragraph has been implemented in the case of the sewage treatment plant in Kraków. To perform the task, the Matlab/Simulink model structure has been adapted to the conditions of the Płaszów Sewage Treatment Plant (Fig. 41).

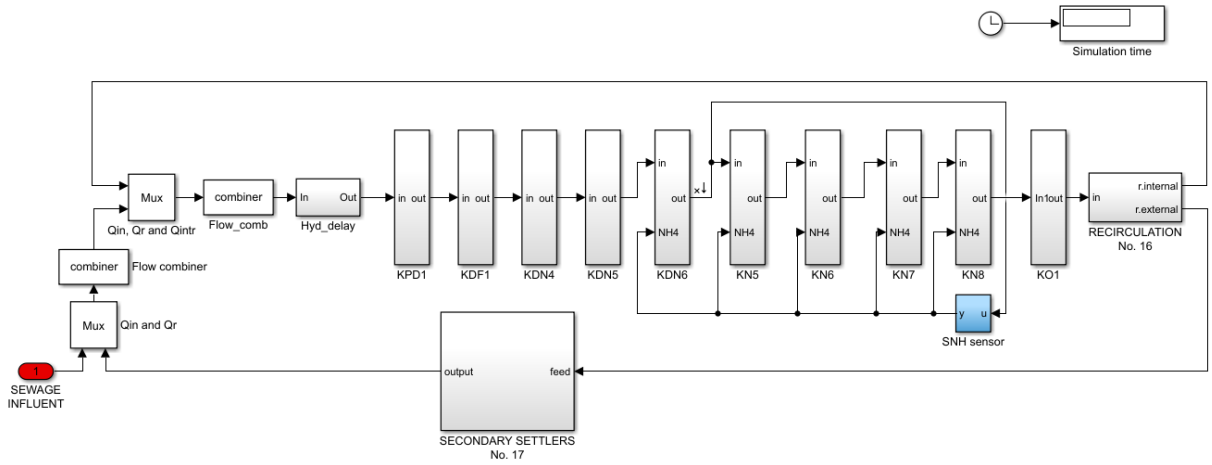

Fig. 41. Model of reactors of wastewater treatment plants based on the BSM1 model

To simulate the operation of the reactor, a numerical model has been made using BSM1 as foundation. The publicly available BSM1 package published on the website and in the [62] has been implemented for this purpose.

While modifying the BSM1 model, the following changes have been adopted:

- Sections names and volumes are obtained from Płaszów documentation;
- Internal and external recirculation is unknown, thus values of recirculation in reactor are adopted in proportion to BSM1;
- Secondary settlers stay as in the BSM1 model, except for the fact that in the Płaszów, there were settling tanks connected (the author entered depth as in Płaszów WWTP with a doubled surface area);
- The carbon content in the process is not included (carbon combiner is deactivated);
- The aeration applies to sections KN1, KN2, KN3, KN4. Oxygenation in KDN3 is off ($KLa = 0$);
- Implementation of the Petersen equation in reactors (Tab. 5) remains unchanged.

The diagram below presents a single oxygenation section of a reactor (Fig. 42).

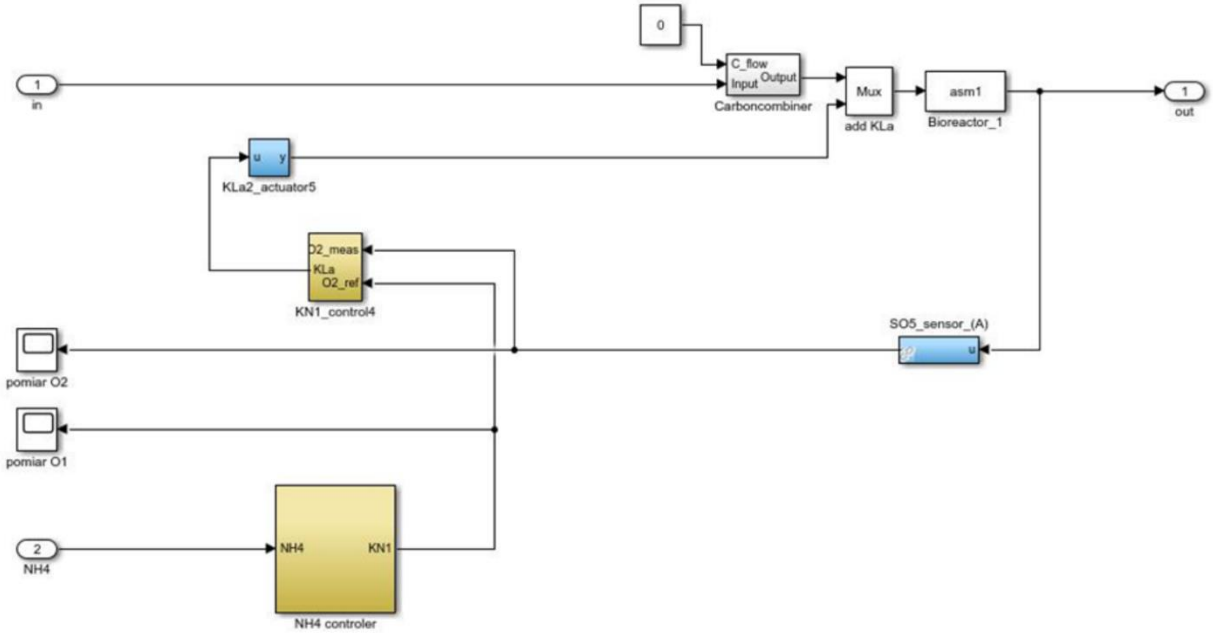

Fig. 42. Simulink block diagram presenting the oxygenated section (KN1, KN2, KN3 or KN4)

The oxygenation controller provided in the BSM1 model has been modified, as described below:

- NO sensor has been replaced by an NH_4^++NH_3 nitrogen sensor by measuring this signal, characteristics describing sensors' operation have not been changed (they are compatible with the BSM1 model documentation);
- The oxygen sensor has not been changed;
- The value of the expected oxygen model is based on the dependency below (Fig. 43). The Min and Max values for oxygen and ammonia are defined for each section separately;

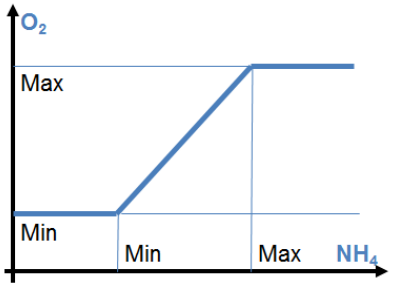

Fig. 43. Relationship between the amount of expected oxygen in the reactor section and the ammonia content in the wastewater

- KLa is calculated based on the expected oxygen difference from the current one and determined similarly to the original BSM1 model based on the difference in actual oxygen content ($O2_{means}$) and expected one ($O2_{ref}$).

5.1.2 Quality supposition of the influent wastewater

Sewage influent parameters are very difficult to measure experimentally and therefore, the plant is generally operated without knowing the parameters. To visualize the operation of the Płaszów Sewage Treatment Plant, a BSM1 simulation framework has been developed and its parameters adapted to the WWTP under investigation. The author collected available data to make such an estimation.

It is assumed that at a given time the amount of outgoing sewage and amount of flowing sewage are the same. The author therefore assumes that sewage influent coincides with outfluent in the wastewater treatment plant in Płaszów. Hence, sewage flow is corrected by outfluent volume obtained from measures of SCADA in Płaszów WWTP – the inflow in the BSM1 model is scaled to the values observed in the outfluent of the treatment plant. Finally, Fig. 44 and Fig. 45show the sewage flow through the WWTP [109]. These values oscillate around 170,000 m^3/day with daily volatility. It can be seen that the weather influences the volume of influent.

In addition, authors use other measurements of the sewage treatment plant from the SCADA system presented in Sec. 4.4 (oxygen reading in the reactor for KDN3, KN1, KN2, KN3, KN4 sections, air flow in the blowers, and estimates of electricity consumption by blowers). Nevertheless, the parameters of the influencing waste water are missing.

Originally default data published within BSM1 are used as sewage parameters (published by IWA[7]). The wastewater parameters can be modelled with constant values of parameters (CONSTANTINFLUENT) or parameters changing characteristics daily (DRYIFNLEUNT, RAININFLUENT, STORMINFLUENT). Both constant and variable input parameters are analyzed in influent signals. These data are considered as input to the BSM1 model of the Płaszów Sewage Treatment Plant. It is worth mentioning that the parameters describing the wastewater will be investigated in the following paragraphs. Fig. 44 and Fig. 45 present exemplary time series of wastewater influent characterizing modelled Plaszów WWTP.

To sum up, wastewater flowing into the treatment plant is described by a matrix called DATAINFLUENT. The structure of the matrix is characteristic for BSM1 model (Sec. 3.3.3), so it consists of the following columns:

- Column 1 – Time vector – changing depending on the length of simulation,
- Columns 2-15 – Wastewater parameters – characteristic for ASM1 model,
- Column 16 – The sewage flow adjusted to the SCADA readings of the sewage treatment plant in Płaszów.

[7] Source http://iwa-mia.org/benchmarking/#BSM1

First, the treatment plant model has adopted a flow consistent with SCADA data and fixed parameters described in the CONSTANTINFLUENT example (Fig. 44).

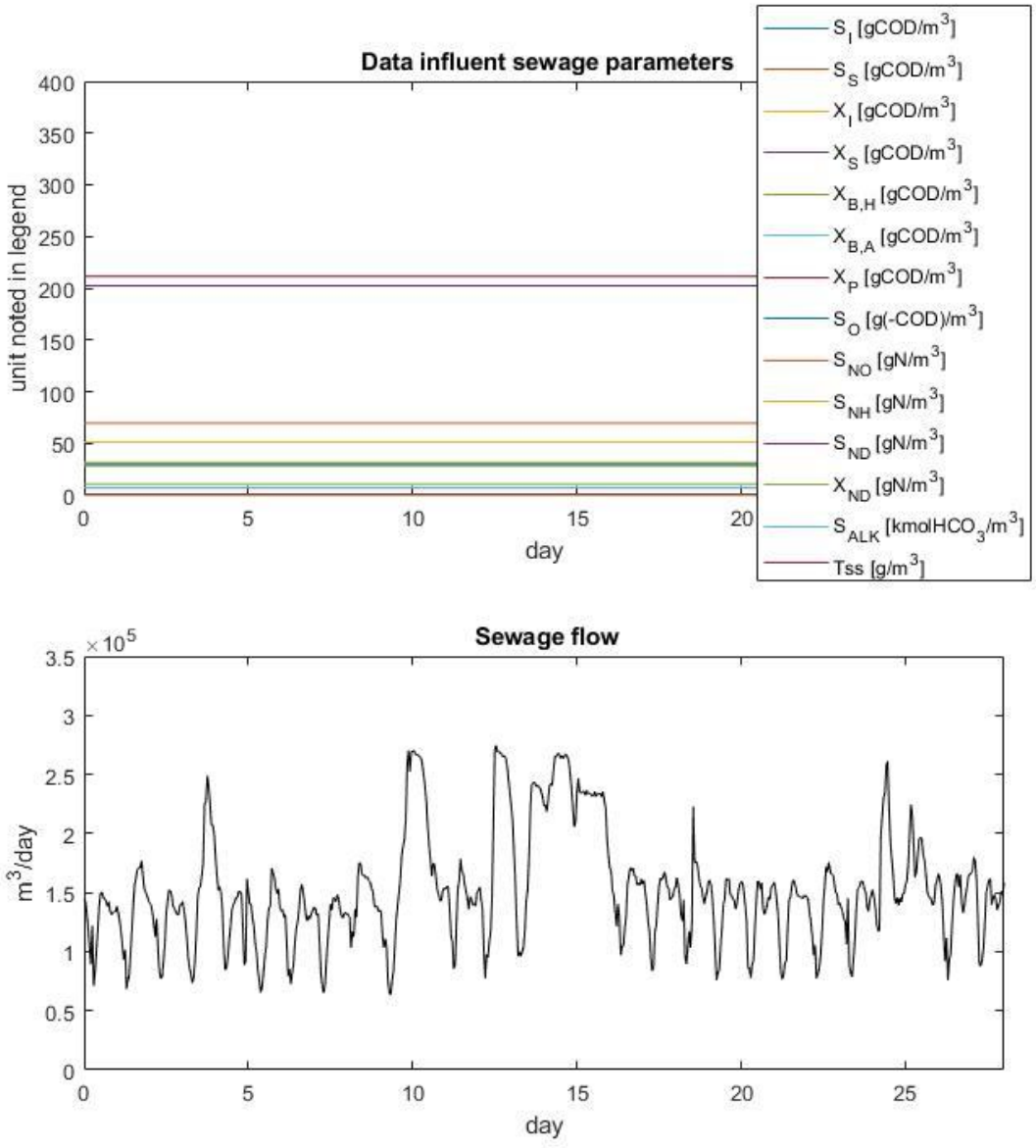

Fig. 44. Sewage influent parameters based on CONSTANTINFLUENT used in the simulation

In the second case, the sewage treatment plant has been examined under the influence of sewage with variable daily parameters simulating dry conditions (Fig. 45).

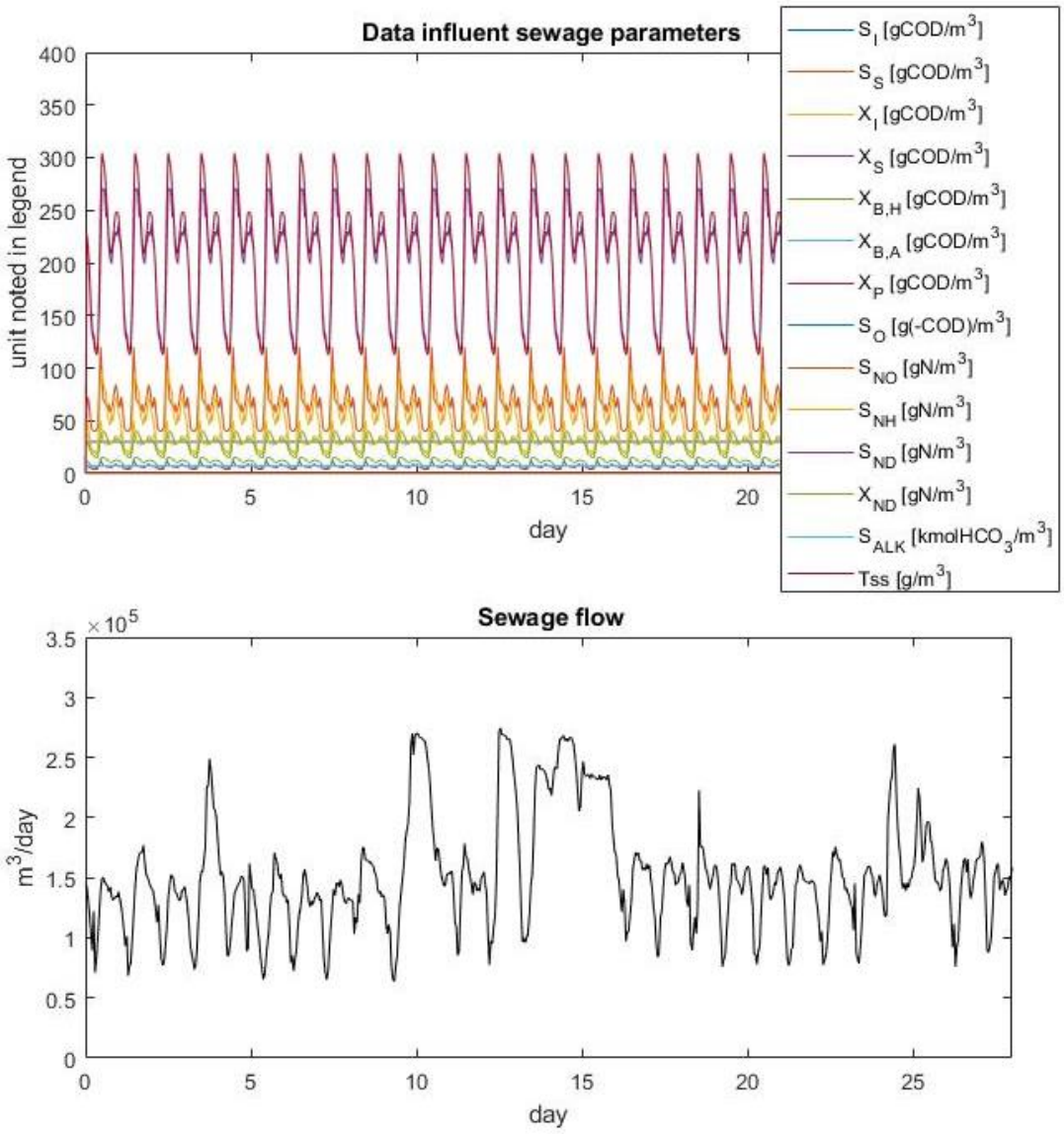

Fig. 45. Sewage influent parameters based on DRYINFLUENT used in the simulation

The data is used in the course of their comparative analysis with simulations in the following chapters.

5.1.3 Simulation of reactors in Płaszów Sewage Treatment Plant

Simulations have been performed on the BSM1 model (described in Sec. 3.3) using input signals based on SCADA data (as in Sec. 4.4). The view of the Matlab/Simulink program with the description of individual parts is shown below (Fig. 46).

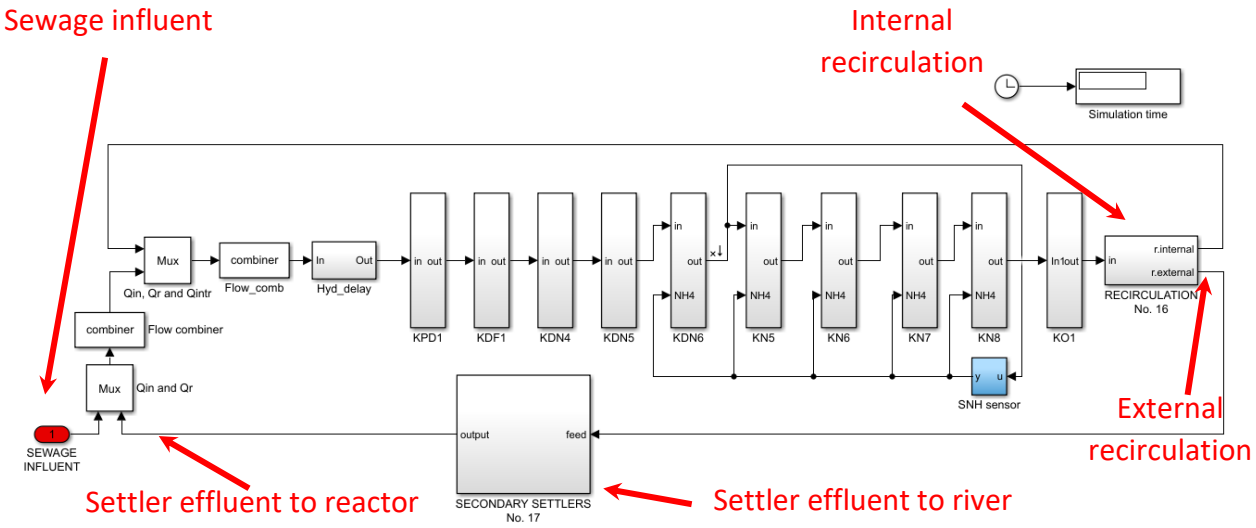

Fig. 46. Schematic of simulation with measurement points marked

The model has been tested in terms of the quality of the outflowing sewage (Fig. 47). As it can be perceived, the variability of the effluent results from the variability in influencing sewage. A constant volume of secondary recirculation has been assumed.

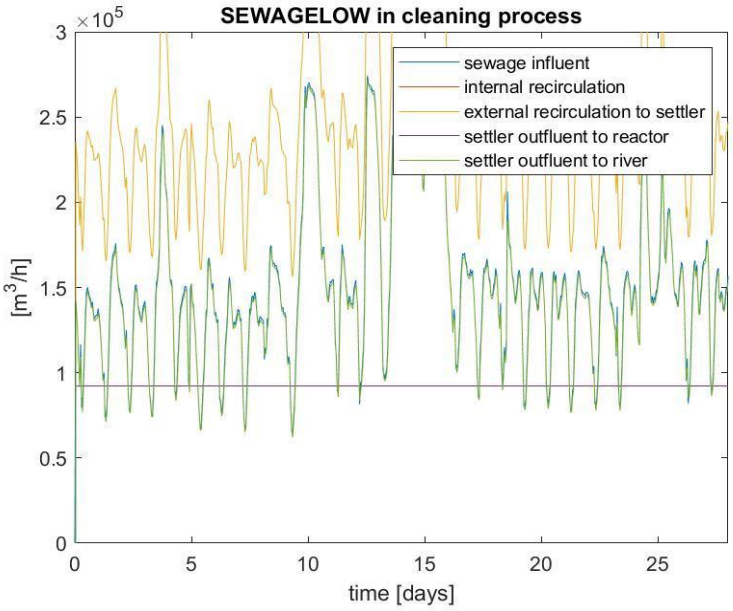

Fig. 47. Sewage flow during cleaning process in the reactors

The simulation results illustrate the plots below in which the author points out the registered amount of oxygen and ammonia contrasted with SCADA data obtained during the operation of the treatment plant.

In the first case, the constant values of the CONSTANTINFLUENT input signal have been used. The resulting oxygen concentration is presented in Fig. 48.

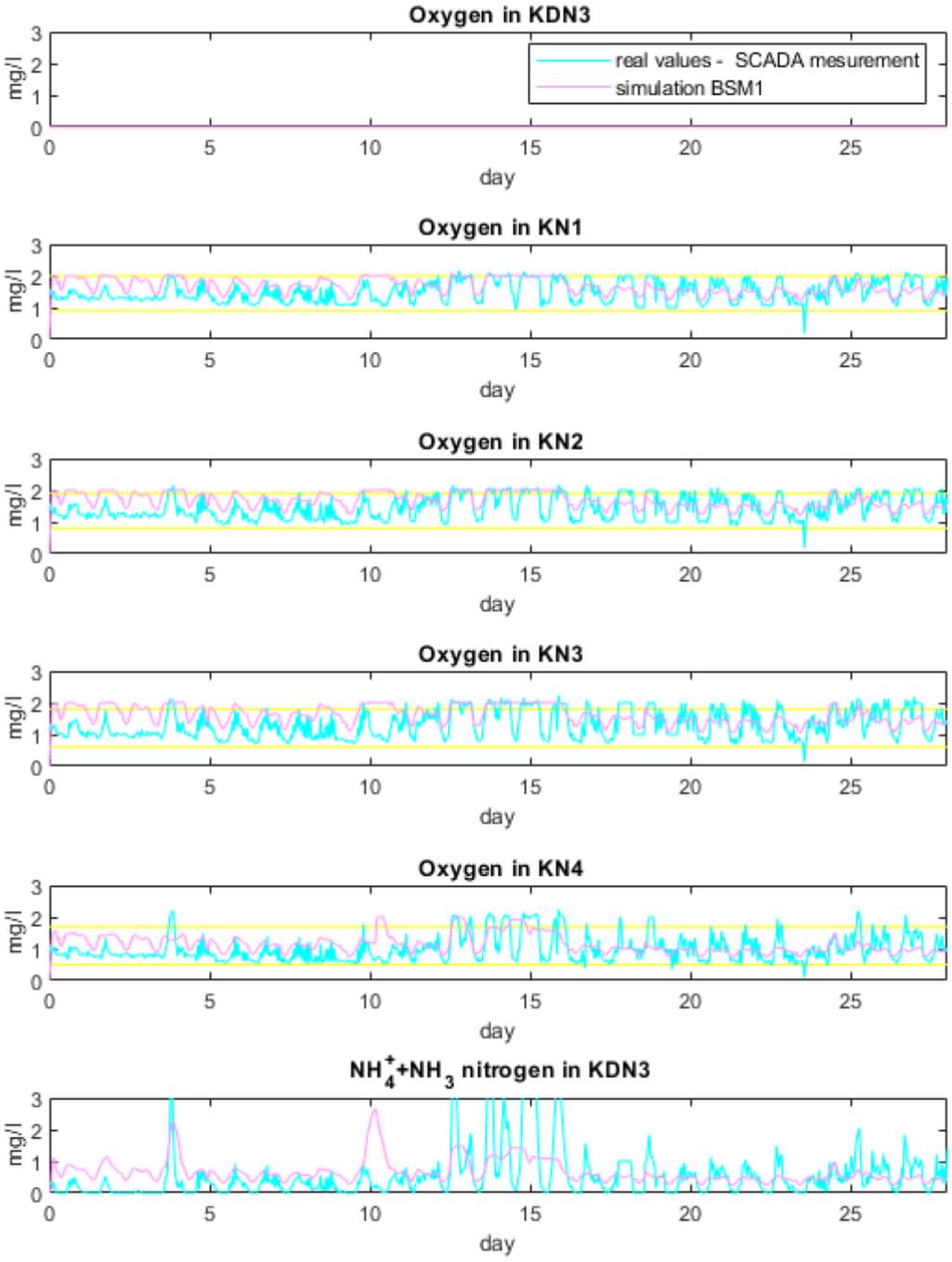

Fig. 48. Simulation results using CONSTAINFLUENT signal as input to WWTP

Further simulation using VARIABLEINFLUENT signals as input to WWTP has been performed. The Fig. 49 presents the plots of both simulations.

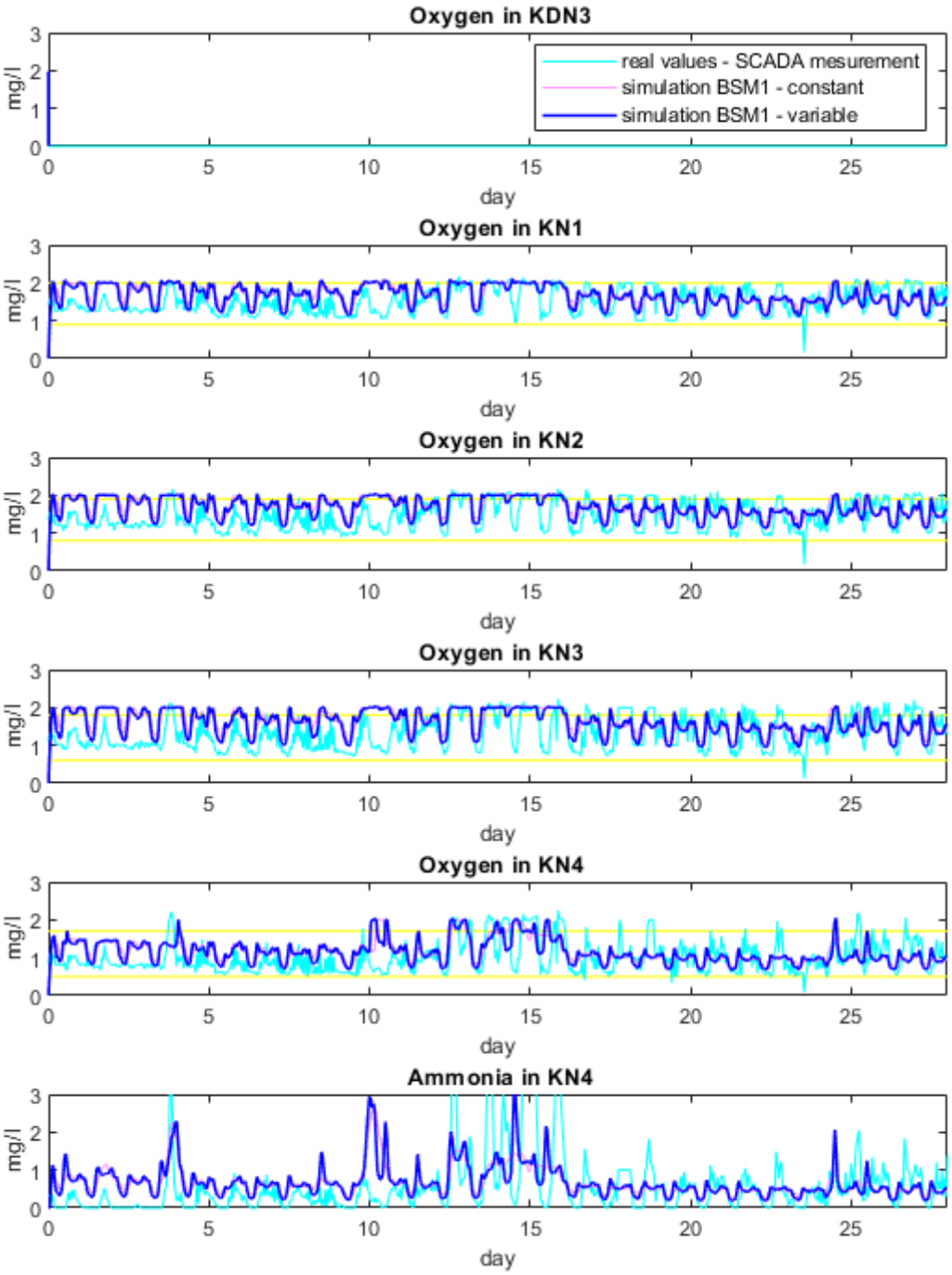

Fig. 49. Simulation results using CONSTAINFLUENT and VARIABLEINFLUENT signals as input to WWTP – O_2 and NH_4^++NH_3 nitrogen (ammonia)

The airflow demand calculated during the WWTP's operation allowed to set the airflow demand (as described in Sec. 5.1.1). The results of simulation presents Fig. 50.

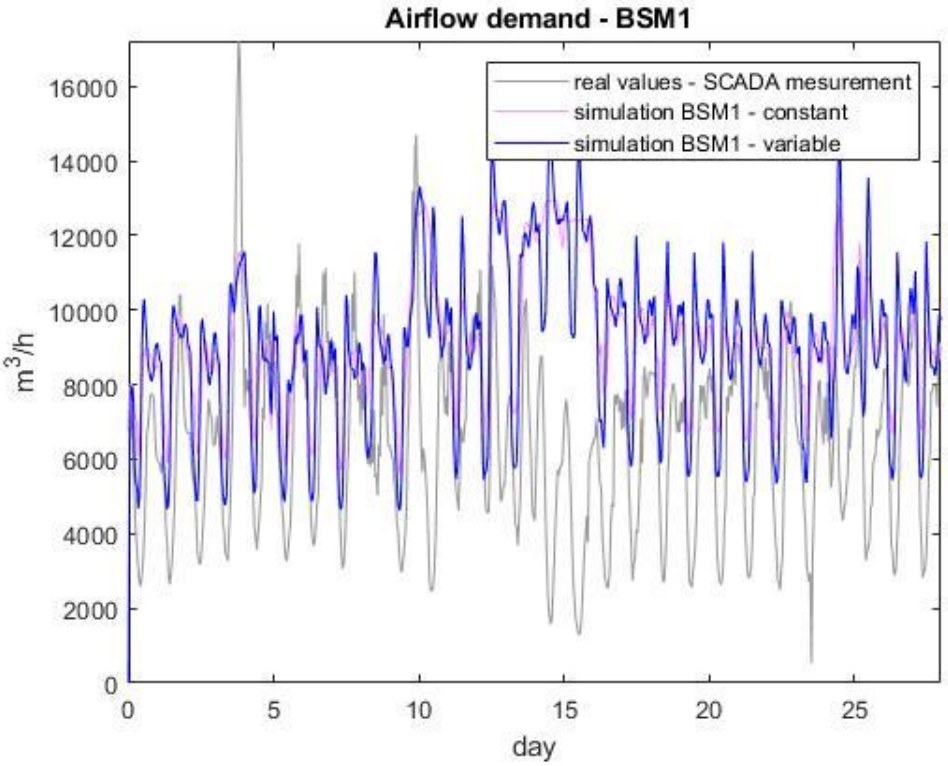

Fig. 50. AIRFLOWDEMAND calculeted with use of CONSTAINFLUENT and VARIABLEINFLUENT signals as input to WWTP

It can be noticed from the given graphics that the variable signal VARIABLEINFLUENT introduces more daily dynamics to the simulation than CONSTAINFLUENT. Moreover, these changes are in line with the measurements. Nevertheless, the wastewater flow, which is given on the basis of SCADA measurements, has a key influence on the characteristics of the treatment process.

Additionally, the treatment process has been explored in terms of the quality of the outgoing sewage. Fig. 51 shows how the value of the NH_4^++NH_3 parameter (SNH) changes during the treatment. A significant improvement in the effluent compared to the influencing value can be seen. The graphic below shows that the effluent reaches the expected degree of purity (less than 15 mg/l content).

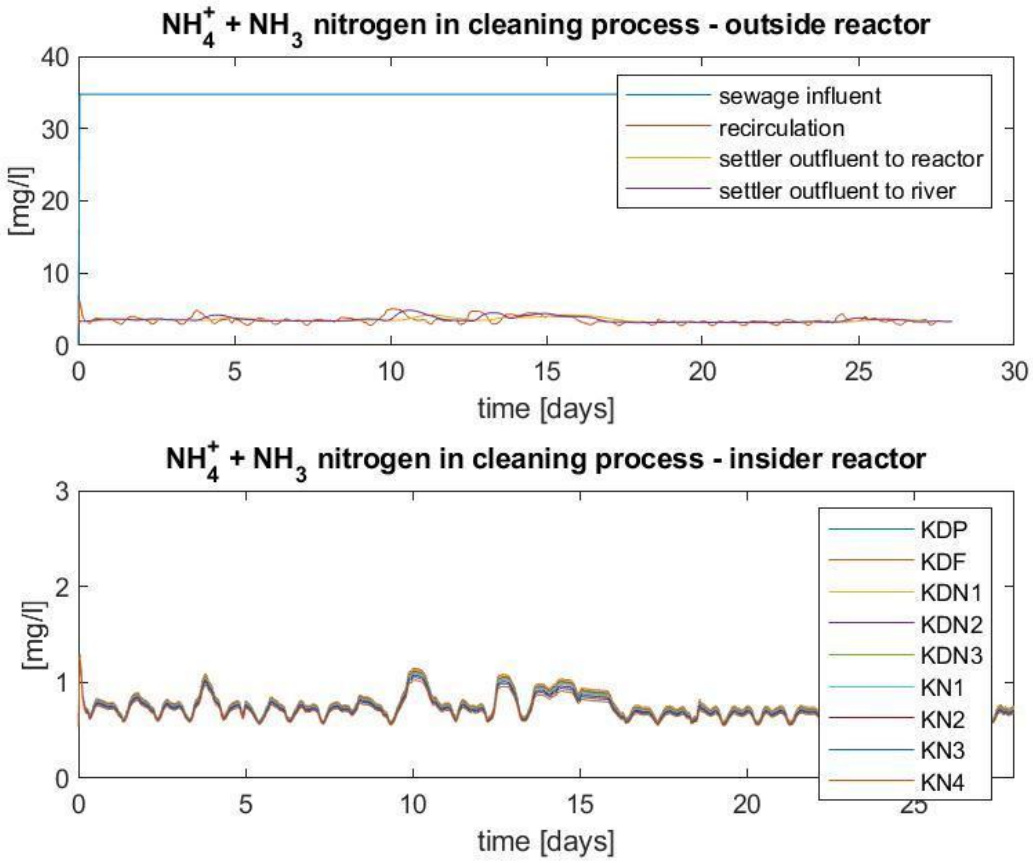

Fig. 51. NH_4^++NH_3 nitrogen in cleaning process

5.2 Aeration system and its integration with reactor

5.2.1 Elaboration of blowers' control algorithm

The wastewater treatment plant reactor model presented above is based on well-documented numerical models. The SCADA data, on the basis of which the characteristics of the blowers have been developed, are helpful in the implementation of the task. The model of operation of blowers has been acquired on the basis of data obtained during the implementation of the GEKON project.

As described in the paragraph (Sec. 3.1), oxygenation control is a key consideration in the operation of wastewater treatment plants. More precisely, the condition of each section of each reactor forces the demand for aerated air at a certain value ("airflow demand"). To fulfill the need, blowers are adjusted to supply the necessary amount of air. The task is carried out in two stages: throttling valves regulate the airflow that is introduced into the wastewater and the pressure of the collectors is adjusted by adjustment of blowers' means. Such a system of operation is also installed in the Płaszów sewage treatment plant (Fig. 52).

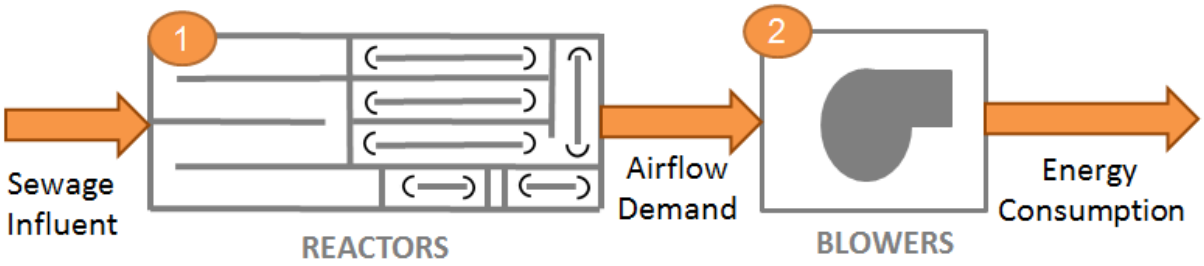

Fig. 52. General scheme of the purification process presented in the dissertation

The control algorithm of Płaszów Sewage Treatment Plant in Kraków is very complex and depends on many parameters. Unfortunately, some cannot be determined by measurement (as described in Sec. 4.3). Therefore, there is a need to make some simplifications. First, blower control based on pressure measurement in the reactor has been replaced by airflow. In this case, the blower controller adjusts the pitch of the blades based on the air demand and not on the basis of pressure as in the original. In operation of real WWTP blowers are controlled by a PID controller. In the case of the modeled blower system, PID control is replaced by a purely proportional controller.

For such a simplified model of blowers, the author proposes a control strategy that controls blowers and their efficiency, giving priority to the most efficient ones. An idea of control is to implement scheduling policy that tries to run the blowers no later than necessary. The assumed solution allows the reduction of electricity by switching off the blower operating for a long time at "idle capacity."

The diagram below demonstrates the implementation of blowers' controller in modelled WWTP (Fig. 53).The operation algorithm presented here is a proprietary approximation of the actual blower control of the sewage treatment plant. This example will be used later in the study.

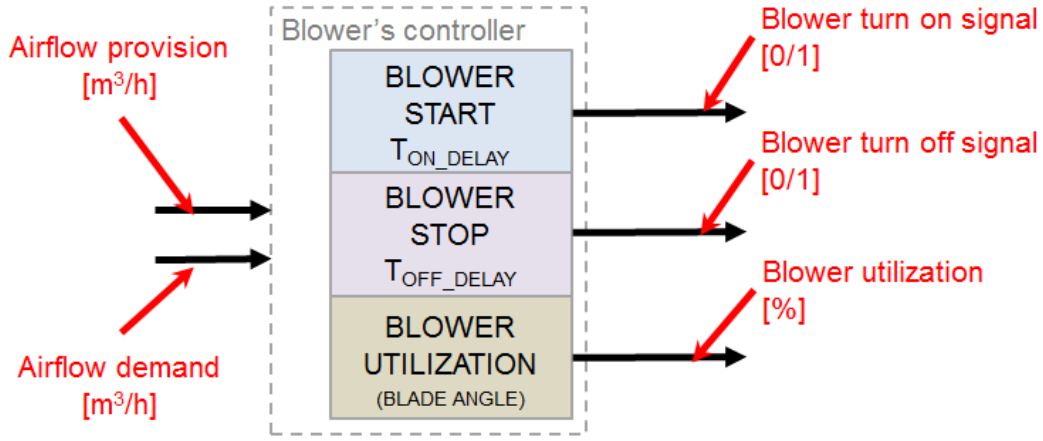

Fig. 53. The scheme of blowers' controller

The controller raises the blowers' utilization ($BLADE_{ANGLE}$) by increasing blades' angle for the longest operating blower as long as airflow in controller $airflow_{PROVISION}$ is lower than expected $airflow_{DEMAND}$. Controller turns on next blower if the previously activate blowers are already working at 100% blade angle $(sum(BLADE_{ANGLE})>B_{ACTIVE}*100)$ for a certain amount of time ($T_{MAX}>T_{ON\_DELAY}$, T_{ON_DELAY} is a constant user defined parameter).However, it is limited by the maximum number of blowers that can be turned on $(B_{ACTIVE}<4)$.When a new blower is to be started (B_{ON}),a controller chooses the first blower in the queue of waiting blowers ordered according to their efficiency (as described in Sec. 4.3).More formally, the rules of implementing the above dependencies are listed below:

$$BLADE_{ANGLE}(n) \nearrow \Leftrightarrow (AIRFLOW_{PROVISION} < AIRFLOW_{DEMAND}) \qquad (17, 18)$$

$$B_{ON}(n) = 1 \Leftrightarrow (\mathrm{sum}(B_{A.}) > B_{ACTIVE} * 100) \wedge (T_{MAX} > T_{ON\_DELAY}) \wedge (B_{ACTIVE} < 4)$$

On the contrary, if $airflow_{PROVISION}$ is higher than $airflow_{DEMAND}$, the controller decreases the blades' angle $(BLADE_{ANGLE})$.A blower working at lower utilization is switched off for user defined T_{OFF_DELAY} constant $(T_{MIN}>T_{OFF\_DELAY})$ when the sum of the blowers' utilization $(BLADE_{ANGLE})$ will not exceed the capacity of the blowers after turning off one blower $(sum(B_{U.})<(B_{ACTIVE}-1)*100)$.Likewise, the minimum number of blowers turned on is a limitation $(B_{ACTIVE}>1)$.The blower that is being stopped (B_{OFF}) is the one currently operating for the longest time at lower utilization. The equations describing the rules:

$$BLADE_{ANGLE}(n) \searrow \Leftrightarrow (AIRFLOW_{PROVISION} > AIRFLOW_{DEMAND}) \qquad (19, 20)$$

$$B_{OFF}(n) = 1 \Leftrightarrow (\mathrm{sum}(B_{A.}) < (B_{ACTIVE} - 1) * 100) \wedge (T_{MIN} > T_{OFF\_DELAY}) \wedge (B_{ACTIVE} > 1)$$

The equations presented above are my implementation of tasks scheduling (Sec. 2.4.3).

5.2.2 Blowers' characteristics

In the section 4.4, the author presented available SCADA data used in simulations. The blower station contains 6 fixed-speed blowers.

Available measurement data have been used to measure the efficiency of the blower. To estimate the efficiency of blowers available data are used –vectors of power of the blower in the relation to air flow. As presented in [113] and [114], this is one of estimates describing blowers efficiency in engineering. Having these two values will allow the performance curve of the blower to be determined (Fig. 54).

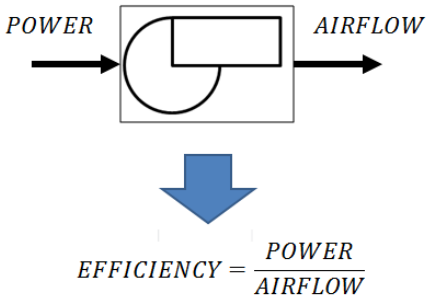

Fig. 54. Method to assess the blowers characteristic[113]

On the basis of available SCADA measurements the plots presenting power consumption for different airflow and blade angle values are presented. For the last blower 6, the acquired data was scarce due to its rare usage. Thus, its characteristic has been assumed to be the same as that of the blower with most similar specifications (blower 3). The results of such simulation are presented in Fig. 55.

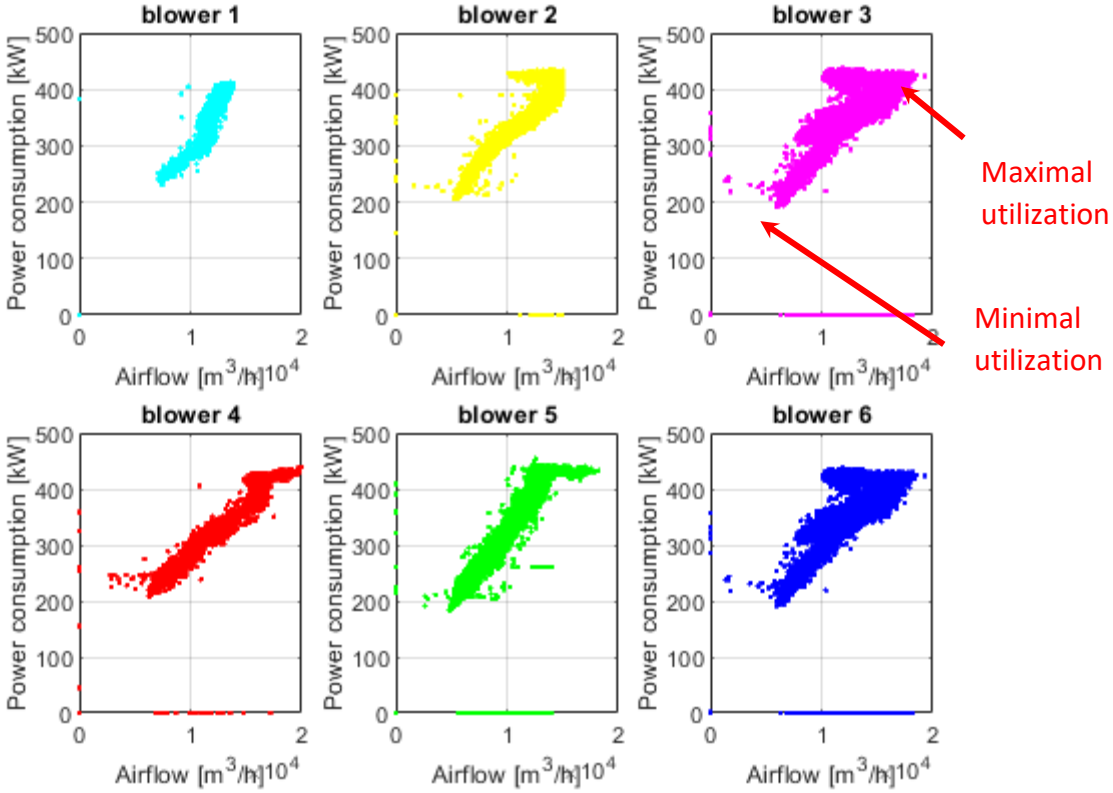

Fig. 55. Measured blower power consumption for different airflow measures and blade angle values

The signals presented above, based on SCADA measurements, are tested. On the basis of these signals, for non-zero probes the linear regression has been calculated[115]. Later, the coefficient of determination R2 has been determined. Values close to 1 indicate the correctness of the fit for performed linear regression[116].Power consumption and airflow are related one to another. The results are presented in the following table (Tab. 10).The linearised characteristics are presented below (Fig. 56).

Tab. 10. Coefficients used in the simulations

Blower	Standard deviation		linear regression	Coefficient of determination
	Airflow [m^3/h]	Power cons. [kW]		
1	751.2	23.2562	y=0.0278*x+31.445	0.8056
2	3498.3	75.8611	y=0.0212*x+107.63	0.9588
3	2937.5	86.7573	y=0.0243*x+74.904	0.6775
4	4153.4	76.2592	y=0.0181*x+106.93	0.9682
5	2646.8	81.1222	y=0.03*x+36.567	0.9597
6	2937.5	86.7573	y=0.0243*x+74.904	0.6775

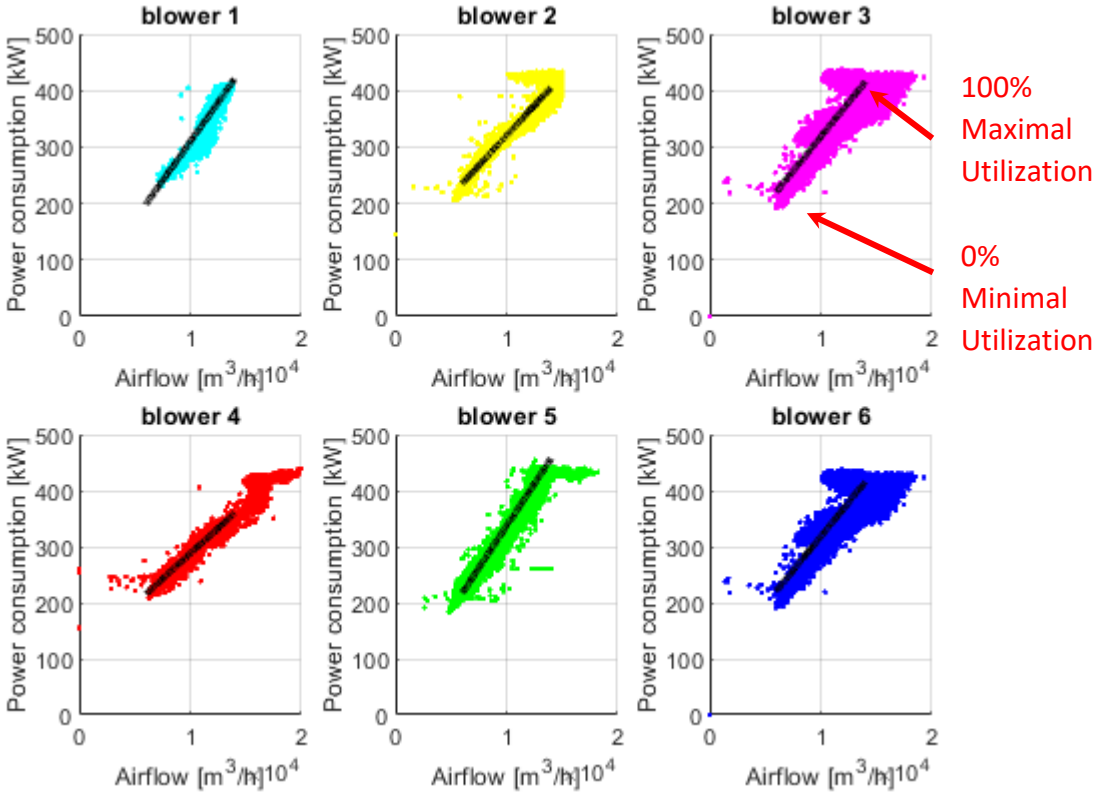

Fig. 56. The characteristics are obtained by fitting SCADA data – proposal

The above graphic shows that the control of the blower utilization affects the air flow and the electricity consumption in a linear relation. It is assumed that the utilization of the blowers is adjusted in the range of 0-100 achieving the lowest and the highest flow respectively. Therefore, blowers' operation point becomes strongly simplified by linearisation (Fig. 57).

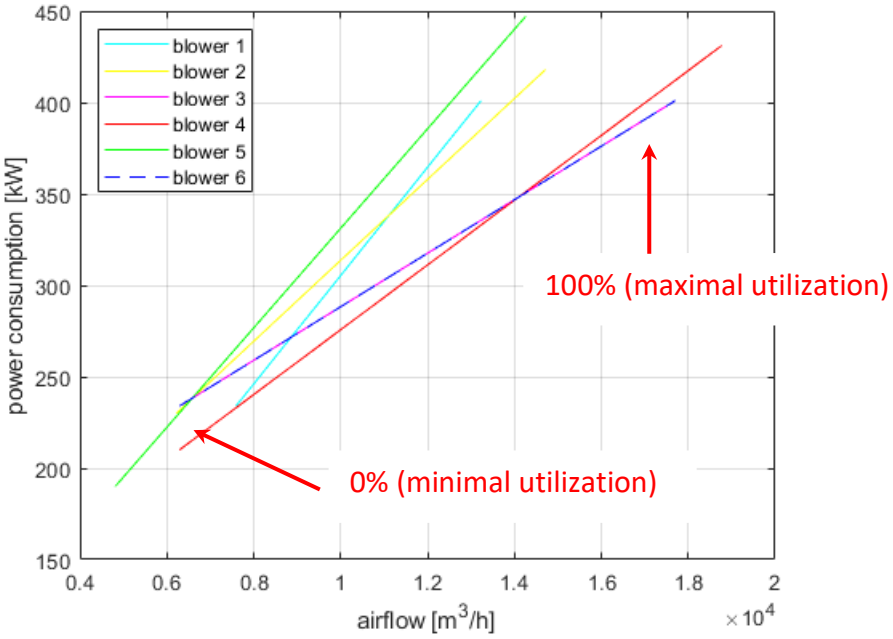

Fig. 57. The characteristics are obtained by fitting SCADA data – summary

To sum up, the following characteristics are used in the simulation. The efficiency curve for individual blowers shows the difference in the achieved flow depending on the efficiency. The first plot presents the airflow in relation to efficiency(Fig. 58).

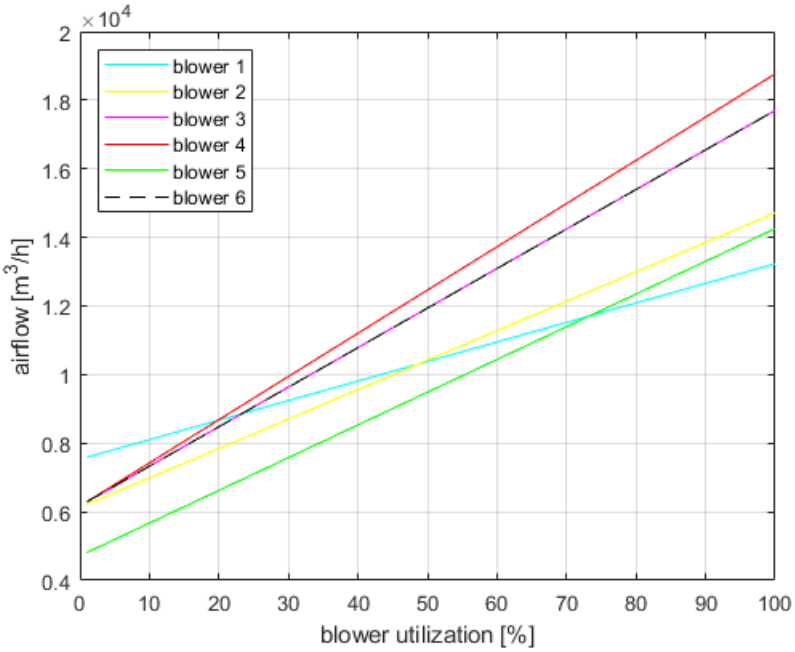

Fig. 58. Control of blowers adopted in the numeric model – airflow in relation to utilization

The power consumption characteristic shows the change in electric energy consumption of the blower depending on its utilization. Here, the differences for individual blowers are similar (Fig. 59).

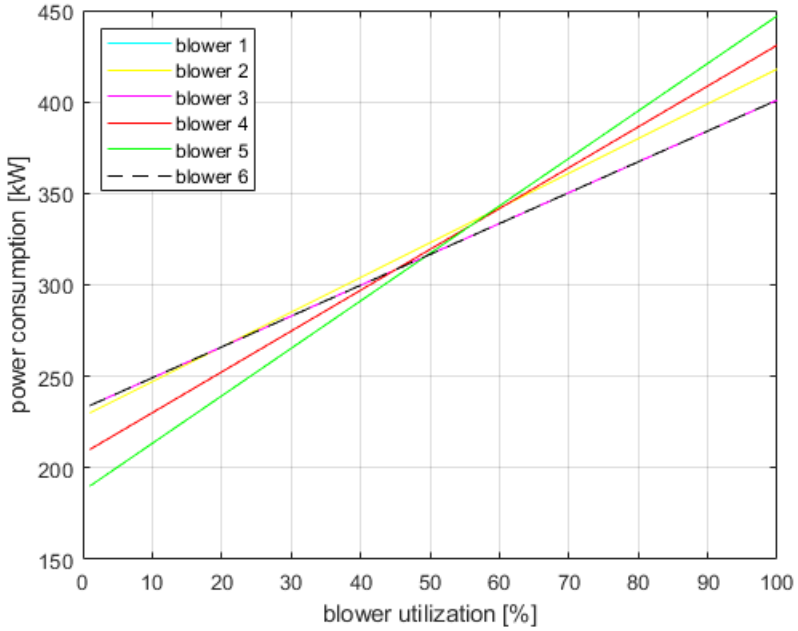

Fig. 59. Control of blowers adopted in the numeric model – power consumption in relation to utilization

To sum up, characteristics of airflow and power consumption for efficiency of the blowers between 0-100% rates (Fig.58 and Fig. 59) are implemented in look-up tables used in a numeric model used in the construction of blower control. At the lowest efficiency 0% rated each blower generates some constant flow. On the other hand, 100% rated efficiency means reaching the maximum capacity. The airflow provision and power consumption discussed above depend on the amount of working blowers and their utilization is determined by the control system (Fig. 60).

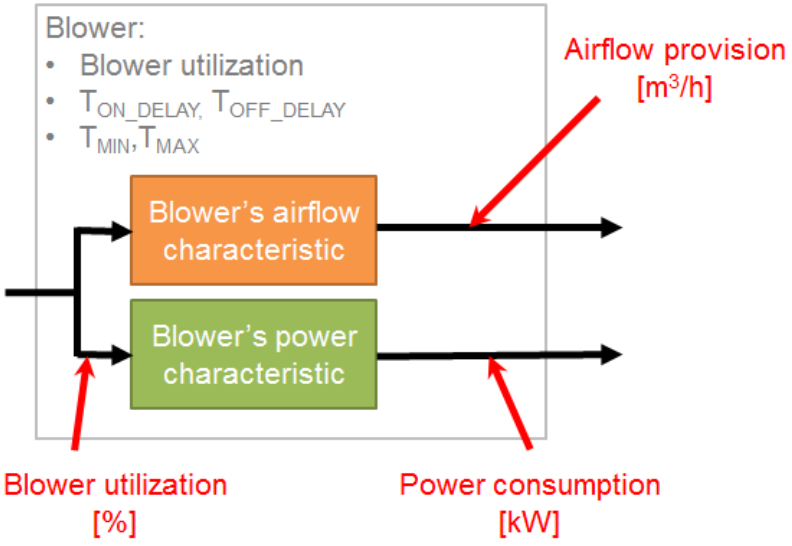

Fig. 60. Control of blowers adopted in the numeric model

Next, in Fig. 61 airflow demand has been demonstrated in the relation to power consumption per airflow unit. The author indicates the lines outlining the particular characteristics. This has been done by calculation of power consumption at unit airflow [in kW/(m^3/h)]. The lines are mapped in one figure to match characteristics of particular blowers (Fig. 62).

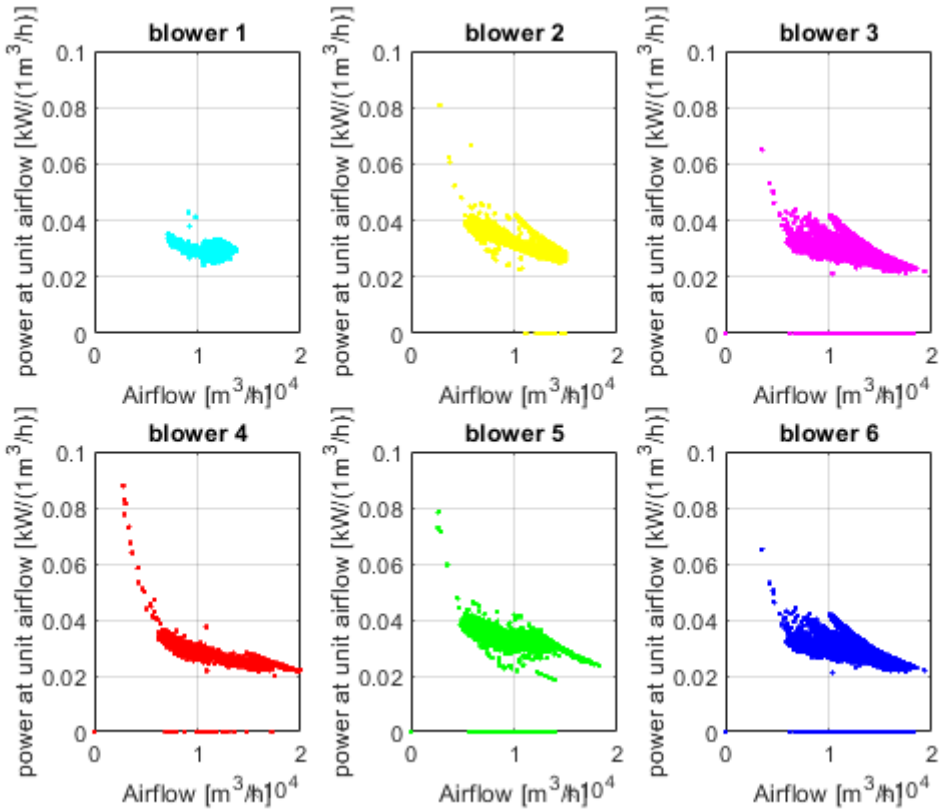

Fig. 61. Blower characteristic curves expressed as power consumption per airflow unit

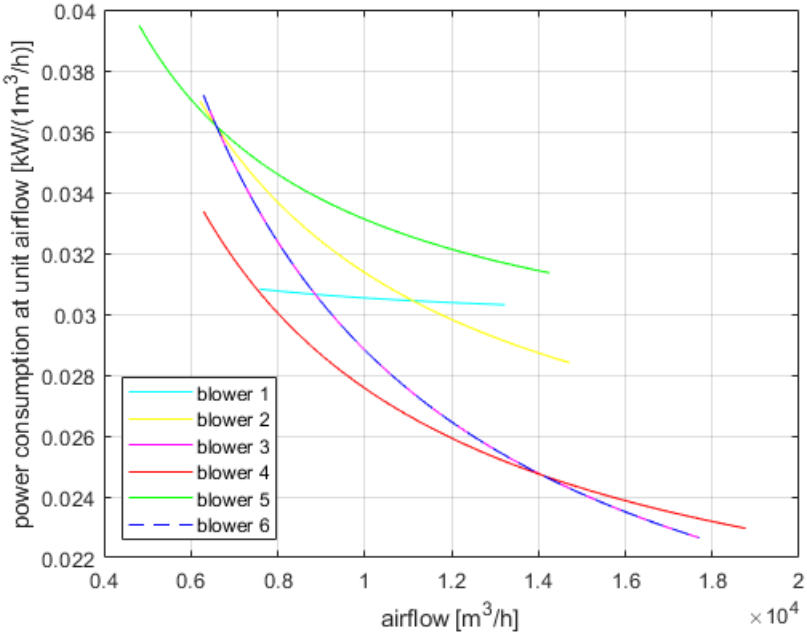

Fig. 62. Blower characteristic curves expressed as power consumption per airflow unit vs airflow - summary

Finally, on the basis of values describing efficiency of particular blowers are calculated. The analysis demonstrates the difference in operation of particular blowers. Presented in this paragraph, estimation of blowers is implemented in numeric model of Płaszów WWTP. On the basis of the efficiency factors in Tab. 11, the performance of particular blowers can be determined (as presented in section 4.3).

Tab. 11. Coefficients used in the simulations

Blower No.	Mean efficiency estimation (blower power/blower airflow)
	[kW/(m^3/h)]
1	0.0305
2	0.0315
3	0.0275
4	0.0264
5	0.0340
6	0.0275

Blowers' control strategy is expected to prioritize the most efficient blower. More precisely, the queue of blowers scheduled to start is proposed on the basis of their efficiency estimate. One can observe that blower with highest efficiency is blower 4, on the other hand blower 5 has the lowest efficiency. In practice, a maximum of 4 blowers are started. Hence, it is fair to conclude that blowers 2 and 5 do not work at all. They can be activated in case of failure of the blower with better efficiency.

5.2.3 Model of blowers in Płaszów WWTP and its simulation

In order to illustrate the operation of the blowers, the author implemented the MATLAB/SIMULINK model that has the characteristics of the air flow and electricity consumption for each blower described depending on the control utilization expressed in percentages (0-100%). The graphic below shows the structure of a single blower (Fig. 63).

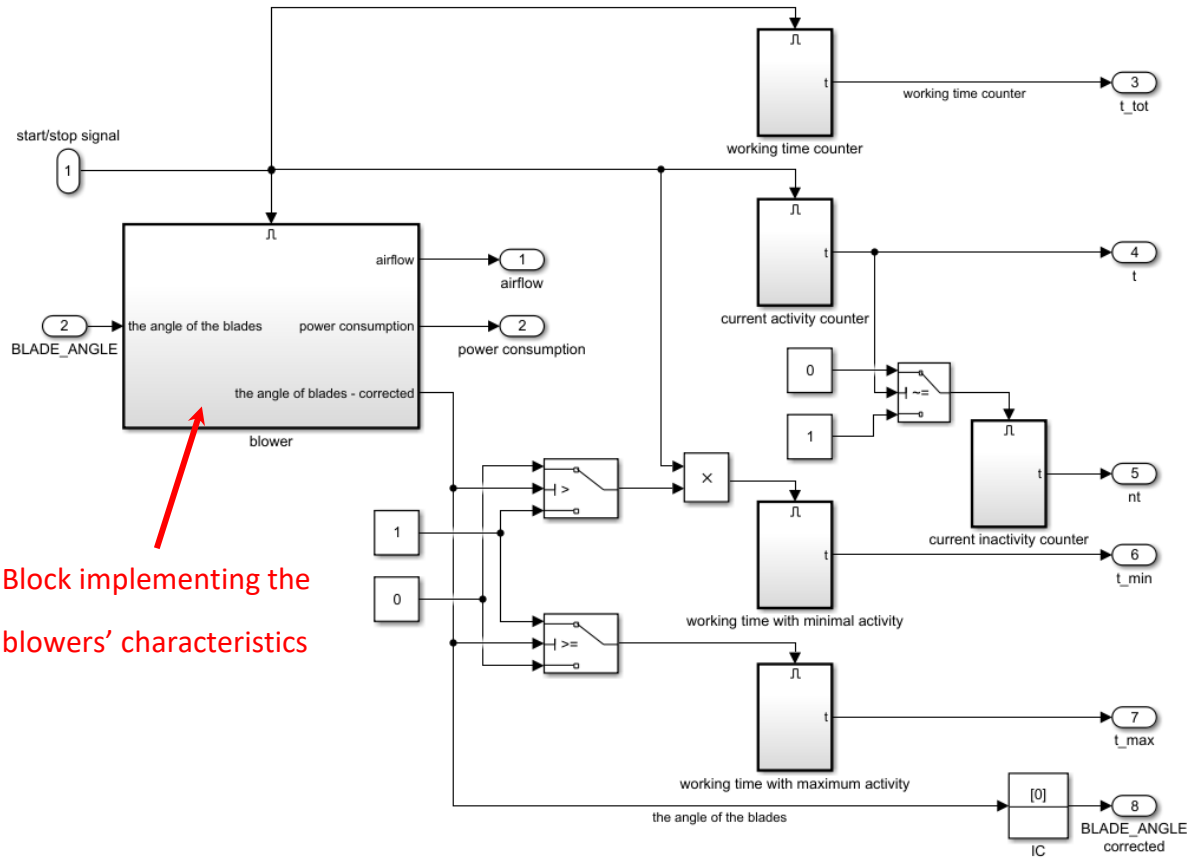

Fig. 63. Internal structure of blowers in model of WWTP in Matlab/Simulink

As blowers control adjustable set points are following:

- *the angle of the blades* – the angle of the blades ($BLADE_{ANGLE}$),
- *start/stop signal* – signals setting switching the blower operation of blower, adjusted by T_{ON_DELAY} and T_{ON_DELAY} defined in controller (Sec. 5.2.1).

The blowers' model outputs with the following operational parameters:

- *t_min* – working time of blowers with minimal activity (adjusted by T_{ON_DELAY}),
- *t_max* – working time of blowers with maximum activity (adjusted by T_{OFF_DELAY}),
- *t_tot* – working time,
- *t* – current activity time,
- *nt* – current inactivity time,

A simulation has been performed in which the input signal is the air flow obtained from the SCADA. The model of the entire aeration system is presented in the graphic below (Fig. 64).

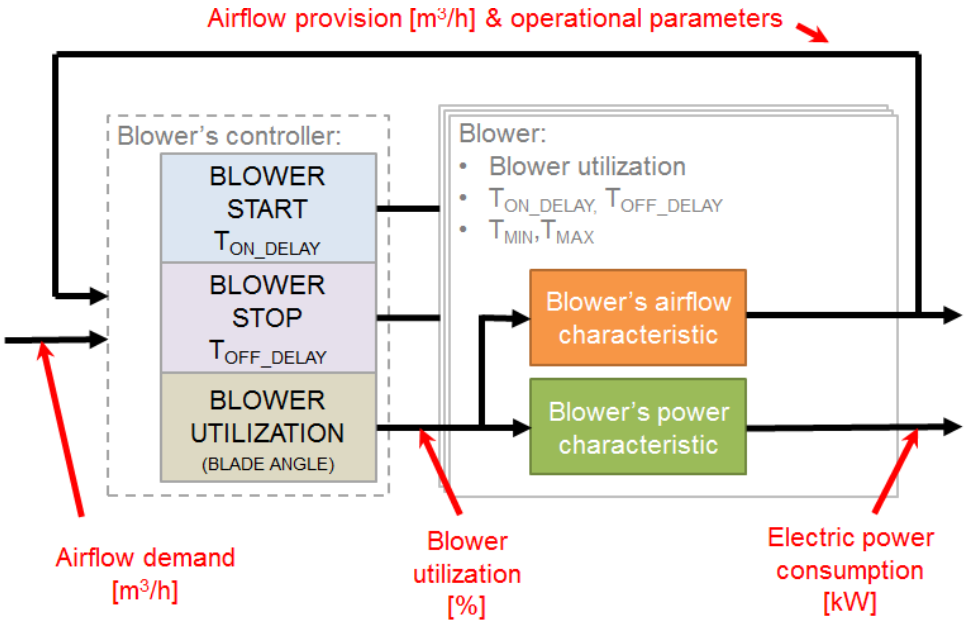

Fig. 64. The detailed plan blower's simulation

In this introductory simulation, the author uses SCADA measurements. The diagram below shows assumed values. The values of summarized airflow demand is presented in graphic below (Fig. 65). The second graphic presents the total power consumption registered during the period. An interesting observation is that the increase in air demand proportionally increases electricity consumption. Simulations are performed with airflow measurement as input. Available power consumption is compared with real data.

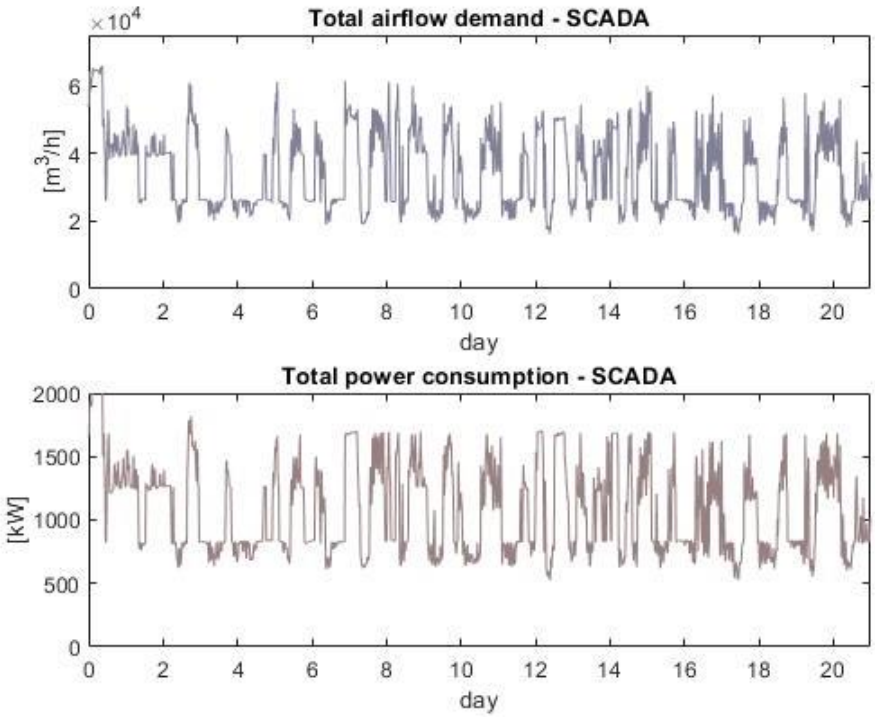

Fig. 65. Observed signals – total airflow in blowers and total power consumption

Simulations have been performed using the blower controller implemented as described above and in chapter 5.2.1.Initially, the blowers' set points, i.e. delay times are the following: T_{OFF_DELAY} equals 1h, T_{ON_DELAY} equals 1h.There is a high convergence of results. The first graph shows such parameters and describes obtained characteristics (Fig. 66).

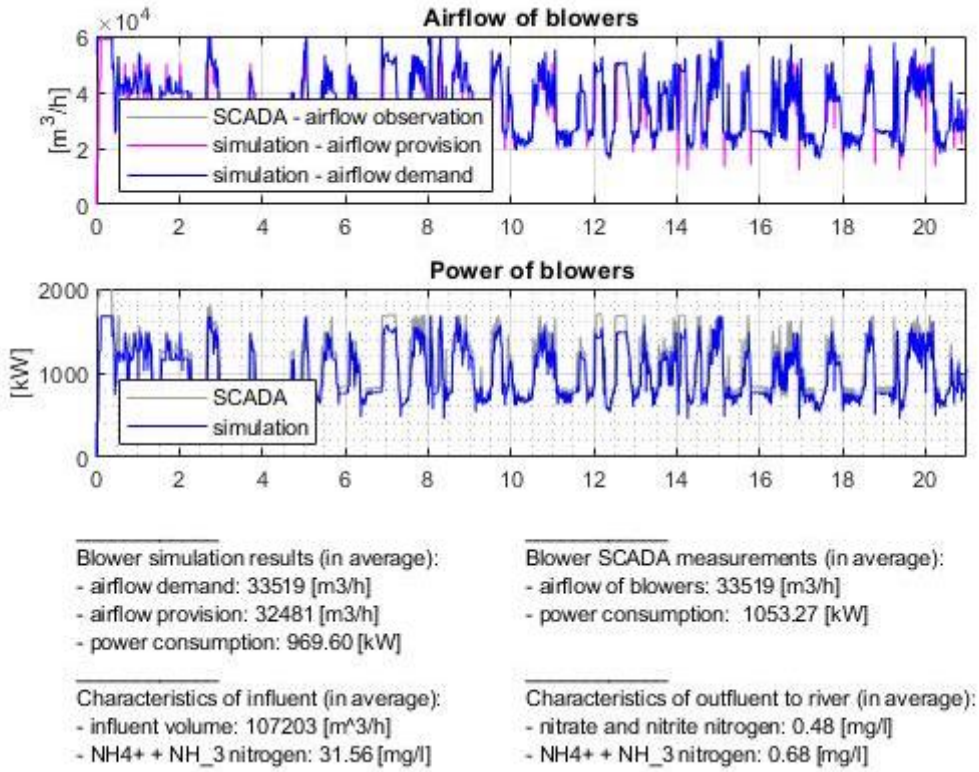

Fig. 66. Results of simulation for T_{OFF_DELAY} equals 1h, T_{ON_DELAY}equals 1hwith SCADA – total airflow and power consumption

The graphic below (Fig. 67) shows the variability of the blowers' efficiency which affects the number of blowers turned on. To summarise, the algorithm that turns the blowers on and off will do its job.

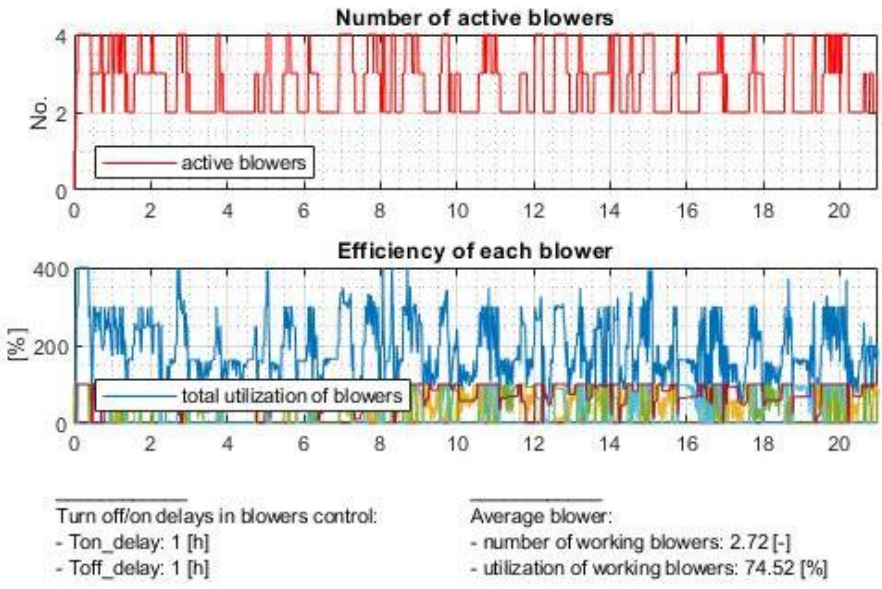

Fig. 67. Results of simulation for T_{OFF_DELAY} equals 1h, T_{ON_DELAY} equals 1h– number of blowers working and their utlization

It is worth mentioning that during this 21 day-long period only 4 blowers are working (are activated in accordance with the efficiency demonstrated in Sec. 5.2.2). As presented in previous paragraphs, this practice is expected.

5.2.4 Simulation utilizing blowers with BSM1 model

The presented approach describes how the control of blowers affects the processes in the reactor. The reverse approach is assumed in this implementation (Fig. 68).The oxygen demand is determined based on the known oxygen and ammonia content in the reactor. Then airflow demand is calculated. Such airflow to reactors lowers the pressure in the collector. The decline in pressure forces blowers to adjust utilization to cover the demand. Finally this blowers' operation is converted into specific electric energy consumption.

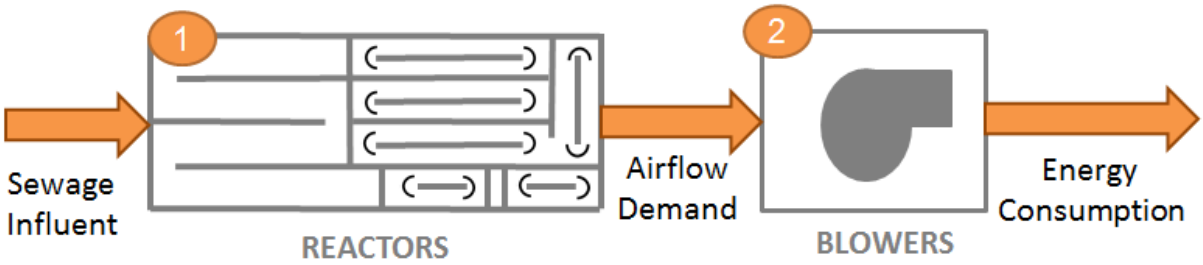

Fig. 68. General scheme of the purification process presented in the dissertation

As presented in Sec. 3.2, the BSM1 model, which simulates the operation of the reactor, derives the demand for oxygen in the form of the time-varying parameter KLa. Further, this parameter is used to develop the oxygen demand in the reactor. The following equation presents in details converting the KLa into airflow (Sec. 3.5.5)

$$OTR_{TOTAL} = KLa \cdot (c^{sat} - c) \cdot V \tag{21}$$

$$AIRFLOW = \frac{OTR}{OTE \cdot CF_1} \tag{22}$$

The value of the correction factor is chosen empirically so that the ranges of obtained oxygen flow correspond to the measurements of SCADA sensors readings. In this case, this value is 3600. Oxygen transfer efficiency is assumed to be 0.3. CF value of parameter was empirically selected so that the results of the BSM1 model and the actual SCADA readings coincide. In this case, this value is 3600.

The following graphic presents the layout of simulation containing reactors and blowers (Fig. 69).

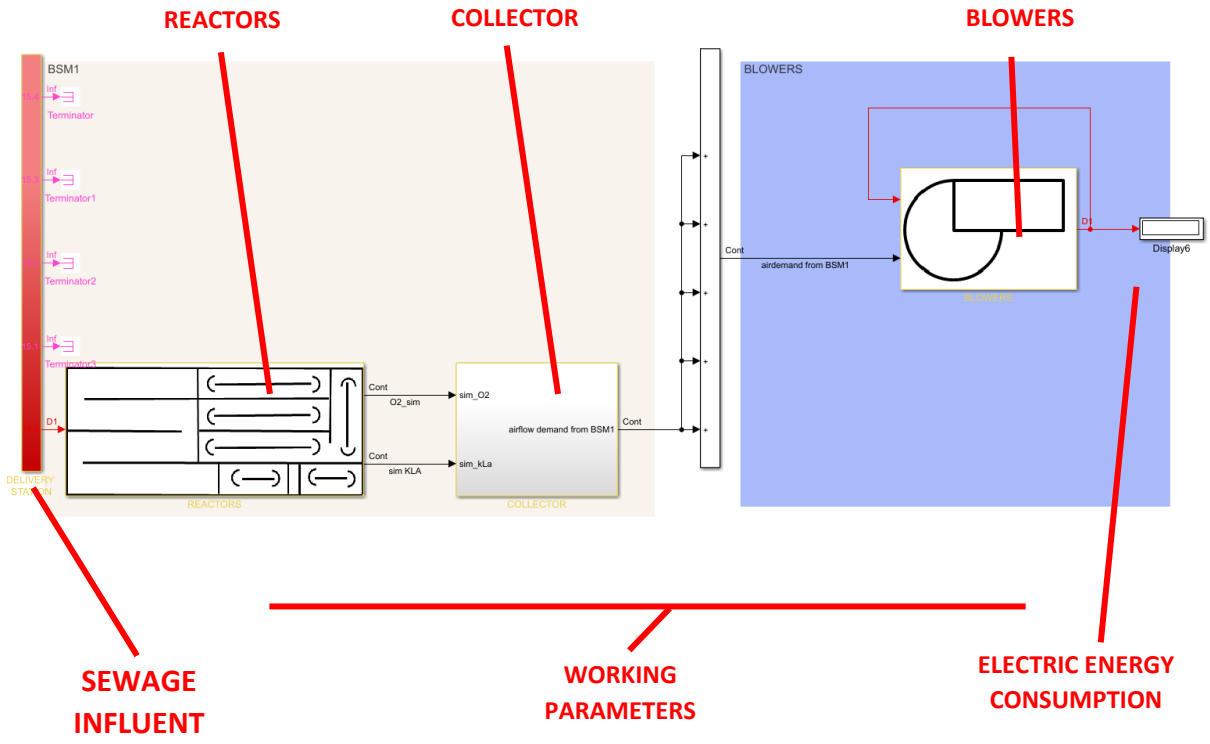

Fig. 69. Model of Płaszów WWTP including the blowers

To sum up, the diagram presented above consists of the following groups:

- REACTORS – the numeric model of the 5 reactors based on the BSM1 model. Estimation of oxygen demand based on sewage quality correlated with SCADA read-outs. Block combines the reactor and blowers by numeric translation of the value of KLa measured by the reactor to airflow demand expected in blowers;
- COLLECTOR – block calculating airflow demand on the basis of KLa, O_2sim;
- BLOWERS – numerical model of blowers. In the treatment plant, the oxygen demand reported from the reactor level is input. The electric power demand is calculated based on the blower operation.

Input and output of the system:

- SEWAGE INFLUENT – values based on literature data and SCADA measurements obtained from a working sewage treatment plant, the output is the value of the KLa factor;
- WORKING PARAMETERS – values observed during WWTP's operation;
- ELECTRIC ENERGY CONSUMPTION – value of power spent during aeration.

A sewage treatment plant model has been prepared along with the analysis of control systems.

The previous paragraphs describe all components of a complete biological wastewater treatment system: input data (Sec. 4.4), reactor model (Sec. 5.1), oxygenation model (Sec. 5.2). In this paragraph, the author considers the case of simulation performed for the system combining BSM1 reactors and blowers(Fig. 70). This description of influent is used for estimation of airflow demand.

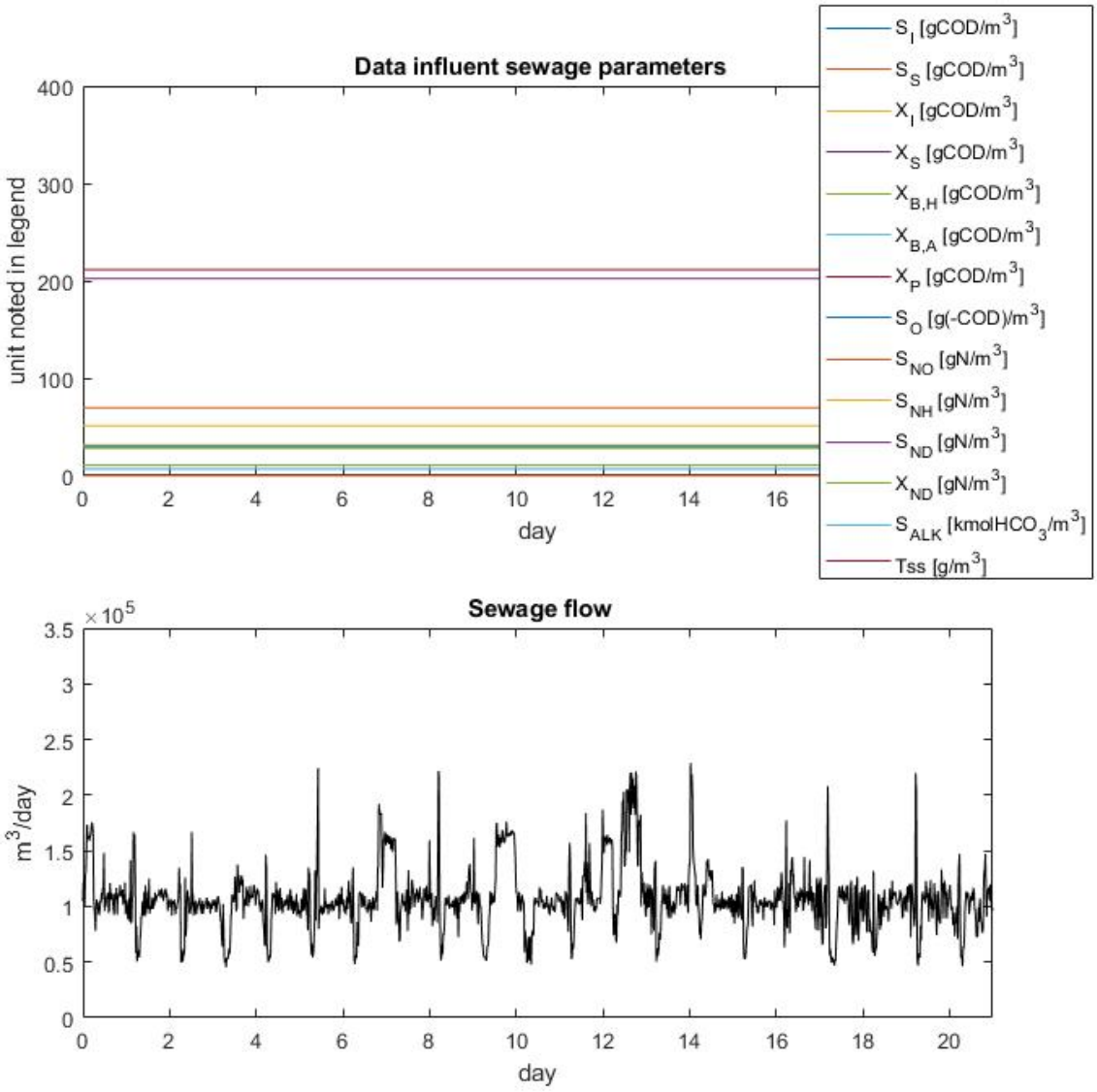

Fig. 70. Matrix DATAINFLUENTused in this simulation

The simulative results are juxtaposed with real SCADA measurements to validate the results of airflow estimation. The simulation model based on BSM1 reflects the internal processes in reactor and airflow demand is estimated on the basis of results. The resulting airflow demand is presented below (Fig. 71).

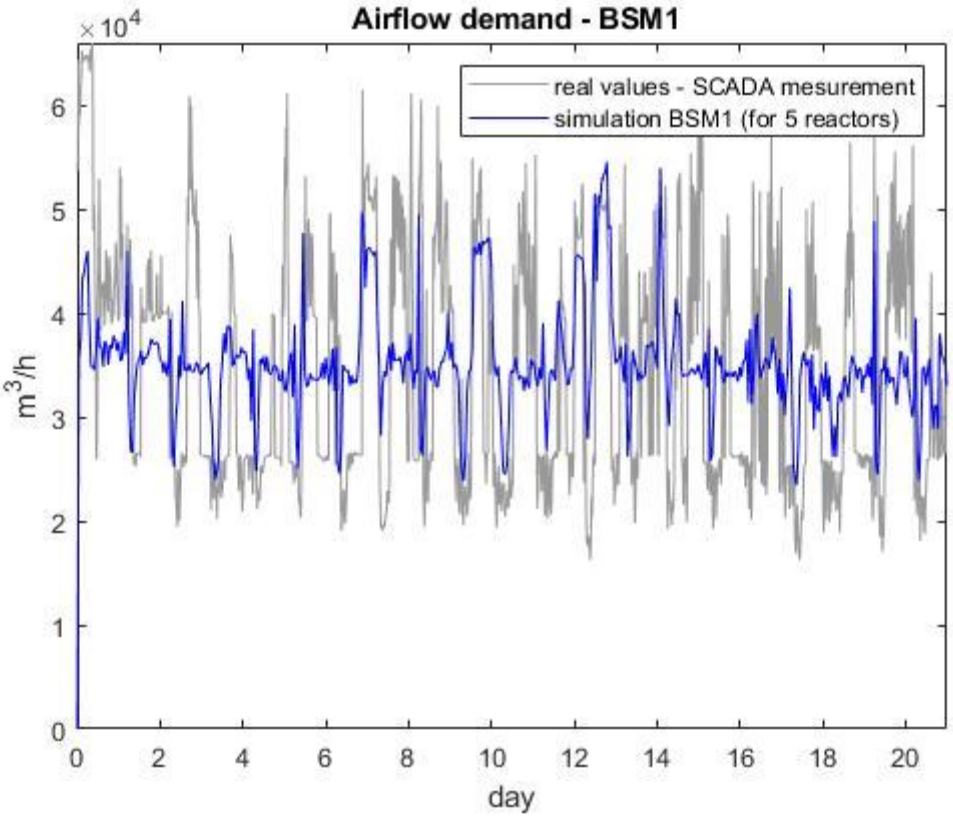

Fig. 71. Airflow demand – real and results of simulation

Later, such estimation of airflow demand is used in model of blowers. This estimation of airflow demand is used by the virtual model of blowers to estimate total power consumed by the blowers. It is worth mentioning that the blowers' characteristics are as in Sec. 5.2.3.

The results of such simulations are presented in graphics below. Fig. 72 presents simulation results that are similar to the measurements of the real object. In particular, it is worth noting that sometimes large changes in influencing wastewater are noticeable in air flow readings and in blower control. This confirms the compliance of the entire facility with the reality. The simulation environment prepared in this way is the subject of further analysis in which the operation of the entire system has been checked in terms of energy optimization. Fig. 73 presents characteristics for parameters describing the operation of blowers' during their operation in simulation. It is worth noting that between 2 and 4 blowers operate in one moment, their performance fluctuates adapting to the demand. Summing up the efficiency of working blowers' (2-4 blowers operate in the range of 0%-100%), the control in the range of 200%-400% of the total efficiency is obtained.

.

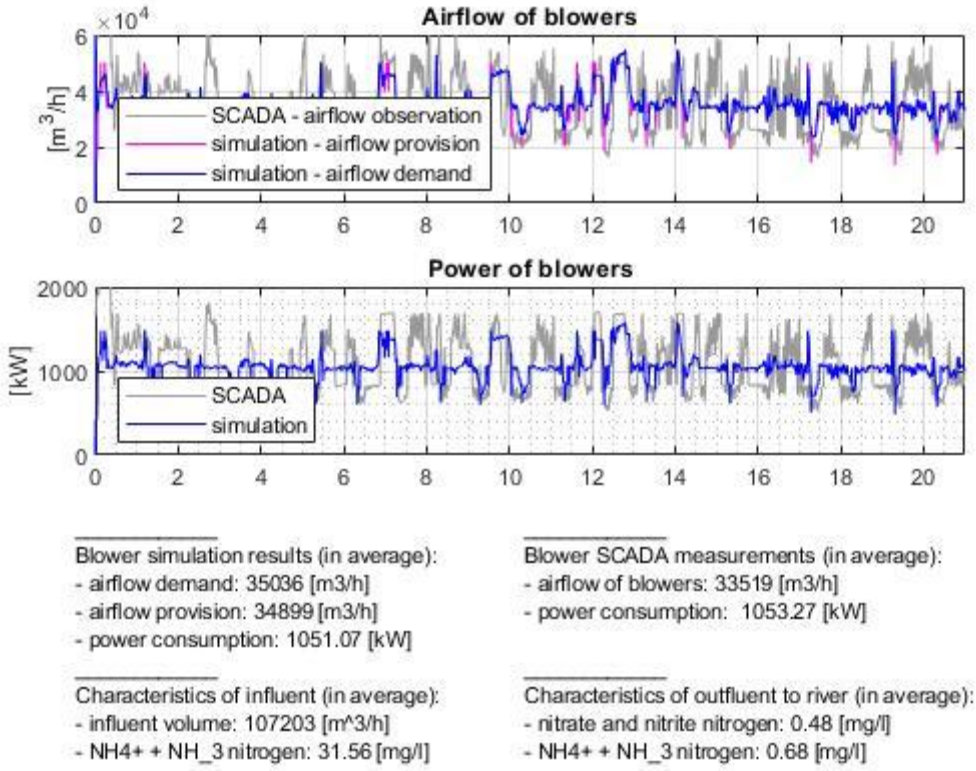

Fig. 72.Results of blowers simulation with control algorithm – measurements

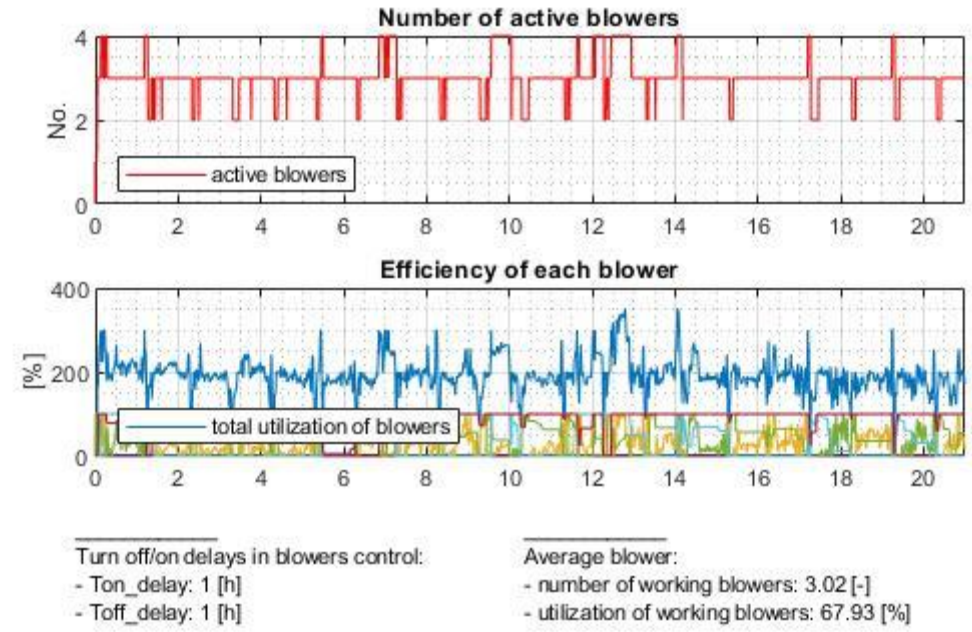

Fig. 73. Results of blowers simulation with control algorithm – characteristics

5.3 Optimizing WWTPs' operation control – state of the art

The model of sewage treatment plant shown in the previous paragraph allows for testing the performance characteristics of the system under various conditions. An interesting topic remains the study of the properties of the treatment plant in terms of reducing electricity consumption in blowers. Thus, how has it been done?

The issues of energy optimization of sewage treatment plants are a broad object of scientific research. It seems right because the process of pumping and blowing air is the most energy-consuming aspect of the treatment plant operation. This paragraph presents the scientific state of the art in this field. Authors propose various optimization techniques to reduce the use of electricity.

Most of the WWTP aeration systems involve a proportional-integral-differential (PID) controller. PID parameters regulation has been done utilizing:

- aeration profiles [117], [118],
- adaptive on-line tuning [119],
- scheduling adjustment of the gain parameter [120], [121],
- neural networks [122],
- model predictive control [123],
- fuzzy controller [95].

In [118], authors optimize aeration profile using MINLP programming technique (Sec. 2.4.2) based on the model of activated sludge tank calibrated and validated with data from a real plant. Authors analyze the profits achieved after utilizing non-uniform aeration (NUA) control instead of uniformly distributed aeration (UDA).

In [119], authors demonstrate an algorithm focused on auto-tuning the PI control parameters to satisfy effluent quality condition and optimizing the nitrogen removal at the same time. Authors research the system utilizing the numeric model performed in BSM1. Control is portioned into two separate PID controllers.

In [117] and [118], authors analyze the modernization of Kaapla WWTP using dissolved oxygen feedback. Authors conclude that large reductions in air consumption can be made with a simple DO control strategy. It increases the process sensitivity to influents' dynamics and impacts the reduction of volumes of aerated air.

Brdys 2002[123] deliberates the hybrid model predictive controller (HMPC) to schedule the efficiency of blowers. The example of the Kartuzy WWTP is described. In [124], authors describe other WWTPs in Poland. The issues connected with fuzzy modeling of the chemical-biological processes for the MPC control strategy of the electrical blowers are presented.

In [125], the author points out some degree of insight into the problem of energy overuse in the activated sludge process at the wastewater treatment plant at Perth, Scotland. The ASM1 model has been used to describe the level of dissolved oxygen in three aeration sections, each containing one mechanical aerator. To solve that issue the KLa value is calculated using the Simulink schematic below (Fig. 74).

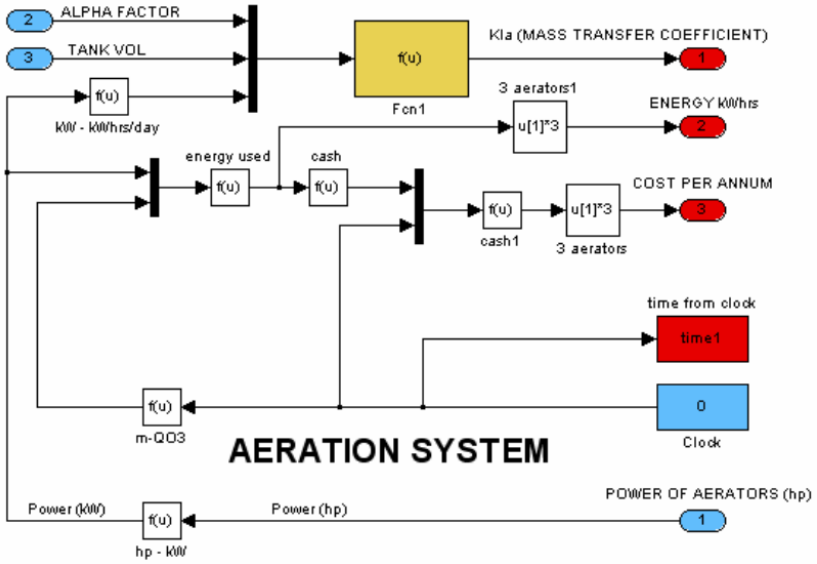

Fig. 74. Representation of Perth Mechanical Aeration system in Matlab/Simulink

In [126], authors base on the analysis that has been obtained from the Detroit Water and Sewerage Department (DWSD), the largest single-site wastewater treatment facility in the United States. The WWTP has been optimized using the Simulated Annealing (SA) algorithm.

The publication [127] presents the energy audit of membrane bioreactor (MBR) in Schilde, Belgium. The publication [128] analyses the benchmark simulation model for membrane bioreactors (BSM-MBR). Aeration energy (AE) is presented in the equation that split into the contributions from fine bubble aeration in the bioreactors and coarse bubble aeration in the membrane unit. The publication [129]shows another version of the AE equation which has been used in SBR WWTPs.

In [130], Larrson analyses the savings with a new aeration and control system. The implementation of ASM1 in WWTP in Sternö, Swedishis is utilized. The author proposes a method to calculate standard aeration efficiency (SAE) (Fig. 75).

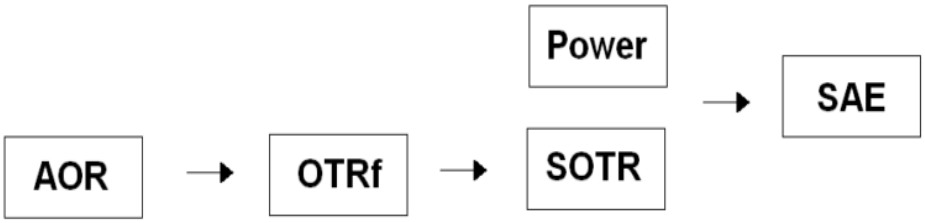

Fig. 75. Overview of calculations to find the SAE [130]

In [131], the author describes the Lancaster (UK) wastewater treatment that works for around 100 000 population. Authors discuss the implementation of the model predictive control (MPC) for wastewater treatment plants to reduce the costs of aeration. A process efficiency of approximately 0.8 kWh/kg BOD is considered to be a good operation.

Olsson and Carlsson[132] presents the step-by-step schematic how level of NH_4^++NH_3 nitrogen in influent is regulated by valve position in diffusors supporting air (Fig. 76).

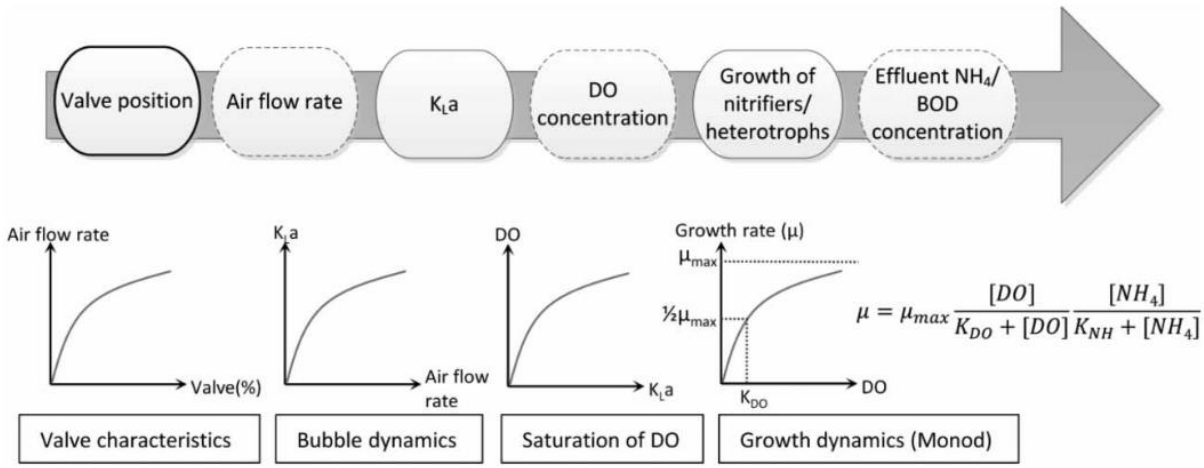

Fig. 76. The interpretation of process from valve position to effluent ammonium concetration [132]

In series of publications *Methods for Energy Optimization in Wastewater Treatment Plants*[91] and [134], authors demonstrate the energy optimization case study of WWTP in San Pedro Del Pinatar, Spain. The reactor is a membrane biological reactor (MBR). The first document discusses variables used in control of processes in the activated sludge system. The adoption of a real-time control system makes the oxygen demand lower and reduces overall energy consumption of the installation to more than 15%. In the second paper, authors present reductions of energy consumption of the San Pedro del Pinatar WWTP using flow modeling and simulation techniques. Authors propose the following stages of optimization: selection of best operating conditions and regulation of airflow injection by the diffusers. Additionally, the determination of age and conditions of air injecting components is important. Their results allow to reach more than 35% of reduction in the overall energy consumption of the facility. Fig. 77 outlines the stages of process that can be optimized (according to [90]).

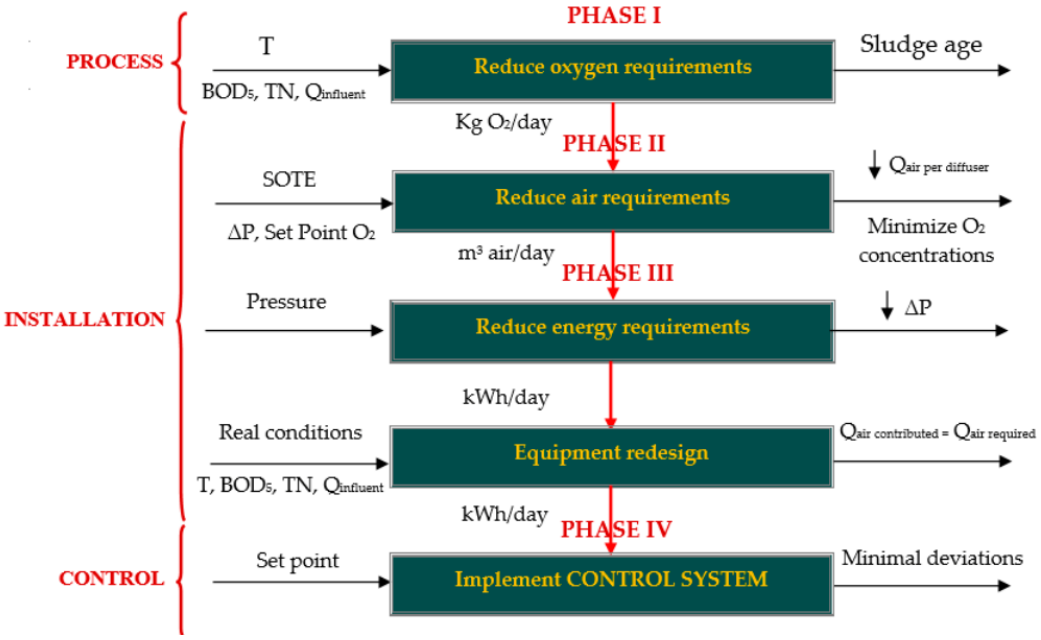

Fig. 77. The electrical analogy of the aeration system model [90]

5.4 Methods used to validate the model

After reviewing the literature, the author notes that the available resources do not show comprehensive models simulating the process of the Krakow-Płaszów wastewater treatment and oxygenation in biological reactors. Previous paragraphs describe the implementation of this sewage treatment plant model based on the BSM1 numerical model. Sample runs present the operation of the numerical model. The modification of parameter could significantly impact the behavior of the simulated treatment plant. The problem concerns both the parameters of the inflowing sewage and parameters. Changing parameters can significantly change the behavior of the model. Moreover, the model requires adoption of parameters to match the real SCADA signals.

The author has performed the following test in order to study the model:

- Characterization of uncertainty with Morris simulation – the sensitivity of wastewater parameters in BSM1 has been examined in terms of their importance in the purification process. For this purpose, the Morris method of sensitivity assessment has been used. More details are in chapter 6;
- Performance check with Kalman filter and its derivatives – in relation to the above assumptions, optimization algorithms have been used to reduce electricity consumption in the sewage treatment plant. Then, in the BSM1 model, critical parameters have been estimated using identification procedures based on the Extended Kalman Filters. The procedure has been initially tested by using synthetic feed rate and concentrations proposed in BSM1. Later, it has been applied to a real object, the Płaszów Sewage Treatment Plant located in Kraków. The analyses described above are described in chapter 7;

- The operation of reactor with blowers modeled in dissertation has been examined in terms of minimization of electric energy consumption. The author analyses how influent characteristics affect the electricity consumption. The example of simulations with statement of results is presented in chapters 8.

5.5 Potential to exploit the model in order to optimize energy consumption

Eventually, the author exploits the model implementing the characteristics of the treatment plant. The author proposes an approach aimed at optimizing the operation of wastewater treatment plants, taking into account the reduction of electricity consumption. In the presented dissertation, the author puts forward control optimization exploiting criteria of electric energy consumption minimization. The blower control algorithms is proposed to reduce electricity consumption in this facility. More precisely, the method of blower efficiency control by adjusting the on/off time of the blowers in the wastewater treatment plant has been implemented. This solution allows to achieve favorable operating points of the blowers guaranteeing lowering electricity consumption. The details of the optimization are presented in the chapter 9.

6 Characterization of model sensitivity

6.1 General description of sensitivity algorithms

Global sensitivity analysis is a numerical tool widely used in computer simulations to check the effect of a set of parameters on the response of a such non-linearities in a numeric system. These methods enable fast testing of a numeric model. Practice proves that importance of some factors can differ significantly. It mainly concerns determining the sensitivity of a given project's profitability to changes in the input parameters of a given numeric model. Three kinds of methods are distinguished [134]:

- the screening – coarse sorting of the most influential numerous inputs,
- the measures of importance – quantitative sensitivity indices,
- deep exploration of the model behavior – measuring the effects of inputs on their all variation range.

Screening methods arebased on discretization of input data in levels. The purpose of this identification is to assess how subtle changes in the input parameters impact simulation results. The numerous combinations of input allow for the selection of the most affecting influent parameter -it allows to reduce the number of input parameters only to the most important ones. Such analysis allows to research realistic structure of the complex models. Such a simple screening simulation is used before other more complex optimization algorithms [135].

A variance-based sensitivity analysis can be performed using the following screening sampling techniques: Sobol and Morris [136].

6.2 Morris screening method

This analysis is based on series of simulations performed with heterogeneously changing parameters to assess the influence of a particulate parameter to the system. A trajectory is set of simulations, in every one parameter it is changed and the parameter changes one at a time. Thus, the number of simulations in the trajectory equals to the number of variables plus one [137]. This is how the trajectories are created. On the basis of these simulations, the elementary effect is calculated [139] and [140]. The elementary effect is the measure of response for a particular parameter that is changed in simulation. The elementary effect is calculated with the equation:

$$ee_j^{(i)}(x) = \frac{\left[f\left(x_1^{(i)}, x_2^{(i)}, \dots, x_{j-1}^{(i)}, x_j^{(i)} + \Delta, x_{j+1}^{(i)}, \dots, x_k^{(i)}\right) - f(X^{(i)})\right]}{\Delta} \tag{23}$$

Where j is the variable obtained at the $i\text{-}th$ repetition. Δ is predetermined multiple of $1/(n\text{-}1)$ where $n$represents number of "levels" of the design. Then, the ee thus calculated is submitted to the statistical analysis (sum of all ee, mean). On the basis of these indicators, the influence of parameters' changes to the operation of the model is characterized.

6.3 Uncertainty algorithms in WWTPs – state of the art

As mentioned above, numeric models of WWTPs are strongly non-linear. Thus, numeric models of WWTP's are widely researched in literature.

The study of uncertainties in models of WWPS is presented in [140]. In this document, three uncertainty sources are discussed: caused by stoichiometric, bio-kinetic and influent parameters; due to hydraulic behavior of the plant and mass transfer parameters or due to the combination of both of them. The Latin hypercube sampling (LHS) is proposed and Monte Carlo simulation procedure is used.

The systematic application of regression analysis to ASM is presented in [141], where the sensitivity of the BSM1 wastewater quality indicator to bio-kinetic parameters and the inflow ASM1 fractions is examined. Regression analysis is also used in [62] to investigate the sensitivity of other process variables, such as nitrate and ammonia in waste water, sludge production and aeration energy.

In [142], a variance-based decomposition method is proposed to investigate the role of 79 ASM2d parameters on the amount of chemical properties of wastewater inside wastewater treatment plant reactors. In this study, sensitivity analysis is used as a way to obtain information about the observability of the model. Indeed, it is expected that parameters that show a significant influence on the model response can be also identified.

In [143], the revised version of Morris method is presented. In this research. DESASS simulator is used. Authors emphasize the significance of sampling. Screening is adopted to most influential parameters of fuzzy control of WWTP. Random sampling can lead to discordant coverage of the parameter space. On the other hand, Morris approach provides sufficient results. Authors propose 70 trajectories in this simulation.

The description of the practical implementation of the algorithm is marked in the next paragraph. The procedure calculates a sensitivity for changes in model's properties. Morris analysis can be performed on many aspects of purification.

The author of the study uses Morris analysis implemented in the novel model of Płaszów WWTP. In particular, such simulation is used to analyze the sensitivity of sewage influencing the treatment process and to validate the impact of process parameters for treatment quality.

6.4 Sensitivity analysis of BSM1 process

6.4.1 Validation of process variables

The dynamics of wastewater treatment based on BSM1 is described with 19 parameters whose values must be considered in simulation. Thus, parameter screening can be carried out to assess the influence of the stoichiometric and kinetic parameters on the BSM1 response, namely the average value of NH_4^++NH_3 nitrogen (SNH) and O_2 (SO) levels in the reactor sections.

In Tab. 12, the assumed variability ranges are presented (based on [140] and [144]). The question to be solved now is to specify the parameters with a key impact on the operation of the treatment plant.

Tab.12. Values of stoichiometric and kinematic parameters considered in the sensitivity analysis ([140][144])

Parameter	Unit	Min	St. Val.	Max
Autotrophic yield Y_A	gCOD/gN	0.23	0.24	0.25
Heterotrophic yield Y_H	gCOD/gCOD	0.64	0.67	0.70
Fraction of biomass yielding part. products f_P	-	0.015	0.08	0.2
Mass N/mass COD in biomassi_{XB}	gN/gCOD	0.04	0.08	0.12
Mass N/mass COD in products from biomass i_{XP}	gN/gCOD	0.05	0.06	0.07
Heterotrophic max. specific growth rate μ_H	day^{-1}	3.0	4.0	5.0
Half-saturation coefficient (hsc) for heterotrophs K_S	$gCOD/m^3$	5.0	10.0	15.0
Oxygen hsc for heterotrophs $K_{O,H}$	gO_2/m^3	0.1	0.2	0.3
Nitrate hsc denitrifying heterotrophs K_{NO}	gNO_3/m^3	0.25	0.5	0.75
Heterotrophic decay rate b_H	day^{-1}	0.29	0.3	0.32
Corr. factor for anoxic heterotrophs growth η_g	-	0.6	0.8	1.0
Correction factor for anoxic hydrolysis η_h	-	0.6	0.8	1.0
Max. specific hydrolysis rate k_h	$gX_s/gX_{BH}CODday$	2.25	3.0	3.75
Hydrolysis hsc of slowly biodeg. substrate K_X	$gX_s/gX_{BH}COD$	0.075	0.1	0.125
Autotrophic max. specific growth rate μ_A	day^{-1}	0.48	0.5	0.53
Ammonia hsc for autotrophs K_{NH}	gNH_3/m^3	0.5	1.0	1.5
Autotrophic decay rate b_A	day^{-1}	0.04	0.05	0.06
Oxygen hsc for autotrophs $K_{O,A}$	gO_2/m^3	0.3	0.4	0.5
Ammonification rate k_a	$m^3/gCOD/day$	0.03	0.05	0.08

In the Morris analysis pictured below, a set of simulations taking into account the variability of input parameters are executed. To make this simulation, the set of trajectories is prepared. In each trajectory, $n+1$ simulations are performed, where n is the number of parameters. In each subsequent simulation, the value of one random parameter changes. Therefore, for 19 wastewater parameters 20 simulations must be performed (Fig. 78).

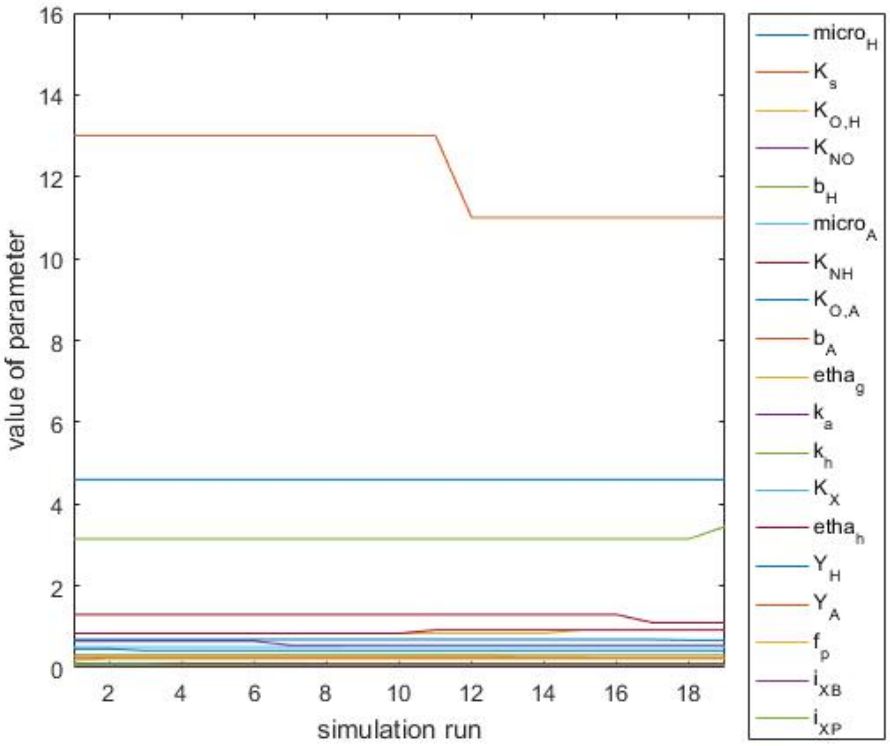

Fig. 78. Example trajectory based on parameters changing in successivesimulations

The presented simulation consists of 10 trajectories. In total, 200 simulations of the sewage treatment plant operation has been made. Values of PAR stoichiometric and kinetic parameters on the Tab. 12have been adopted as in the figure above (Fig. 78). Only one of the 19 analyzed values changes in each simulation. The results of the simulation are SNH and SO measurements (NH_4^++NH_3 nitrogen in KDN3 and O_2 in sections KDN3, KN1, KN2, KN3, KN4). The sum of absolute values has been calculated for the measurements' time vectors. This value becomes an elementary effect and becomes the basis for further analysis. The resulting elementary effects are presented in the graphic (Fig. 79).

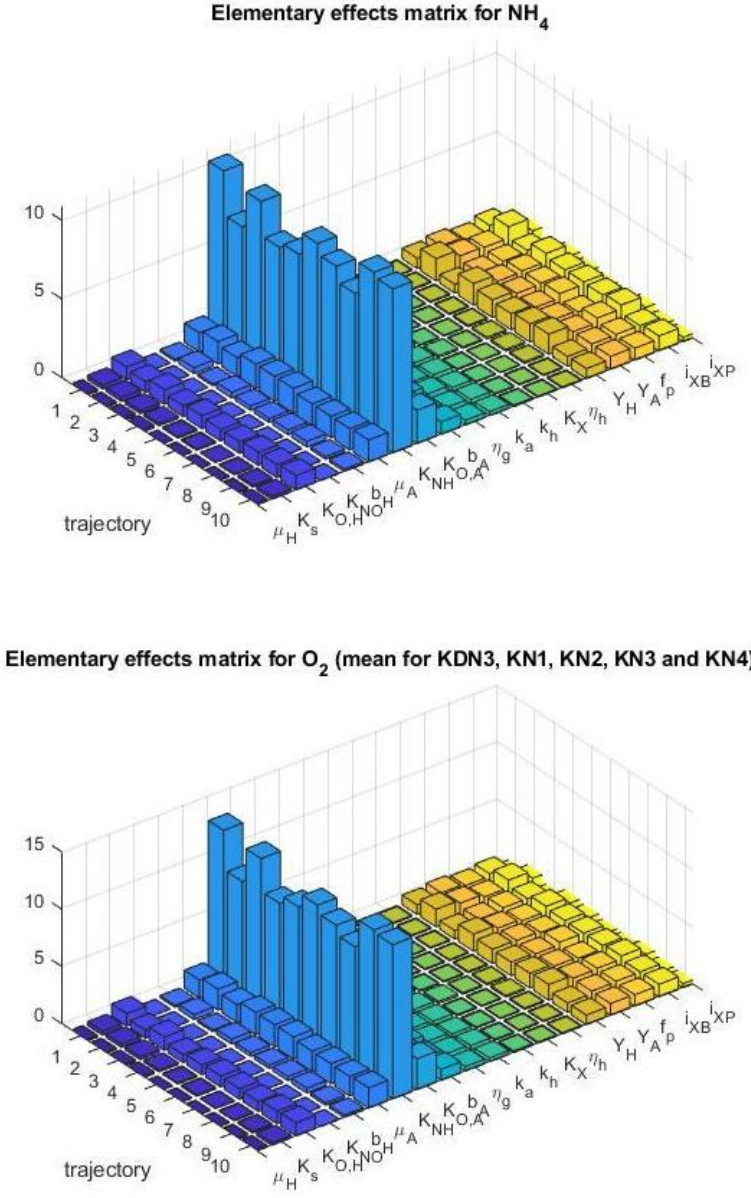

Fig. 79. The matrixes of elementary-effects achieved in Morris simulation

Finally, after calculating the mean value and standard deviation, the effect of particular parameters on the operation of the treatment plant can be assessed. The first graphic(Fig. 80) manifest mean values and standard deviation for NH_4^++NH_3 nitrogen values. The second one (Fig. 81) shows the mean values and standard deviation for O_2 values in individual sections of the rector.

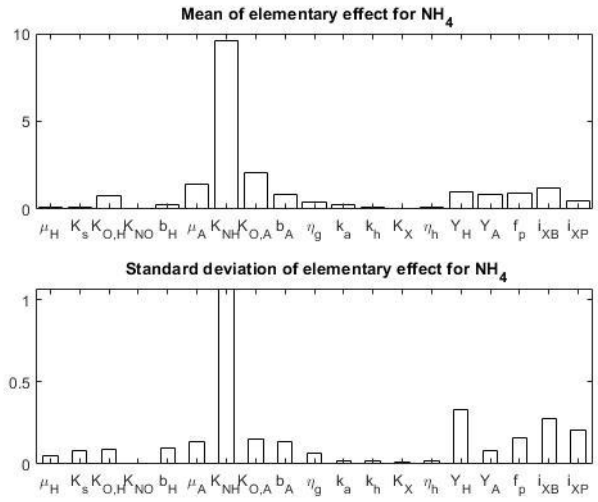

Fig. 80.The mean and standard deviation for NH_4^++NH_3 nitrogen (SNH) and O_2 (SO) in Morris simulation

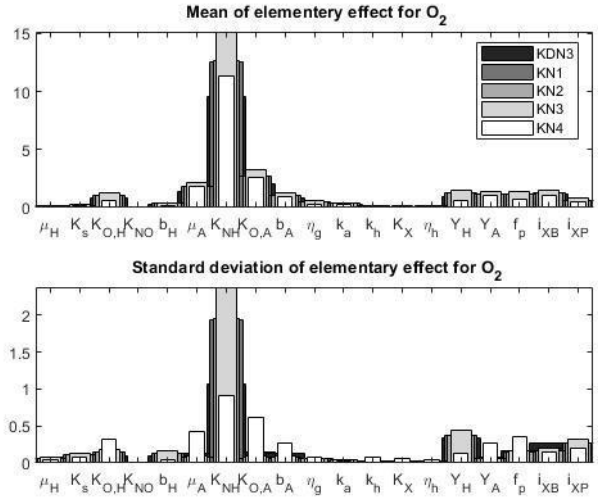

Fig. 81. The mean and standard deviation for NH_4^++NH_3 nitrogen (SNH) and O_2 (SO) in Morris simulation

The analysis reveals that ammonia half-saturation coefficient for autotrophic biomass (K_{NH}) has a decisive role in the wastewater treatment. Indeed, the parameter directly impacts aerobic growth of autotrophs. It is also worth noting that the change in half saturation coefficient K_{NH} for autotrophs has the highest impact comparing with other half heterotrophic saturation coefficients (K_{NO}, $K_{O,H}$). Moreover, it should be observed that the means and standard deviations of elementary effects for both NH_4^++NH_3 nitrogen (SNH) and O_2 (SO) responses show the same trend. It means that the process is in general non-linear (as expected) due to the complexity of the biological process. Finally, sensitivity diagrams say

that several process parameters are not reflected in the values of NH_4^++NH_3 nitrogen (SNH) and O_2 (SO) [145].

6.4.2 Validation of influent parameters

BSM1 model defines several key parameters that affect both influent and the purification process themselves. Thus, it can be assumed that the selected quality parameters in incoming sewage have a key impact on the treatment process.

Tab. 13 presents the nominal value set in Płaszów that is based on BSM1. Those values are included to the DATAINFLUENT reference signal that is included in the ASM1 package[78]. The minimal and maximal values are defined as reference values limiting the possible range of parameter variation in the Morris simulation.

Tab.13.List of ASM1 variables[71] and their values considered in the sensitivity analysis [62]

No	Parameter	Influent parameter	Constant value set in BSM1	Płaszów WWTP		
				Minimal value	Nominal value set in Płaszów	Maximal value
1	Soluble inert organic matter	S_I	30	29	30	31
2	Soluble inert organic matter	S_S	69.5	64.5	69.5	74.5
3	Particulate inert organic matter	X_I	51.2	46.2	51.2	56.2
4	Slowly biodegradable substrate	X_S	202.32	192.3	202.32	212.3
5	Active heterotrophic biomass	X_{BH}	28.17	25.17	28.17	31.17
6	Active autotrophic biomass	X_{BA}	0	0	0	0
7	Particulate products arising from biomass decay	X_P	0	0	0	0
8	Oxygen	S_O	0	0	0	0
9	Nitrate and nitrite nitrogen	S_{NO}	0	0	0	0
10	NH_4^++NH_3 nitrogen	S_{NH}	31.56	26.56	31.56	46.56
11	Soluble biodegradable organic nitrogen	S_{ND}	6.95	6.55	6.95	7.55
12	Particulate biodegradable organic nitrogen	X_{ND}	10.59	9.59	10.59	11.59
13	Alkalinity	S_{ALK}	7	6	7	8
14	Total Suspended Solids	TSS	211.2675	191.26	211.2675	231.26
15	Flow rate	Q	18 446	111 000	120 000	130 000

This part analyses the effect of the above influent parameters on the value of NH_4^++NH_3 nitrogen (SNH) and O_2 (SO) in the treatment plant. In total, 160 simulations of the sewage treatment plant operation have been made. Influent parameters based on the Tab. 12 have been adopted as in the figure above. Only one of the 15 analyzed values changes in each simulation. Next, the simulation results in measurements in reactor - NH_4^++NH_3 nitrogen (SNH) in KDN3 and O_2 (SO) in sections KDN3, KN1, KN2, KN3, KN4.

Simulation presented below consists of 10 trajectories(Fig. 82). In each trajectory, 15 parameters are changed. As in previous simulation, the sum of absolute values has been calculated for the measurements' time vectors.

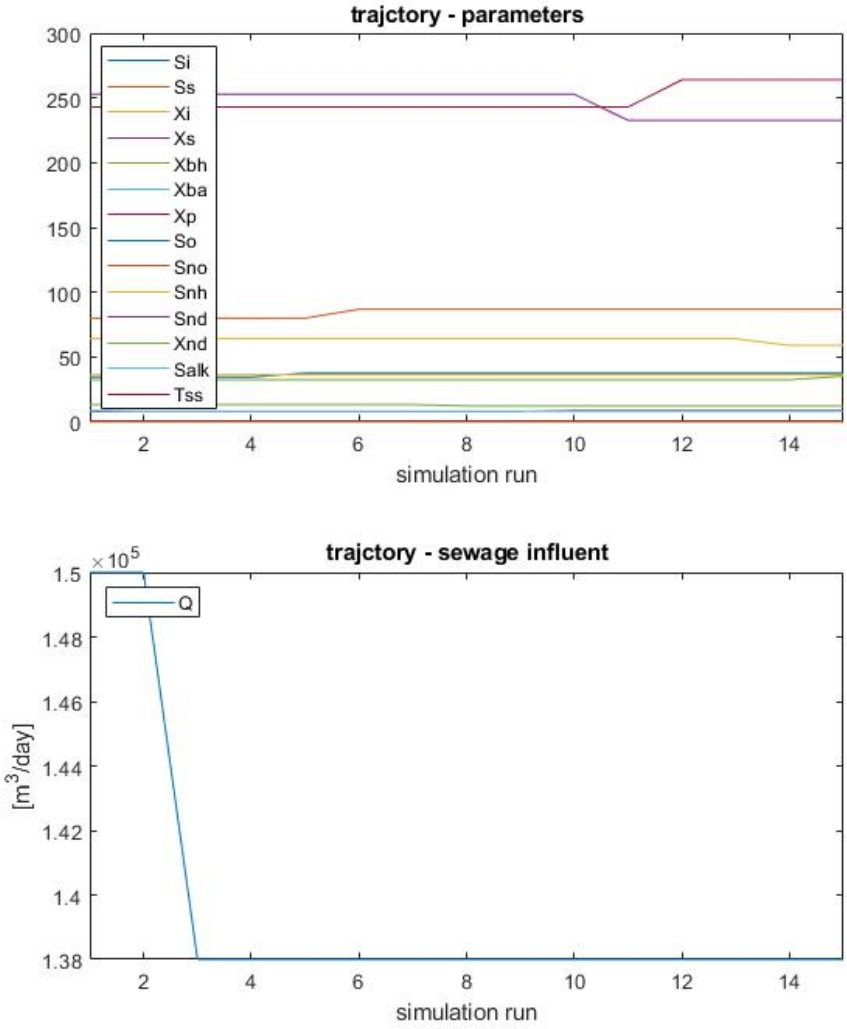

Fig. 82. Example trajectory based on parameters changing in successive simulations

This value becomes an elementary effect and becomes the basis for further analysis. The resulting elementary effect is presented in the graphic below(Fig. 83).

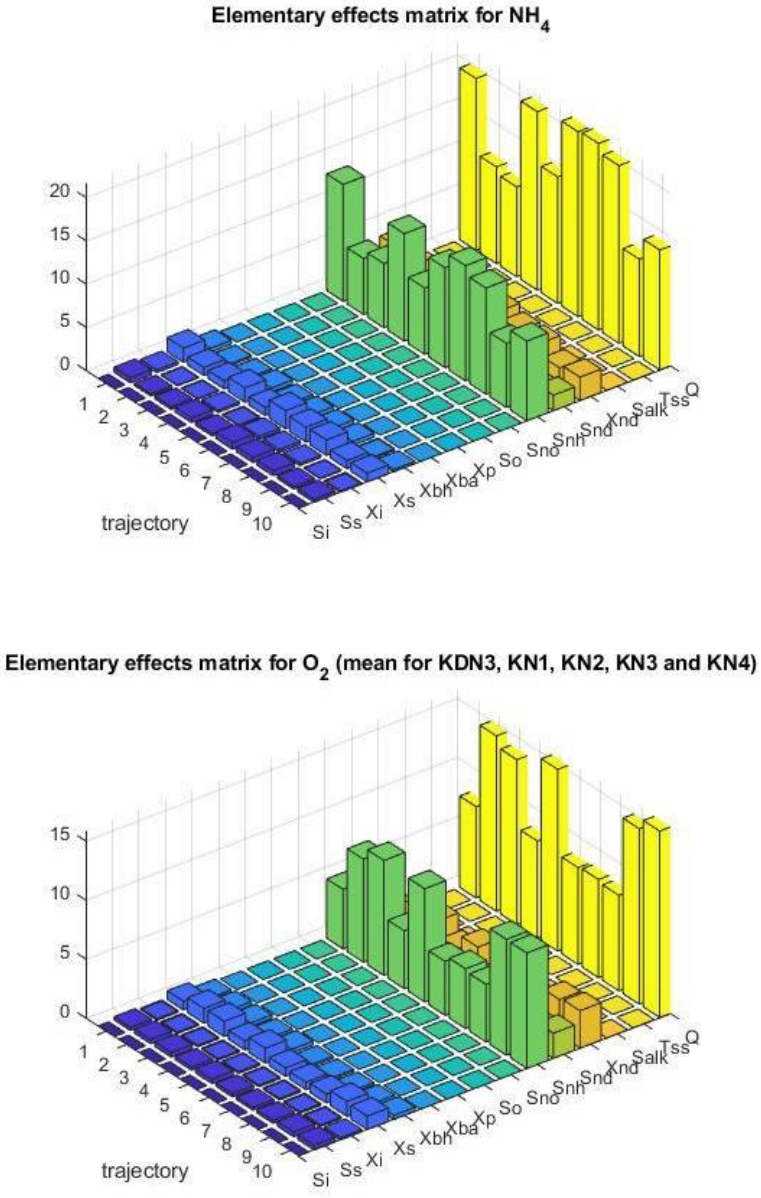

Fig. 83. The matrixes of elementary-effects achieved in Morris simulation

Finally, after calculating the mean value and standard deviation, the effect of particular parameters on the operation of the treatment plant can be assessed. Fig. 84 shows mean values and standard deviation for values of NH_4^++NH_3 nitrogen (*SNH*). Fig. 85 pictures the mean values and standard deviation for O_2 (*SO*) values in individual sections of the rector.

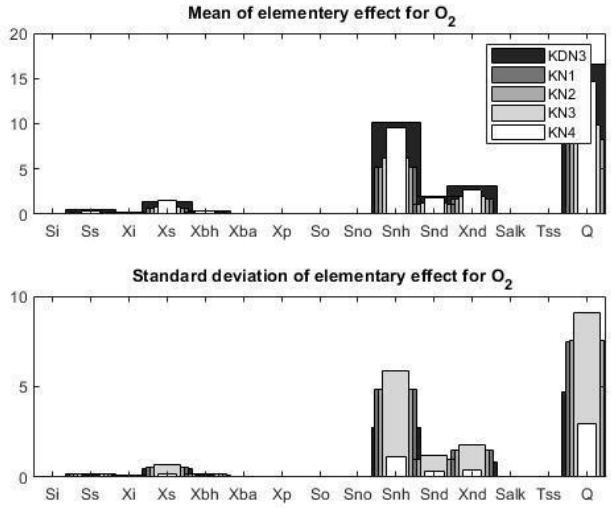

Fig. 84. The mean and standard deviation for NH_4^++NH_3 nitrogen (SNH) and O_2 (SO) in Morris simulation

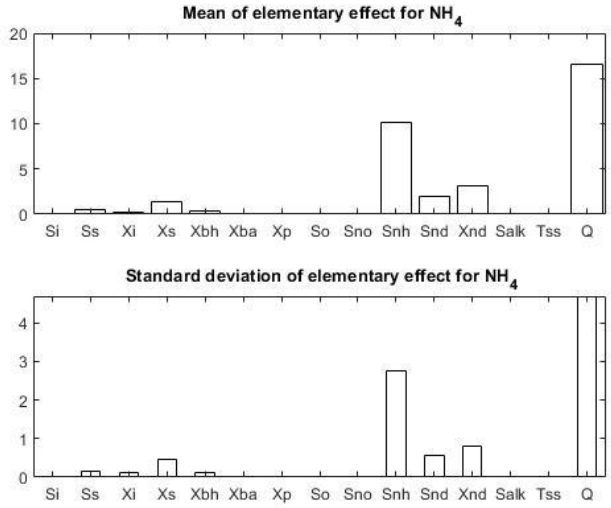

Fig. 85. The mean and standard deviation for NH_4^++NH_3 nitrogen (SNH) and O_2 (SO) in Morris simulation

To sum up, the analysis of sewage treatment plant sensitivity to change of influent parameters, several conclusions can be drawn. As in the analysis of the variables of the BSM1 process (stoichiometric and kinematic parameters respectively), the value representing ammonia compounds is of the greatest importance. It seems obvious that the content of ammonia and dissolved oxygen in sewage is influenced by sewage into treatment plants.

Finally, the author validates how mean and standard deviation of airflow demand is affected by changes of parameters in influent. Here, as in the above considerations, influent NH_4^++NH_3 nitrogen (SNH) has the greatest contribution. Figure below(Fig. 86) presents the results.

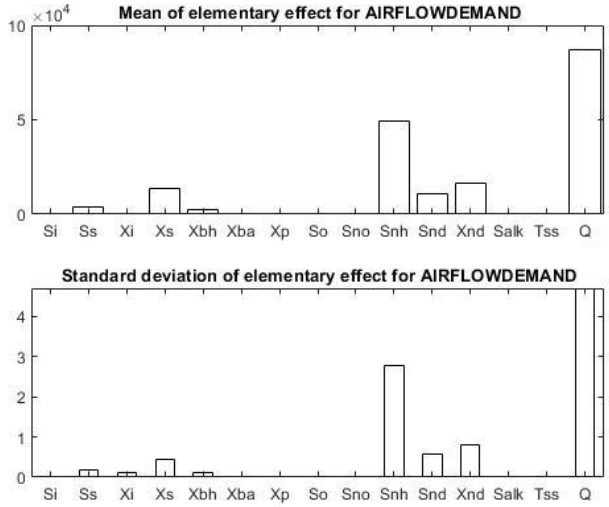

Fig. 86. Mean and standard deviation airflow demand in Morris simulation

6.5 Summary of Morris validation

Summarizing the above observations, the author can conclude that Morris sensitivity analyses have proved that the parameters describing the NH_4^++NH_3 nitrogen in wastewater (S_{NH}) have the greatest impact on the treatment process. Therefore, a considerable attention must be paid for ammonia parameters during wastewater treatment process.

7 State estimation based on Kalman filter

7.1 Procedures based on Kalman filter - introduction

7.1.1 Bayesian optimization implemented in model validation

In the first two paragraphs of the work, a numerical model of the treatment plant is presented which unfortunately is very non-linear. Therefore, the analysis of the operation of such an object requires the use of special techniques that will be resistant to the nonlinearities of the model's operation.

The Bayes' observer is used with the assumption that the treatment process has the properties of the Markov chain (equation 24). Reactors' state depends only upon the current state and not upon all the previous history of state.

$$p(x_t|x_{0:t-1}) = p(x_t|x_{0t-1}) \tag{24}$$

Recursive Bayesian Estimators (RBE) is a method for estimation of an unknown probability density function, which is recursive over time, using mathematical model of process and incoming measurements. The main feature of the Bayes' filter is the ability to recursively determine the state probability distribution based on a known input history and observation[146].

Bayesian optimization consists of main components [147]:

- Prior – Choose some prior measure over the space of possible objectives *f*;
- Innovation - Combine prior and the likelihood to get a posterior measure over the objective given some observations;
- Use the posterior to decide where to take the next evaluation according to some acquisition/loss function.

State estimation with Bayesian probability process consists recirculating calculation as presented above. The most likely x_t value can be determined from such probability distributions p. So in the model the previous state from the moment $t-1$ is taken into account and includes the update from the measurement.

The Bayesian optimization described above has been used to develop various numeric methods that are used for state estimation of various nonlinear models. Bayesian optimization techniques are implemented in Kalman filters that are used in model validation.

7.1.2 Mathematical concept of Kalman Filters

One can imagine a situation where uncertain measurements of the processes can be simultaneously visualized by a numerical model that is expressed by transition and observation equations. The calculations based on such a model allow implementation of the dedicated algorithms correcting the measurements even in high uncertainty.

Kalman Filter (KF) can be used to reconstruct variables that are not measured or to reduce the effect of noise in the available measurements. The idea was invented by Hungarian scientist Kalman in 1960[148]. Kalman filter is based on linear equations discretized in the time domain. Filters based on Kalman idea are the numeric algorithms computing the state estimates of the nonlinear system using the specified state transition and measurement likelihood functions. The idea can be presented with the following diagram (Fig. 87).

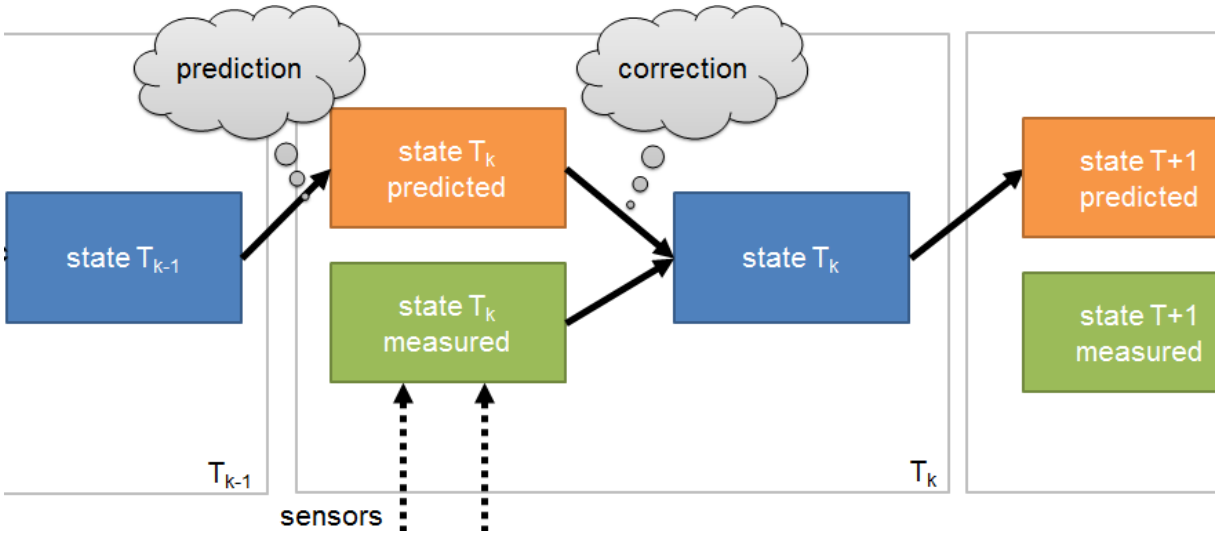

Fig. 87. Kalman filter used in optimal state estimation

We assume the following variables:

- state x, state estimation $\hat{x}$
- input u,
- output m,
- process noise w,
- measurement noise y,
- time k.

Mathematically, the Kalman filter model assumes the new state x_k at time k evolved from the state x_{k-1} at $(k-1)$ according to equation below. Matrix A is a state transition model, matrix B is an input observation model [149].

$$x_k = A \cdot x_{k-1} + B \cdot u_k + w_k \tag{25}$$

At time k an observation (or measurement) y_k of the true state x_k is made according to the equation below. Output function maps the simulated state into space observed by measurements.

$$y_k = C \cdot x_k + v_k \tag{26}$$

Vector $w_k$is the process noise and vector v_k is measurement noise. They are assumed to be zero mean Gaussian white noises with covariance matrices $w_k \sim N(0, Q_k)$ and $v_k \sim N(0, R_k)$ respectively. The Kalman algorithm is a two-step process: prediction and correction (measurement update).

In the prediction step, the Kalman Filter produces estimates of the current state variables, along with their uncertainties using model expresses in matrix A. Prediction is expressed in the following equations:

- ✓ Project state ahead

$$x'_{k(prediced)} = A \cdot x_{k-1} + B \cdot u_k \tag{27}$$

- ✓ Project the error covariance ahead

$$P'_{k(predicted)} = A \cdot P_{k-1} \cdot A^T + Q \tag{28}$$

Correction (measurement update) is the next stage when state prediction is compared to measured state values.

- ✓ Compute the Kalman gain

$$K_k = \frac{P'_{k(prediced)} \cdot H^T}{HP'_{k(predicted)}H^T + R} \tag{29}$$

- ✓ Upgrade the state estimate using measurement z_k

$$x_k = x'_{k(prediced)} + K_k\left(z_k - Hx'_{k(prediced)}\right) \tag{30}$$

- ✓ Update the error covariance

$$P_k = (I - K_k H)P'_{k(predicted)} \tag{31}$$

The Kalman gain is the relative weight given to the measurements and current state estimate. The product of Kalman gain and difference between the predicted and measured state indicates the signification of simulation to the output value. A new state estimation and its error covariance are output. After update of state estimate x_k and error covariance P_k, the cycle begins again. The overview of Kalman filter is presented below (Fig. 88).

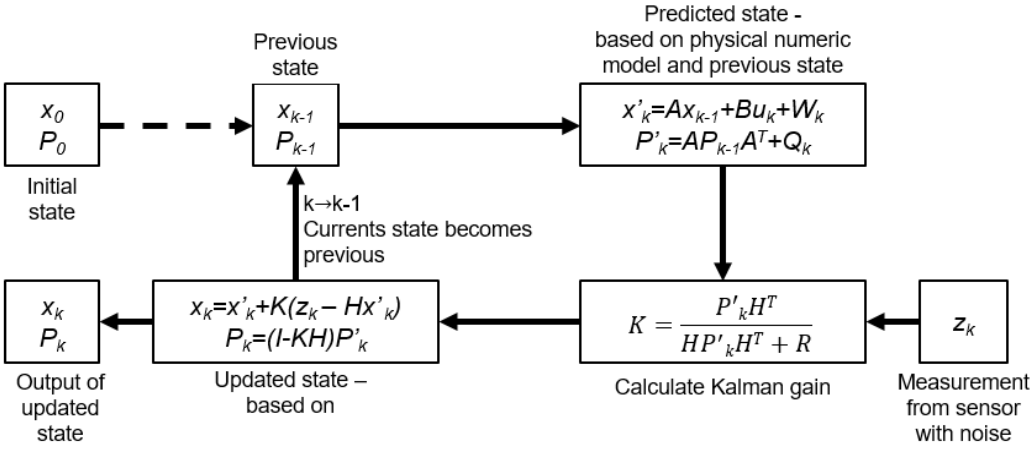

Fig. 88. The overview of Kalman Filter (based on [150])

Symbols used in equations are:

- u_k, z_k – control and measurement vector, the first one indicates the magnitude of any input state value controlled in the situation; the second one contains real-world measurement received in moment k,
- x_k, x_{k-1} – newest and previousestimate of the current „true" state,
- P_k,P_{k-1} – newest and previous estimate ot the average error covariance matrix,
- A, B, H, C – state transition matrix, control matrix, conversion matrix, observation matrix respectively,
- K_k – Kalman gain in step *k,*
- Q, R – estimated covariance matrices of u_k (process noise) and v_k (error noise).

State measurements are needed for satisfactory performance in many applications. For linear systems, standard solution are available like Kalman filter. Prediction for non-linear systems is much more challenging. One can take two approaches [132]:

- One approach is to linearize the nonlinear system at each sampling time and then apply the linear solutions to the linearized model (Extended Kalman Filter). This approach is ad-hock solution for non-linear systems;
- Observer designs that explicitly account for nonlinearities can use deterministic approaches (sample based methods like a particle filter) or stochastic observers (moving horizon estimation).

Extender Kalman Filter (EKF) can be used for non-linear functions of the state. Extended Kalman Filter (EKF) simplifies non-linear function to linear using linear transition in a selected point [151]. Values $w_k$and$v_k$correspond to estimated noise and error in the system and measurements.

The literature [152]describes the process w_k and observation v_k disturbances in two ways. First, it takes into account in state transition and observation functions as non-additive noise formulation. Secondly, it extracts it as the component of the sum of the equation (additive noise formulation).

In the case of non-additive noise formulation process function $f()$ depends on both previous state x_{k-1} and input u_k. Output is described with observation function $h()$ that is non-linear reaction based on state x_k and observation noise v_k (Fig. 89).

$$x_k = f(x_{k-1}, u_k, w_k) \tag{32}$$

$$y_k = h(x_k, v_k) \tag{33}$$

In further considerations only the case of additive noise is analyzed – process and observation noises are both assumed to be zero mean multivariate Gaussian noises with covariance $Q_k$and $R_k$respectively (Fig. 89).

$$x_k = f(x_{k-1}, u_k) + w_k \tag{34}$$

$$y_k = h(x_k) + v_k \tag{35}$$

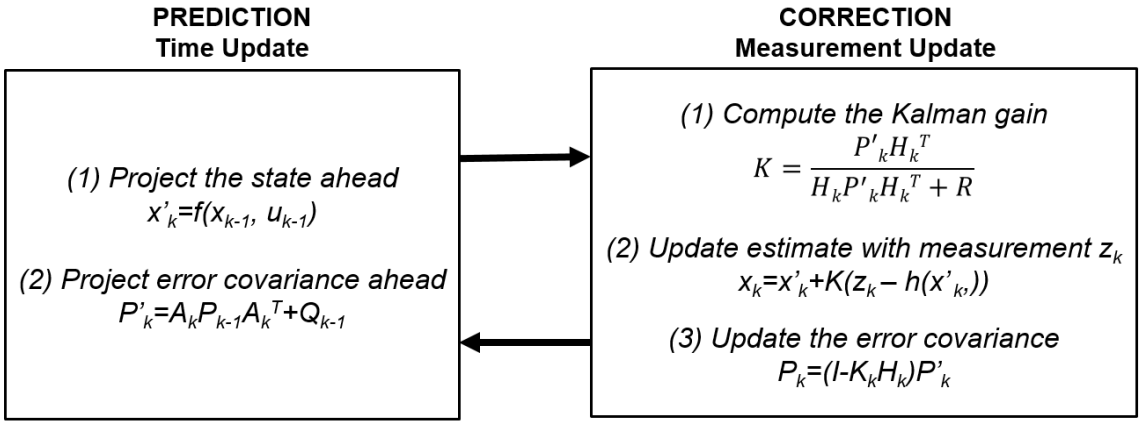

Fig. 89. The overview of Extended Kalman Filter (based on [149])

Extended Kalman Filter makes the non-linear function into linear function using Taylor Series, it helps in getting the linear approximation of a non-linear function. This way best available linear estimate is achieved. We are assuming that functions F and H are differentiable at a points $x_k$and x_{k-1}.

For state function $f()$

$$f(x_{k-1}, u_k) \approx f(x_{k-1}, u_k) + \frac{\partial f(x_{k-1}, u_k)}{\partial x_{k-1}}(x_{k-1} - u_k) \tag{36}$$

For measurement function $h()$

$$h(x_k) \approx h(x_{k-1}) + \frac{\partial h(x_{k-1})}{\partial x_k}(x_{k-1}) \tag{37}$$

The partial derivatives lead toJacobian functions - the best linear approximation of the function $F$and Hnear the point $x$in time k.

$JF = \frac{\partial f(x_{k-1}, u_k)}{\partial x_{k-1}}$ – state transition Jacobian

$JH = \frac{\partial f(x_{k-1})}{\partial x_k}$ – measurement Jacobian

Finally the non-linear function can be presented linearly as in classic Kalman filter

$$f(x_{k-1}, u_k) \approx f(x_{k-1}, u_k) + JF(x_{k-1} - u_k) \tag{38}$$

$$h(x_k) \approx h(x_{k-1}) + JH(x_{k-1}) \tag{39}$$

A nonlinear task can be replaced with a linear one after calculating the cost of the Jacobian matrix value at each step of the simulation. Such a task can be solved with the classic Kalman filter described in the previous paragraphs. Although linearization used in the EKF filter gives correct results in the case of small non-linearities. Although it is worth noting that the Kalman filter limits issues like: difficulties in analytical calculation of the Jacobian matrices in state transition or measurement functions, high computational cost to find the numerical version of Jacobian and finally EKF is not optimal if the system is highly nonlinear.

EKF is suitable for parameter estimation of complex non-linear numeric models. As such following numeric problems must be solved with EKF [153]:

- determination of the structure of the dynamic relationships between inputs u, state variables x, and outputs y (model structure identification), prediction especially when measurement data has a lot of noise,
- determination of the current and future values of the state variables (state estimation and prediction),
- estimation of the inaccessible state variables that are not measured (state reconstruction),
- computation of values for the parameters that appear in the identified model structure (parameter estimation); In this dissertation second EKF will be implemented to estimate the unknown parameters (paragraph below),
- simultaneous determination of the values of x and (combined state and parameter estimation, or adaptive estimation and prediction).

Another modification of Kalman Filter for non-linear systems is Unscented Kalman Filter (UKF). This concept was introduced in 1997 by Julier and Uhlman[154]. It is expected to deal with the most non-linear cases. Unscented transformation captures the propagation of the statistical properties of state estimates through nonlinear functions.

The basic idea underlying the algorithm is to apply unscented transformations to a set of points (Sigma Points) representing a random variable, to estimate the probability density function of another random variable: the state in the next step (time update), or the output of the system (measurement update). Each sigma point stores mean and covariance of the estimated state that is used as input to the state transition and measurement functions. UKF filter is implemented in software by following equations [155]:

$$x[k+1] = f(x[k], us[k]) + w[k] \tag{40}$$

$$y[k] = h(x[k], um[k]) + v[k] \tag{41}$$

$$w[k] \sim (0, Q[k]), v[k] \sim (0, R[k]) \tag{42}$$

The nonlinear measurement function h relates x to the measurements y at time step k. By us and um denoted are additional input arguments. The state transition and measurement equations are for an M-state discrete-time nonlinear system and have additive process and measurement noise, w and v with zero mean and respectively Q and R covariance matrices. Value of $\hat{x}$ is the state estimate and $\hat{x}\,[k_a|k_b]$ denotes the state estimate at time step k_a using measurements at time steps $0,1,\ldots,k_b$.

Like the EKF, the unscented Kalman filter can be used only for models with Gaussian noises. For the estimation of the state with non-Gaussian noises particle filters are used which are based on the sequential Monte Carlo method [156].

To sum up, the table below (Tab. 14) shows the computational cost associated with the discussed Kalman filter and its modifications[157]:

Tab.14. Comparison of Kalman Filter with its modifications[157]

State estimator	Model	Assumed distribution	Computational cost
Kalman filter (KF)	Linear	Gaussian	Low
Extended Kalman Filter (EKF)	Locally linear	Gaussian	Low (without numerical Jacobians) Medium (with numerical Jacobians)
Unscented Kalman Filter (UKF)	Nonlinear	Gaussian	Medium

This model's linearity is a crucial issue. A significant non-linearity of the numerical model of WWTP's has been demonstrated. Thus, in further simulations implementations of EKF and UKF are investigated.

7.1.3 State estimation using Kalman filter

The Kalman filter consists of two stages - prediction and correction. During the prediction, the numeric model is used to calculate the behavior one step ahead. During the correction, the model uses the measured data. In the case when one state in vector does not have equivalent in measurements, the covariance "entails" unmeasured state during the correction step [158] and[159]. Such a phenomenon allows for the determination of the parameter value by entering one into the model as a state.

In models like WWTP not all state variables are measured, so we have only output measurements and state estimation provides a way to reconstruct the state of the system. Therefore, the literature has been checked for the implementation of such an approach in a sewage treatment plant and an own solution has been proposed.

7.1.4 State estimators in WWTPs – literature review

The concept of state estimation of WWTP to reduce consumption using the Kalman filter is presented in numerous publications.

The first attempts of state estimation took place at the beginning of the 80'. Beck [153] presents on-line real-time state estimation and prediction in operational control of the activated sludge process. Mass balance across the aerator yield the 5 nonlinear ordinary differential equations simulating the dynamic nitrification mode. States consist of the following sewage parameters x_i: ammonium-N, nitrite-N, nitrate-N, Nitrosomonas bacteria; Nitrobacter bacteria (all in g/m^3).

In publication [160], an on-line estimation of suspended solids in pilot-scale Membrane Bio-Reactor (MBR) using a Kalman observer is presented. Authors construct state-space model $X(t)$ that is n-dimensional state vector of the suspended solids (SS) concentration in the reactors. The test of Kalman State Observer has been designed for the dynamic estimation of SS in the biological tanks of WWTPs' reactors.

In publication[161], state estimation for large-scale wastewater treatment plants is presented. Authors utilize two numeric techniques: Extended Kalman Filter and Moving Horizon Estimation.

Chai [162]investigates the use of the standard Kalman Filter, the Extended Kalman Filter, and the Unscented Kalman Filter in state estimation of a typical biological WWTP and compare the differences in performance of these estimation approaches. Author analyses the states of the model grouped into the concentration of soluble components S_j and particulate components X_j.

The concept of the Kalman filter has been used many times in the task of sewage treatment plants simulated with ASM models of reactor. Some examples are highlighted below.

Zeng and Liu [163]develop a distributed state estimation scheme for wastewater treatment processes in the context of extended Kalman filtering. In presented control algorithm is based on ASM1. Authors have extracted state vector $X(t)$ that contains 78 state variables with 48 variables measurable. The distributed scheme is compared with a centralized extended Kalman filtering scheme under dry conditions.

One of the first works addressing the problem of model state and parameter estimation is [164], where the Extended Kalman Filter (EKF) was applied to the ASM nr.1 in 1991. E. Ayesa published a detailed explanation of using modified non-linear Kalman Filter (EKF). EKF is implemented in model of WWTP based on IAWPRC and uses unknown numerical values of the state and parameter of sewage parameters as states. In the proposed application, measurement vector consists of 7 measurable parameters such as: COD, TKN, NH.

In [165], EKF has been used in ASM2 model, in [166] with a reduced ASM, in [167] with ASM2 and in [162] with ASM3. In [168], a proper orthogonal decomposition of BSM1 is carried out for estimating as many as 145 state variables of all reactors of the plant via EKF. A measurement vector counts 49, 3 states are uncontrolled input to the WWTP plant.

7.2 State estimation to check performance of WWTP model

7.2.1 Sewage influent estimation using Kalman filters

The previous paragraph (Sec. 4.3.7) introduces a parameter estimation using Kalman filter. This method can be an effective way of estimating the unknown parameters of wastewater affecting only and exclusively on the basis of measurements made within the process. In order to validate the algorithm in this task, a simulation study on synthetic data has been performed. The process consists of two independent approaches.

Performance check simulation. First, the reference simulation is performed. Based on the assumed input data, the NH_4^++NH_3 nitrogen (SNH) and O_2 (SO) values in the reactors are counted. Such measurements show what values of the state of the reactor are expected with the known inflow sewage. This task is illustrated by the Fig. 90 below.

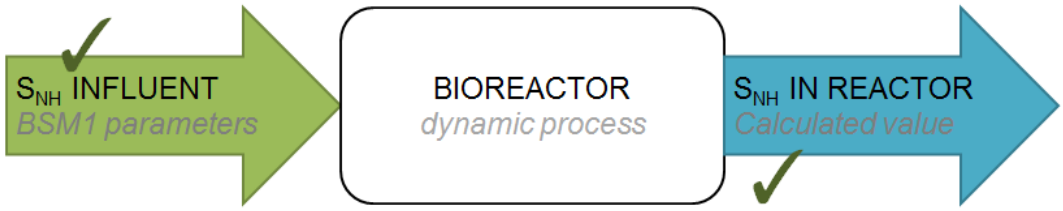

Fig. 90. The reference run calculating synthetic data

Parameter estimation simulation. In the second step, parameter of NH_4^++NH_3 nitrogen (SNH) istreated asunknown, its value is adopted from synthetic sensor measurements obtained during the reference simulation. The simulation begins with the initialization value of the SNH influent state and sensors' measure. Next, the simulation aims to estimate the value of the influent of SNH to validate whether it matches the measurements obtained from previous simulations. The comparison of the estimated SNH value with the value for reference stimulation allows estimating the effectiveness of the algorithm. This task is presented by the Fig. 91.

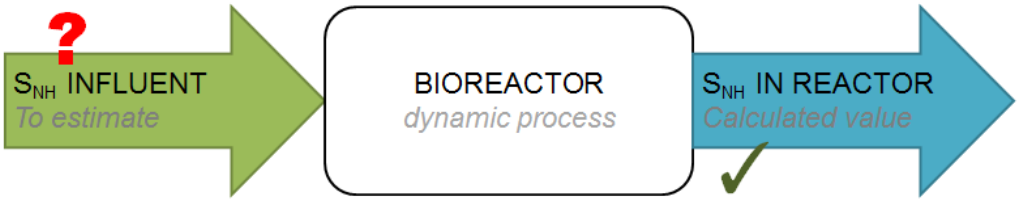

Fig. 91. The schematic of parameter estimation based on synthetic data

This idea of state estimation using Kalman filters is presented in [169].

7.2.2 Implementation of Kalman state estimator in Płaszów WWTP

Discussed in p. 6.2 sensitivity analysis has shown that the NH_4^++NH_3 nitrogen (SNH parameter) has the greatest impact on the purification process. Therefore, the analysis will be limited to SNH estimation in the inflowing sewage. The parameters will be adopted according to the Tab. 15.

The paragraph describes the implementation of Kalman state estimator. In this case, the state estimation is based on the reference simulation.

Tab.15. List of ASM1 variables[71]

No	Parameter	Influent parameter	Constant value set in BSM1
1	Soluble inert organic matter	S_I	30
2	Soluble inert organic matter	S_S	69.5
3	Particulate inert organic matter	X_I	51.2
4	Slowly biodegradable substrate	X_S	202.32
5	Active heterotrophic biomass	X_{BH}	28.17
6	Active autotrophic biomass	X_{BA}	0
7	Particulate products arising from biomass decay	X_P	0
8	Oxygen	S_O	0
9	Nitrate and nitrite nitrogen	S_{NO}	0
10	NH_4^++NH_3 nitrogen	S_{NH}	31.56
11	Soluble biodegradable organic nitrogen	S_{ND}	6.95
12	Particulate biodegradable organic nitrogen	X_{ND}	10.59
13	Alkalinity	S_{ALK}	7
14	Total Suspended Solids	TSS	211.2675
15	Flow rate	Q	18 446

As presented in previous chapters (Sec. 6), selected parameters pay a crucial role during the operation of the wastewater treatment. In the discussed solution, the estimation procedure is used to estimate the NH_4^++NH_3 nitrogen of incoming sewage (SNH parameter). More precisely, two states are assumed in this implementation of the Kalman filter:

- NH_4^++NH_3 nitrogen (S_{NH}) influent as a parameter to be estimated,
- NH_4^++NH_3 nitrogen (S_{NH}) measured in KDN3 section in WWTP.

In Sec.7.1, the idea of using the Kalman filter in wastewater treatment plant is discussed. It is mentioned that for the analysis of non-linear objects such as sewage treatment plants the following options can be considered:

- Extended Kalman filter,
- Unscented Kalman filter.

The following parameters have been used in the particular Kalman simulations (Tab. 16):

Tab.16. Parameters used in the particular simulations

Simulation length	EKF
Pre run period	EKF
Process noise covariance matrix	EKF
Measurement Noise covariance matrix	EKF
Alpha	UKF
Beta	UKF
Kappa	UKF

The simulation has been performed on synthetic data, which was obtained along with the documentation of the BSM1 model (Fig. 92). Sewage flow increased in proportion to the conditions of the Płaszów WWTP (here the average of sewage flow is around 200 000 m^3/h). Other parameters due to a lack of reliable comparative points remain original.

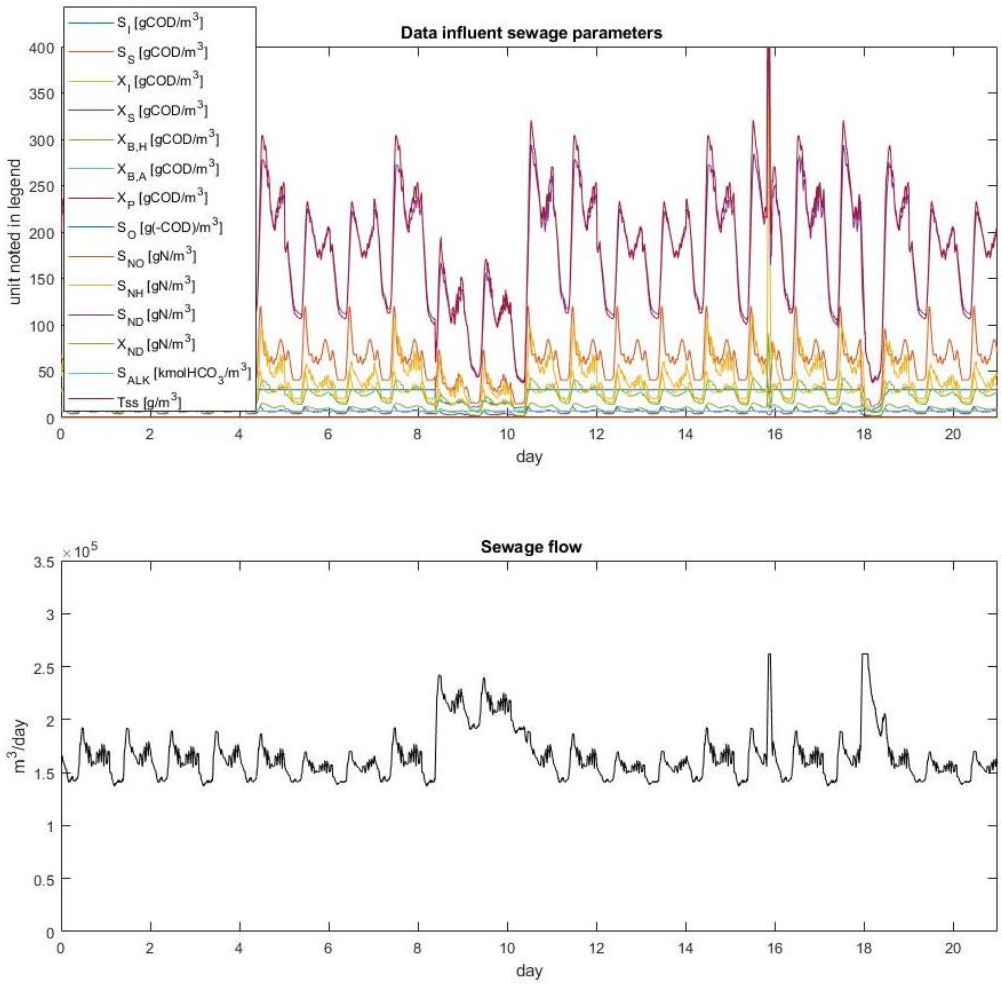

Fig. 92. Plots presenting synthetic data used in the reference simulation

Each week we can distinguish different weather conditions. These three weeks are the basis for further analysis in which the operation of the reactor model is examined (Fig. 91).

- ❖ Week 1 (dryweek) is characterized dry weather conditions. In practice, the values change throughout the day cycle. This week is designed to allow a week long period to stabilize the simulation;
- ❖ During week 2 (rainweek) two-day rains have been introduced. Under these conditions, the flow increases to approx. 250 000m^3/h and as a result of separation the waste water contamination parameters are reduced;
- ❖ Week 3 (stormweek) contains a storm in which the impact of sewage increases dynamically and sewage parameters change.

The results of the above simulation are the reference base for further simulations in which the inflow sewage parameters are estimated. The results of the simulation of the parameter estimation algorithms are discussed below. The simulation lasts 21 days.

The first week is devoted for "a start-up" - establishing a steady state (as described in the documentation of the BSM1 model [57]). Exactly at the beginning of day 7, a new value of SNH influent is “injected.” Thus, a two-week simulation is carried out in which the SNH influent value is dynamically estimated. The task of the parameter estimation algorithm is to bring the model state out of distortion and return to equilibrium. At this point, a reference simulation is used as equilibrium and it shows how the simulation should look like in a no-disturbance case. Therefore, for SCADA measurements, additional tests have been carried out to show the operation of the simulation for the ranges discussed in Tab. 17.

Tab.17. Parameters set in the simulation

PARAMETER TYPE	Low Value	Intermediate Value	High Value
Process noise covariance matrix	[0.20.20.20.2]	[0.20.20.20.2]	[0.20.20.20.2]
Measurement Noise cov matrix	[0.2]	[0.7]	[1.2]
Alpha	0.2	0.7	1.2
Beta	1	1.5	2
Kappa	0.5	1	1.5
Initial influent NH_4^++NH_3 nitrogen (S_{NH})	0 -100		

Two independent simulations are performed: reference simulation and an estimation.

First, a reference simulation is performed. As already mentioned, the reactor model is based on the BSM1 model. It has been proved in the previous sections that NH_4^++NH_3 nitrogen (S_{NH}) in influent and its volume affects the cleaning process the most. Thus, NH_4^++NH_3 nitrogen (S_{NH}) has been estimated for incoming sewage (Fig. 91). A reference simulation has been performed in which it has been checked what values of ammonia in the reactor are registered. The idea of reference run are shown in the graphs below(Fig. 93).

- NH_4^++NH_3 nitrogen influent is taken from BSM1 model,
- NH_4^++NH_3 nitrogen sensor are saved as a result of the simulation,

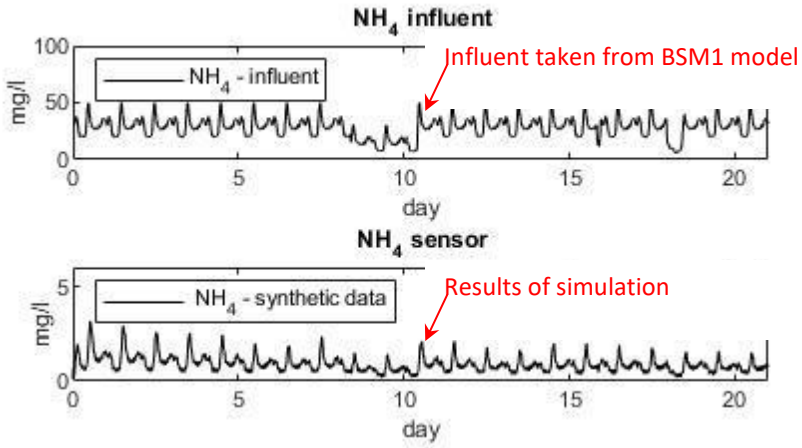

Fig. 93. Values of NH_4^++NH_3 nitrogen for influent and sensors - reference simulation

Then, the results obtained in this way will be used to check whether the parameter estimation using the Kalman filter coincides with the simulation results (Fig. 94).

- NH_4^++NH_3 nitrogen sensor from the reference simulation (a reference point for further analyzes),
- NH_4^++NH_3 nitrogen influent is considered unknown and therefore is the object of the estimation.

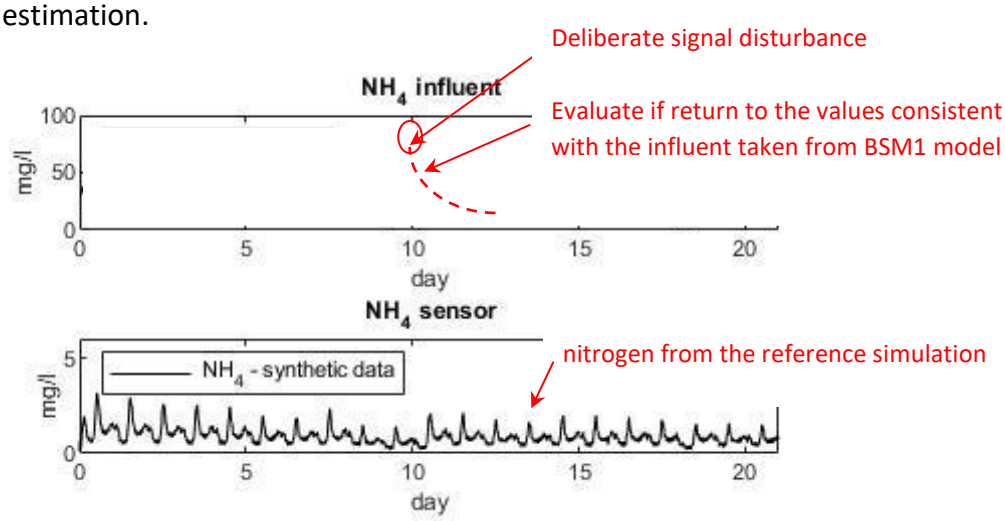

Fig. 94. Values of NH_4^++NH_3 nitrogen for influent and sensors – idea of state estimation

7.2.3 Determination of EKF covariance matrices in simulation

The operation of the estimation depends on the settings of the Kalman filter parameters. Therefore, the simulations with different values of process and measurement noise covariance matrices are performed. To validate the values of the noise covariance matrices, the author considers running simulations with variable covariance matrices. The following values are taken into consideration:

- Process noise covariance matrices:
  $[0.02, 0.02;\ 0.02\ 0.02]$, $[0.8, 0.8;\ 0.8, 0.8]$, $[0.32, 0.32;\ 0.32, 0.32]$,
- Measurement noise covariance matrices:
  $[0.25]$, $[1]$, $[4]$.

Next simulation presents the test of covariance matrices (Fig. 95).

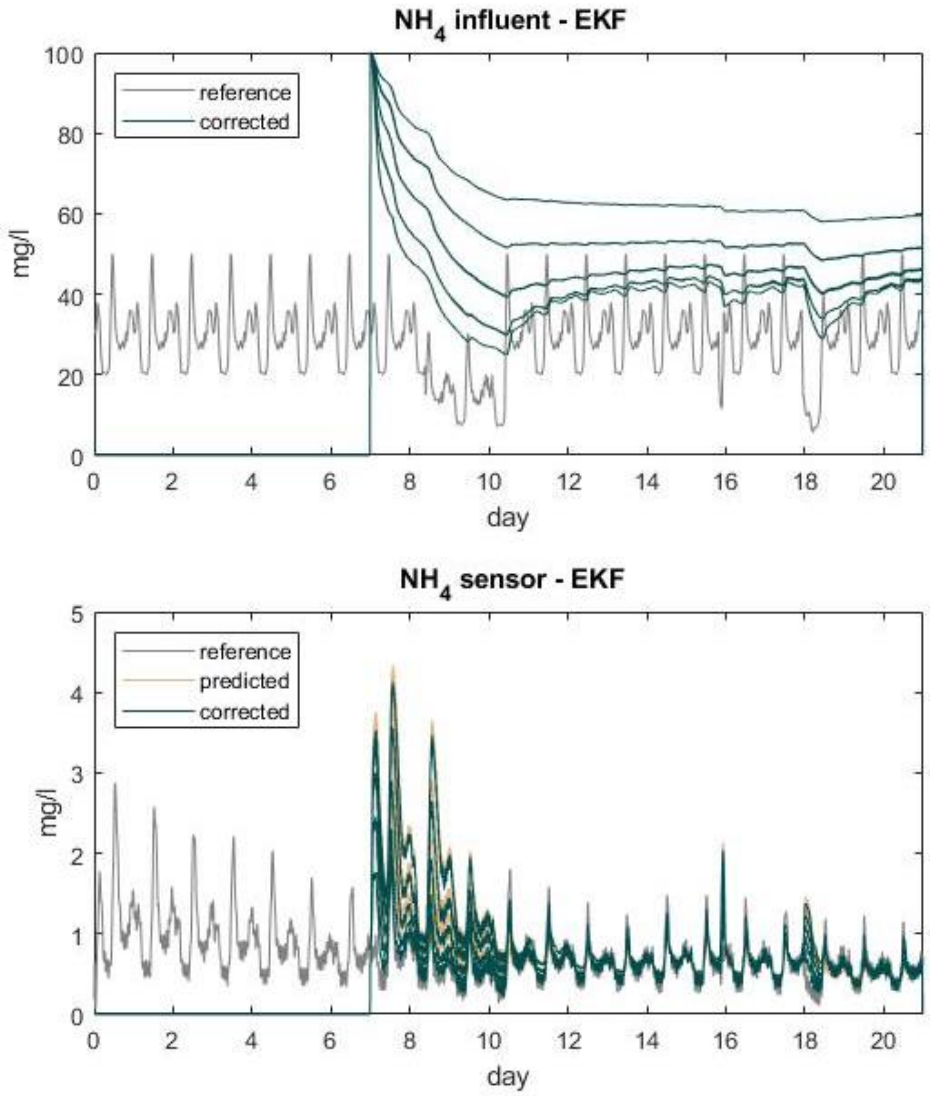

Fig. 95. Results of EKF estimation for different values of process noise covariance matrices

Additional calculations are made to investigate the shown ones. Importantly, the only meaningful reference is to measure the SNH in the reactor. Therefore, this value is checked for each estimation against the reference (measured) values. In order to represent the mathematical relationship, root mean square error ($RMSE$) is calculated[170].

$$RMSE = \sqrt{\frac{\sum_{t=1}^{n}(A_t - F_t)}{n}} \tag{43}$$

Where:

A_t– actual data
F_t – forecast
n – number of probes

In Fig. 96 result with a lower $RMSE$ in reference with measurement is marked and the appropriate value of the covariance matrix has been written.

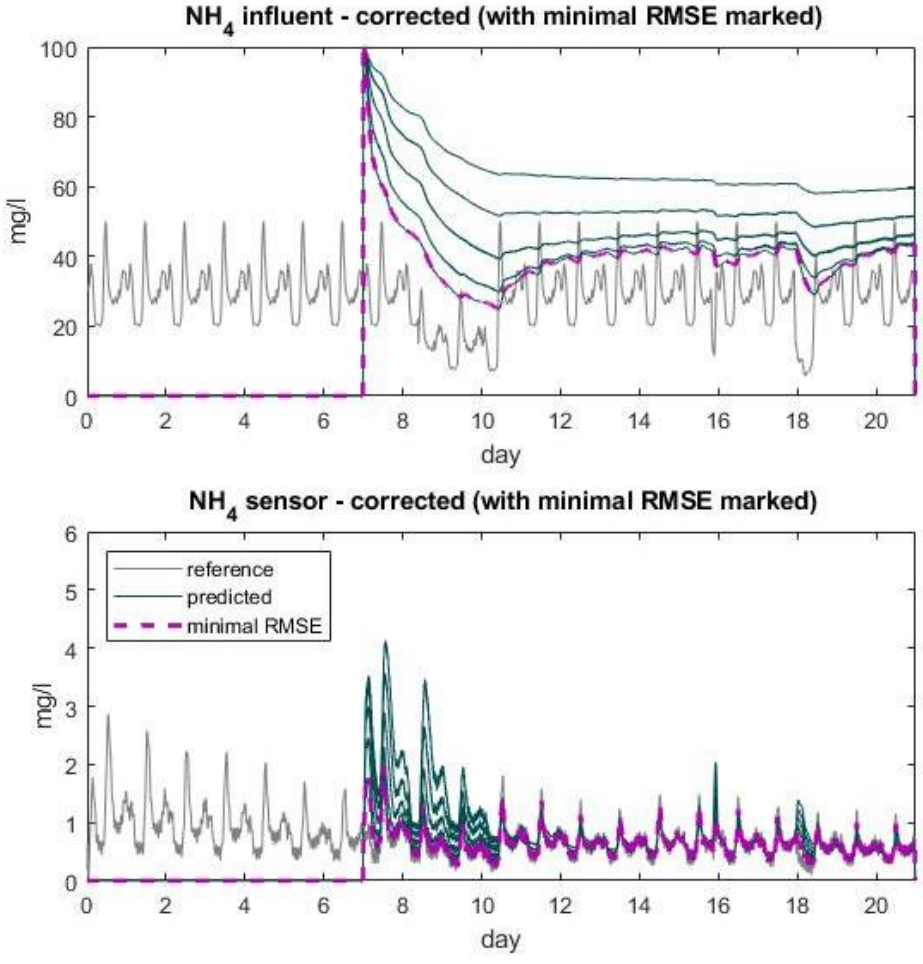

Most suitable parameters selected for EKF:
InitialNH4influent:100
InitialState: [100 0]
processNoiseCovMatrix: [0.32 0.32]
measurementNoiseCovMatrix:0.25

Fig. 96. Results of EKF estimation for different values of process noise covariance matrices – with minimal RSME marked

7.2.4 EKF in estimation for different initial values of influent

In the analyzed case, extreme values of NH_4^++NH_3 nitrogen (S_{NH}) influent are "injected," they correspond to the state of complete purity of the wastewater and extreme pollution:

- 0 mg/l,
- 100 mg/l.

The first simulation results are performed for EKF with initial conditions between 0 – 100. The precise values are 0-25-50-75-100 (Fig. 97).Lines presenting the corrected NH_4^++NH_3 nitrogen (S_{NH}) are approaching one value. Importantly, this line coincides with the reference values (drawn in the background).

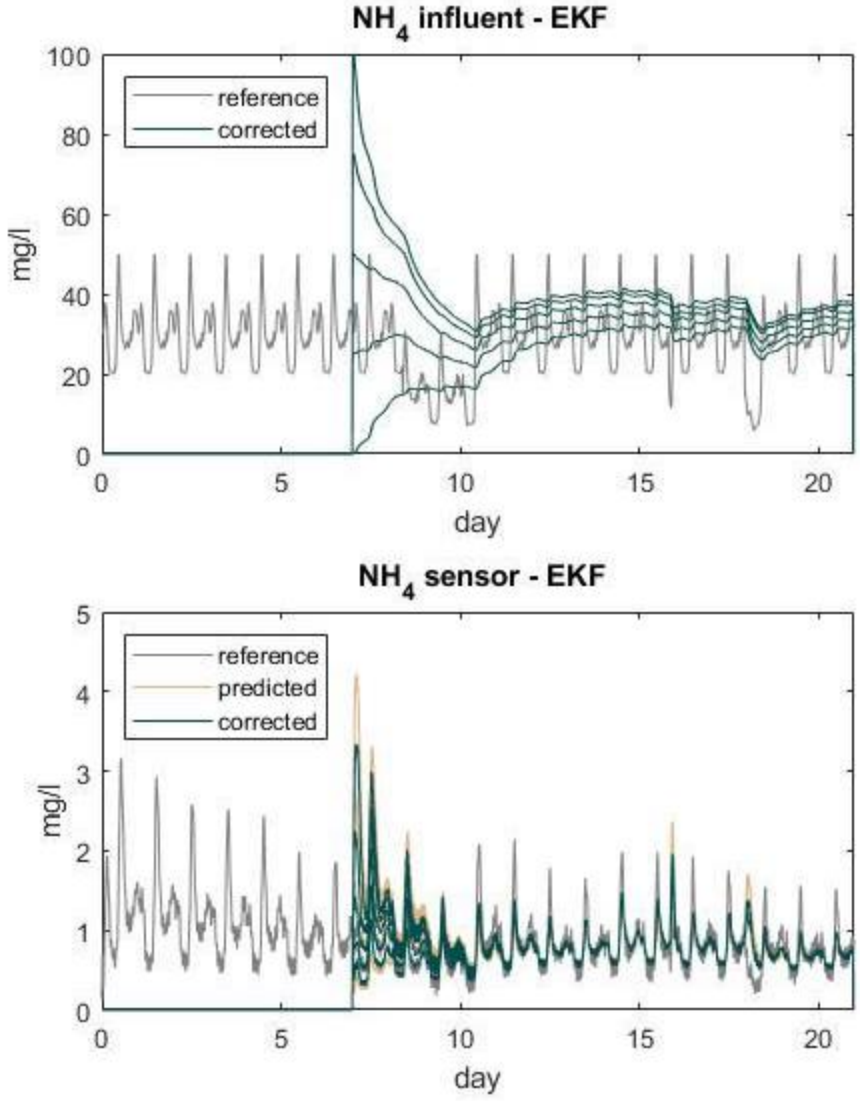

Fig. 97. Simulation results for EKF with initial conditions between 0 – 100

It can be noticed that the EKF correctly estimates the value of NH_4^++NH_3 nitrogen (S_{NH}) in the sewage. The convergence of the estimate is correct, while the value converges to the value of 50 mg/l.

7.2.5 UKF in estimation for different initial values of influent

The next simulation implements the previously discussed Unscented Kalman Filter (Sec. 7.1.2). In this case, a reference simulation was also used as described for EKF (Fig. 98).

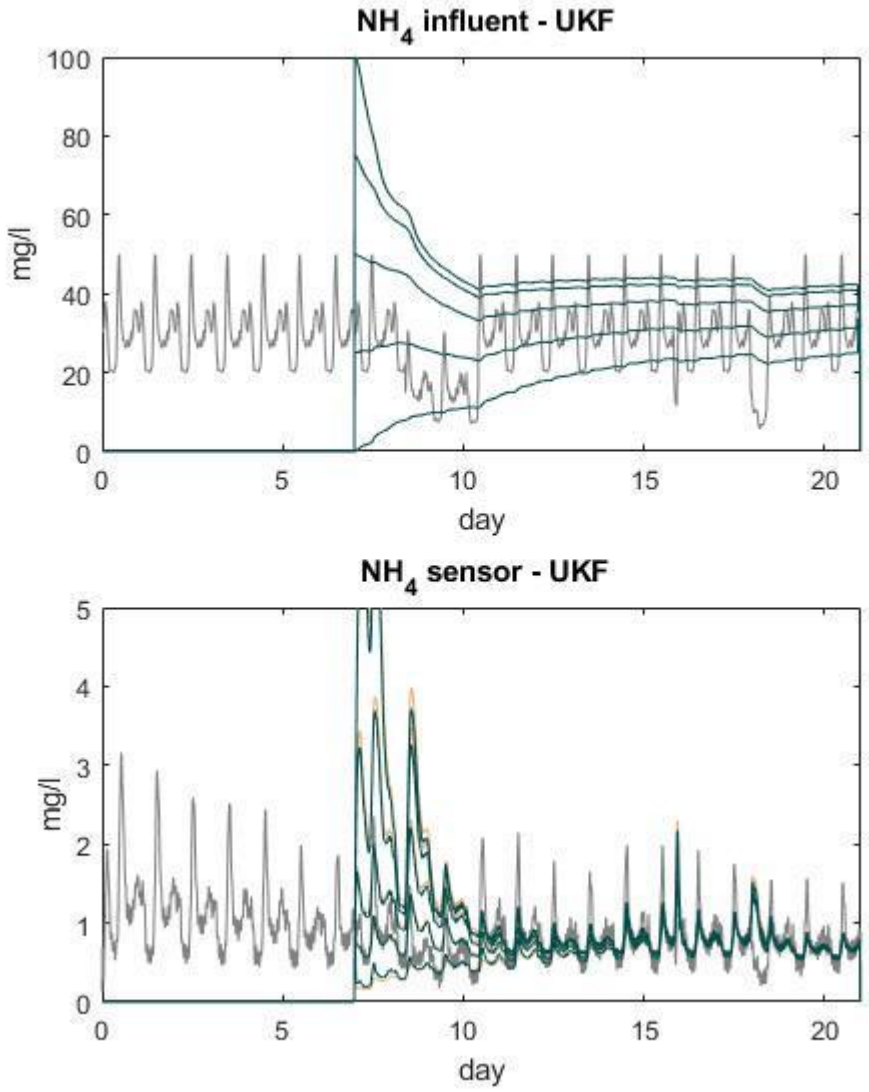

Fig. 98. Simulation results for UKF with initial conditions between 0 – 100

It can be noticed that the UHF simulation, like EKF, correctly estimates the value of NH_4^++NH_3 nitrogen (S_{NH}) in the sewage. Nevertheless, from the above figures it can be concluded that in this case UKF works worse than the analogous simulation from EKF. The Performance of UKF is rather disappointing. Therefore, only EKF will be used for further identification.

7.3 Parameter identification using EKF

7.3.1 Description of the analyzed numeric cases

The sensitivity analysis in Sec. 6 has demonstrated sensitivity of WWTP to change of influent. However, only selected influent parameters have a greater impact on the operation of the treatment plant. Hence, the number of parameters has been limited to 1. The implementation of EKF and UKF filters discussed in Sec. 7.2estimates NH_4^++NH_3 nitrogen (S_{NH}) influent parameters in relation to NH_4^++NH_3 nitrogen in the reactor calculated in the reference simulation. It is only validation of the performance of the model on the basis of synthetic data. The conclusions of the analysis indicate that EKF can be used to estimate incoming sewage parameters.

In this case, available SCADA measurements describing the operation of a real object have been used. More specifically, the available measurements of NH_4^++NH_3 nitrogen (S_{NH}) in the reactor are used. State estimation is implemented to identify the unknown parameter. The influent NH_4^++NH_3 nitrogen (S_{NH}) is chosen as the second unknown state in this case. A correctly configured Kalman filter should lead to the estimation of the unknown parameter to possible values despite the lack of precise measurements. This idea of simulation is presented below (Fig. 99).

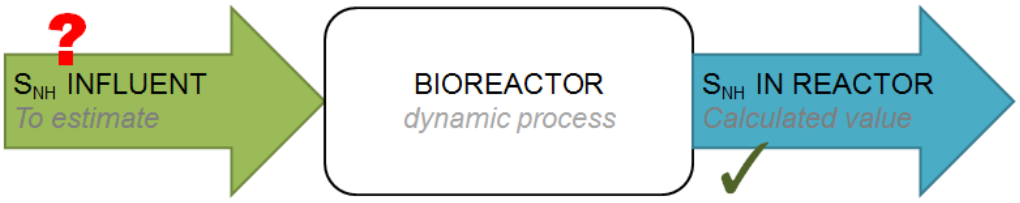

Fig. 99. Schematic of parameter estimation based on synthetic data

7.3.2 Selection of 21-day SCADA signal

Unknown parameters of sewage influent are presented on the basis of BSM1 model data. Parameters describing CONSTANTINFLUENT signal from BSM1 are selected (Sec. 3.3.3). This is how DATAINFLUENT variable that simulates the influent to the WWTP is built (Fig. 100).

In this simulation the unknown influent NH_4^++NH_3 nitrogen (S_{NH}) is estimated on the basis of available measurements of this parameter in the reactor.

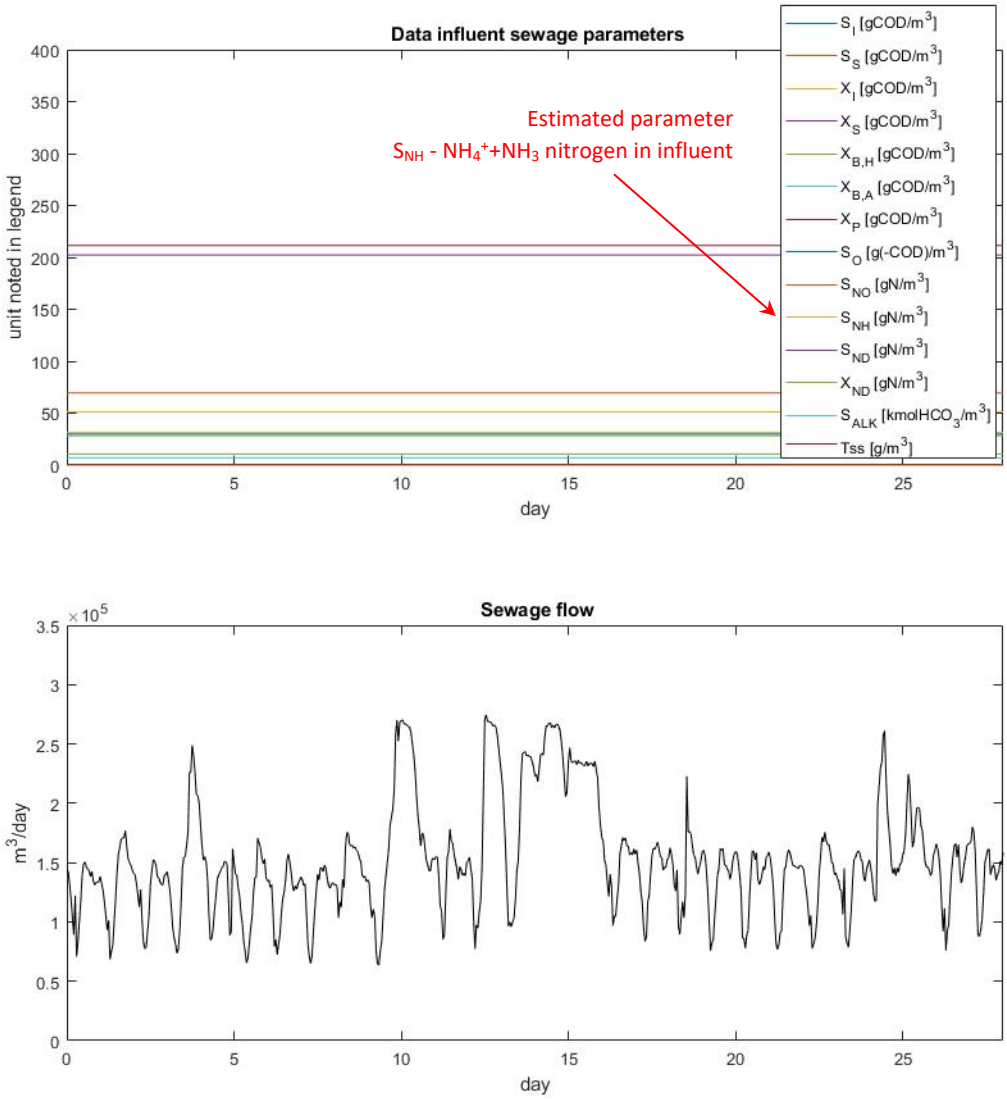

Fig. 100. Example of SCADA measurements – influent data based on sensors

The above input data requires validation. Out of the above data, the S_{NH}, which describes the content of ammonia flowing into the wastewater, seems to be of particular interest. In CONSTANTINFLUENT input signal value of parameter is assumed constant (more precisely, this value is 31.56). This value originates from the BSM1 model, so it is worth customizing this value to the case of the sewage treatment plant in Płaszów Sewage Treatment Plant in Kraków. Therefore, simulations of the Kalman state estimators are performed in order to estimate the unknown influent parameters. For such estimation EKF and UKF are implemented.

At this point, measurements obtained in the reactors' SCADA system are used as a reference. First, the data presented in the figure below have been obtained (based on the available SCADA data from 2015). To perform next analyses, 21- day period (3 weeks) has been selected as presented in the graphics. SCADA measurements are: sewage flows (in effluent), O_2 in reactors' sections KDN, KN1, KN2, KN3 and finally NH_4^++NH_3 nitrogen in KDN4 (as described in Sec. 4.2). The author presents these measurements data below (Fig. 101).

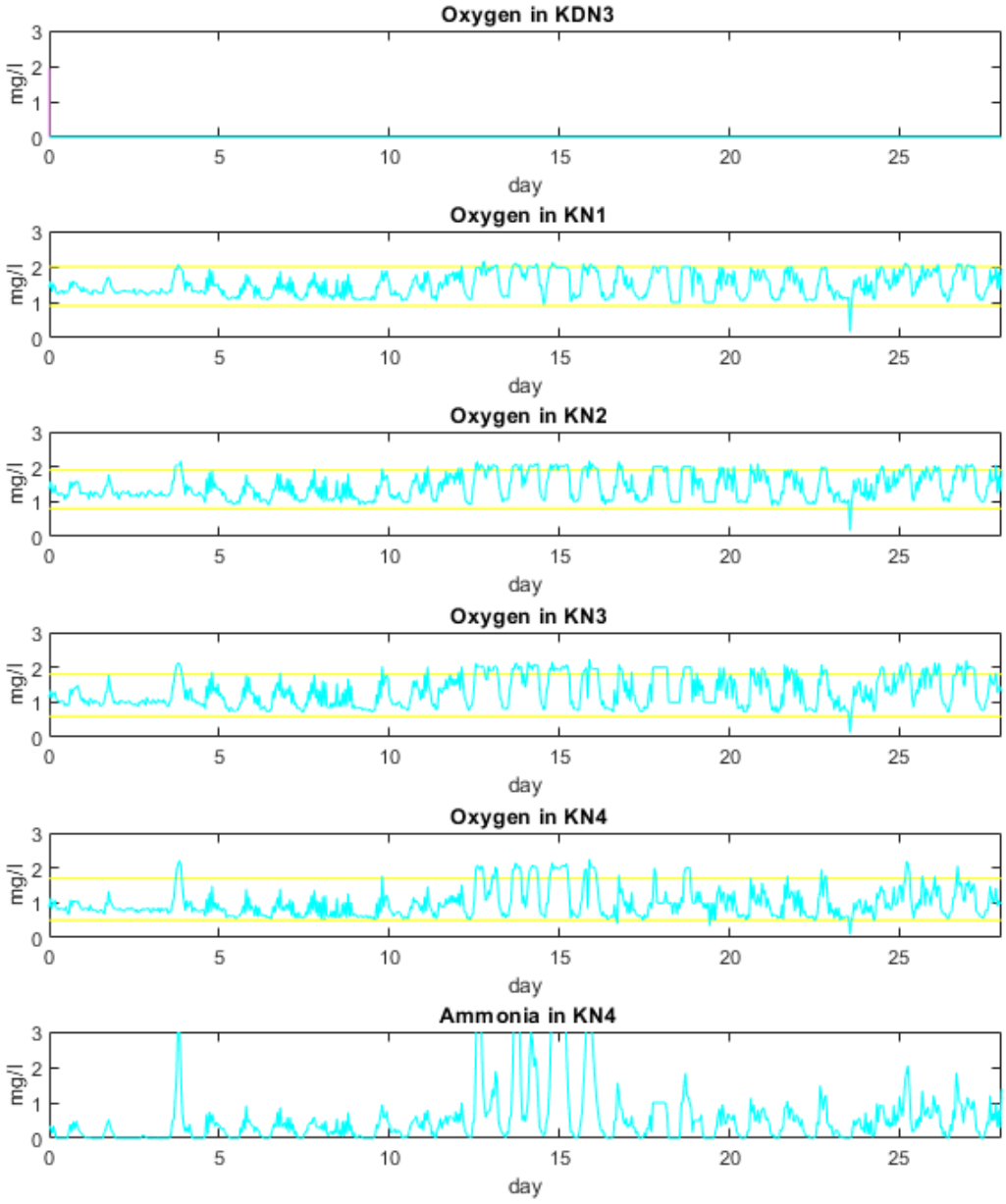

Fig. 101. Example of SCADA measurements – in each section O_2 (SO) sensor andNH_4^++NH_3 nitrogen (SNH)

Fig.102 pictures the measurements in NH_4^++NH_3 nitrogen (S_{NH}) and sewage flow. It is worth underlining variability WWTP's operation depending on the day of observations. Such unpredictability is caused by variations in environmental conditions - day, rain, storm etc. (as described in 3.2.1).

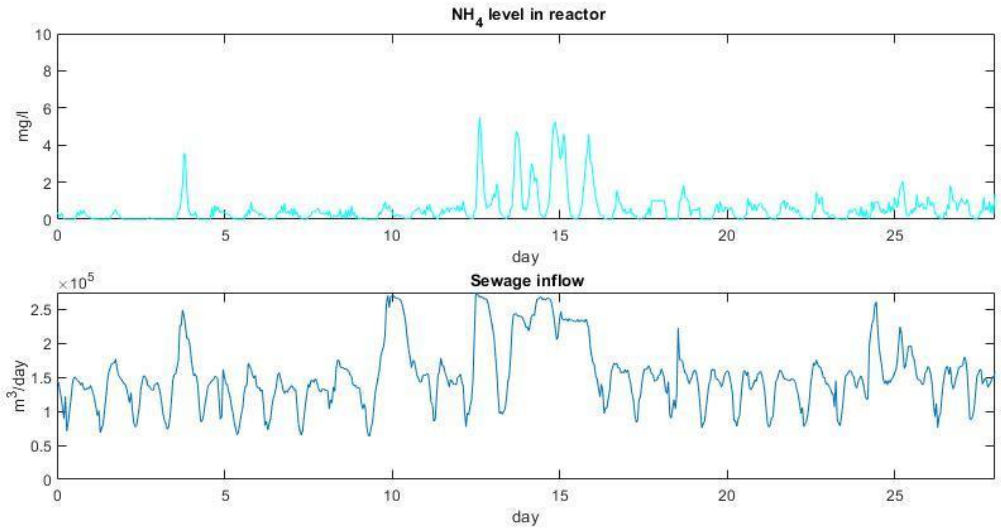

Fig. 102. Example of SCADA measurements – NH_4^++NH_3 nitrogen (SNH)and sewage flow sensors

The corresponding airflow is presented in the Fig. 103.

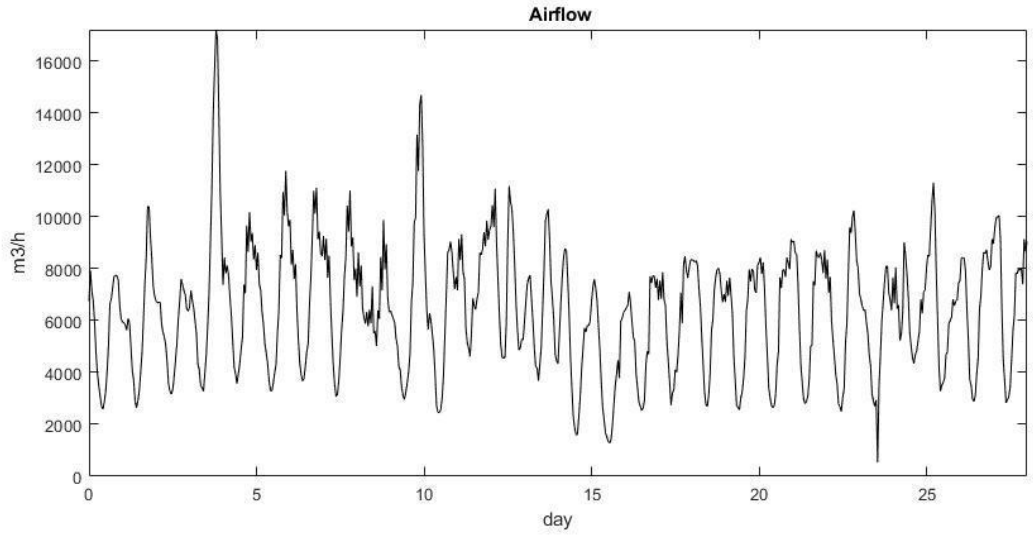

Fig. 103. Example of SCADA measurements – airflowsensor

7.3.3 Determination of EKF covariance matrices in simulation

For this simulation, the estimation plan is similar including inter alia covariance matrices presented in Sec. 7.2.3. Thanks to this, the consistency of the results can be compared. The results of simulations are presented in the following figure (Fig. 104).

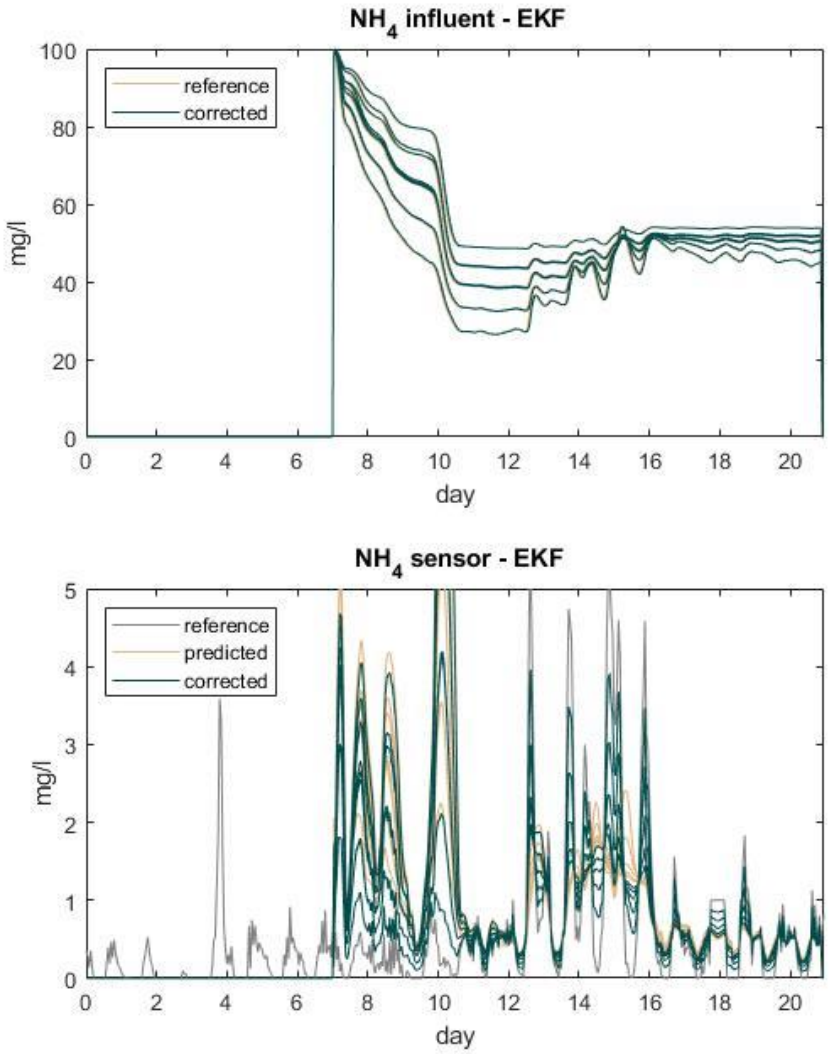

Fig. 104. Results of EKF estimation for different values of process noise covariance matrices

It is worth mentioning that the value of NH_4^++NH_3 nitrogen (S_{NH}) is slowly setting down to optimum despite the lack of measurements in the Kalman filter. One can find that the measure of NH_4^++NH_3 nitrogen reaches optimum for all simulations performed with different values process noise covariance matrices.

Out of the above results, the most favorable value of process noise covariance matrices has been. More precisely, each result is compared with the result of the reference simulation. The minimal root mean square error ($RMSE$) is calculated (Fig. 105)and its track is marked with the dashed line. Noise covariance matrix parameter, equal to 0.25, has given the best results.

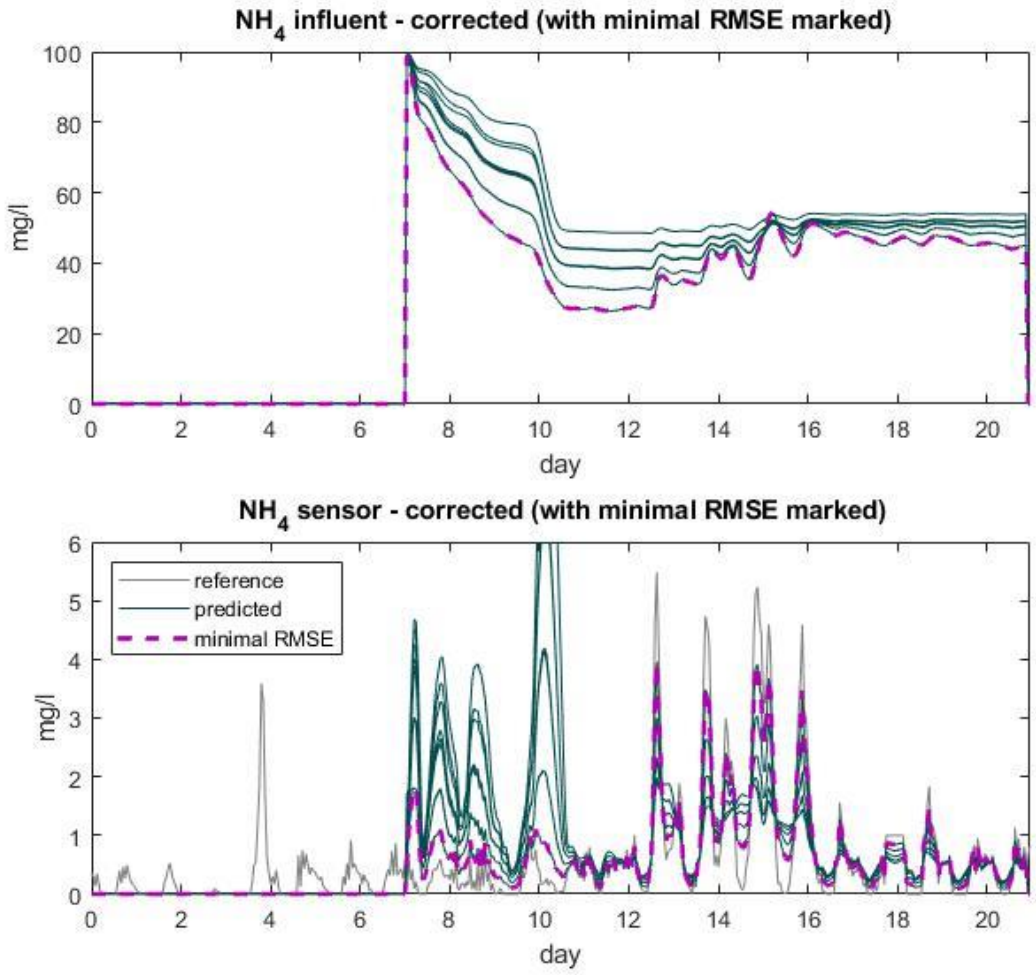

Most suitable parameters selected for EKF:
InitialNH4influent:100
InitialState: [100 0]
processNoiseCovMatrix: [0.32 0.32]
measurementNoiseCovMatrix:0.25

Fig. 105. Results of EKF estimation for different values of process noise covariance matrices – with minimal RSME marked

7.3.4 EKF in estimation for different initial values of influent

Results of EKF simulations with different starting initial NHTINFLUENT are presented below.

The values of NH_4^++NH_3 nitrogen (S_{NH}) influent are as follows: 0, 25, 50, 75, 100 mg/l. Results are presented in Fig. 106. Presented results are in line with previous results (Sec. 7.2.3).

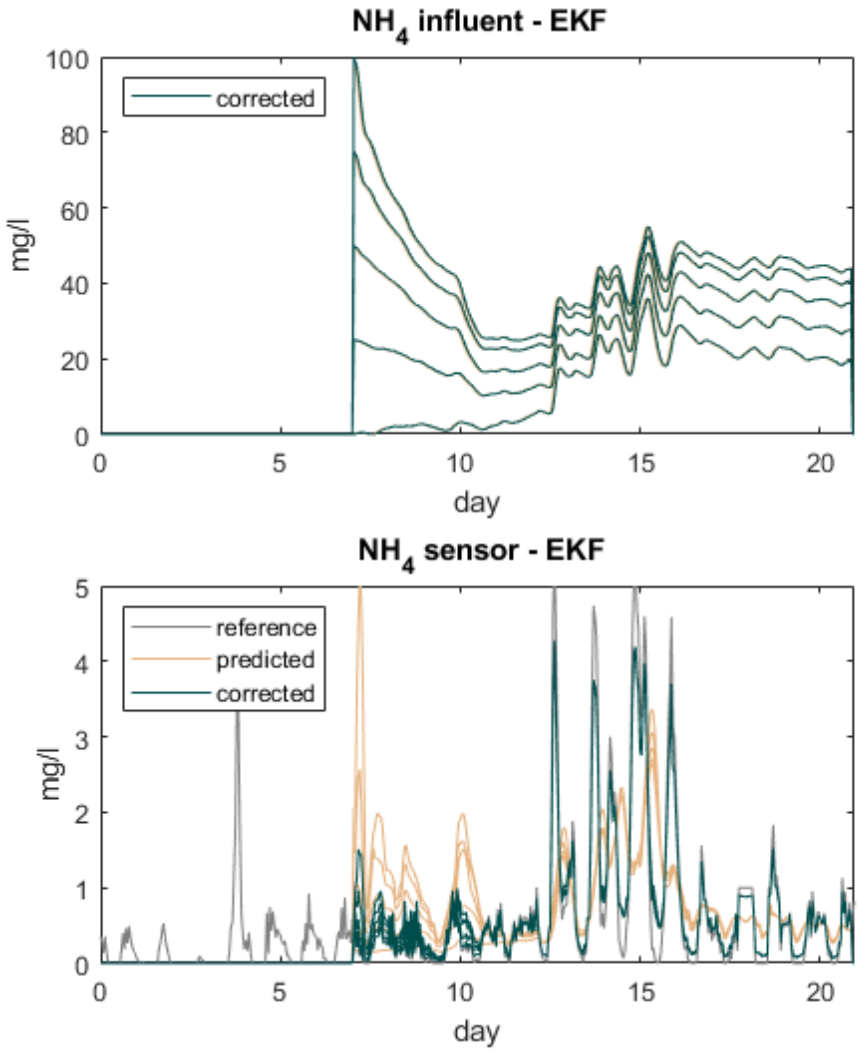

Fig. 106. Simulation results for EKF with initial conditions between 0 – 100

7.4 Summary of state estimation based on Kalman filter

Taking into account the earlier validation based on Morris, it is worth noting that the key parameters of the influencing wastewater are their volume and the NH_4^++NH_3 nitrogen parameter (Sec. 6).

Summarizing the above observations, the author can conclude that the analysis of the state observer using the Kalman filter proves the convergence of the BSM1 model to the assumed value of NH_4^++NH_3 nitrogen (31.56 mg/l) in influent (Sec. 7).

Taking into account the above facts, it can be said that the model is ready for further analysis taking into account the energy minimization criterion. The figure below shows how the above simulations are used in an optimization task (Fig. 107).

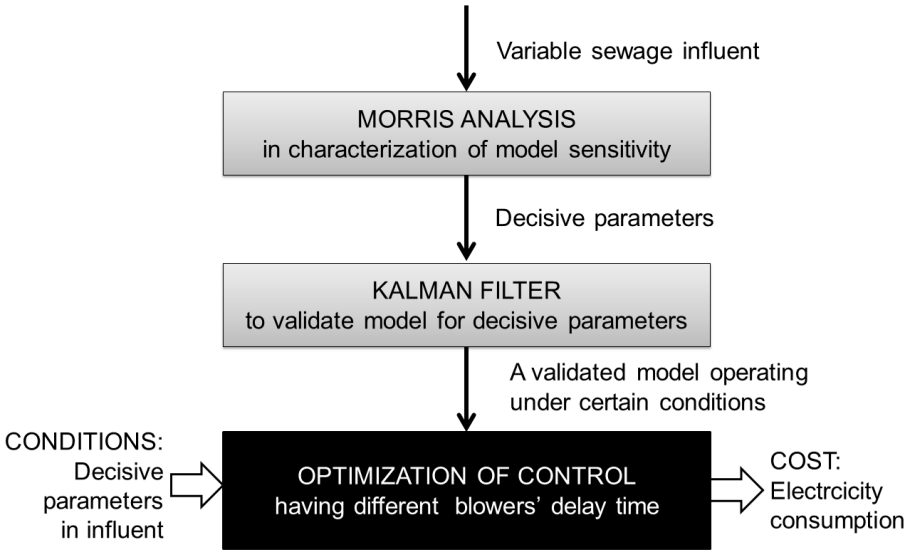

Fig. 107. The idea of optimization based on the discussed model

8 Testing the operation of reactor with blowers under variable conditions

8.1 Introduction to this paragraph

Heretofore, some theoretical issues of optimization in the field of energy have been presented and numeric model of a sewage treatment plant has been described and validated. The previous chapters present the operating procedure of a biological reactor in a sewage treatment plant. Contamination of sewage influent can vary which affects the treatment process. Thus, depending on the quality of sewage, expected oxygen level in reactors changes. The content of oxygen in reactors is controlled by air pumped to reactors. Blowers adjust the pressure to maintain the expected airflow. Their operation consumes significant amount of electric power and its adjustment is expected. The question of the impact of the quality of wastewater affecting the operation of wastewater treatment plants remains open.

In this paragraph, the author presents the results of simulations carried out to reduce the electricity consumption of facilities such as sewage treatment plants.

Taking into account the above-described models of the reactor (based on BSM1) and blowers (based on the characteristics), they have been used to simulate the complete treatment process (Fig. 108).

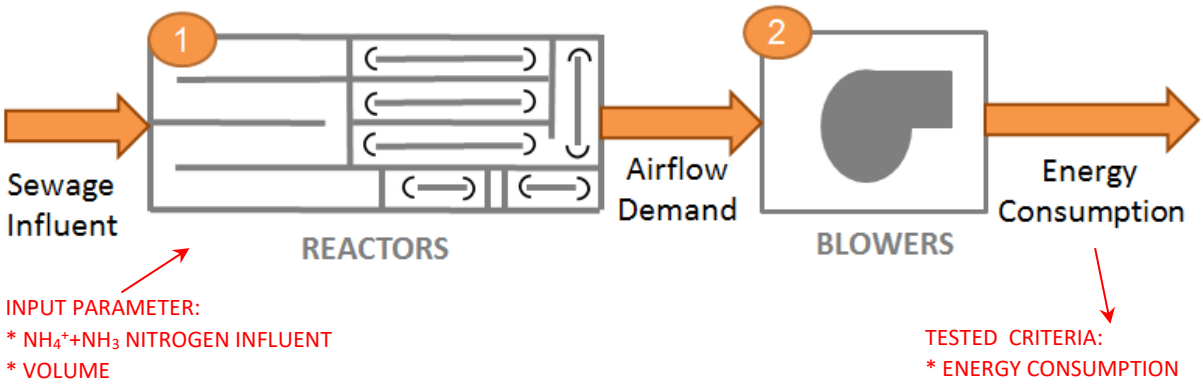

Fig. 108. General view of the optimization task

Such system is the object simulation that allows to analyze the process in terms of minimization of electric energy consumption. Such numeric process is based on the complex implementation of wastewater treatment integrated with aeration.

Using the numerical model of the wastewater treatment plant together with oxygenation presented above, which is based on the wastewater treatment plant in Płaszów Sewage Treatment Plant in Kraków, the author will discuss control options to reduce electric energy consumption during the purification process. Potentially, the modernization of pumps can give even 30% of savings and aeration can save up to 50% of electricity [9].

In the analyses presented in this chapter, parameters of the influencing sewage presented below are used (Fig. 109).

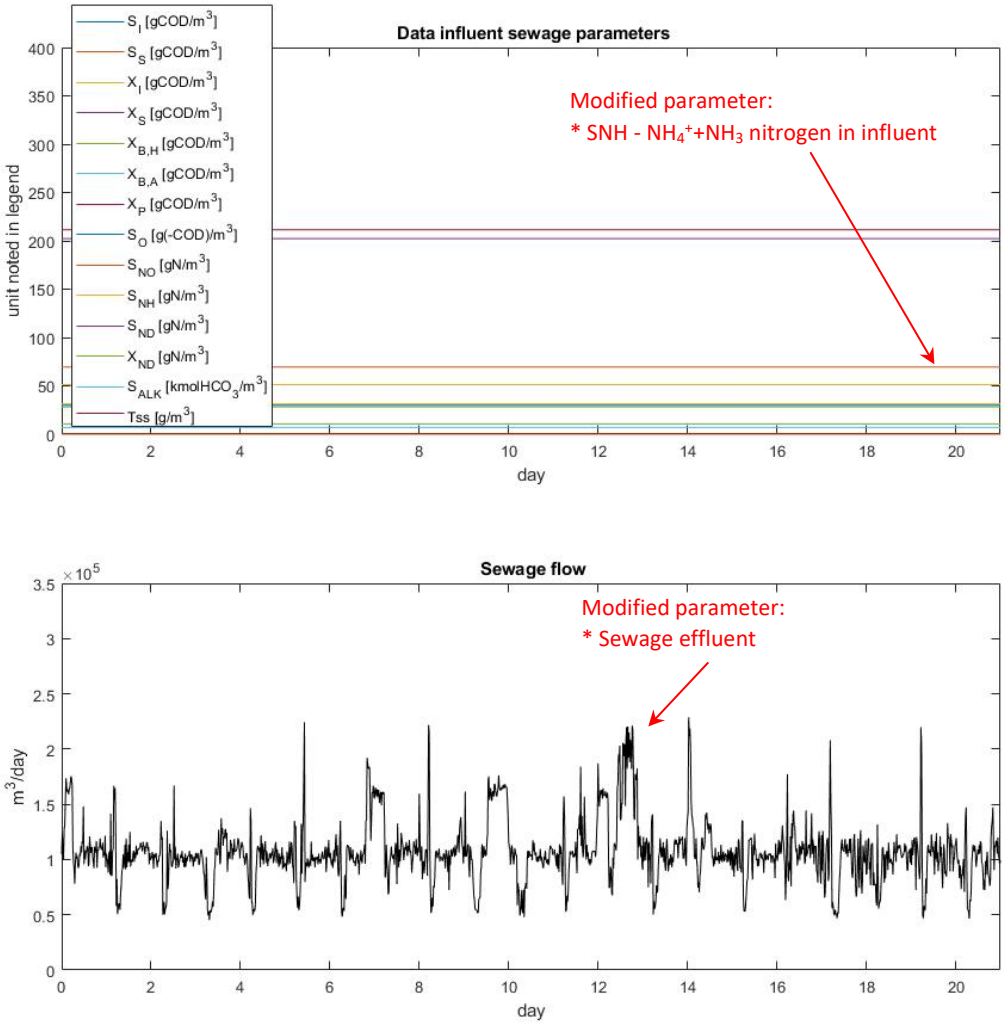

Fig. 109. Parameters of sewage influent used in simulations

The simulation is performed for a presented influent. First, the airflow demand is calculated. Such resulting airflow is the influent to blowers in Sec. 8.2and8.3.

8.2 How quality of sewage influent impacts the electricity consumption

In previous chapters, it has been investigated that NH_4^++NH_3 nitrogen (S_{NH}) in influent has the greatest influence on the process. Thus, this value is changed to validate the impact on electricity consumption. The values of SNH influent are: 20,30,40 and 50 mg/l.

A detailed results of simulations for extreme values are presented below.

The first figure (Fig. 110) presents the simulation for lowest NH_4^++NH_3 nitrogen. It shows that total airflow demand and total power of blowers is low. This is due to the fact that low NH_4^++NH_3 nitrogen causes low air demand and thus only 4 blowers operate at minimal utilization.

The second graphic (Fig. 111) presents the number of blowers and average utilization for a period of simulation

Graphic (Fig. 112) presents the simulation for highest NH_4^++NH_3 nitrogen. In this situation, total airflow demand and total power of blowers significantly exceed SCADA measurements. The fact is that the blower needs to be operated at high utilization.

Figure (Fig. 113) shows the variability of blower operation for this case. The blowers are dynamically turned on/off according to the previously presented algorithm.

The performance of the treatment plant has been investigated at intermediate values of NH_4^++NH_3 nitrogen. The observed measurements are shown in the table below (Tab. 18).

Tab. 18. Results of simulations with variable influent NH_4^+ + NH_3 nitrogen

Influent		Average effluent		Average blowers operation parameters (stop and start delay: 1h)		
Mean of sewage volume	NH_4^++NH_3 nitrogen	Nitrate and nitrite nitrogen	NH_4^++NH_3 nitrogen	Average power	Average number of blowers	Average utilization of blowers
[m^3/day]	[mg/l]	[mg/l]	[mg/l]	[kW]	[-]	[%]
107 203	20	0.41	0.68	931.77	2.81	60.46
	30	0.46	0.68	1045.28	3.04	65.05
	40	0.51	0.69	1144.05	3.12	76.87
	50	0.54	0.69	1240.81	3.31	82.31

These results allow the assumption that the relationship between the NH_4^++NH_3 nitrogen of the influent and the NH_4^++NH_3 nitrogen content inside of the reactor is increasing. Moreover, NH_4^++NH_3 nitrogen monotonically (increasingly)affects the operation of the blowers and, consequently, the electricity consumption in the facility.

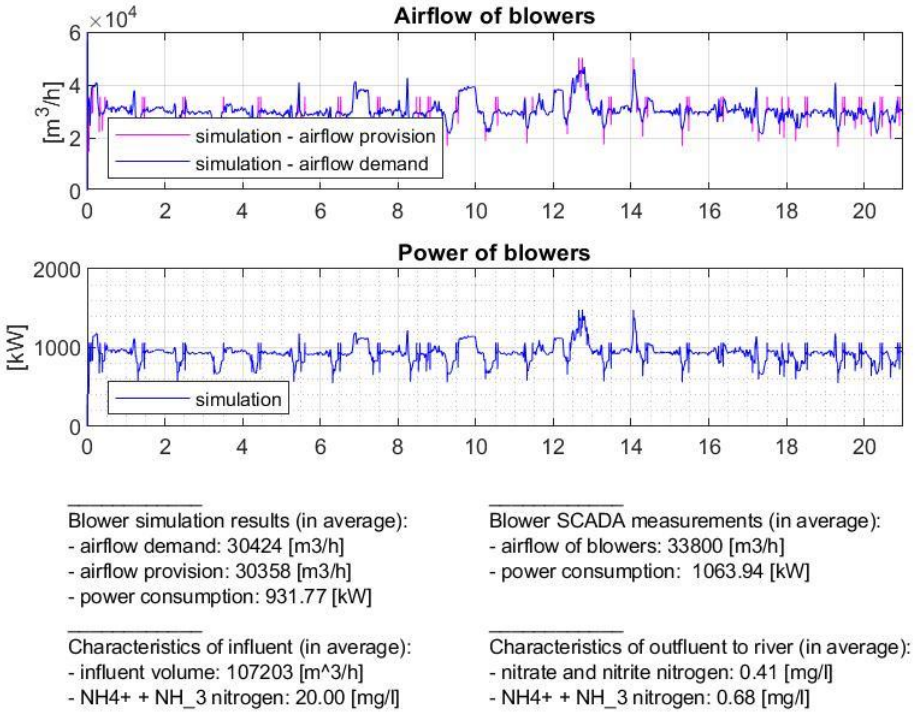

Fig. 110. Total airflow and total power for maximal NH_4^++NH_3 nitrogen

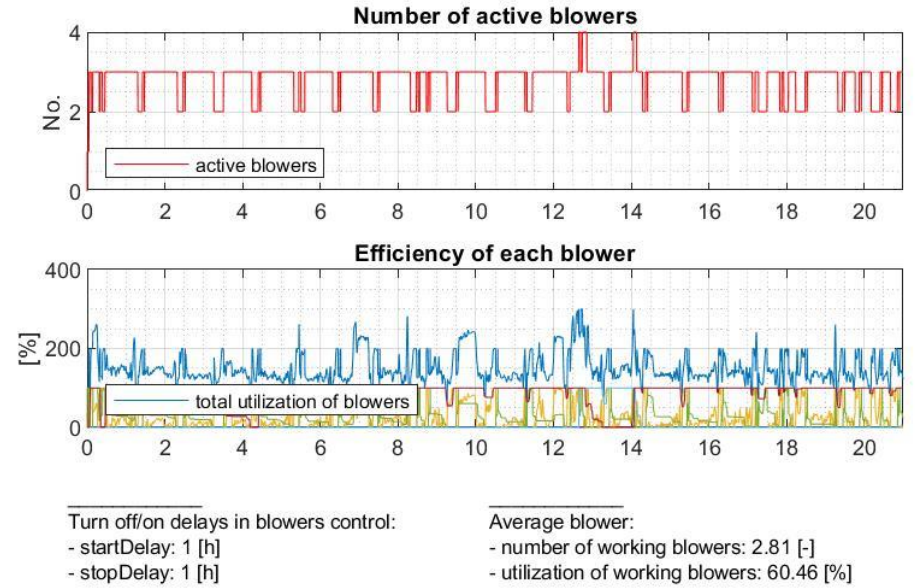

Fig. 111. Characteristics of simulation for maximal NH_4^++NH_3 nitrogen

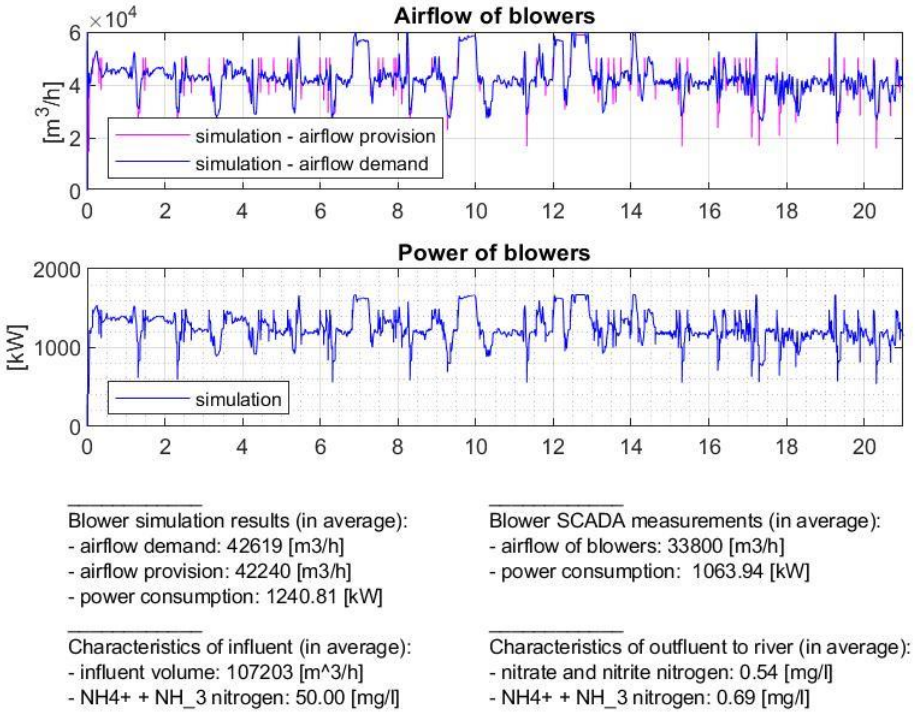

Fig. 112. Total airflow and total power for maximal NH_4^++NH_3 nitrogen

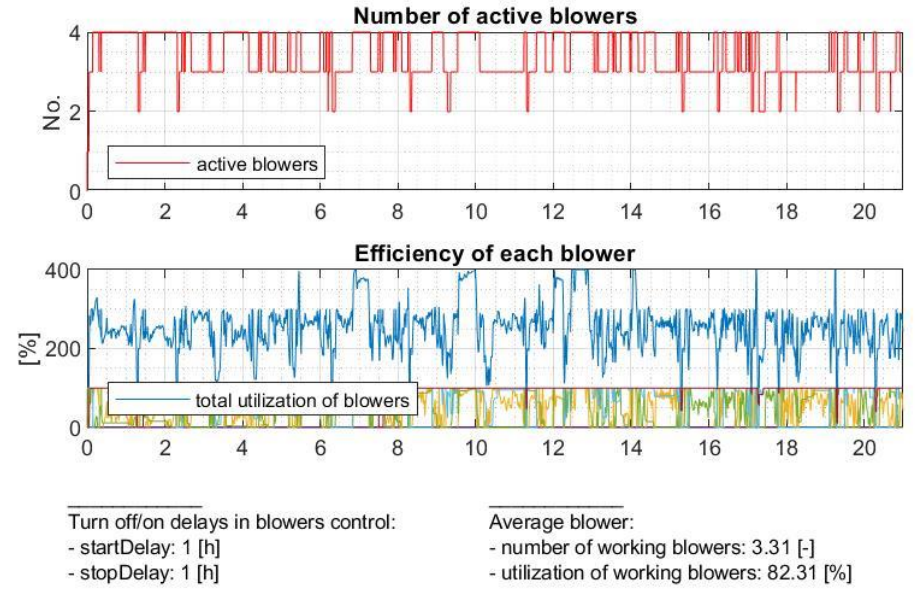

Fig. 113. Characteristics of simulation for maximal NH_4^++NH_3 nitrogen

Results for average effluent parameters are demonstrated in the figures below (Fig. 114).

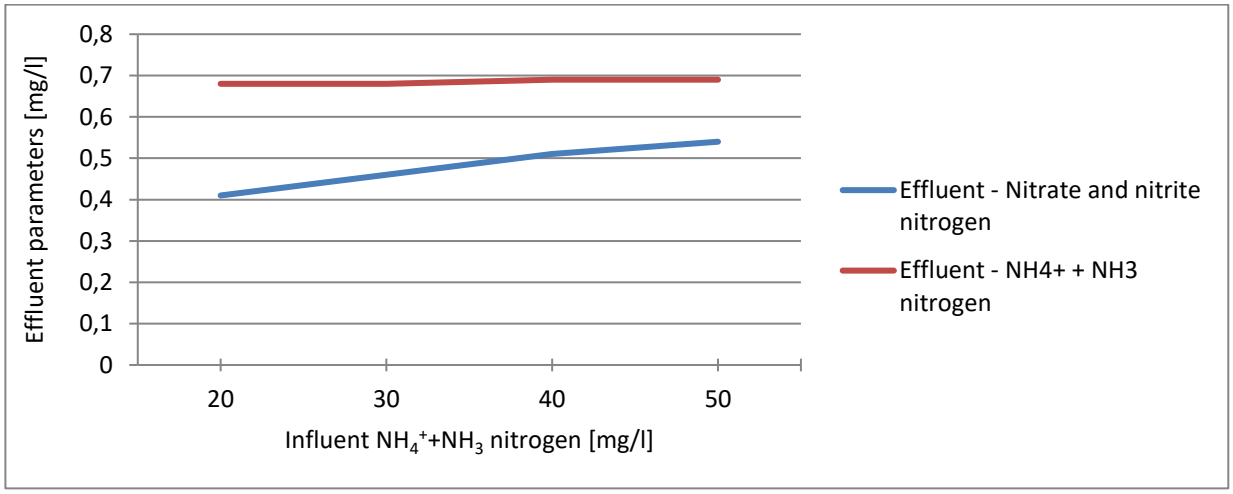

Fig. 114. Plots presenting effluent parameters:
1) Nitrate and nitrite nitrogen (S_{NO})
2) NH_4^++ NH_3 nitrogen (S_{NH})

The change in the quality of the sewage influent affects the performance of the observed blowers during the treatment process (Fig. 115). It can be seen that the utilization of the blower increases with the deterioration of the quality of the waste water.

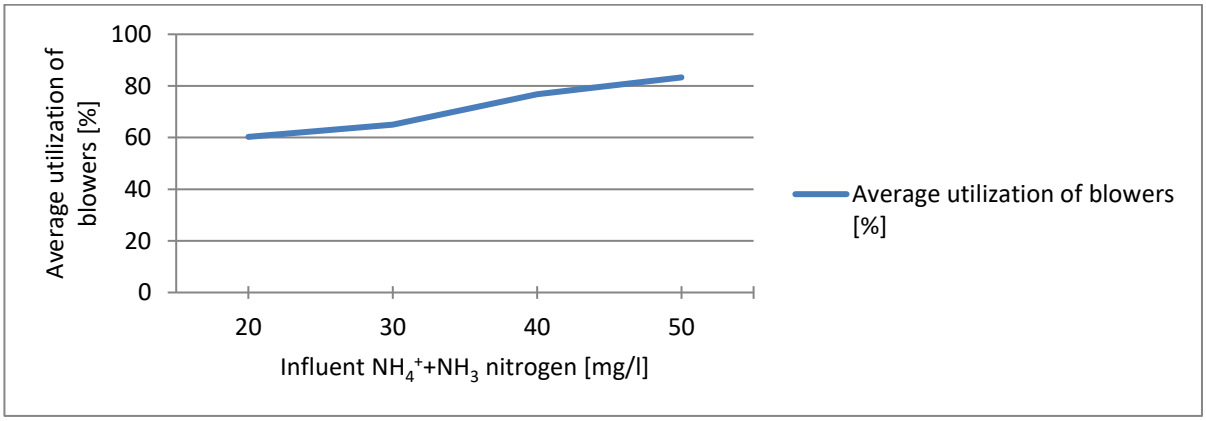

Fig. 115. Plot presenting average power needed to clean m^3 of sewage in one hour

Summarizing the calculations, it can be concluded that influent NH_4^++NH_3 nitrogen (S_{NH}) strongly impacts the wastewater treatment process. Nevertheless, the deterioration of the influencing effluent does not significantly change the effluent. Such behavior is the most desirable. The controller adapts to changing wastewater quality maintaining the effluent in desirable quality. The customization of blowers' use clearly indicates this operation in action.

8.3 How the volume of influent wastewater affects the consumption of electricity

The second experiment investigates how volume change for wastewater influent affects the process. The flow values have been selected corresponding to the physically possible situations in the Kraków sewage treatment plant. The mean of sewage volume ranges from 50 000m^3/day to 200 000m^3/day. The analysis assumes a constant quality of wastewater, regardless of its quantity.

The graphics below show the results of individual simulations for the extreme values of the influencing wastewater. It is worth noting that the results have been compared to the SCADA measurements for this case.

The first figure (Fig. 116) shows that total airflow demand and total power of blowers is low. This is due to the fact that low sewage flow causes low air demand and thus only 4 blowers operate at minimal efficiency are required.

The second graphic (Fig. 117) presents the number of blowers and average utilization for a period of simulation.

Graphic (Fig. 118) presents the simulation for highest sewage influent. In this situation, total airflow demand and total power of blowers significantly exceed SCADA measurements. The situation results from the fact that the increased influence of sewage causes an increase in the total demand for air.

This situation is well reflected in the next drawing (Fig. 119). Such a high demand for oxygen forces the maximum number of blowers (four) to operate at maximum utilization. As before, the first 7 days the model spends to stabilize.

Finally, the performance of the treatment plant has been investigated with mean of sewage volume at intermediate values. The set of results is shown in the table below (Tab. 19).

Tab.19. Results of simulations with variable volume of influent

Influent		Average effluent		Average blowers operation parameters (stop and start delay: 1h)		
Mean of sewage volume	NH_4^++NH_3 nitrogen	Nitrate and nitrite nitrogen	NH_4^++NH_3 nitrogen	Average power	Average number of blowers	Average utilization of blowers
[m^3/day]	[mg/l]	[mg/l]	[mg/l]	[kW]	[-]	[%]
50 000	31.56	0.30	0.63	623.45	2.07	52.59
100 000		0.46	0.67	1003.95	2.97	63.09
150 000		0.67	0.71	1371.94	3.89	69.21
200 000		0.91	0.74	1609.57	4.00	92.18

As in the previous chapter (Sec. 8.2), on the basis of these results, a monotonically increasing dependence of the amount of wastewater influencing the internal measurements of wastewater quality in the reactor has been assumed. This also monotonically (increasingly)affects the electricity consumption.

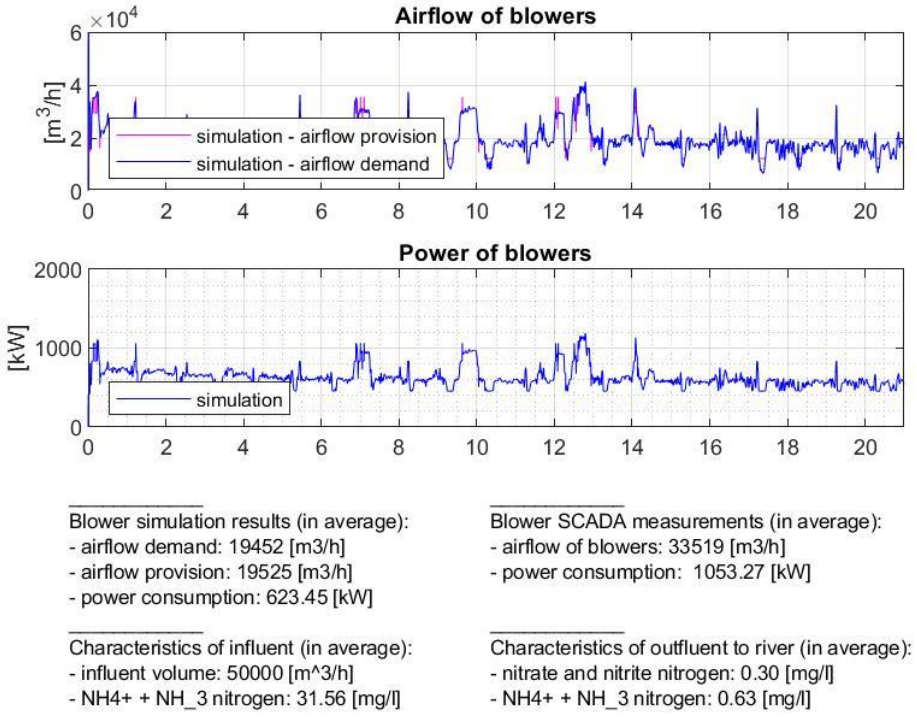

Fig. 116. Total airflow and total power for minimal mean of sewage volume

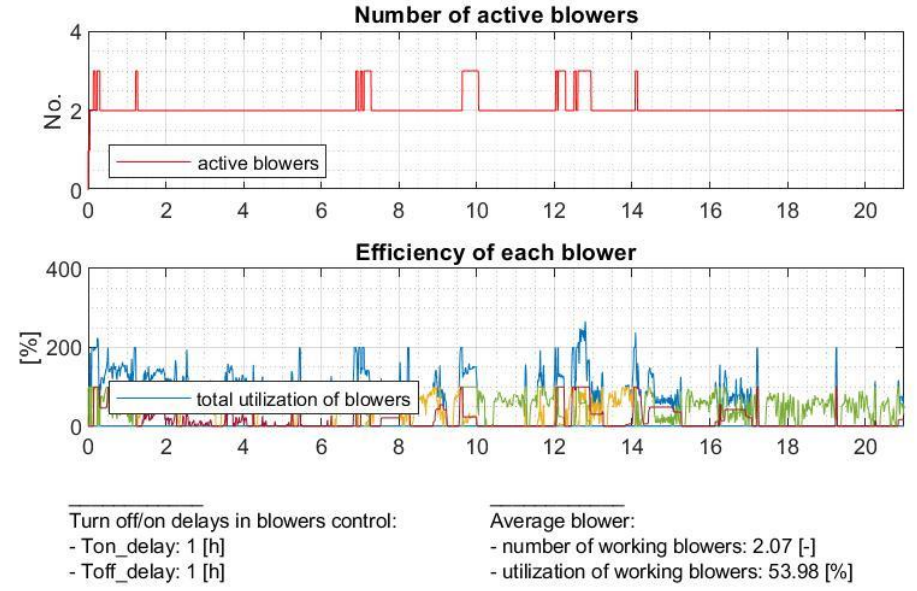

Fig. 117. Characteristics of simulation for minimal mean of sewage volume

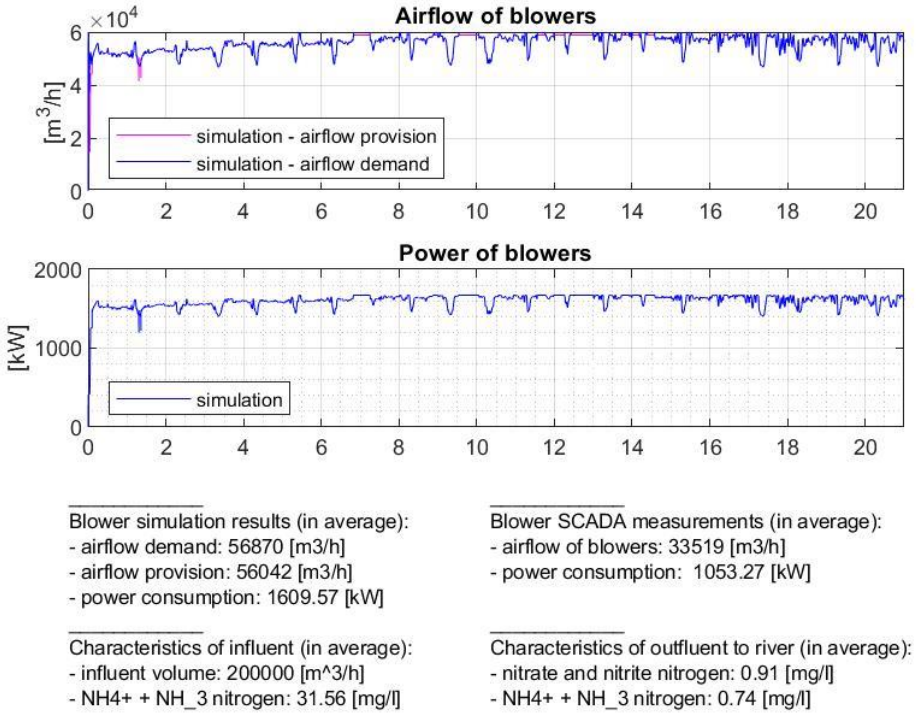

Fig. 118. Total airflow and total power for maximal mean of sewage volume

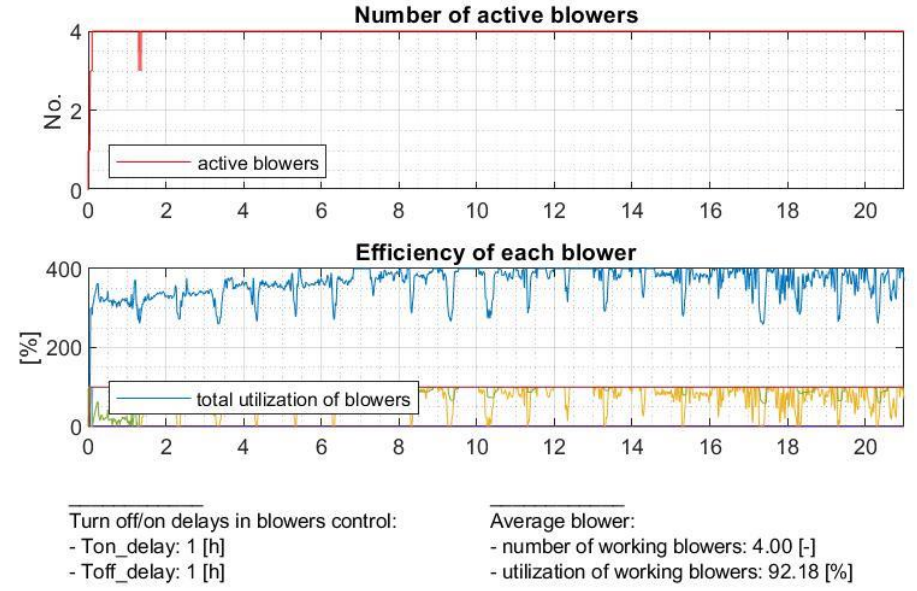

Fig. 119. Characteristics of simulation for maximal mean of sewage volume

The plot below (Fig. 120) presents the average effluent on mean of sewage volume flowing to the reactor. It can be seen that with increased inflow into the treatment plant, the quality of the effluent in the reactor deteriorates.

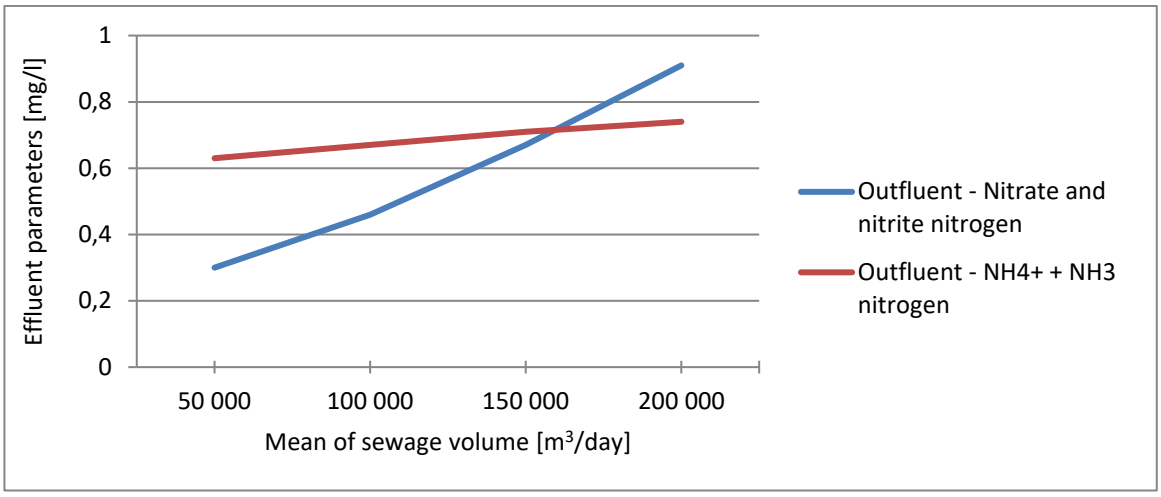

Fig. 120. Plots presenting effluent parameters:
1) Nitrate and nitrite nitrogen (S_{NO})
2) NH_4^++NH_3 nitrogen (S_{NH})

The characteristic of the power in the relation to the mean of influent is similar. For low mean of sewage volume (50 000 m^3/day) blowers only use half of their rated power. For the highest assumed influent (200 000 m^3/day) the expected performance of the blowers increases to almost 100%. It can be easily observed that the change of influent affects the average power needed to clean m^3 of sewage in one hour (Fig. 121).

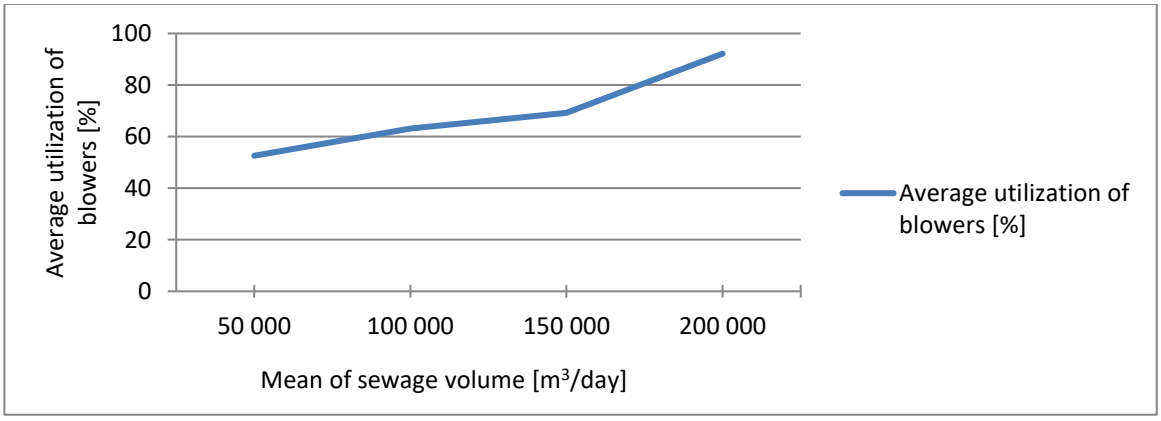

Fig. 121. Plot presenting average power needed to clean m^3 of sewage in one hour

8.4 Discussion of results

The paragraph presents the operation of the numerical model of the sewage treatment plant as a whole. The modeled sewage treatment plant has been launched under various operational conditions. The quality of the wastewater and volume of influent affect the electricity consumption. This action is reflected in the characteristics for the simulation (the number of blowers connected and their efficiency).

The runs with introduced extreme values of the diagnosed key parameters in the influencing sewage (NH_4^++NH_3 nitrogen and flow volume).In particular, it has been shown that the NH_4^++NH_3 nitrogen (S_{NH} parameter) of influent wastewater has a key impact on the treatment process and therefore on energy demand. Moreover, the volume of effluent significantly influences the electricity consumption of the blowers. The results for all simulations are shown in the tables.

Observing the graphs showing the total air flow and electricity consumption of blowers, it can be seen that in the full compliance of simulations with the SCADA measurements has not been achieved. Nevertheless, the results satisfied the author– the observed cyclicality of the simulation results coincides with the actual observations. The results presented in this paragraph confirm the expected behavior of the numerical environment of the sewage treatment plant.

The model developed in this way is the basis for launching optimization algorithms aimed at reducing the consumption of electricity. The report [1] shows the operation of the control system in an actual wastewater treatment plant.

9 Control optimization for minimization of energy consumption

9.1 Influence of blowers delay times on energy consumption

Earlier chapters of the work inspected the operation of the sewage treatment plant model. The operation of the reactor system with blowers was demonstrated in accordance with the measurement data. Now the blowers themselves are analyzed in terms of their performance to optimize electricity consumption. This study investigates in particular the electric energy consumption in relation to real airflow (Fig. 122).

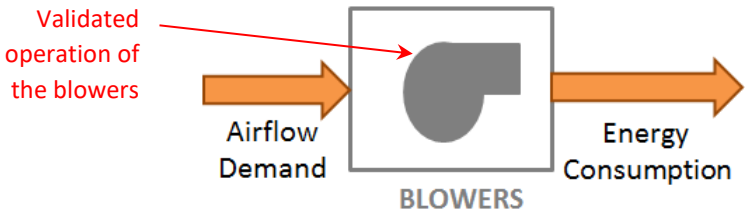

Fig. 122. Scheme of action simulated in this analysis

Sec. 5.2.1 mentions controlling the blowers by changing the efficiency and turning them on and off after some delay. What is their impact on electricity consumption? Is there any good criterion for optimizing electricity consumption? The analyses in this chapter perform to answer these questions. In this case, the author uses the airflow registered in SCADA system as input to model of blowers. The aforementioned model of blowers in WWTP is used in comparison with the values of electricity consumption obtained in simulation with the values from real measurements. The simulation has been performed for different values of the switch-on (T_{ON_DELAY}) and switch-off (T_{OFF_DELAY}) delay times (Fig. 123). The presented algorithm is an original implementation of task scheduling (sec. 2.4.4).This blower switch delay algorithm is a form of the tasks scheduling algorithm implementing the lazy approach.

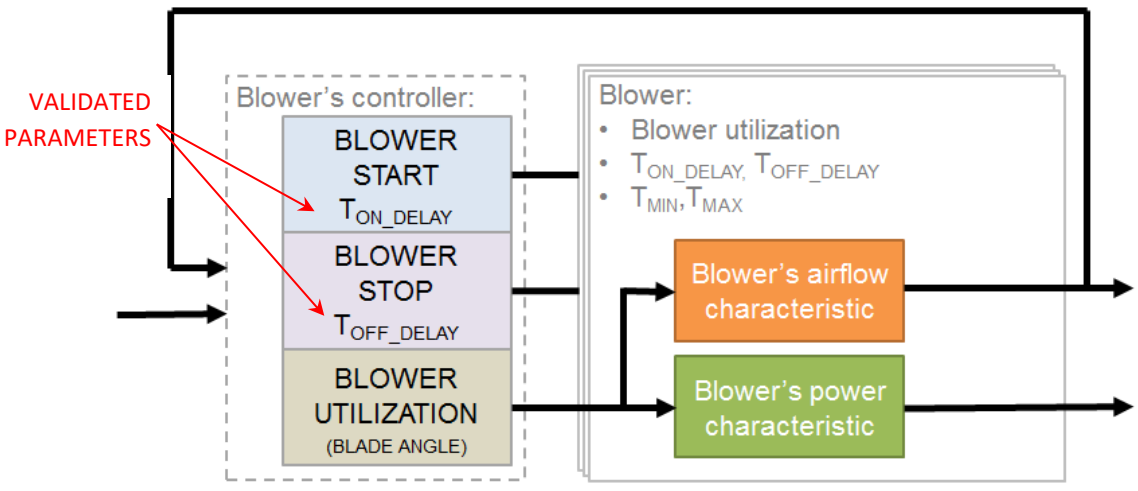

Fig. 123. Detailed plan of performed simulation

The values of T_{ON_DELAY} and T_{OFF_DELAY} have been selected based on the observation of the SCADA signal. The following times are specifically proposed: 1h, 2h and 4h. In this simulation, the input value is airflow demand based on the SCADA measurement.

The result of the analyses are shown in the Tab. 20 with Fig. 124 and Tab. 21 with Fig. 125.

Tab. 20. Average power for different delay times during simulation

T_{OFF} delay [h] / T_{ON} delay [h]	1	2	4
1	969.60	993.66	1015.12
2	938.93	960.54	983.52
4	886.58	912.02	993.08

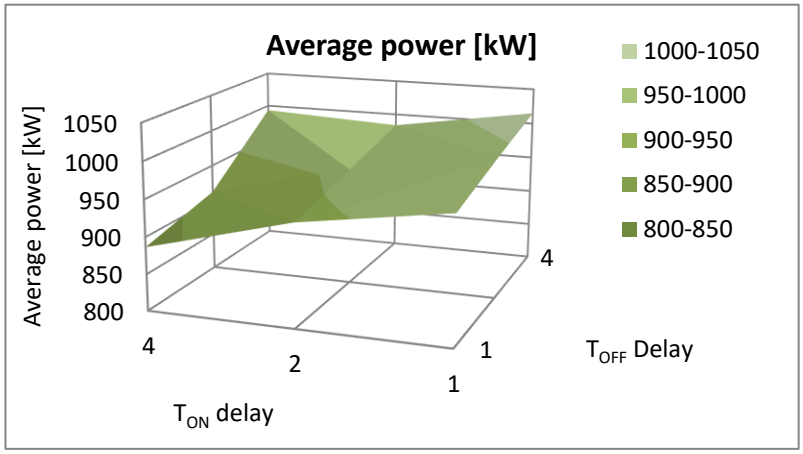

Fig. 124. Average power for different delay times during simulation

Tab. 21. Average utilization of working blowers during simulation for different delay times during simulation

T_{OFF} delay [h] / T_{ON} delay [h]	1	2	4
1	74.52	71.11	65.58
2	75.76	73.56	67.52
4	78.44	75.76	71.09

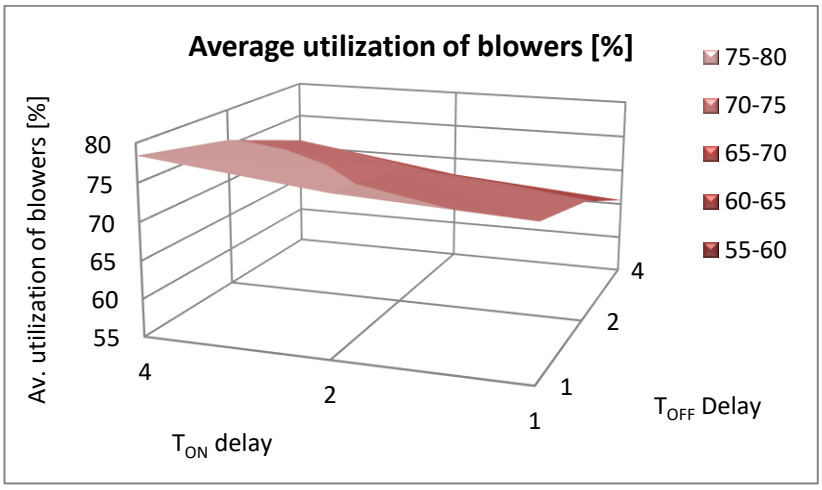

Fig. 125. The detailed plan of performed simulation

The results presented above (Tab. 20 with Fig. 124 and Tab. 21 with Fig. 125) clearly show that the delay in switching the blowers on and off has a significant impact on the operation of the blowers, which results in a change in electricity consumption.

Let's assume that electric energy consumption for T_{ON_DELAY} and T_{OFF_DELAY} equal 1h will be denoted as 100%. In this case T_{ON_DELAY} (switch on time) increased to 4h will reduce the electricity consumption to 91,43% of its initial value. On the other hand, prolonging the T_{OFF_DELAY} (switch off time) of the blowers to 4h increases low utilization runtime, causing increase of electricity usage to 104,69% of the initial value. Generally speaking, on the basis of these charts one direct conclusion can be proposed. Forcing the blowers to procrastinate switching (higher T_{ON_DELAY}) causes operation of the blowers at more favorable operating points, resulting in a reduced power of the installation. At the same time, forcing the blowers to run longer (higher T_{OFF_DELAY}) causes the operation at lower efficiency points resulting higher electricity consumption.

It is worth highlighting one fact. When the blower operates for elongated time (higher T_{OFF_DELAY}) airflow supplied by blowers ($airflow_{PROVISION}$) covers one expected from BSM1 ($airflow_{DEMAND}$).On the other hand, delaying the moment when the blower switches on (higher T_{ON_DELAY}) slightly worsens the quality of the airflow supplied by blowers ($airflow_{PROVISION}$) compared to one expected from BSM1 ($airflow_{DEMAND}$). It can be assumed that delayed switching on (higher T_{ON_DELAY}) of a new blower might force those already operating to work with maximal, however still insufficient capacity. This deficiency of airflow will be taken into account as one of the optimization criteria in the next chapter (Sec. 9.2).

The simulation results for the cases giving two marginal results of electricity consumption are described below.

Fig. 126 presents the airflow and power for blowers operating with 1h for start delay(T_{ON_DELAY}) and 4h for stop delay (T_{OFF_DELAY}). However, periodic deviations of airflow can be noticed. This happen when the blower shuts down and other blowers have to overcompensate the missing airflow. The characteristics of blowers' operation are shown in Fig. 127. Here as well, one can observe that this blowers' configuration causes the blowers to turn on quickly and then it is turned off after a longer period.

By contrast, Fig. 128 presents the simulation results for blowers operating with 4h for start (T_{ON_DELAY}) and 1h for stop (T_{OFF_DELAY}). One may notice that at certain periods the blown air does not cover the demand. The situation is caused by an extended switch-on delay of the blower which has been previously switched off. Fig. 129 shows that there are often fewer blowers in operation at any given time. This action is due to the elongation of time when the blowers are turned on.

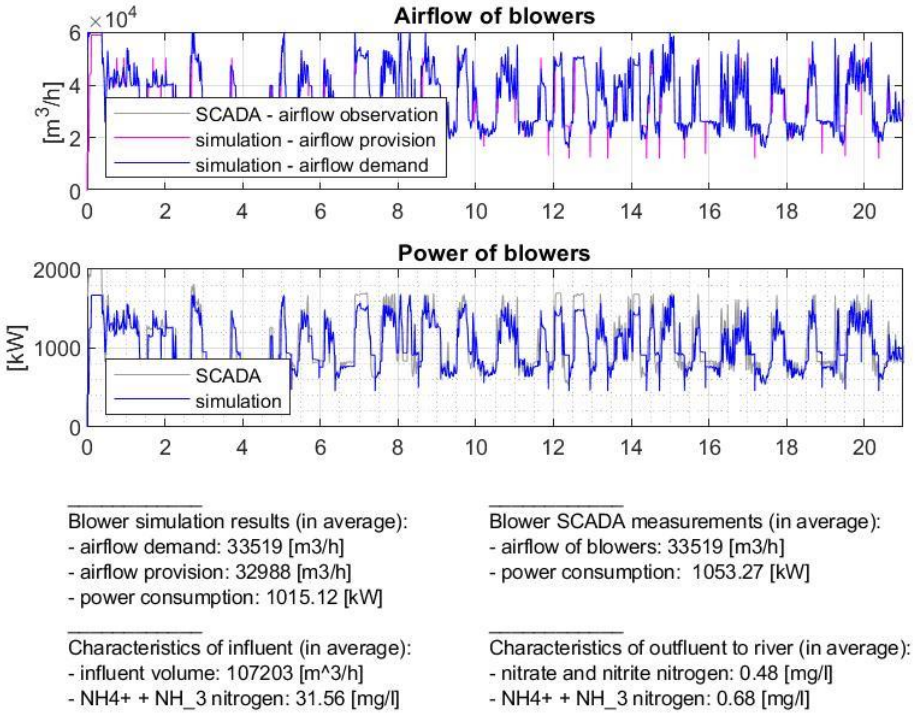

Fig. 126. Total airflow and total power for T_{ON_DELAY} equal 1h and T_{OFF_DELAY} equal 4h

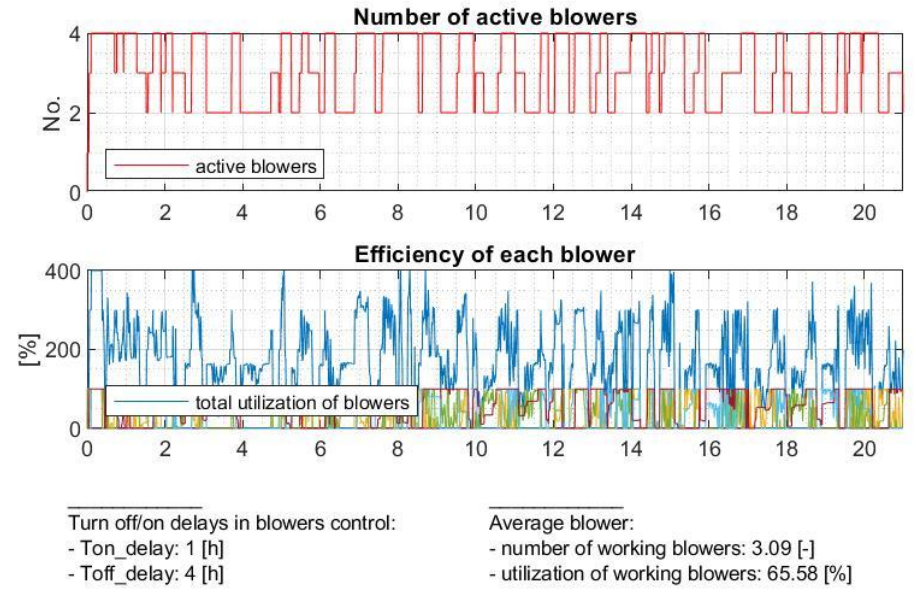

Fig. 127. Characteristics of simulation for T_{ON_DELAY} equal 1h and T_{OFF_DELAY} equal 4h

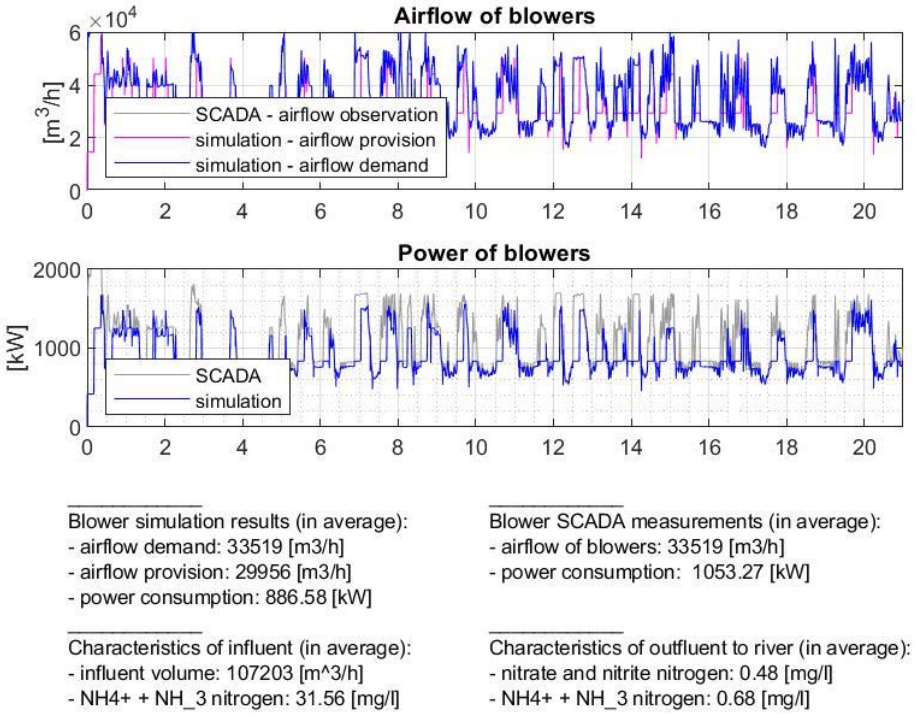

Fig. 128. Total airflow and total power for T_{ON_DELAY} equal 4h and T_{OFF_DELAY} equal 1h

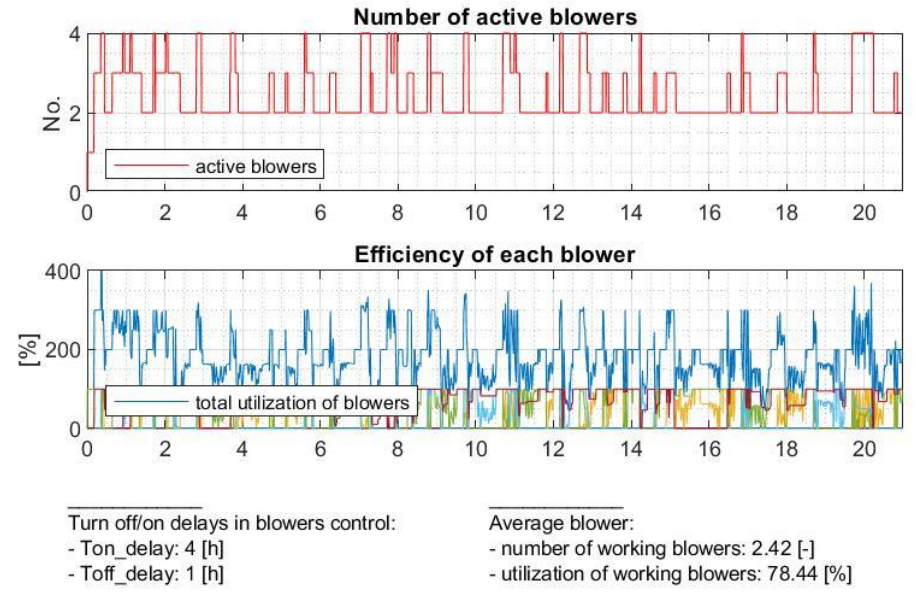

Fig. 129. Characteristics of simulation for T_{ON_DELAY} equal 4h and T_{OFF_DELAY} equal 1h

9.2 Control optimization to reduce electricity consumption

During the simulation presented in Sec. 9.1, it can be observed that the blowers do not turn on time, which causes delayed activation and a certain period of insufficient oxidation. However, temporary hypoxia is acceptable when it is replenished in later periods. It is clearly seen in the for T_{ON_DELAY} equal 4h and T_{OFF_DELAY} equal 1h (cited Fig. 130 from Sec. 5.2.4).

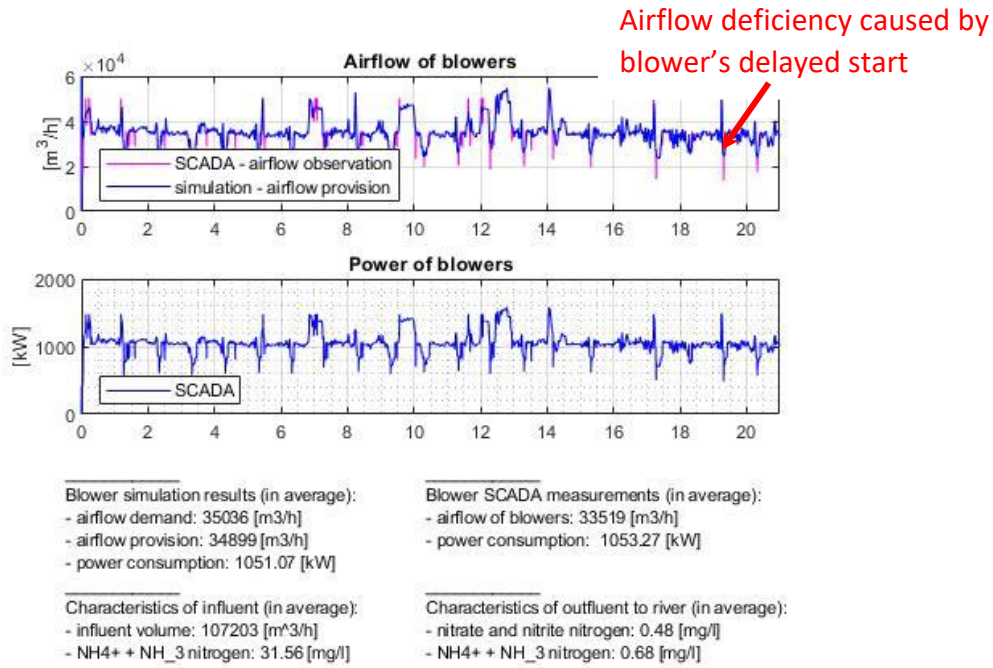

Fig. 130. Total airflow and total power for T_{ON_DELAY} equal 4h and T_{OFF_DELAY} equal 1h

Finally, this section examines the case of the control optimization of the blower reactor system (as presented in Sec. 2.4). The analysis of electricity consumption by blowers for various parameters of influencing sewage is the final stage of the dissertation. This time, all analyzed input parameters have been taken into account. The cost criterion is electricity consumption. The modelled case is described graphically in the figure below (Fig. 131).

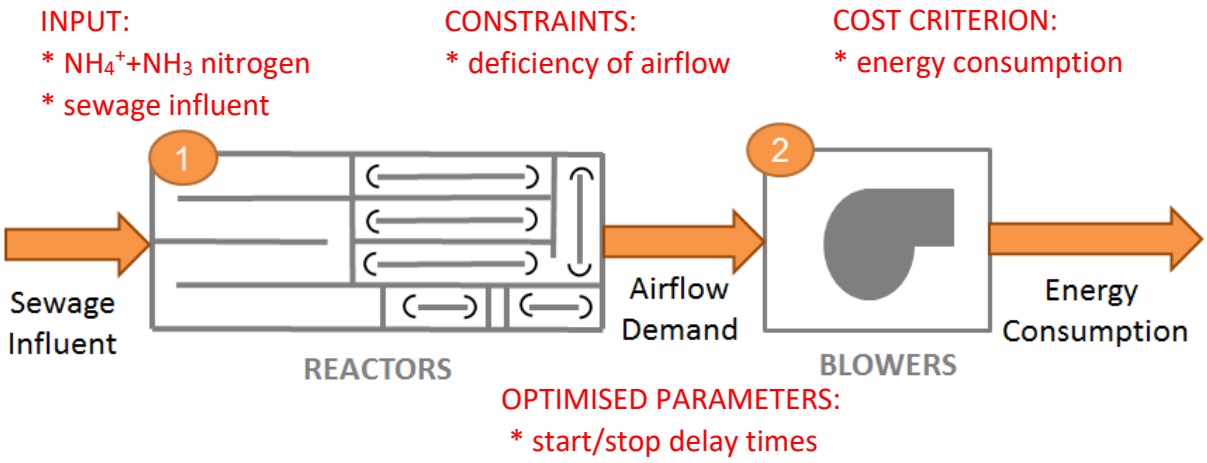

Fig. 131. The idea of simulations used in this chapter

It should be borne in mind that the model of sewage treatment plant is very complex. Electricity consumption is not linearly dependent on input parameters including imposed constraints. The task can present optimization problem with following characteristics:

- COST CRITERION⇨The goal of optimization is to reduce power electric energy consumption in the model of WWTP. (Sec. 5.2);
- INPUT⇨ Influent NH_4^++NH_3 nitrogen and volume – the different qualities of the incoming waste water must be taken into account in the operation of the treatment plant (Sec. 6 , Sec. 7 and Sec. 8);
- INTERNAL CONSTRAINTS⇨The value of airflow expected by BSM1 model ($airflow_{DEMAND}$) it is not fully covered by airflow feed from blowers ($airflow_{PROVISION}$). The disturbance differ for different delay times of the controlled blowers (Sec. 9.1);
- OPTIMISED PARAMETERS ⇨ Start/stop delay times in blowers' control allow for considerable energy savings. The longer the delay time of the blowers, the lower the electricity consumption.

The limitations described above are considered as the boundary conditions for this optimization. In a sense, the problem appears to be the optimal control task. Unfortunately, the classic case of optimal control requires a continuous function (implementation of the equations shown in Sec. 2.4.3).However, the relation between the continuous function of electricity consumption as a relation of influent NH_4^++NH_3 nitrogen and volume is very complex. Therefore, the author chooses grid search approach– calculation of specific cases in order to determine the directions of optimal control. The adopted calculations are for a small number of samples. Hence, this algorithm will prove successful despite the fact that the computational complexity of this algorithm has been demonstrated [59], [171].

A set of 81 simulations has been performed in which the input parameters of wastewater change in accordance with quality of influent(as in Sec. 8.2) and volume of influent (as in Sec. 8.3). For each simulation, it has been checked how the value of airflowDEMAND and airflowPROVISION differ for various delay times of sewage treatment plants(as in Sec. 9.1). The result of simulations is presented below (Tab. 22).

The simulation result for $T_{ON\_DELAY} = 4$ and $T_{OFF\_DELAY} = 1$ is in bold. In accordance with Sec. 9.1 for these blower control parameters, the most efficient blower operation points are obtained, resulting in the highest energy savings.

Tab. 22. Result of simulations

SIM NR.	BLOWERS' DELAY		INFLUENT PARAMETERS		MEAN SUPPLIED AIRFLOW		ENERGY CONSUMPTION
	T_{ON_DELAY}	T_{OFF_DELAY}	NH_4^++NH_3nitrogen	Influent volume	Reactor demand	Provision by blowers	
	[h]	[h]	[m^3/h]	[mg/l]	[m^3/h]	[m^3/h]	[kW]
1	1	1	20,00	50000	17937,15	18078,87	587,12
2				100000	29733,42	29624,52	886,19
3				150000	40789,44	40754,58	1202,54
4			30,00	50000	20390,50	20449,22	650,94
5				100000	34072,01	33930,84	1026,80
6				150000	46784,68	46717,65	1393,56
7			40,00	50000	22821,16	22782,76	710,55
8				100000	38344,04	38144,63	1136,24
9				150000	52146,26	51453,29	1502,56
10		2	20,00	50000	17937,15	18079,35	587,68
11				100000	29733,42	29572,42	888,27
12				150000	40789,44	40736,00	1205,61
13			30,00	50000	20390,50	20497,73	652,93
14				100000	34072,01	33910,85	1030,44
15				150000	46784,68	46713,20	1396,53
16			40,00	50000	22821,16	22854,88	714,35
17				100000	38344,04	38088,19	1140,51
18				150000	52146,26	51384,93	1503,16
19		4	20,00	50000	17937,15	18091,27	590,02
20				100000	29733,42	29601,13	893,39
21				150000	40789,44	40703,02	1211,42
22			30,00	50000	20390,50	20488,32	654,23
23				100000	34072,01	33958,92	1038,54
24				150000	46784,68	46647,33	1399,58
25			40,00	50000	22821,16	22880,83	718,94
26				100000	38344,04	38140,22	1151,04
27				150000	52146,26	51426,01	1506,81
28	2	1	20,00	50000	17937,15	18067,31	586,71
29				100000	29733,42	29581,73	885,87
30				150000	40789,44	40714,63	1201,10
31			30,00	50000	20390,50	20481,44	650,93
32				100000	34072,01	33754,87	1017,31
33				150000	46784,68	46507,54	1381,15
34			40,00	50000	22821,16	22657,92	703,61
35				100000	38344,04	37607,29	1115,40
36				150000	52146,26	51384,37	1499,93
37		2	20,00	50000	17937,15	18065,54	586,95
38				100000	29733,42	29441,10	881,86
39				150000	40789,44	40680,97	1203,84

40			30,00	50000	20390,50	20494,85	653,43
41				100000	34072,01	33633,78	1017,89
42				150000	46784,68	46696,23	1394,76
43			40,00	50000	22821,16	22714,15	708,40
44				100000	38344,04	37603,58	1121,03
45				150000	52146,26	51190,43	1495,56
46		4	20,00	50000	17937,15	18091,27	590,02
47				100000	29733,42	29461,52	890,61
48				150000	40789,44	40627,68	1208,66
49			30,00	50000	20390,50	20523,25	655,95
50				100000	34072,01	33865,37	1031,08
51				150000	46784,68	46713,05	1401,13
52			40,00	50000	22821,16	22747,56	711,38
53				100000	38344,04	37978,18	1142,42
54				150000	52146,26	51391,11	1505,49
55	**4**	**1**	**20,00**	**50000**	**17937,15**	**18050,58**	**585,44**
56				**100000**	**29733,42**	**29191,60**	**870,61**
57				**150000**	**40789,44**	**40512,83**	**1193,53**
58			**30,00**	**50000**	**20390,50**	**20294,06**	**639,31**
59				**100000**	**34072,01**	**33294,65**	**997,09**
60				**150000**	**46784,68**	**46031,96**	**1359,50**
61			**40,00**	**50000**	**22821,16**	**22280,57**	**687,43**
62				**100000**	**38344,04**	**36985,19**	**1094,05**
63				**150000**	**52146,26**	**51173,31**	**1491,96**
64		2	20,00	50000	17937,15	18060,56	586,76
65				100000	29733,42	29175,74	870,64
66				150000	40789,44	40576,81	1200,12
67			30,00	50000	20390,50	20307,60	641,81
68				100000	34072,01	33313,37	1002,47
69				150000	46784,68	46456,54	1378,66
70			40,00	50000	22821,16	22246,14	687,38
71				100000	38344,04	36750,14	1091,31
72				150000	52146,26	51180,11	1494,41
73		4	20,00	50000	17937,15	18087,92	589,57
74				100000	29733,42	29187,61	875,80
75				150000	40789,44	40478,57	1203,57
76			30,00	50000	20390,50	20340,94	645,77
77				100000	34072,01	33397,62	1010,68
78				150000	46784,68	46690,34	1399,40
79			40,00	50000	22821,16	22357,73	695,40
80				100000	38344,04	37349,52	1117,41
81				150000	52146,26	51313,10	1502,66

The average for particular blowers switch on/off delay times (TON_DELAY and $TOFF\_DELAY$) is calculated in order to simplify the analysis of results. Table below presents the average results for individual TON_DELAY and $TOFF\_DELAY$ parameters (Tab. 23).

Tab. 23. Abstract of simulation results

SIM NR.	BLOWERS' DELAY		SUPPLIED AIRFLOW				ENERGY CONSUMPTION	
	T_{ON_DELAY}	T_{OFF_DELAY}	Reactor demand	Provision by blowers	Mean Deficiency	Mean Deficiency	Mean Energy	Change of Energy
	[h]	[h]	[m³/h]	[m³/h]	[m³/h]	[%]	[kW]	[%]
1-9	1	1	33668,74	33548,48	120,26	0,46	1010,72	100
10-18		2	33668,74	33537,50	131,24	0,54	1013,27	100,25
19-27		4	33668,74	33548,56	120,18	0,53	1018,22	100,74
28-36	2	1	33668,74	33417,46	251,29	0,83	1004,67	99,40
37-45		2	33668,74	33391,18	277,56	0,91	1007,08	99,64
46-54		4	33668,74	33488,78	179,96	0,70	1015,19	100,44
55-63	**4**	**1**	**33668,74**	**33090,53**	**578,22**	**1,70**	**990,99**	**98,05**
64-72		2	33668,74	33118,56	550,19	1,66	994,84	98,43
73-81		4	33668,74	33244,82	432,92	1,34	1004,47	99,38

Turning to the analysis of the presented results, it can be concluded that evidently the case of operation with $T_{ON\_DELAY}=4h$ and $T_{ON\_DELAY}=1h$ gives lower energy consumption for operation for different influent quality. Extending the T_{ON_DELAY} value from 1 hour to 4 hours can reduce the electricity consumption by 1,95% (the situation is similar to that described in Sec. 9.1).

Fig. 132 presents the summary how the quality of sewage influent differentiates $airflow_{PROVISION}$ pushed by blowers from $airflow_{DEMAND}$ from BSM1. $T_{ON\_DELAY}=4h$ and $T_{OFF\_DELAY}=1h$ results with maximal around 600m³/h deficiency of supplied airflow (at the same time, the average air flow is approximately 35000-40000m³/h).

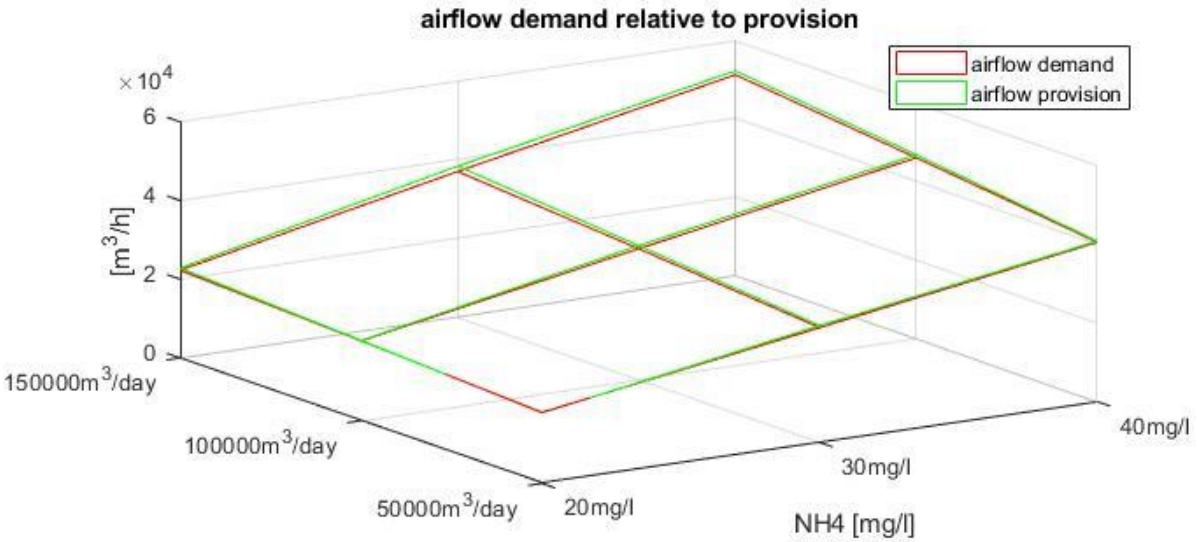

Fig. 132. How variable influent differentiates $airflow_{PROVISION}$ from $airflow_{DEMAND}$ for for the case of T_{ON_DELAY}=4h and $T_{ON\_DELAY}=1h$

This gives an $airflow_{PROVISION}$ from $airflow_{DEMAND}$ difference up to 1,70% (Fig. 133). The momentary oxygen deficiency in the reactor can be made up for later once the necessary number of blowers has been turned on (after T_{ON_DELAY}).The authors of the work [126] indicate that the potential energy gains outweigh the costs of such an operation.

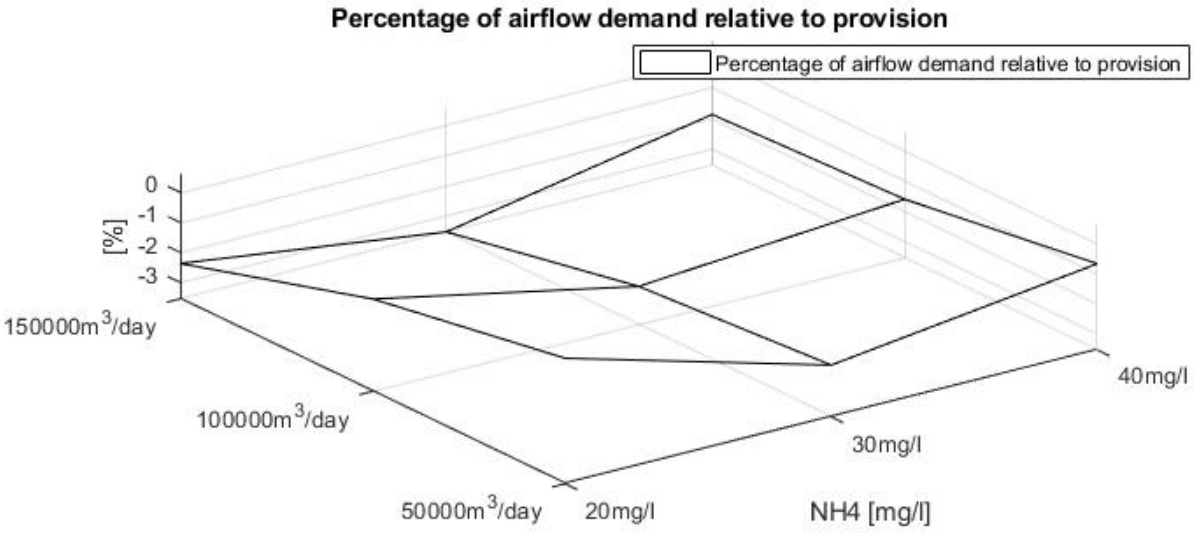

Fig. 133. Airflow deficiency (how variable influent differentiates $airflow_{PROVISION}$ from $airflow_{DEMAND}$) for for the case of T_{ON_DELAY}=4h and T_{ON_DELAY}=1h

Finally, in the Fig. 134, the author shows how variable influent impacts mean power of installation for $T_{ON\_DELAY}=4h$ and $T_{ON\_DELAY}=1h$.

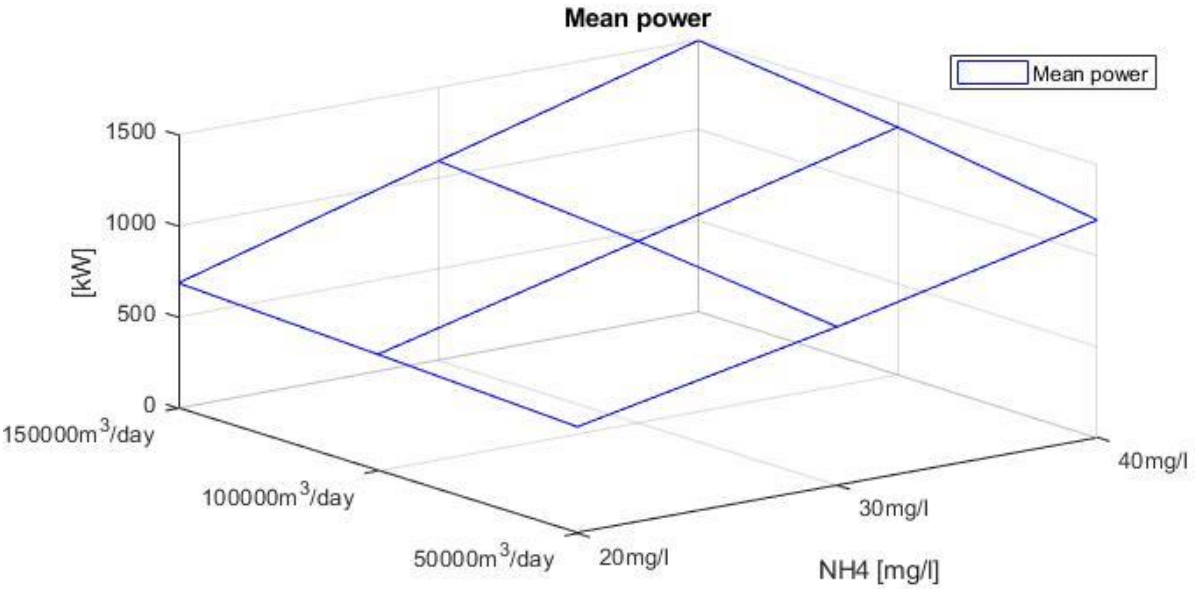

Fig. 134. How variable influent impactsmean power of installation for for the case of T_{ON_DELAY}=4h and T_{ON_DELAY}=1h

To sum up, elongation the blower activation time (T_{ON_DELAY}) will bring real savings. The potential airflow deficiency must be taken into account. Nevertheless, increased efficiency in order to maintain the necessary amount of blown air is a possibility to reduce airflow almost without being scarified by effluent quality. The potential gains outweigh the costs. The conclusions are in line with the study [126] which describes the similar case. Nevertheless, the indicated deterioration in the quality of wastewater in the process means that such changes should be introduced very carefully.

9.3 Conclusion of simulations respecting optimization of blowers control

A numerical model of blowers in the WWTP has been used to control oxygenation in order to reduce electricity consumption. The validation of the model confirms the correctness of the model in terms of the tested characteristics. The simulation environment significantly simplifies the conduct of experiments. Thanks to this solution, the experiments can go beyond the standard scenarios available in a real sewage treatment plant.

The blowers are checked in terms of the control algorithm. The simulations performed in Sec. 9.1 suggest the implementation of task scheduling in control of blowers in WWTP. The entire range of operating conditions of the sewage treatment plant has been taken into account in the simulations. At the beginning, the blower activation time (T_{ON_DELAY} and T_{OFF_DELAY}) are sat as 1h. Changing their values to 4h have an impact on the electricity consumption of the blowers, allowing a slight change in the electric energy consumption. The simulation results show the average power of the blowers can be reduced even to 91,43% of original value. At the same time, the power of blowers increases up to 104,69% of initial value. Based on these results, it can be concluded that in order to reduce electric energy consumption the period of operation of the blowers should be extended at the maximum capacity and at the same time the working time at the minimum capacity should be shortened.

It should be borne in mind that experimenting with oxygenation affects the sensitive process of bacterial growth in wastewater. Therefore, this risk must be taken into account in the further implementation of this control. The problem has been examined in Sec. 9.2.To solve the task, 81 simulations have been carried out in the treatment plant facility as a whole (from the impact of wastewater to electricity consumption).The calculations are a practical attempt to solve the optimal control for this object. Due to complexity of the model, the optimal solution has been found with the use of grid search. Based on paragraph 9.1, it is known that the blower delay should be as long as possible. Extending the switch-on value will reduce the electricity consumption to 98,05% of its initial value. On the other hand, prolonging the shutdown time of the blowers increases airflow deficiency, reaching 1,70%. To sum up, the discussed results are ambiguous. After elongation of T_{ON_DELAY}time reduction in consumption of electric energy can be observed, whereas such action worsens the oxygenation process. Nevertheless, forcing the blower of the sewage treatment plant to be turned on later brings real savings, even after taking into account the increased efficiency in order to maintain the necessary amount of blown air.

10 Summary

10.1 Numeric model of wastewater plant as the basis of optimization

The work presented above discusses the issues of optimization of control in industrial utilities exploiting criteria of electric energy consumption minimization. The sewage treatment plant has been selected for analysis due to the large share of total electricity usage. The author has undertaken the study of blowers model in terms of electric energy consumption. The rightness of the choices has been confirmed by the high electric energy consumption with simultaneous environmental impact. The work uses available data from the wastewater treatment plant in Płaszów Sewage Treatment Plant in Kraków.

Complex standard simulation algorithms, such as ASM1 model and its implementations are used to model wastewater treatment plants. The review suggests the use of a BSM1 environment for plant simulation. A detailed analysis of the model and measurement data allowed to build a model of reactors and blowers. The study has shown a complexity of internal operation and non-linearity of the sewage treatment plant. This numerical object is the basis for further optimization of operation in terms of reducing electricity consumption.

A review of the available tools and algorithms for model validation is presented. To accomplish the task, the author prepared his own implementation of some of them. The properties of the treatment process are examined.

More specifically, Morris' analysis has revealed the most crucial parameters. Summarizing the observations, the author can conclude that Morris sensitivity analyzes have proved that the parameters describing the NH_4^++NH_3 nitrogen in wastewater (S_{NH}) have the greatest impact on the treatment process. Therefore, a considerable attention must be paid for ammonia parameters during wastewater treatment process.

Later, the author implemented the state estimation to check the performance of WWTP and parameter identification utilizing the observations of state estimators grounded on Kalman Filter (EKF and UKF). The changed values of the NH_4^++NH_3 nitrogen and value of influencing coincided with the expected values. By these calculations, the author proves the convergence ofBSM1 model. The state of the art proves that the task of determining the energy optimal control in a facility is not a trivial task.

10.2 General conclusions and reference to thesis

The author starts his work with the thesis:

> *Comprehensive modeling of the industrial facilities like wastewater treatment plants can be used in optimization of control leading to minimization of electric energy consumption.*

The following calculations are performed in order to validate this statement.

First, the operation of the numerical model of the sewage treatment plant as a whole has been examined. The modelled sewage treatment plant has been launched under various operational conditions – the runs with introduced extreme values of the diagnosed key parameters in the wastewater treatment process and in influencing sewage. The quality of the influencing effluent affects the consumption of electricity. Based on the above analyses, it has been demonstrated that the quality of the influent wastewater has an impact on the electricity consumption in the treatment plant. In particular, it has been proved that the NH_4^++NH_3 nitrogen (S_{NH} parameter) of influent wastewater has a key impact on the treatment process and energy demand. Later, it is noted that the volume of influent is another factor affecting the process by increasing consumption of electricity. Moreover, the volume of influent also impacts the electricity consumption of the blowers. The results presented in the work confirm the expected behavior of the numerical environment of the analyzed installation. This behavior is consistent with common sense, thus confirming the correctness of the design assumptions adopted earlier. The results are similar to the observations presented in SCADA measurements.

Next, the author focuses on control respecting the minimization of electricity consumption. The analyzed object has been researched in terms of the control algorithm. The results of the conducted simulations suggest that the change of the of start/stop delay times of the blowers has an impact on the electricity consumption. Extending the start delay time of the blowers allows a significant reduction in the consumption of electric energy. The simulations performed use task scheduling control technique. The procedures tested with validated model underline the rationality of the conducted investigation.

Finally, the author utilizes the model to optimize electric energy consumption in blowers. The author proposed optimal control on the basis grid search to solve non-linear optimal control problem. Nevertheless, the optimization algorithm shown in this way has been limited to running a simulation for selected input values. The optimization solution is therefore a suboptimal solution. Delaying the activation of the blowers leads to short situations in which the amount of oxygen deviates from the demand. The difference between the reactor demand and the actual airflow reaches a noticeable level. However, hypoxia in the rectors of biological wastewater treatment plants must be taken into consideration during optimization reducing electric energy consumption. Fortunately, the amount of oxygen in the reactor can slightly fluctuate. Hence, oxygen deficiencies can be made up by increasing the efficiency of blower after it is switched on.

Summarizing, the author describes some specific conclusions from the work:

- The influent quality, especially NH_4^++NH_3 nitrogen, and its volume lead to the observation of the impact of to the consumption of electricity;
- Better operation points can be achieved by blocking the blowers leading to switching in better performance. Technically, simulation blowers with extended delay in switching on reduces electric power of the installation to 91,43% of its initial value;
- It should be noted that for blowers' station use more than 1MWof electric energy consumption. Saving 1%in their operation corresponds to10kW of electric energy. When the blower operates continuously a whole year with a similar power it translates to 87.6 MWh. A reduction of 8.57% of electric energy consumption has the potential to save up to750 MWh yearly;
- The simulation of the treatment plant as a whole has shown the possibility of reducing the consumption to 98.05% of the initial value. On the other hand, delaying the activation of the blowers leads to short situations in which the amount of oxygen deviates from the demand. The airflow deficiency reaches1,70%;
- Hypoxia in the rectors must be taken into consideration. Oxygen deficiencies can be made up by increasing the efficiency of blower after it is switched on because the amount of oxygen in the reactor can slightly fluctuate;
- It ought to be concluded that complex optimization algorithms can be used to model wastewater treatment plants and optimize their operation in terms of energy to decrease its consumption leading to reduction operational costs andCO_2 emission.

With the above results the author confirms the assumption of thesis that *comprehensive modeling of the industrial facilities like wastewater treatment plants can be used in optimization of control leading to minimization of electric energy consumption.*

The author declares the following issues are characterized by originality:

- The implementation discussed in the dissertation is an in-depth case study of an existing sewage treatment plant in Kraków Płaszów. The presented work is a complete realization that integrates various issues in this WWTP. What is worth emphasizing is that such a comprehensive numerical model of Płaszów Sewage Treatment Plant in Kraków is the novelty. The previously described literature examples deal with other objects and do not cover operation of this wastewater treatment as a whole;
- The author presents a novel method of controlling the blowers by changing the time that on/off blowers turn on and off. This control algorithm allows some savings of several percent in electricity consumption. The method of changing the control itself has been described in the literature, but the implementation of it in a comprehensive position is another innovative part of the dissertation.

The conducted experiments do not exhaust the possibilities. It is easy to imagine other scenarios that can be carried out using the numerical model of the treatment plant. However, the author is limited to the experiments described in detail above. Further research may be done in the future.

10.3 Implementation of research and commercialization potential

Presented dissertation touches important issue in all wastewater treatment plants – the process of blowing air during wastewater treatment is being studied in more detail. This is the crucial process in wastewater treatment in municipal installations. Due to the high electricity consumption of the blowers, even a small reduction of the amount of electric energy consumed can achieve significant savings. The saving declared in the report can be achieved by changing the method of switching on/off the blowers. The implementation presented in the dissertation is adopted to the case of one existing object of Płaszów WWTP. The proposed control assessment complements the work already carried out under the GEKON project.

The author is limited to the detailed experiments discussed above. There is a scope for further model development. The analyses modelling wastewater treatment can be extended by another parameters observed within treatment. Process simulations may consider other parameters, such as the presence of carbon and assessment of the amount of phosphorus in the effluent sewage. Nevertheless, every change required an in-depth configuration of many aspects.

The presented control algorithm is not the only way to modify the operation of blower. Other scenarios can be validated by using the numerical model of the treatment plant. In particular, validation of other control techniques and the implementation of additional criteria for assessing seems promising.

There is potential for commercialization since the solution of switching blower on/off is deployable in other facilities. A reader can propose the implementation of such optimization algorithms for reduction of electricity consumption in other wastewater treatment facilities. This is due to the fact that in each wastewater treatment plant there is a field to tune the control parameters taking into account electricity consumption without any observable impact on the purification process. Nevertheless, all such changes must be made after a detailed analysis of the object. Each treatment plant is specific, therefore an implementation based on the numeric model requires an independent in-depth analysis.

11 Literature

[1] "MPWiK Kraków – Zintegrowany System Efektywności Energetycznej w Oczyszczalni Płaszów," 2019. https://www.astor.com.pl/klienci-astor/wdrozenia/10368-mpwik-krakow-zintegrowany-system-efektywnosci-energetycznej-w-oczyszczalni-plaszow.html.

[2] P. Małka, "Zintegrowany System Efektywności Energetycznej jako istotny element podnoszący niezawodność systemów wodociągowo-kanalizacyjnych," *Gaz, Woda I Tech. Sanit.*, vol. 1, no. 4, pp. 36–38, 2017, doi: 10.15199/17.2017.4.10.

[3] A. Biedrzycka and N. B. Inżynieryjne, "Kierunek : pasywna oczyszczalnia Płaszów," pp. 14–17, 2016.

[4] F. Apostolos, P. Alexios, P. Georgios, S. Panagiotis, and C. George, "Energy efficiency of manufacturing processes: A critical review," *Procedia CIRP*, vol. 7, pp. 628–633, 2013, doi: 10.1016/j.procir.2013.06.044.

[5] "Industrial sector energy consumption," pp. 127–140, 2013.

[6] Z. C. Guo and Z. X. Fu, "Current situation of energy consumption and measures taken for energy saving in the iron and steel industry in China," *Energy*, vol. 35, no. 11, pp. 4356–4360, 2010, doi: 10.1016/j.energy.2009.04.008.

[7] T. Skoczkowski, "Zużycie energii i energochłonność w przemyśle chemicznym w Polsce," no. February, 2017, doi: 10.15199/62.2017.2.4.

[8] C. A. Ramírez, M. Patel, and K. Blok, "The non-energy intensive manufacturing sector. An energy analysis relating to the Netherlands," *Energy*, vol. 30, no. 5, pp. 749–767, 2005, doi: 10.1016/j.energy.2004.04.044.

[9] Feng Liu, Alain Ouedraogo, Seema Manghee, and Alexander Danilenko, "A primer on energy efficiency for municipal water and wastwater utilities," vol. ESMAP.

[10] "Tuam Wastewater treatment plant aeration capacity preliminary raport," no. March 2009, 2010.

[11] K. Mizuta and M. Shimada, "Benchmarking energy consumption in municipal wastewater treatment plants in Japan," *Water Sci. Technol.*, vol. 62, no. 10, pp. 2256–2262, 2010, doi: 10.2166/wst.2010.510.

[12] I. Bodik and M. Kubaska, "Energy and Sustainability of Operation of a Wastewater Treatment Plant," *Environ. Prot. Eng.*, vol. 39, no. 2, pp. 15–24, 2013, doi: 10.5277/EPE130202.

[13] A. Masłon, J. Czarnota, A. Szaja, J. Szulzyk-Cieplak, and G. Łagód, "The enhancement of energy efficiency in a wastewater treatment plant through sustainable biogas use: Case study from Poland," *Energies*, vol. 13, no. 22, 2020, doi: 10.3390/en13226056.

[14] T. Uhl, *Audyt energetyczny i opracowanie strategii energetycznej dla Oczyszczalni Ścieków MPWiK S.A. w Płaszowie*. 2013.

[15] A. H. Reilly and K. A. Hynan, "Corporate communication, sustainability, and social media: It's not easy (really) being green," *Bus. Horiz.*, vol. 57, no. 6, pp. 747–758,

2014, doi: 10.1016/j.bushor.2014.07.008.

[16] E. R. Stafford and C. L. Hartman, “PROMOTING THE VALUE OF Sustainably Minded PURCHASE BEHAVIORS,” *Mark. News*, vol. 47, no. 1, pp. 28–33, 2013, [Online]. Available: http://search.ebscohost.com.ezproxy.liv.ac.uk/login.aspx?direct=true&db=bth&AN=84690449&site=eds-live&scope=site.

[17] P. Dossow, T. Kern, and A. Guminski, “Relevance and potential for industrial on-site electrcicity generation on european scale,” no. 4, pp. 1–22.

[18] I. Gruber and D. Stead, “Urban strategies for Waste Management in Tourist Cities,” 2016.

[19] K. Vatopoulos and D. Andrews, *Study on the state of play of energy efficiency of heat and electricity production technologies*. 2012.

[20] D. Elango, M. Pulikesi, P. Baskaralingam, V. Ramamurthi, and S. Sivanesan, “Production of biogas from municipal solid waste with domestic sewage,” *J. Hazard. Mater.*, vol. 141, no. 1, pp. 301–304, 2007, doi: 10.1016/j.jhazmat.2006.07.003.

[21] M. Serdar, M. Serdar, M. Serdar, and M. Serdar, “Use of sludge generated at WWTP in the production of cement mortal and concrete,” *J. Croat. Assoc. Civ. Eng.*, vol. 68, no. 03, pp. 199–210, 2016, doi: 10.14256/JCE.1374.2015.

[22] I. Zsirai, “Sewage Sludge as Renewable Energy,” *J. Residuals Sci. Technol.*, vol. 8, no. 4, pp. 165–179, 2011.

[23] M. Devine, “Engines? Turbines? Both? Choosing Power for CHP Projects,” no. August, 2013, [Online]. Available: http://www.carolinacat.com/documents/choosing-power-for-chp-projects.aspx.

[24] L. Houdková, J. Boráň, J. Pěček, and P. Šumpela, “Biogas - A renewable source of energy,” *Therm. Sci.*, vol. 12, no. 4, pp. 27–33, 2008, doi: 10.2298/TSCI0804027H.

[25] A. Matuszewska, M. Owczuk, A. Zamojska-Jaroszewicz, J. Jakubiak-Lasocka, J. Lasocki, and P. Orliński, “Evaluation of the biological methane potential of various feedstock for the production of biogas to supply agricultural tractors,” *Energy Convers. Manag.*, vol. 125, no. October, pp. 309–319, 2016, doi: 10.1016/j.enconman.2016.02.072.

[26] D. Schneider and B. Željko, “Analysis of a sustainable system for energy recovery from municipal waste in Croatia,” *Manag. Environ. Qual. An Int. J.*, vol. 22, no. 1, pp. 105–120, 2011, doi: 10.1108/14777831111098516.

[27] S. A. Opatokun, V. Strezov, and T. Kan, “Product based evaluation of pyrolysis of food waste and its digestate,” *Energy*, vol. 92, pp. 349–354, 2015, doi: 10.1016/j.energy.2015.02.098.

[28] Y. Cao and A. Pawłowski, “Sewage sludge-to-energy approaches based on anaerobic digestion and pyrolysis: Brief overview and energy efficiency assessment,” *Renew. Sustain. Energy Rev.*, vol. 16, no. 3, pp. 1657–1665, 2012, doi: 10.1016/j.rser.2011.12.014.

[29] P. Król and G. Krajačić, “Energy Analysis of Municipal Waste in Dubrovnik,” *Acta*

Innov., vol. 28, no. 40, pp. 40–48, 2018.

[30] G. Vaudano, U. F. Ri, and T. Hakala, “DEMOnstration of large SOFC system fed with biogas from WWTP,” no. 2, 2016.

[31] A. Midtsjø, “Power Production from Low Temperature Heat Sources,” no. June, 2009.

[32] I. Vankeirsbilck, “Energetical, Technical and Economical considerations by choosing between a Steam and an Organic Rankine Cycle for Small Scale Power Generation,” *First Int. Semin. ORC Power Syst. ORC 2011*, 2011.

[33] T. Sawik, *Badania operacyjne dla inżynierów zarządzania*. Kraków: Wydawnictwo AGH, 1998.

[34] C. Moser, D. Brunelli, L. Thiele, and L. Benini, “Real-time scheduling for energy harvesting sensor nodes,” *Real-Time Syst.*, vol. 37, no. 3, pp. 233–260, 2007.

[35] M. Zhu, X. Y. Liu, L. Kong, R. Shen, W. Shu, and M. Y. Wu, “The charging-scheduling problem for electric vehicle networks,” *IEEE Wirel. Commun. Netw. Conf. WCNC*, vol. 4, pp. 3178–3183, 2014, doi: 10.1109/WCNC.2014.6953026.

[36] C. Moser *et al.*, “Lazy Scheduling for Energy Harvesting Sensor Nodes,” *Comput. Eng.*, 2007.

[37] T. Khatib, A. Mohamed, and K. Sopian, “A review of photovoltaic systems size optimization techniques,” *Renew. Sustain. Energy Rev.*, vol. 22, pp. 454–465, 2013, doi: 10.1016/j.rser.2013.02.023.

[38] D. Zhang and L. Papageorgiou, “Optimal scheduling of smart homes energy consumption with microgrid,” *ENERGY 2011, First …*, no. c, pp. 70–75, 2011, [Online]. Available: http://www.thinkmind.org/index.php?view=article&articleid=energy_2011_4_30_50148.

[39] Y. Yang, S. Zhang, and Y. Xiao, “An MILP (mixed integer linear programming) model for optimal design of district-scale distributed energy resource systems,” *Energy*, vol. 85, no. 0, pp. 433–448, 2015, doi: http://dx.doi.org/10.1016/j.energy.2015.03.101.

[40] C. A. Floudas and X. Lin, “Continuous-time versus discrete-time approaches for scheduling of chemical processes: A review,” *Comput. Chem. Eng.*, vol. 28, no. 11, pp. 2109–2129, 2004, doi: 10.1016/j.compchemeng.2004.05.002.

[41] Q. Zhang, A. Sundaramoorthy, I. E. Grossmann, and J. M. Pinto, “A discrete-time scheduling model for continuous power-intensive process networks with various power contracts,” *Comput. Chem. Eng.*, vol. 84, pp. 382–393, 2016, doi: 10.1016/j.compchemeng.2015.09.019.

[42] H. Bozkurt, A. Quaglia, K. V. Gernaey, and G. Sin, “A mathematical programming framework for early stage design of wastewater treatment plants,” *Environ. Model. Softw.*, vol. 64, no. 0, pp. 164–176, 2015, doi: http://dx.doi.org/10.1016/j.envsoft.2014.11.023.

[43] D. Newbery, G. Strbac, and I. Viehoff, “The benefits of integrating European electricity markets,” *Energy Policy*, vol. 94, pp. 253–263, 2016, doi: 10.1016/j.enpol.2016.03.047.

[44] S. P. Burger, S. Edu, and M. Luke, “Business Models for Distributed Energy Resources: A Review and Empirical Analysis An MIT Energy Initiative Working Paper,” 2016.

[45] P. Król, A. Gallina, and G. Bazior, “Metody zarządzania handlem energią elektryczną na rynku międzynarodowym.”

[46] “EUPHEMIA Public Description,” 2015.

[47] A. Olędzki, Z. Busko, K. Jawórek, K. Kędzior, K. Nazarczuk, and A. Olędzki, “Zarys Dynamiki i Automatyki Układów,” 1991, [Online]. Available: https://bcpw.bg.pw.edu.pl/Content/767/PDF/01zdau_poczatek.pdf.

[48] I. Ross, “A primer on Pontryagin’s principle in optimal control,” 2015, [Online]. Available: https://bcpw.bg.pw.edu.pl/Content/767/PDF/01zdau_poczatek.pdf.

[49] D. M. Rosewater, D. A. Copp, T. A. Nguyen, R. H. Byrne, and S. Santoso, “Battery Energy Storage Models for Optimal Control,” *IEEE Access*, vol. 7, pp. 178357–178391, 2019, doi: 10.1109/ACCESS.2019.2957698.

[50] L. I. Minchala-Avila, L. E. Garza-Castañón, A. Vargas-Martínez, and Y. Zhang, “A review of optimal control techniques applied to the energy management and control of microgrids,” *Procedia Comput. Sci.*, vol. 52, no. 1, pp. 780–787, 2015, doi: 10.1016/j.procs.2015.05.133.

[51] P. Toint, “BFO : a simple ‘ brute-force ’ optimizer and its self optimization,” *Marseille*, no. April, 2010.

[52] “Hyperparameter optimization.” https://en.wikipedia.org/wiki/Hyperparameter_optimization.

[53] A. Glazunova and E. Aksaeva, “Development of Methods for Research of Electric Power System Flexibility,” *E3S Web Conf.*, vol. 209, 2020, doi: 10.1051/e3sconf/202020902011.

[54] G. Parlier, H. Guéguen, and F. Hu, “Smart brute-force approach for distribution feeder reconfiguration problem,” *Electr. Power Syst. Res.*, vol. 174, pp. 1–17, 2019, doi: 10.1016/j.epsr.2019.04.015.

[55] “Hyperledger Iroha API docs.” https://hyperledger.github.io/iroha-api/#overview.

[56] D. Zhang, Z. Zhang, L. Chen, S. Li, Q. Huang, and Y. Liu, “Blockchain Technology Hyperledger Framework in the Internet of Energy,” *IOP Conf. Ser. Earth Environ. Sci.*, vol. 168, no. 1, 2018, doi: 10.1088/1755-1315/168/1/012043.

[57] F. Lombardi, L. Aniello, S. De Angelis, A. Margheri, and V. Sassone, “A Blockchain-based Infrastructure for Reliable and Cost-effective IoT-aided Smart Grids,” *Living Internet Things Cybersecurity IoT - 2018*, pp. 1–6, 2018, doi: 10.1049/cp.2018.0042.

[58] P. Król, K. Nowakowski, and G. Bazior, “Zastosowanie technologii Hyperledger w zadaniu optymalizacji energetycznej.”

[59] J. Błażewicz, W. Cellary, R. Słowiński, and J. Węglarz, *Badania Operacyjne dla Informatyków*. WNT, 1983.

[60] Centrum Innowacyjnych Technologii Sp. z o.o, “Biologiczne reaktory membranowe

MBR."

[61] M. Arnell, *Performance Assessment of Wastewater Treatment Plants*. .

[62] G. Sin, K. V. Gernaey, M. B. Neumann, M. C. M. van Loosdrecht, and W. Gujer, "Global sensitivity analysis in wastewater treatment plant model applications: Prioritizing sources of uncertainty," *Water Res.*, vol. 45, no. 2, pp. 639–651, 2011, doi: 10.1016/j.watres.2010.08.025.

[63] Z. Dymoczewski, J. Oleszkowicz, and J. Sozański, "Poradnik eksploatora oczyszczalni ścieków." Poznań, 1997.

[64] R. Wójcik, "WYBRANE WSKAŹNIKI FIZYKO-CHEMICZNE WODY," 2019. https://brasil.cel.agh.edu.pl/~09skmolfa/indexa35e.html?file=kursA#BZTn.

[65] M. Mańczak and M. Balbierz, "Instrukcje do przedmiotu oczyszczanie ścieków 2," no. 2, 2018.

[66] C. Wang, Lawrence K. ; Yung-TSe, Hung; Howard, H Lo ; Yapijakis, *Handbook of Industrial and Hazardous Wastes Treatment*. 2004.

[67] U. Jeppsson and G. Olsson, "A General Description of the IAWQ Acrtivated Sludge Model No. 1," *Dep. Ind. Electr. Eng. Autom.*, no. 1, p. 444, 1996.

[68] M. Henze, W. Gujer, T. Mino, and M. C. M. van Loosdrecht, "Activated Sludge Models ASM1, ASM2, ASM2d and ASM3," *IWA Publ.*, p. 121, 2000, doi: 10.1007/s13398-014-0173-7.2.

[69] M. Henze, C. P. . Grady, W. Gujek, G. Marais, and T. Matsuo, "ACTIVATED SLUDGE MODEL NO. 1," 1987.

[70] J. Copp, "The COST Simulation Benchmark: Description and Simulation Manual."

[71] J. Alex *et al.*, "Benchmark Simulation Model no. 1 (BSM1)," vol. 1, no. 1, 2008.

[72] "RISE: C-FOOT-CTRL Development of dynamic model for carbon footprint estimation Deliverable," 2016. [Online]. Available: https://ec.europa.eu/research/participants/documents/downloadPublic?documentIds=080166e5ac61383c&appId=PPGMS.

[73] "MASSFLOW - Technical reference." http://www.massflow.kr/Site/Technical.aspx.

[74] D. J. Batstone and I. Angelidaki, "Anaerobic digestion model No 1 (ADM1)," vol. 1, no. 1, 2002.

[75] U. Jeppsson *et al.*, "Benchmark Simulation Model no . 2 (BSM2)," *Water Sci. Technol.*, vol. 1, no. 1, p. 99, 2018.

[76] C. Rosen and U. Jeppsson, "Aspects on ADM1 Implementation within the BSM2 Framework," *Tech. Rep.*, no. May, pp. 1–37, 2006.

[77] U. Jeppsson, C. Rosen, J. Alex, J. Copp, K. V Gernaey, and M. Pons, "Towards a benchmark simulation model for plant-wide control strategy performance evaluation of WWTPs," pp. 287–295, 2006, doi: 10.2166/wst.2006.031.

[78] J. Alex *et al.*, "Benchmark Simulation Model no . 1 (BSM1)," *Lutedx*, vol. TEIE-7229,

no. 1, pp. 1–62, 2008.

[79] K. V Gernaey, D. Vrecko, C. Rosen, and U. Jeppsson, “BSM1 versus BSM1 _ LT : Is the Control Strategy Performance Ranking Maintained ?,” vol. 1, no. 1, 2006.

[80] I. W. A. Tg, C. Rosen, and J. Alex, “BSM2 Plant - Wide Wastewater Treatment Plant Modelling Supported by IWA ICA and SAIA specialist groups several,” no. May, pp. 1–5, 2007.

[81] U. Jeppson, “Modifications to BSM1, BSM1_LT and BSM2,” pp. 1–5, 2005.

[82] Aerzen, “Aeration Blowers in the Wastewater Industry in North America,” 2012, [Online]. Available: http://vertassets.blob.core.windows.net/download/116613d5/116613d5-d2a2-42c3-b3a5-a17700a0d648/whitepaperaerationblowerwastwaterindustry2.pdf.

[83] L. Düppe, “What The kLa Tells You About The Oxygen Transfer In Your Bioreactor,” 2020. https://www.infors-ht.com/en/blog/what-the-kla-tells-you-about-the-oxygen-transfer-in-your-bioreactor/.

[84] B. Steven, “Modeling wastewater aeration systems to discover energy savings opportunities,” pp. 1–11, 2003.

[85] M. K. Stenstrom and D. Rosso, “Aeration,” p. 92, 2010.

[86] Z. He, A. Petiraksakul, and W. Meesapya, “Oxygen-Transfer Measurement in Clean Water,” *J. KMITNB*, vol. 13, no. 1, pp. 14–19, 2003.

[87] *Aeration: A Wastewater Treatment Process*. .

[88] I. Fändriks, “Alternative Methods for Evaluation of Oxygen Transfer Performance in Clean Water,” pp. 1–101, 2011.

[89] R. A. Zaveri, R. C. Easter, J. E. Shilling, and J. H. Seinfeld, “Modeling kinetic partitioning of secondary organic aerosol and size distribution dynamics: Representing effects of volatility, phase state, and particle-phase reaction,” *Atmos. Chem. Phys.*, vol. 14, no. 10, pp. 5153–5181, 2014, doi: 10.5194/acp-14-5153-2014.

[90] A. B. L. Avilés, F. del C. Velázquez, and M. L. P. del Riquelme, “Methodology for energy optimization in wastewater treatment plants. Phase I: Control of the best operating conditions,” *Sustain.*, vol. 11, no. 14, 2019, doi: 10.3390/su11143919.

[91] J. Yanjun, “An Alternative Mathematical Model for Oxygen Transfer Evaluation in Clean Water,” no. 1, pp. 1–10, 2015, [Online]. Available: https://www.wwdmag.com/sites/wwdmag.com/files/A New Model for Oxygen Tranfer Model in Clean Water-JH-Water online (1).pdf.

[92] R. Piotrowski, M. A. Brdys, K. Konarczak, K. Duzinkiewicz, and W. Chotkowski, “Hierarchical dissolved oxygen control for activated sludge processes,” *Control Eng. Pract.*, vol. 16, no. 1, pp. 114–131, 2008, doi: 10.1016/j.conengprac.2007.04.005.

[93] R. Piotrowski, M. A. Brdys, and D. Miotke, *Centralized dissolved oxygen tracking at wastewater treatment plant: Nowy dwor gdanski case study*, vol. 9, no. PART 1. IFAC, 2010.

[94] W. Krawczyk, R. Piotrowski, M. A. Brdys, and W. Chotkowski, “Modelling and Identification of Aeration Systems for Model Predictive Control of Dissolved Oxygen – Swarzewo Wastewater Treatment Plant Case Study,” *IFAC Proc. Vol.*, vol. 40, no. 4, pp. 43–48, 2007, doi: 10.3182/20070604-3-MX-2914.00076.

[95] R. Piotrowski and T. Ujazdowski, “Designin Control Strategies of Aeration system in Biological WWTP,” 2020.

[96] T. J. Casey, “Diffused Air Aeration Systems for the Activated Sludge Process Design Performance Testing,” *Aquavarra Res. R&D Publ.*, no. August, 2009.

[97] “Das OTT Produkt-Handbuch,” 2016.

[98] C.-F. Lindberg, *Control and Estimation Strategies Applied to the Activated Sludge Process*. 1997.

[99] M. Arnell and U. Jeppsson, “Aeration System Modelling - Case Studies From Three Full-scale Wastewater Treatment Plants 9th IWA Symposium on Systems Analysis and Integrated Assessment,” no. June, 2015.

[100] S.-Y. Leu, D. Rosso, L. E. Larson, and M. K. Stenstrom, “Real-Time Aeration Efficiency Monitoring in the Activated Sludge Process and Methods to Reduce Energy Consumption and Operating Costs,” *Water Environ. Res.*, vol. 81, no. 12, pp. 2471–2481, 2009, doi: 10.2175/106143009X425906.

[101] Z. Zhu, R. Wang, and Y. Li, “Evaluation of the control strategy for aeration energy reduction in a nutrient removing wastewater treatment plant based on the coupling of ASM1 to an aeration model,” *Biochem. Eng. J.*, vol. 124, pp. 44–53, 2017.

[102] “CHAPTER 6 Suspended Growth Models,” no. GPS-X documentation, pp. 95–120.

[103] A. Biedrzycka, “Utylizacja osadów ściekowych, Veolia Water Systems Sp. z o.o.,” pp. 20–22, 2008.

[104] “Platforma Systemowa Wonderware w Oczyszczalni Ścieków Płaszów II,” pp. 1–6, 2007.

[105] P. Małka, M. Frączek, and S. A. Mpwik, “System sterowania oraz aparatura kontrolno pomiarowa Oczyszczalni Ścieków Płaszów,” 2007.

[106] O. Projektu, P. Zakończony, P. Oczyszczalnia, and Ś. Płaszów, “Oczyszczalnia Ścieków Płaszów II w Krakowie - Opis projektu (projekt zakończony),” 2020. https://wodociagi.krakow.pl/o-firmie/projekty-unijne/oczyszczalnia-sciekow-plaszow-ii-w-krakowie.html.

[107] “AMTAX sc - Data Sheet DOC053.52.00138.Jan06.”

[108] “Oxygen Transfer Technology Efficiency by Design OTT GROUP.”

[109] T. Kudłacz; and M. Musiał-Malago, “Funkcjonalne miasto w teorii i praktyce na przykładzie Krakowa i Krakowskiego Obszaru Metropolitarnego,” *J. Chem. Inf. Model.*, vol. 53, no. 9, pp. 1689–1699, 2019.

[110] “The urban waste water treatment directive,” *Inst. Water Off. J.*, vol. 28, no. 4, pp. 14–15, 1992.

[111] “Dyrektywa rady z dnia 21 maja 1991 r. dotycząca oczyszczania ścieków komunalnych (91/271/EWG),” 1991.

[112] “HV-TURBO® centrifugal turbo compressor.”

[113] “Fans - Efficiency and Power Consumption.” https://www.engineeringtoolbox.com/fans-efficiency-power-consumption-d_197.html.

[114] T. Mathson and M. Ivanovich, “AMCA’s Fan Efficiency Grades : answers to Frequently asked Questions,” *AMCA Int. inmotion*, vol. 9, pp. 8–13, 2011.

[115] J. Pyka and I. Foltynowicz, “Aproksymacja metodą najmniejszych kwadratów,” no. x, pp. 182–201, 2017, [Online]. Available: www.staff.amu.edu.pl/ ~zcht/pliki/ Aproksymacja.pdf.

[116] E. Brzychczy, “Weryfikacja modeli ekonometrycznych opracowanych dla potrzeb analizy charakterystyk techniczno-ekonomicznych kopalni węgla kamiennego.”

[117] X. Liu, Y. Jing, G. Olsson, and Z. Yuan, “Finding the optimal aeration profiles and do profiles in a plug-flow biological wastewater treatment reactor with a theoretical approach,” *IFAC Proc. Vol.*, vol. 19, pp. 2715–2720, 2014.

[118] M. C. Ozturk, F. Martin Serrat, and F. Teymour, “Optimization of aeration profiles in the activated sludge process,” *Chem. Eng. Sci.*, vol. 139, pp. 1–14, 2016, doi: 10.1016/j.ces.2015.09.007.

[119] M. F. Rahmat, S. I. Samsudin, N. A. Wahab, M. C. Razali, and M. S. Gaya, “Decentralized adaptive PI with adaptive interaction algorithm of wastewater treatment plant,” *J. Teknol. (Sciences Eng.*, vol. 67, no. 5, pp. 15–21, 2014, doi: 10.11113/jt.v67.2837.

[120] a. Thunberg, A.-M. Sundin, and B. Carlsson, “Energy optimization of the aeration process at Käppala wastewater treatment plant,” *10th IWA Conf. Instrumentation, Control Autom.*, 2009.

[121] L. Åmand and B. Carlsson, “Aeration control with gain scheduling in a full-scale wastewater treatment plant,” *IFAC Proc. Vol.*, no. August, pp. 7146–7151, 2014, doi: 10.3182/20140824-6-za-1003.01892.

[122] X. Du, J. Wang, V. Jegatheesan, and G. Shi, “Dissolved oxygen control in activated sludge process using a neural network-based adaptive PID algorithm,” *Appl. Sci.*, vol. 8, no. 2, 2018, doi: 10.3390/app8020261.

[123] M. A. Brdys, W. Chotkowski, K. Duzinkiewicz, K. Konarczak, and R. Piotrowski, *Two - Level Dissolved Oxygen Control for Activated Sludge Processes*, vol. 35, no. 1. IFAC, 2002.

[124] K. Szabat and C. T. Kowalski, “Fuzzy models of the biological-chemical processes in the water-water treatment plant,” pp. 230–241.

[125] M. Henderson, “Energy Reduction Methods in the Aeration Process at Perth Wastewater Treatment Plant,” 2002.

[126] A. R. Asadi, A. Verma, and K. Yang, “Wastewater effluents & Optimizing Aeration

Process," *Proc. Int. Conf. Ind. Eng. Oper. Manag.*, pp. 808–812, 2016.

[127] A. Fenu *et al.*, "Energy audit of a full scale MBR system," *Desalination*, vol. 262, no. 1–3, pp. 121–128, 2010, doi: 10.1016/j.desal.2010.05.057.

[128] T. Maere, B. Verrecht, S. Moerenhout, S. Judd, and I. Nopens, "BSM-MBR: A benchmark simulation model to compare control and operational strategies for membrane bioreactors," *Water Res.*, vol. 45, no. 6, pp. 2181–2190, 2011, doi: 10.1016/j.watres.2011.01.006.

[129] S. Gabarrón, M. Dalmau, J. Porro, I. Rodriguez-Roda, and J. Comas, "Optimization of full-scale membrane bioreactors for wastewater treatment through a model-based approach," *Chem. Eng. J.*, vol. 267, pp. 34–42, 2015, doi: 10.1016/j.cej.2014.12.097.

[130] V. Larsson, "Energy savings with a new aeration and control system in a mid-size Swedish wastewater treatment plant," no. December, 2011.

[131] M. O'Brien, J. Mack, B. Lennox, D. Lovett, and A. Wall, "Model predictive control of an activated sludge process: A case study," *Control Eng. Pract.*, vol. 19, pp. 54–61, 2011, doi: 10.1016/j.conengprac.2010.09.001.

[132] L. Amand, G. Olsson, and B. Carlsson, "Aeration control - A review," *Water Sci. Technol.*, vol. 67, no. 11, pp. 2374–2398, 2013, doi: 10.2166/wst.2013.139.

[133] A. B. L. Avilés, F. Del Cerro Velázquez, and M. L. P. Del Riquelme, "Methodology for energy optimization in wastewater treatment plants. Phase II: Reduction of air requirements and redesign of the biological aeration installation," *Water (Switzerland)*, vol. 12, no. 4, 2020, doi: 10.3390/W12041143.

[134] B. Iooss, "A review on global sensitivity analysis methods," no. around 30.

[135] A. Saltelli, P. Annoni, I. Azzini, F. Campolongo, M. Ratto, and S. Tarantola, "Variance based sensitivity analysis of model output. Design and estimator for the total sensitivity index," *Comput. Phys. Commun.*, vol. 181, no. 2, pp. 259–270, 2010, doi: 10.1016/j.cpc.2009.09.018.

[136] M. Jaxa-Rozen and J. Kwakkel, "Tree-based ensemble methods for sensitivity analysis of environmental models: A performance comparison with Sobol and Morris techniques," *Environ. Model. Softw.*, vol. 107, pp. 245–266, 2018, doi: 10.1016/j.envsoft.2018.06.011.

[137] M. D. Morris, "Factorial Sampling Plans for Preliminary Computational Experiments," *Quality*, vol. 33, no. 2, pp. 161–174, 1991.

[138] P. Ekström, "Eikos A Simulation Toolbox for Sensitivity Analysis," *Master's*, no. February, p. 41, 2005.

[139] F. Campolongo, J. Cariboni, and A. Saltelli, "An effective screening design for sensitivity analysis of large models," *Environ. Model. Softw.*, vol. 22, no. 10, pp. 1509–1518, 2007, doi: 10.1016/j.envsoft.2006.10.004.

[140] G. Sin, K. V. Gernaey, M. B. Neumann, M. C. M. van Loosdrecht, and W. Gujer, "Uncertainty analysis in WWTP model applications: A critical discussion using an example from design," *Water Res.*, vol. 43, no. 11, pp. 2894–2906, 2009, doi:

10.1016/j.watres.2009.03.048.

[141] X. Flores-Alsina, I. Rodriguez-Roda, G. Sin, and K. V. Gernaey, “Uncertainty and sensitivity analysis of control strategies using the benchmark simulation model No1 (BSM1),” *Water Sci. Technol.*, vol. 59, no. 3, pp. 491–499, 2009, doi: 10.2166/wst.2009.871.

[142] A. Cosenza, G. Mannina, P. A. Vanrolleghem, and M. B. Neumann, “Variance-based sensitivity analysis for wastewater treatment plant modelling,” *Sci. Total Environ.*, vol. 470–471, pp. 1068–1077, 2014, doi: 10.1016/j.scitotenv.2013.10.069.

[143] M. V. Ruano, J. Ribes, A. Seco, and J. Ferrer, “An improved sampling strategy based on trajectory design for application of the Morris method to systems with many input factors,” *Environ. Model. Softw.*, vol. 37, pp. 103–109, 2012, doi: 10.1016/j.envsoft.2012.03.008.

[144] S. Sharifi, S. Murthy, I. Takács, and A. Massoudieh, “Probabilistic parameter estimation of activated sludge processes using Markov Chain Monte Carlo,” *Water Res.*, vol. 50, pp. 254–266, 2014, doi: 10.1016/j.watres.2013.12.010.

[145] P. Król, A. Gallina, M. Lubieniecki, T. Uhl, and T. Żaba, “Sensitivity analysis of a municipal wastewater treatment plant model,” *MATEC Web Conf.*, vol. 252, p. 05010, 2019, doi: 10.1051/matecconf/201925205010.

[146] P. I. Frazier, “A Tutorial on Bayesian Optimization,” no. Section 5, pp. 1–22, 2018, [Online]. Available: http://arxiv.org/abs/1807.02811.

[147] J. Gonzalez, “Intruduction to Bayesian Optimization.”

[148] R. E. Kalman, “A New Approach to Linear Filtering and Prediction Problems,” *ASME–Journal Basic Eng.*, vol. 82, pp. 35–45, 1960, doi: 10.1007/BF00248635.

[149] G. Welch and G. Bishop, “An Introduction to the Kalman Filter,” pp. 1–16, 2006.

[150] M. van Biezen, “Lectures in The Kalman Filter.” http://www.ilectureonline.com/lectures/subject/SPECIAL TOPICS/26/190.

[151] C. Keatmanee, J. Baber, and M. Bakhtyar, “Simple Example of Applying Extended Kalman Filter Simple Example of Applying Extended Kalman Filter,” *1st Int. Electr. Eng. Congr.*, no. March 2015, 2014.

[152] D. G. Bleser, “Using the Kalman filter Extended Kalman filter.”

[153] M. B. Beck, “Operational estimation and prediction of nitrification dynamics in the activated sludge process,” *Water Res.*, vol. 15, no. 12, pp. 1313–1330, 1981, doi: 10.1016/0043-1354(81)90004-X.

[154] S. J. Julier and J. K. Uhlmann, “New extension of the Kalman filter to nonlinear systems,” *Signal Process. Sens. Fusion, Target Recognit. VI*, vol. 3068, p. 182, 1997, doi: 10.1117/12.280797.

[155] E. A. Wan and R. van rer Merwe, “The Unscented Kalman Filter for Nonlineaer Estimation,” *Medizinische Welt*, vol. 33, no. 13, pp. 475–479, 2000.

[156] S. Konatowski, P. Kaniewski, and J. Matuszewski, “Comparison of Estimation Accuracy

of EKF, UKF and PF Filters," *Annu. Navig.*, vol. 23, no. 1, pp. 69–87, 2017, doi: 10.1515/aon-2016-0005.

[157] MATHWORKS, "Extended and Unscented Kalman Filter Algorithms for Online State Estimation." https://www.mathworks.com/help/control/ug/extended-and-unscented-kalman-filter-algorithms-for-online-state-estimation.html (accessed Sep. 12, 2019).

[158] F. Haugen, "State estimation with Kalman Filter," *Kompend. Kyb. 2 ved Høgskolen i Oslo*, pp. 101–127, 2007.

[159] S. Boyd, "Lecture 8 The Kalman filter," pp. 1–28, 2008, [Online]. Available: www.stanford.edu/class/ee363/lectures/kf.pdf.

[160] S. Beltrán, I. Irizar, H. Monclús, I. Rodríguez-Roda, and E. Ayesa, "On-line estimation of suspended solids in biological reactors of WWTPs using a Kalman observer," *Water Sci. Technol.*, vol. 60, no. 3, pp. 567–574, 2009, doi: 10.2166/wst.2009.302.

[161] J. Busch *et al.*, "State estimation for large-scale wastewater treatment plants," *Water Res.*, vol. 47, no. 13, pp. 4774–4787, 2013, doi: 10.1016/j.watres.2013.04.007.

[162] Q. Chai, B. Furenes, and B. Lie, *Comparison of State Estimation Techniquest, Appliced to a biological Wastewater Treatment Process*, vol. 40, no. 4. IFAC, 2007.

[163] J. Zeng, J. Liu, T. Zou, and D. Yuan, "State Estimation of Wastewater Treatment Processes Using Distributed Extended Kalman Filters," no. Cdc, pp. 6721–6726, 2016.

[164] E. Ayesa, J. Florez, J. L. Garcia-Heras, and L. Larrea, "State and coefficient estimation for the activated sludge process using a modified Kalman filter algorithm," *Water Sci. Technol.*, vol. 24, no. 6, pp. 235–247, 1991.

[165] H. Zhao and M. Kümmel, "State and parameter estimation for phosphorus removal in an alternating activated sludge process," *J. Process Control*, no. 5, pp. 341–351, 1995, doi: 10.1016/0959-1524(95)00006-C.

[166] "State observers for a biological wastewater nitrogen removal process in a sequential batch reactor," *Bioresour. Technol.*, vol. 79, no. 1, pp. 1–14, 2001, doi: 10.1016/S0960-8524(01)00041-4.

[167] T. Rutkowski and M. A. Brdys, *the Hybrid Estimation Algorithm for Wastewater Treatment Plant*, vol. 40, no. 9. IFAC, 2007.

[168] X. Yin and J. Liu, "State estimation of wastewater treatment plants based on model approximation," *Comput. Chem. Eng.*, vol. 111, pp. 79–91, 2018, doi: 10.1016/j.compchemeng.2018.01.003.

[169] P. Król, A. Gallina, and T. Uhl, "Sewage influent estimation in BSM1 model of Płaszów WWTP," 2021.

[170] S. Saigal and D. Mehrotra, "Performance Comparison of Time Series Data Using Predictive Data Mining Techniques," *Adv. Inf. Min.*, vol. 4, no. 1, pp. 57–66, 2012, [Online]. Available: http://www.bioinfo.in/contents.php?id=32.

[171] E. A. G. de Souza, M. S. Nagano, and G. A. Rolim, "Dynamic Programming algorithms and their applications in machine scheduling: A review," *Expert Syst. Appl.*, vol. 190, no. September 2021, p. 116180, 2022, doi: 10.1016/j.eswa.2021.116180.